Title
ENERGY & ENVIRONMENT DIVISION ANNUAL REPORT, 1977

Permalink
https://escholarship.org/uc/item/7q1868h9

Author
Budnitz, R.J.

Publication Date
1978-08-25

UC-13
LBL-6877
C.1

Energy & Environment Division

Annual Report 1977

13

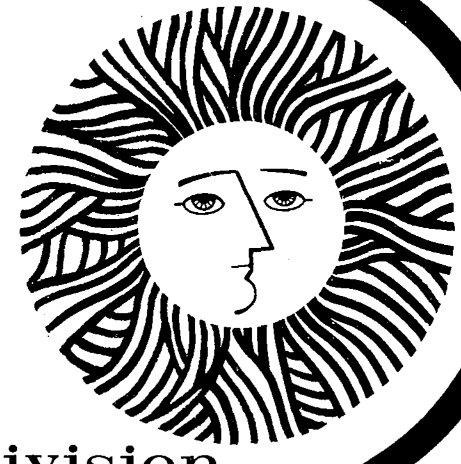

Energy & Environment Division

Lawrence Berkeley Laboratory
University of California, Berkeley

Prepared for the U.S. Department of Energy under Contract No. W-7405-ENG-48

LBL-6877 c.1

Printed in the United States of America
Available from
National Technical Information Service
U. S. Department of Commerce
5285 Port Royal Road
Springfield, VA 22161
Price: Printed Copy, $ 9.00 Domestic; $18.00 Foreign
Microfiche, $ 3.00 Domestic; $ 4.50 Foreign

LBL-6877
UC-13
TID-4500-R66

ENERGY & ENVIRONMENT DIVISION ANNUAL REPORT

1977

Robert J. Budnitz
Head, Energy & Environment Division
and
Associate Director, LBL

Editorial Committee
Jeffrey Kessel, Chairperson

Susan M. Gillett
Ronald L. Ritschard
Frank Robben
Hal Rosen
Peter Rowe

Technical Editing
by
Josephine A. Camp
Gloria Chua
Robert Hendrickson

Energy & Environment Division
Lawrence Berkeley Laboratory
University of California
Berkeley, California 94720

LAWRENCE BERKELEY LABORATORY
UNIVERSITY OF CALIFORNIA
ENERGY & ENVIRONMENT DIVISION

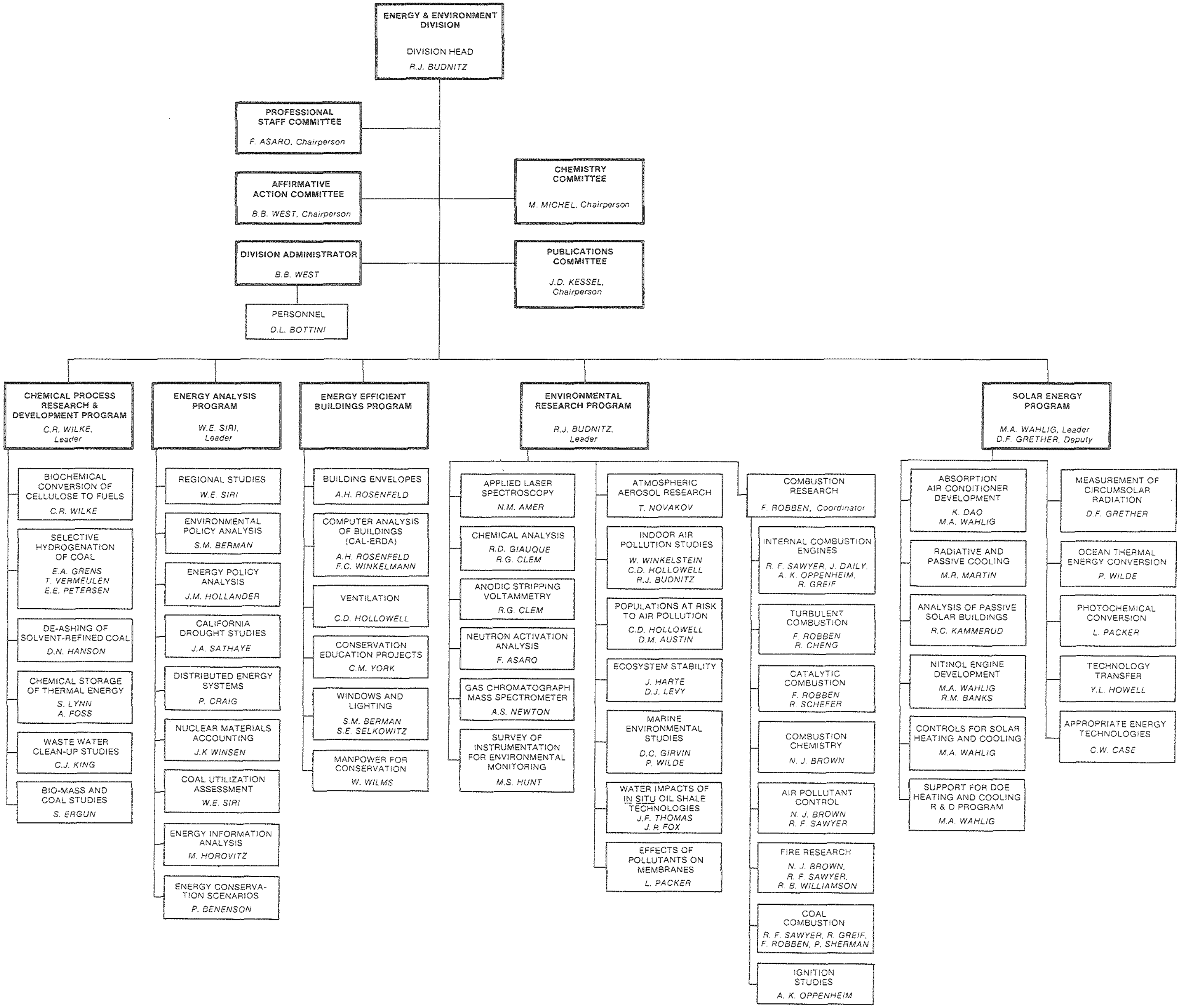

MAY 1978

Energy and Environment Division Staff*

Yogesh Agrawal
Nabil Amer
Roy Anaclerio, Jr.
Brandt Andersson
Anthony Anninos
Reginal Anson
Kenneth Arnold
Frank Asaro
Janette Bacon
Myra Baker
Ridgway Banks
Peter Benenson
William Benner
Paul Berdahl
James Berk
Samuel Berman
Prem Bhardwaja
Henryk Birecki
Carl Blumstein
Tom Borgers
Dorothy Bottini
Patricia Bronnenberg
Nancy Brown
Robert Budnitz
Walter Buhl
Charles Case
Felipe Catalan
Peter Chan
Shih-Ger Chang
Robert Cheng
Holly Ching
Mark Christensen
Robert Clear
Ray Clem
Paul Condon
Steven Cosner
Paul Craig
John Daily
Kim Dao
Mark Davidson
Joshua Dayan
Edward Dean
Richard Diamond
James Dillworth
Linda Dioguardi
Raymond Dod
Harry Dwyer
Sabri Ergun
Anthomy Fisher
Sharon Forsberg
Alan Foss
Phyllis Fox
Raymond Freitas
Denise Fynmore
Roberta Garrett
Robert Gerlach
Robert Giauque
Susan Gillett
Donald Girvin
C. Roger Glassey
Ralph Greif
Edward Grens
Donald Grether
David Grimsrud
Lara Gundel
Anthony Hansen
Donald Hanson
Takeshi Harima
John Harte
Alvin Hebert
Frederick Henderson
Heidi Hill
James Hirsch
Alfred Hodgson
Craig Hollowell
Kenneth Hom
Mark Horovitz
Arlon Hunt
Mary Quinby-Hunt
Alan Jassby
Julie Jones
Edward Kahn
Ronald Kammerud
Stephen Kanzler
Michael Kelly
Jeffrey Kessel
C. Judson King, III
Mathilde Kland
Tetsuya Konishi
Leonard Kunin
Yvonne Ladson
Alan Laird
Elliot Lapan
Mark Levine
Donald Levy
Chin-I Lin
Billy Long
Scott Lynn
John Maguire
Michael Majteles
Glenn Markoe
Samuel Markowitz
Marlo Martin
Gary Mason
Ashwani Mathur
Joanne McCarthy
Roxie McLeod
Janet McQuillan
Rolf Mehlhorn
Karl Mellander
Helen Michel
Harry Miller
Howard Mitchell
Hani Mohamed
Duane Mosier
Dana Mukamel
Don Murphy
Jean Nelson
Anthony Nero, Jr.
Amos Newton
Tihomir Novakov
Antoni Oppenheim
Maria Ossa
William Oswald
Huseyin Ozbek
Lester Packer
Patrick Pagni
Rebecca Palmer
Eugene Petersen
Sidney Phillips
Thomas Powell
Alexandre Quintanilha
Clayton Radke
John Rees
Mohammad Riaz
Robert Risebrough
Ronald Ritschard
Franklin Robben
Hal Rosen
Steven Rosenberg
Arthur Rosenfeld
Peter Rowe
Henry Ruderman
Laurie Sampietro
James Sandusky
Jayant Sathaye
Robert Sawyer
Robert Schefer
Leon Schipper
Richard Schmidt
Nancy Schorn
Susan Schwartz
Aldo Sciamanna
Stephen Selkowitz
Steven Selvin
Richard Sextro
Pauline Sherman
Paul Shieh
John Shively
Ellen Shurtleff
Harrison Sigworth, Jr.
Melvin Simmons
William Siri
Angela Smothers
Robert Sonderegger
Ralph Stewart
Lawrence Talbot
S. Tangnu
Mark Tatro
Elisha Tel-Or
Jerome Thomas
Launey Thomas, III
Gregory Traynor
Patria Vega De Castro
Rudolph Verderber
Theodore Vermeulen
Jerel Vogt
Michael Wahlig
Robert Walker, Jr.
Barbara West
Kenneth Wilcox
Pat Wilde
Charles Wilke
Wellford Wilms
Frederick Winkelmann
Warren Winkelstein
Anita Winkler
Linda Wroth
Ren-Der Yang
Winifred Yen
Carl York
Sharran Zeleke

---

* Not including Graduate Student Research Assistants.

Contents

ENERGY ANALYSIS

SOLAR ENERGY

ENERGY EFFICIENT BUILDINGS

CHEMICAL PROCESS RESEARCH AND DEVELOPMENT

ENVIRONMENTAL RESEARCH

INSTRUMENTATION DEVELOPMENT

COMBUSTION RESEARCH

Energy Analysis

INTRODUCTION

From that moment in the distant past when one of our ancestors learned to use fire, Homo sapiens was launched on a never-ending quest for more energy and ways to spend it. From man's original and highly personal consumption of 500 Btu per hour to fuel muscle and metabolism, the per capita consumption of energy (in the United States) has risen past the 40,000 Btu per hour mark. For the growing U.S. population, now well past 200 million, the flow of energy hovers at 75 QBtu per year on its exponential rise. Along with this enormous flow of energy has come an uneasy awareness that the many benefits of energy come wrapped in disturbing and difficult-to-solve problems labelled environmental, economic, social, and health impacts and constraints.

It is this set of strongly interconnected impacts to which the Energy Analysis Program directs its attention, aided by a bag of diagnostic computer models and massive banks of data. In general, analyses fall into two major categories. One embraces the impacts of specific energy technologies and fuels, such as nuclear, coal combustion and conversion, and geothermal sources, together with economic, environmental and institutional constraints on their use.

The second category includes assessments of regional--meaning local, state, and multistate--impacts of alternative future energy supply systems and energy growth. For integrated regional assessments sponsored by the Department of Energy (DOE) Assistant Secretary, Environment, LBL has been assigned the states of California, Nevada and Hawaii.

The major subprograms spring from national energy policy, contemplated and enacted, and energy technology R & D pursued by DOE. Together with the other national laboratories, LBL participates in a National Coal Utilization Assessment, which examines the consequences of, and constraints on, accelerated use of coal in the U.S. Similarly, an enviornmental-health assessment of the National Energy Policy Act has been undertaken, encompassing all the energy technologies, economic drives and regulations it calls for.

Complementing these continuing subprograms are analytical studies centered on special energy-related issues, problems, and policy. Among such studies are analyses of the impacts of the severe California drought on electricity supply and demand for 1977 and 1978, when hydroelectricity, which normally supplies one-fourth of the state's electricity, would be severely reduced. Among impacts anticipated were significantly higher electricity rates and greater air pollution from increased oil burning to compensate for hydroelectric losses.

Various aspects of energy conservation, for example its effects on employment and capital, have been examined and others are under continuing study.

The security of nuclear material has become a sensitive issue. To explore possibilities for improvement, studies were undertaken which examined procedures currently employed in nuclear material accounting, and developed a game-theoretical approach to decision making on actions to be taken vis-a-vis material unaccounted for in periodic inventories of nuclear materials in fuel reprocessing and fabrication plants.

Aside from analyses of technology-specific problems, assessments conducted by the LBL program have involved economic impacts, water resource and quality issues related to energy supply, air quality effects, siting of facilities, and health effects. The findings of such assessments are intended primarily to aid DOE and other agency decision makers in formulating policy and energy technology R & D programs.

IMPACTS OF FUTURE COAL USE IN CALIFORNIA

R. Brandi, P. Chan, D. Ermak, M. Horovitz, J. Kooser,
R. Nyholm, R. Ritschard, H. Ruderman, J. Sathaye,
R. Sextro, and W. Siri

INTRODUCTION

This project details the preliminary methodology and results of an ongoing asssessment of the impacts of future (to year 2000) coal use in California. The assessment forms an integral part of the National Coal Utilization Assessment (NCUA) being conducted cooperatively by six of the Department of Energy national laboratories.

A common basis for these assessments has been adopted. An initial set of four national coal utilization scenarios was constructed, featuring alternative coal technologies for comparative assessments. Each scenario, disaggregated to the regional level, specifies the type and number of facilities and fuel for each region for the time span from 1976 to 2000. Lawrence Berkeley Laboratory is responsible for the integrated assessment of the scenarios for the State of California. In conducting the assessments, candidate sites for facilities are selected on the basis of which analyses are to be performed to evaluate the impacts on air quality, water and other resources, local and state economy, and health and safety.

ACCOMPLISHMENTS DURING 1977

Energy supply scenarios for California were disaggregated from the four Pacific Region scenarios developed by Brookhaven National Laboratory. These scenarios specify in detail the quantities of major energy supply sources for 1975, 1978, and 2000. Major sources include coal, petroleum, natural gas, solar and geothermal, and electricity supply by type of generation. Each of these four scenarios emphasizes different amounts and types of coal use. The first scenario, or the Recent Trends scenario, extrapolates current low quantities of coal use in California. The second and third scenarios call for increased coal use for conversion to synthetic fuels and for electricity generation, respectively. The fourth scenario postulates increased coal use for both electricity generation and synthetic fuels production. In California, coal use is assumed only for electricity generation and for industrial production; scenarios 1 and 2 are therefore identical as are scenarios 3 and 4, except for minor differences in natural gas supply in the latter two scenarios.

Statewide economic impacts and pollutant residuals were calculated for the Recent Trends scenario (scenario 1). Economic impacts include estimates of direct capital and manpower requirements for construction and operation of all facilities required for energy supply, and estimates of consequent changes in value added and indirect manpower requirements. Instate capital outlays and manpower requirements generally decrease over time, although these show an irregular behavior since many of the energy facilities are built in large discrete units. The construction of coal-related facilities to generate power from the single coal-fired power plant assumed in this scenario requires roughly $400 million (1974 constant dollars), a small outlay compared to a total capital requirement of $11 billion for all the energy facilities. The manpower requirements are also a relatively small fraction of the total. The direct and indirect value added both decrease, although irregularly, through to 2000. However, over the twenty-five year period, 1975-2000, the direct economic impacts constitute an increasing fraction of the total economic impacts. This indicates a shift away from capital-intensive to more labor-intensive energy facilities.

Of the statewide pollutant residuals, air pollutants from coal-related facilities are of significance to this study. In California these coal facilities include coal trains and a coal power plant. Quantities of the three major pollutants emitted by these facilities--particulates, oxides of nitrogen, and sulfur oxides--were estimated. These amount to less than ten percent of the statewide emissions of these pollutants by energy and transportation facilities during the 1975-2000 period.

To permit detailed analysis of impacts on water resources, air quality and health and safety aspects, site regions were selected to accommodate the power plants specified in the four NCUA scenarios for California. The area of the region was determined by the type of impacts analyzed. For example, since water resources impacts were analyzed at the aggregated sub-area (ASA) level, locations of all power plants were specified by ASA regions. Each ASA region is an aggregation of counties. On the other hand, for air quality and health impacts analysis the coal-fired power plant sites were designated at a more specific (sub-county) level.

The siting analysis for this assessment utilized an exclusionary siting methodology in which areas of California were eliminated from consideration as potential power plant sites on the basis of selected criteria. The exclusionary criteria were:

(1) air quality maintenance areas (AQMA's)

(2) zone III earthquake intensity areas

(3) areas with significant biological resources

(4) urbanized areas as defined in the 1970 census and projected urbanized areas of 1990

(5) prime agricultural lands and agricultural preserves

(6) coastal areas

(7) special state and federal lands

These exclusionary criteria eliminated substantial portions of California; secondary criteria were then applied to evaluate the remaining areas. These secondary criteria are of two types. The first, called avoidance criteria, took into account those features of alternatives which would not necessarily prevent power plant construction but which nevertheless represent some additional constraint or added costs. For example, flood-prone areas were avoided although power plants can be designed to withstand floods. Second, certain opportunities exist which make some areas more desirable than others for power plant sites, such as proximity to rail transportation or transmission lines. These are referred to as opportunity criteria. The majority of the exclusionary criteria were mapped on transparent overlays, which resulted in a map of permissible areas for coal power plant locations within which site areas could be selected by application of secondary criteria.

Based on these criteria an 800 MWe coal power plant stipulated in all four 1985 California scenarios was sited in ASA 1802 in Tehama County (North Central California). For the year 2000 an additional 800 MWe unit was added at the same site along with six other 800 MWe units, two at each of three sites in southeastern California. For the water resource impact analysis all water-consuming power plants were sited by ASA regions.

Freshwater requirements for power plants in 1975 were small (32,000 acre-ft), since most of the power plants were located near the coast and used sea water for cooling. By 2000, however, the freshwater requirements for the new, inland power plants specified in the California scenarios will be as high as 400,000 acre-ft per year. Comparisons of projected water demands with developed supplies have indicated that freshwater shortages will occur in many areas by 2000. The 400,000 acre-ft per year demand for power plants will then pose an additional burden on developed supplies.

By the year 2000 statewide water requirements for scenarios 1 and 2, the Recent Trends and Accelerated Synfuels scenarios, are 20 percent larger than requirements for scenarios 3 and 4, the High Coal Electric and High Coal Electric and Accelerated Synfuels scenarios. This difference is due to the expanded use of less efficient nuclear capacity in scenarios 1 and 2, and the out-of-state siting of some of the coal capacity in scenarios 3 and 4.

The inland siting of most of these nuclear power plants in central California (ASA 1803), a water-deficient region with groundwater overdraft, poses a serious freshwater availability problem. Supplies of cooling water will therefore have to come from agricultural waste waters or from water transfers from other users. Similarly, water for coal power plants in the southwestern desert region (ASA 1806) will have to come from uncertain groundwater sources, from agricultural waste waters, or the transfer of water from other users.

Air quality impacts due to coal combustion in the 800 MWe coal power plant in North Central California were investigated. Coal used in the power plant was assumed to have a heat content of 12,000 Btu per pound, a sulfur content of one percent, and an ash content of ten percent. The power plant was assumed to have scrubbers and precipitators as pollution control equipment. The pollutant concentrations were estimated using a short-range (50-60 Km) Gaussian Plume Model with first-order chemistry and a flat surface with choice of surface cover types for deposition. Due to data limitations, climatological data for Sacramento, California was assumed to approximate the weather conditions at the Southern Tehama County site.

The model indicates that the levels of major pollutants, particulates (TSP), SO_2, and NO_X, produced solely by the power plant are lower than the annual average federal or state Ambient Air Quality Standards for all three pollutants. These pollutants also fall below the short term 1-hour, 3-hour, and 24-hour standards, with the only exception being the 24-hour TSP standard. The plant emissions exceed this standard by 50 percent. Moreover, TSP and NO_X concentrations have been fairly high in the surrounding communities, with TSP levels exceeding the primary TSP standard by a factor of 2. Power plant emissions will add to these ambient background pollutants, thus further aggravating the TSP pollutant problem.

Health and safety impacts resulting from this air pollution and from the mining, processing and transportation of coal were estimated from data and information contained in the Brookhaven National Laboratory's "Handbook for the Quantitation of Health Effects." Sulfates and TSP are the only two major pollutants for which we have adequate quantitative data on health impacts. For this preliminary assessment we estimated the effects of sulfates on mortality rates. It was assumed that the power plant will be sited so that the population within ten kilometers of the plant will be small, and hence the effects of the high concentrations of TSP close to the source can be neglected.

The areal distribution of annual average sulfate concentration levels at ground level was estimated by using the air pollution model. This was superimposed on a map of the region to estimate the population distribution exposed to each sulfate concentration level. The product (mean sulfate concentration X population at risk) coupled with a linear dose response relationship provided an estimate of the mortality rate associated with sulfate pollutants. For the 800 MWe coal-fired power plant sited in Tehama County, the rate was estimated as 0.3 fatalities per year. It should be emphasized that this figure has large uncertainties associated with it, and at this stage should not be used for drawing quantitative conclusions.

The mining health effects and accidents were assumed to be proportional to the trip-miles incurred. The expected annual fatalities for mining range from 1 to 4.8, while for transportation the estimate is three fatalities per year. Most of the transportation fatalities result from accidents between trains and motor vehicles occurring at rail-highway crossings.

PLANNED ACTIVITIES FOR 1978

Future work will address several issues that appear to dominate the use of coal in California. Tasks associated with each issue have been selected to assist in a partial resolution of the issues by providing essential information and comparative analyses of the alternatives. The following research areas are planned for next year:

1. The siting decision-making process in California
2. Water supply problems for coal-fired power plants in California
3. Ambient air quality constraints and source trade-offs for coal use in California

4. Impacts of alternative technologies for coal use in California

5. Coal resource availability problems for California

REFERENCE

1. Energy Analysis Program Staff, Impacts of Future Coal Use In California (Interim Report), Lawrence Berkeley Laboratory Report, UCID-3941, July 1977.

EFFECTS OF THE DROUGHT ON CALIFORNIA ELECTRICITY SUPPLY AND DEMAND

J. Sathaye, R. Sextro, C. Blumstein, H. Ruderman,
R. Ritschard, J. McMahon, E. Kahn, D. Kirshner,
R. Brandi, R. Watkins, P. Chan, J. Kay, K. Taso,
L. Kelleher, B. Greene, B. Krieg, I. Lasater,
L. Vincent, and P. Benenson

INTRODUCTION

The extended drought in California has been the focus of public and private concern and attention for the past two years. By the end of the rainfall and runoff period in the spring of 1977, the statewide runoff was about 20 percent of normal, and reservoir storage levels were 50 percent of normal. With hydroelectric generation consequently reduced to half its normal output (1977) and with further reductions to follow, what alternative sources of energy and capacity would take up the slack should the drought continue into 1978?

This study, initiated in the spring of 1977, examined the question in some detail, including assessments of the attendant impacts on reliability, prices and environmental consequences. Also included was an analysis of remedial measures that could be implemented to alleviate the impacts, or to reduce demand for energy and peak capacity through conservation and load management strategies. An additional purpose of the study was to further develop assessment methodologies which bear on these issues, such as quantifying bulk power system reliability using the loss-of-load-probability (LOLP) method, and measuring the relative impact of differing resource mixes on electricity prices.

The project proceeded in two phases. The first, ending in June 1977, assessed the situation for the summer of 1977,[1] and the second, ending in January 1978,[2] analyzed the prospective situation for 1978. Some of the main results of the study are summarized below. Results from both phases of the project have been combined for brevity.

Electricity Demand

In response to California Energy Resources Conservation and Development Commission (CERCDC) requests under their contingency planning authority, the four major electric utilities in California submitted a set of month-by-month resource plans for 1977 and 1978, showing the expected peak power and energy loads for each service area. In order to supplement the 1977 demand figures given by the Pacific Gas & Electric Company (PG&E), we estimated the effects of decreased water availability upon electricity requirements in the agricultural sector, and the effects of water conservation programs on overall energy requirements for water use in the residential and industrial sectors.

The increased reliance upon groundwater as surface water supplies diminish during the drought will have a major effect on electricity requirements in this sector. Although accounting for only four percent of the total electrical energy load, agricultural electricity use increased 20 percent between 1975 and 1976, the first year of the drought. Electricity sales by sector are summarized in Table 1. Our estimate for total electrical energy demand for agricultural pumping for PG&E in 1977 was 5.9 TWh, up nearly 20 percent over 1976. This was based upon: 1) expected ground- and surface-water deliveries to agriculture, 2) energy requirements by irrigation methods, 3) water requirements by crop type, and 4) estimates of planted acreages for the major crops in the Central Valley.

In the residential and industrial sectors, reduced water use will result in lower energy usage in these areas. In the residential sector, the largest energy use related to water is water heating. Overall, full implementation of water conservation programs could lead to a 35 percent reduction in water consumption and a concomitant drop in electrical energy use of close to 40 percent. At the expected water conservation savings rate, the effect in the PG&E service area was estimated to be about 900 GWh, which nearly offsets the increase in agricultural pumping.

The single largest energy impact of reduced water supplies is the surface water pumping requirements for the State Water Project (SWP) and the federal Central Valley Project (CVP). In a normal year, the CVP uses about 1600 GWh for pumping water to agricultural customers in the San Joaquin Valley. The SWP would have used nealy 5300 GWh in 1977. Due to reduced water deliveries, these figures are estimated to be 900 GWh and about 1700 GWh, respectively, for an overall savings of nearly 4500 GWh, or three percent of the total statewide demand.

As noted in Table 1, 1977 sales of electricity through September have increased only slightly over statewide sales for 1976 and have actually decreased for the PG&E service

Table 1. California Electricity Sales[a] (TWh)

Billing Category	1975 State	1975 PG&E	1976 State	1976 PG&E	10-76 to 9-77 State	10-76 to 9-77 PG&E
Residential	43.53	20.09	45.06	20.77	45.88	21.11
Commercial	40.94	17.63	43.13	18.39	43.39	18.15
Industrial	39.34	15.24	41.30	16.47	42.64	16.96
Agricultural	5.47	4.11	6.58	4.98	7.05	5.35
Other	16.08	5.65	16.28	5.73	14.60	4.59
TOTAL	145.35	62.72	152.35	66.33	153.57	66.15

[a] Data from CERCDC, Form EU-06, Electric Utility Sales Report.

area. In reviewing the 1977 demand situation prior to our assessment of potential 1978 demand for electricity, there appear to be several factors having a greater effect than previously thought. Agricultural energy sales did not increase as much as predicted, apparently due to water conservation practices adopted by farmers, such as drip and sprinkler irrigation techniques, which save energy as well as use water more efficiently. Residential water conservation, at least in northern California, substantially exceeded the expected savings. As noted above, this will also lead to reduced energy usage. In addition, several other factors appear to have had an effect as well: 1) voltage reduction programs instituted by the utilities, 2) substantial price increases for electricity over previous years, 3) generally lower temperatures prevailed during weekdays in the summer, and 4) a heightened conservation consciousness induced in part by the drought and public information campaigns.

Electricity Supply

The principal effect of the drought, as illustrated by the data presented in Table 2, is reduced hydroelectric generation, with PG&E most seriously affected. In order to meet its summer loads, PG&E will have to rely upon purchased energy and capacity from the southern California utilities, as well as out-of-state sources.

The shortfall in hydroelectric supplies will primarily be made up by oil-fired generation; nearly 70 percent of the total statewide capacity is oil- or gas-fired. In the past few years, the amount of natural gas available as boiler fuel has declined, especially for the utilities in southern California.

A review of the 1977 supply situation in California reveals few major difficulties in meeting peak loads and energy demands. A number of factors contributed to this, including the generally lower summer temperatures which, combined with conservation, reduced peak demand.

For 1978, in the event of a continuing drought, the supply situation does not change drastically from 1977. As shown in Table 2, hydroelectric generation continues to decline, although not as dramatically as in 1977. The thermal generation picture changes somewhat for 1978 as approximately 640 MWe of the additional new capacity will be available by August. In addition, PG&E has 1060 MWe at the Diablo Canyon (nuclear) power plant that is presently in the licensing process. However, it is uncertain whether this plant would be available for the peak load period during the summer. In our assessment of the capacity available and the reliability and reserve margins for next summer, we have analyzed two cases, with and without Diablo Canyon on-line.

Reliability of both the PG&E supply system and the coordinated electricity supply system in California was estimated for the various supply options, using the loss-of-load-probability method. Our calculations indicate that for 1978 peak loads there is sufficient capacity to reliably meet the statewide coincident peak loads forecast by the utilities. For the PG&E system we have estimated the amount of additional capacity support required to meet the system loads reliably, with and without the inclusion of Diablo Canyon. The total support necessary depends upon the estimate of the peak load for PG&E. Using the utility predicted load, PG&E would require 1900 MWe of outside support without Diablo Canyon and about 1300 MWe of similar support if Diablo were available for load in August. Support of this magnitude is available from other utility companies, as indicated in their supply forecasts; however, it does require significant loading of the substantial transmission line capacity linking PG&E with the Pacific Northwest and with the southern California utilities.

Impacts

The increased use of oil as fuel for generation of electricity has increased emissions of air pollutants, most notably NO_x and SO_x. Since almost all the thermal generating facilities operated by Southern California Edison and the Los Angeles Department of Water and Power are in the South Coast Air Basin, a basin already

Table 2. Hydroelectric supply in California (GWh) .

Service Area	1975[a,b]	Percent of Total Supply to Service Area	1976[a]	Percent of Total Supply to Service Area	1977[c]	Percent of Total Supply to Service Area	1978[d]	Percent of Total Supply to Service Area
In-State Supply								
PG&E	30521	43	17812	24	9667	13	8733	11
SCE	6300	11	4075	7	4603	7	3527	5
LADWP	2319	11	2012	9	1156	6	830	4
SDG&E	52	0.6	30	0.3	45	0.4	7	0.06
Total Hydroelectric Supply[e]	39191	25	23928	14	15471	9	13097	7
Total Electrical Energy Supply for State[e]	157336		166265		171168		177911	

[a] Source: Quarterly Fuel and Energy Summary, Volume 2, Number 4, 4th Quarter, 1976, CERCDC.
[b] 1975 has slightly higher than normal runoff levels.
[c] Source: Combined Response of California Electric Utilities, Docket 77-EA-1, May 11, 1977, CERCDC.
[d] Source: Combined Response of California Electric Utilities, Docket 77-EA-1, August 5, 1977, CERCDC.
[e] These totals exclude those utilities not included in the loads and resources listed in Reference c above. The largest of those omitted are the Imperial Irrigation District and Pacific Power and Light. In 1975, 1589 GWh of hydroelectric energy were generated by these utilities, while for 1976, 1024 GWh were generated by these hydroelectric resources.

burdened with air pollution, transfers of energy to PG&E from these utilities will add to this pollution. The possibility of gas transfers from PG&E, which has been the only major utility in California with sizable quantities of P-5 gas (for use in electric generation plants), to these southern California utilities was investigated as a method of offsetting the incremental emissions due to energy transfers to PG&E. Our calculations indicate that transfer to these utilities of about 15 percent of the natural gas available to PG&E during the summer months would reduce the incremental NO_x emissions by about a factor of three, and the incremental SO_x emissions would be reduced to nearly zero in the South Coast Air Basin. As it turned out southern California gas suppliers had large quantities of excess gas available during the summer of 1977; hence no gas transfers from PG&E to these electric utilities took place. However, overall NO_x emissions increased nearly 70 percent in 1977 over the 1976 levels.

For 1978 these NO_x emissions are likely to increase another 10 percent due to shortages in hydroelectricity generation, and energy transfer to PG&E would add as much as an additional 10 percent to the power plant SO_x and NO_x emissions during the peak summer months. However, overall SO_x emissions in this basin are expected to decrease as the sulfur content of the fuel oil drops from a 1977 average of .32 percent to .22 percent as a result of mandated California Air Resources Board regulations.

The increased reliance on oil-fired generation has had an impact on electricity prices as well. In 1977 average prices in the PG&E system jumped nearly 30 percent, almost all of which was due to fuel cost adjustments. We analyzed the price effects in the PG&E system of the supply and demand scenarios for 1978, including the differences due to a continued drought vs. return to a normal hydro year. It turns out that this latter difference is the most important, with the average price about 20 percent higher under the assumption that 1978 is a drought year rather than a normal year for hydroelectric generation. The differences between having Diablo Canyon on-line and relying on oil-fired generation are less than three percent for either a dry or wet year. Similarly, the differences among the demand scenarios established for the PG&E system are also quite small, with prices lower by about three percent for the highest demand case because the fixed charges and returns on invested capital are distributed over a broader sales base, so that the unit costs decrease.

Conservation and Remedial Measures

The initial phase of this study was completed shortly before the summer peak loads; hence we focused primarily on operational energy conservation measures, as opposed to institutional or hardware changes that would have effects in the longer term. The major short lead-time measures include changes in building operational procedures, such as reduction in lighting, air conditioning thermostat set-point changes, deferral of some residential, commercial or industrial loads away from the summertime peak hours (noon to six at night). Such conservation or load management measures would have positive benefits, especially in a drought year. The capacity margins would be increased as peak loads are reduced. Additionally, the amount of oil burned would decrease, which would benefit air quality in areas such as the South Coast Air Basin. Water conservation, as noted earlier, will have energy conservation benefits also. Agriculture, which accounts for 85 percent of the water use in California, can employ conservation strategies that would help stretch diminished water supplies and reduce pumping energy requirements as well.

Energy conservation did have an effect in 1977, as both peak loads and energy demand were below 1976 levels for PG&E. Additional emphasis on conservation in 1978 will also be important, and we investigated three categories of actions that could be taken: conservation programs that emphasize public awareness, accelerated implementation of time-of-use rates as load management devices, and incentive programs to encourage participation in voluntary load shedding programs during time of peak load.

REFERENCES

1. J. A. Sathaye, et al., Effects of the Drought on California Electricity Supply and Demand, Lawrence Berkeley Laboratory Report, LBL-6356, June 1977.
2. J. A. Sathaye, et al., Potential Electricity Impacts of a 1978 California Drought, Lawrence Berkeley Laboratory Report, LBL-6871, January 1978.

WATER REQUIREMENTS FOR FUTURE ENERGY PRODUCTION IN CALIFORNIA

J. Sathaye and R. L. Ritschard

INTRODUCTION

The Federal Water Resources Council (WRC) conducted a 1975 National Water Assessment to evaluate the nation's water resources. Part of this assessment was designed to estimate the impact of future national energy development on water resources. This energy development includes various types of electric power plants, production of synthetic fuels, coal and uranium mining, oil and gas extraction, and other conversion processes. The Energy Analysis Program at Lawrence Berkeley Laboratory conducted this analysis for the state of California.

The objective of this study was to determine water requirements of energy technologies and their implications, with emphasis on emerging technologies, for aggregated water subareas (ASA's) in California (Fig. 1). The first phase of this study provides projections and demands for energy and water resources as perceived by regional and state groups responsible for or involved in energy planning.[1] The second phase of the study was designed to calculate the water requirements for the level of energy development specified by an Energy Research and Development Administration (ERDA) scenario for the year 2000 and by utility projections as reported by the Federal Power Commission (FPC) for 1985. The implications of these water requirements on competing water users are explored briefly.

SCENARIOS

California electricity demand projections by each ASA for 1985 were supplied by Oak Ridge National Laboratory (ORNL). These figures are based on a set of energy supply and demand calculations specified by ERDA. The total electricity generation for California amounted to 0.718×10^{15} Btu's, assuming transmission losses of 10 percent. The utilities' projections as reported by the FPC were used to estimate the specific types of electrical capacity needed to meet this demand. Appropriate load factors used in the estimation were derived from utility data or the energy demand projections.

California electricity demand projections for 2000 were arrived at by disaggregating the Pacific scenario for 2000 developed by Brookhaven National Laboratory (BNL). This scenario is based on a set of energy demand and supply figures provided by ERDA. Figures for energy demand by each ASA in the Pacific region were supplied by ORNL. Assuming 10 percent transmission losses, the total electricity generation for California was estimated at 1.391×10^{15} Btu. Projections of individual types of electrical capacity for 2000 to meet this energy demand were estimated by a process of successive elimination. The Pacific fuel mix scenario provided by BNL served as a guideline constraint on the capacities of individual types of power plants.

RESULTS

Cooling water for electricity generation will form the major portion of water requirements for future energy development in California. Since almost all the power plants in 1975 were located along the coast, freshwater requirements for cooling amount to only 32,000 acre-feet/year. Coastal siting restrictions and development of geothermal resources located inland will increase these water requirements to 1.4 million acre-feet/year by 2000. The diminishing potential for future water development along with overcommited water resources could pose a serious constraint to siting electrical capacity of this magnitude in California by the year 2000.

Fig. 1. Aggregated subareas of California. (XBL 776-8970B)

Coastal siting restrictions may require new power plants to be sited inland. As a result very little new capacity is added in coastal water subareas 1801, 1804, and 1805. Capacity additions in subarea 1806, which has a costal zone, will occur inland in the desert region, resulting in 230,000 acre-feet/year of additional water requirements. Currently almost 85 percent of the water to this area is imported from the Colorado River and from northern California. Therefore the cooling water requirement may have an adverse impact on competitive water users. Utilities may resort to deep groundwater supplies or to dry or wet/dry towers to reduce water requirements. Water requirements for fossil and nuclear fueled plants in subareas 1802, 1803 and 1804 are not as high. Water supplies, although limited, are more easily available to these areas, as compared with subarea 1806. Additional water supplies would primarily come from conjunctive use of surface and groundwater basins and agricultural waste waters. In some instances it may also prove more economical for the farmer to transfer water from agricultural uses to the utilities.

Geothermal capacity by the year 2000 accounts for nearly 925,000 area-feet/year of the total 1.4 million acre-feet/yr water requirement. Extensive development of geothermal resources (~17,600 MWe) coupled with high cooling water requirements lead to this estimate.[2] Water supplies appear adequate in the Imperial Valley (subarea 1806) to meet the requirements.[4] These supplies could come from two rivers, the New and Alamo, which are fed by agricultural waste waters. In the Mono Lake area (subarea 1807) and Surprise Valley (subarea 1802) substantial development of surface water supplies has occurred in the past. Future water supplies would depend primarily on development of groundwater basins. However, data on groundwater basins in these regions are superficial; safe yields from the groundwater basins are therefore not known.[3]

Table 1 summarizes the freshwater requirements for power plant cooling by aggregated subarea within California for 1975, 1985 and 2000. The enormous increase in cooling water requirement between 1975 and 2000 is accounted for by three major factors: (1) inland siting of most of the new power plants; (2) higher proportion of water consumptive electricity capacity by 2000; and (3) high fraction of geothermal (hydrothermal) electrical capacity in 2000.

REFERENCES

1. J. Sathaye and R. Ritschard, Survey of Water Requirements for Future Energy Development in California and Nevada, Lawrence Berkeley Laboratory Report, LBL-6872, April 1977.

2. U. S. Geological Survey, Assessment of Geothermal Resources of the United States--1975, Circular 726, 1975.

3. California Department of Water Resources, California's Groundwater, Bulletin No. 118, September 1975.

4. M. Goldsmith, Engineering Aspects of Geothermal Development in the Imperial Valley, California Institute of Technology, EQL Memorandum No. 20, December 1976.

Table 1. Freshwater requirements (acre-feet).

Aggregated Subarea	Power Plant Type	1975	1985	2000
1801	Nuclear	0	0	0
	Oil	0	0	0
1802	Nuclear	9613	15837	35500
	Coal	0	10686	32058
	Geothermal	0	0	111457
1803	Nuclear	0	0	132275
	Oil	*	1350	0
1804	Oil	6624	8700	5625
	Combined Cycle	0	5630	10479
1805	Nuclear	0	0	0
	Oil	0	0	0
1806	Nuclear	0	16981	178428
	Oil	15822	11302	1357
	Coal	0	0	42343
	Combined Cycle	0	8915	27558
	Solar	0	630	18774
	Geothermal	0	21000	254415
1807	Geothermal	0	0	557340
TOTAL		32059	101031	1408109

*Less than one acre-foot.

A STUDY OF NUCLEAR MATERIAL ACCOUNTING

H. Ruderman

INTRODUCTION

The Nuclear Regulatory Commission (NRC) has sponsored a study to address in a systematic fashion several major issues concerning the value of material accounting for safeguards purposes. The tasks of concern are as follows:

(1) To examine the implications on material accounting of deliberate diversion of nuclear material;

(2) To determine the validity of the MUF (Material Unaccounted For) concept to establish assurance concerning the possible diversion of SNM (Special Nuclear Material);

(3) To provide an economic analysis to permit a cost comparison of varying the inventory frequency in a periodic inventory system.

The first phase study began in July 1976. Results of this phase were published by NRC in NUREG-0290,[1] June 1977.

A function outline of the study is shown in Fig. 1. LBL is the prime contractor for the project. Science Applications, Inc., provided

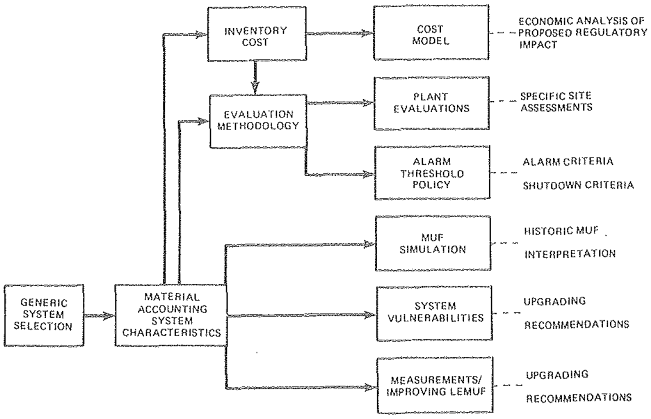

Fig. 1. Nuclear material accounting study functional outline. (XBL 782-7193)

the MUF simulation model, the analysis of accounting systems vulnerability, and evaluation of methods for improving measurements of MUF. The inventory costs model was developed by Professor J. Winsen of U.C. Berkeley. The core of the study was the evaluation methodology, which is based upon the theory of games. The game theoretic model was developed by Dr. Melvin Dresher and Mr. Sidney Moglewer. The model was set up at LBL and used to analyze three generic plant systems. The formulation of the inventory cost and game theoretic models and the analysis of some of the results are presented in this report.

INVENTORY COST MODEL

This portion of the study examined the financial effects of changing the frequency at which an inventory of SNM is taken at a plant. Increasing inventory frequency would decrease the limit of error on MUF (LEMUF) but would entail additional costs. The model provides the framework for calculating the effect of such a change on future cash flow. The model includes the direct labor and materials costs for performing the cleanout inventory, as well as the costs due to loss of production while taking inventory. The latter costs depend upon how close to capacity the plant is operating. The model has been applied to the three generic plants described below.

THE STATISTICAL HYPOTHESIS TESTING APPROACH

The materials accounting system at a plant keeps track of inputs and outputs of SNM by taking inventory at regular intervals. If there were no measurement errors, process gains or losses, or diversion, the book inventory would equal the physical inventory. Due to measurement errors, biases, recording errors, and diversion, the two inventories may differ. This difference, called MUF, may have both random and deterministic components.

NRC presently uses a statistical hypothesis testing approach to analyze MUF data.[2] MUF is considered a random variable with a known standard deviation determined by measurement errors. A null-hypothesis that the measured MUF is a sample drawn from a normal distribution with zero mean (i.e., no diversion or process errors) and known variance is set up. The null-hypothesis is rejected if MUF exceeds a preset level called the alarm threshold. In this case the plant may be shut down and a cleanout inventory taken. The plant will normally remain shut down until the cause of the excessive MUF is determined.

The alarm threshold is chosen by balancing the probability of false alarms against the probability of undetected losses. If the alarm threshold is set higher, there will be fewer false alarms, but small losses will be less likely to be detected. Currently the alarm threshold is set at twice the standard deviation of the measuring error distribution (LEMUF). This would lead to a false alarm rate of approximately 5 percent under conditions of no diversion.

THE GAME THEORETIC APPROACH

As an alternative to statistical hypothesis testing for making decisions about MUF, the game theoretic approach models the situation as a game between two players, a diverter and a defender. Under the assumption that the objectives of the two players are in conflict and that there is no possibility of collusion, a continuous two-person zero-sum game has been set up. The game incorporates the objectives or goals of both players, the strategies available to them, and any random or chance events.

The game as formulated in the first phase consists of three moves:

(1) The diverter removes an amount x of SNM.

(2) An inventory is taken in which the MUF is measured to be u.

(3) Based on whether u is less than or greater than the alarm threshold, a, the defender estimates that an amount y_1 and y_2 has been diverted and takes appropriate action based on these values.

The alarm threshold is known to both players, whereas x is known only by the diverter, and y_1 and y_2 are known only by the defender. The diverter has one strategic variable, the amount diverted, in the range $0 \leq x \leq k$, where k is the amount of material at the plant that is vulnerable to diversion. Similarly, the defender has two strategic variables in the range $0 \leq y_1, y_2 \leq k$.

Move 2 is a chance move because it involves measuring errors. We assume that u is normally distributed with mean x and known variance σ. This means that the probability that $u < a$ is given by

$$F(a,x) = \int_{-\infty}^{a} \frac{1}{\sqrt{2\pi}\sigma} \exp\left[-(u-x)^2/2\sigma^2\right] du$$

The objective of the diverter is to divert sufficient material to be a credible threat. The defender, who may be the plant management, or NRC, or both, tries to minimize his penalties. The payoff function is formulated in terms of penalties to the defender. The payoff function used is

$$M(x,y) = x + \beta + cy - b \min(y,x) + e|y-x|$$

where:

x	is the amount diverted,
y	is the defender's estimate of x,
β	is the (fixed) cleanout inventory cost,
cy	is the (variable) recovery search cost,
$b \min(y,x)$	is the value to the defender of recovering the material diverted, and
$e\|y-x\|$	is the penalty to the defender for wrongly estimating the amount diverted.

The payoff may be decomposed into two parts depending on the value of u.

$$M[x,y(u),u(x)] = \begin{cases} M_1(x,y_1) & \text{if } u < a \\ M_2(x,y_2) & \text{if } u \geqslant a \end{cases}$$

The expected payoff of the game is given by

$$M(x,y) = M_1(x,y_1)\, F(a,x) + M_2(x,y_2)\, G(a,x)$$

where $F(a,x)$ is the probability that $u < a$, and $G(a,x)$ is the probability that $u \geqslant a$. The complete payoff function is

$$\begin{aligned} M(x,y_1,y_2) = {} & [x + c_1 y_1 - b_1 \min(y_1,x) \\ & + e_1 |y_1 - x|]\, F(a,x) \\ & + [x + \beta + c_2 y_2 - b_2 \min(y_2,x) \\ & + e_2 |y_2 - x|]\, G(a,x) \end{aligned}$$

Note that M is piecewise continuous in x; there are changes in slope at $x = y_1$ and $x = y_2$.

Mathematically, the objective of the diverter is to maximize M, whereas the defender tries to minimize M. Solutions to the game for the defender are the points y_1^*, y_2^* for which

$$v(x,y_1^*,y_2^*) = \min_{y_1,y_2} \max_{x} M(x,y_1,y_2) \quad .$$

In general, the diverter has a mixed strategy, i.e., there are two or three values of x at which M is optimal. The diverter selects among these amounts with fixed probabilities which depend on the plant parameters. The defender, on the other hand, has a pure strategy. There is one set of values with $y_1^* < y_2^*$, that minimizes the payoff.

ANALYSIS OF GENERIC PLANTS

Three generic plants were selected for evaluation: 1) a small mixed oxide fabrication plant, 2) a large mixed oxide plant and 3) a large reprocessing plant. Using results of the inventory cost model, the value of β for each of the plants was determined. The amount of material vulnerable to diversion k was taken to be 3.0 kg, and σ, the standard deviation of the measurement error distribution, was estimated for each plant. The other plant parameters (c_1,c_2,b_1,b_2,e_1,e_2) were chosen using rule-of-thumb estimates. A sensitivity analysis of the results to these parameters is in progress.

Some results for plant #1, the small mixed oxide facility, are shown in Fig. 2. The value of the payoff and the defender's estimates of the amount diverted are plotted against the alarm threshold. All values are in units of σ (0.3 kg of plutonium). The penalty to the defender is large when the alarm threshold is much higher or lower than its optimal value of 1.91. For this value of a, even if $u < a$, the defender should estimate that there has been some material diverted. At higher alarm thresholds, he should estimate that even more has been diverted. This is in contrast to the current practice where if MUF is below the alarm threshold, it is assumed that no diversion has occurred.

An analysis of the diverter's optimal strategy at $a = 1.91$ shows that he should divert 0, 1.1 or 10 σ of material with probability 3/8, 1/2, 1/8, respectively. Only infrequently would he try to divert the full amount available. Usually he would divert none or an amount less than the alarm threshold. If the diverter follows his optimal strategy, then the distribution of MUF is trimodal. The probability that $u < a = 2\,\sigma$ is 0.77 compared with a probability of almost 0.98 if there were no diverter operating.

As a result of this study, it appears that the present procedure for periodic inventories to determine MUF can be an effective procedure in most cases for estimating diversion and taking necessary follow-on action. What needs improvement is the current practice of reliance on purely statistical hypothesis testing to make judgments about diversion. The game theoretic approach permits an alternative hypothesis to be tested in which an optimal diverter is at work. The analysis of generic plants shows that this approach can determine the optimal setting of the alarm threshold and can also

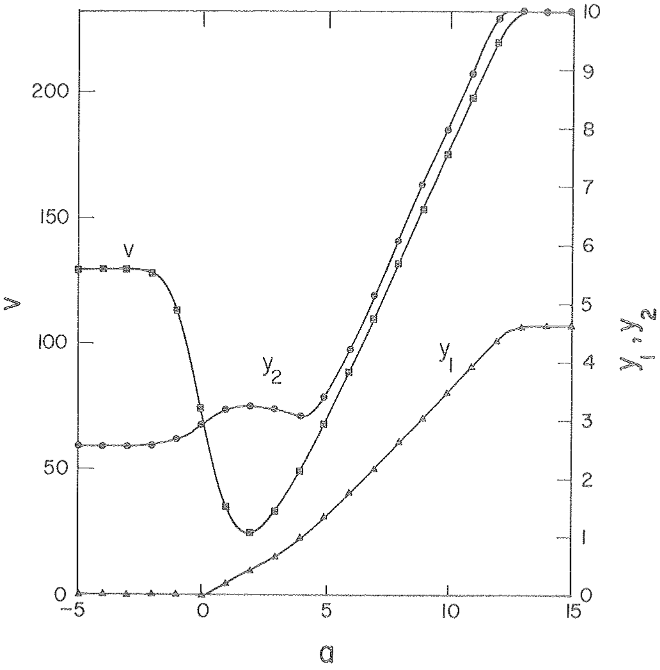

Fig. 2. Optimal payoff and diverter strategies as a function of alarm threshold for Plant 1. (XBL 781-2)

provide an estimate of the amount diverted even if the alarm threshold is not exceeded. If the optimal alarm threshold is low, as is the case with the large reprocessing plant, there will be excessive downtime for cleanout and recovery. Thus, safeguards requirements may impose an upper bound on plant size.

EXTENSIONS OF THE MODEL

In phase 2 of this study, currently in progress, a thorough sensitivity analysis of the results for the three plants is being undertaken. The model is being extended to include the alarm threshold as a strategic variable for the defender. In the variable alarm threshold model, the value a is selected by the defender for each inventory period. The diverter does know its value. This phase will be completed in January 1978.

A third phase will start in 1978. The study will examine the cooperative game aspects of safeguards. It is expected that this analysis will lead to a multi-person non-zero-sum game when the possibility of collusion between players is incorporated.

REFERENCES

1. Lawrence Berkeley Laboratory, A Study of Nuclear Material Accounting, Nuclear Regulatory Commission, NUREG-0290, Volume 1, 1977.
2. J. L. Jaech, Statistical Methods in Nuclear Material Control, U.S. Atomic Energy Commission, TID-26298, December 1973.

THE LAKE COUNTY ECONOMY: POTENTIAL SOCIOECONOMIC IMPACTS OF GEOTHERMAL DEVELOPMENT*

L. Vollintine and J. A. Sathaye

While much of the nation's attention has been focused recently on the environmental problems of large-scale domestic energy production (coal strip mining, nuclear power plants, offshore oil production, etc.), northern California is currently experiencing its own energy development project. This is the Geysers geothermal energy development area in Lake, Sonoma, Napa and Mendocino Counties (Fig. 1). In response to concerns regarding the potential impacts of this development, ERDA's (now DOE), Division of Biomedical and Environmental Research, funded a modest effort to provide an Integrated Assessment of the Geysers development and impact on Lake County.

One of the purposes of this assessment was to gather and refine the available basic demographic and economic data from the various agencies, departments, and business establishments in Lake County, and then, based on the data collected, project the potential socioeconomic impacts of geothermal development.

THE LAKE COUNTY ECONOMY

Lake County is a sparsely populated, rural county whose economic base is centered around recreation, retirement, and agriculture. Recently the county has been experiencing a population growth rate greater than projected by the county's general plan, with a definite shift in age distribution towards older retired people. Employment is highly seasonal (varying from 8-22%) and is composed mainly of government, trade, services, and agricultural workers. The largest single component of personal income (33%) is government transfer payments. These factors, when combined with the pleasing rural environment of Clearlake and the coast range mountains, produce a unique situation that is hostile to, and yet desirous of, geothermal development.

POTENTIAL IMPACTS

We investigated five main areas of potential socioeconomic impact from geothermal development. These areas are: employment, schools, public protection, transportation, and county finances. While the Geysers area represents the largest commercial geothermal facility in the world, and the only one in the U.S., most of the present 500 MWe of development are located just outside the county in northern Sonoma County.

Many of the present impacts on Lake County are small. Yet with active exploration proceeding into Lake County, four new power plants now under construction, and estimates by the Jet Propulsion Lab of an ultimate potential of ten times present capacity, it is felt that extensive data collection, impact projection, and land-use planning is needed to avoid disastrous consequences. The Geysers represents the only domestic, commercially-proven geothermal area capable of significant near-term expansion.

To date, we have found that geothermal development has had only limited effect on reducing the county's unemployment rate. Most geothermal workers are highly skilled and move from place to place with the jobs. Some local contractors for road and construction work have been kept busy as drilling permits are granted. There is the potential of a reverse effect on employment as unskilled, unemployed people are attracted to the county for jobs which are not available.

There appears to have been some growth in the Middletown School District in southern Lake County as geothermal workers have moved into the county. Yet other school districts in the county are also growing, probably due to factors not attributable to geothermal development. In the areas of public protection

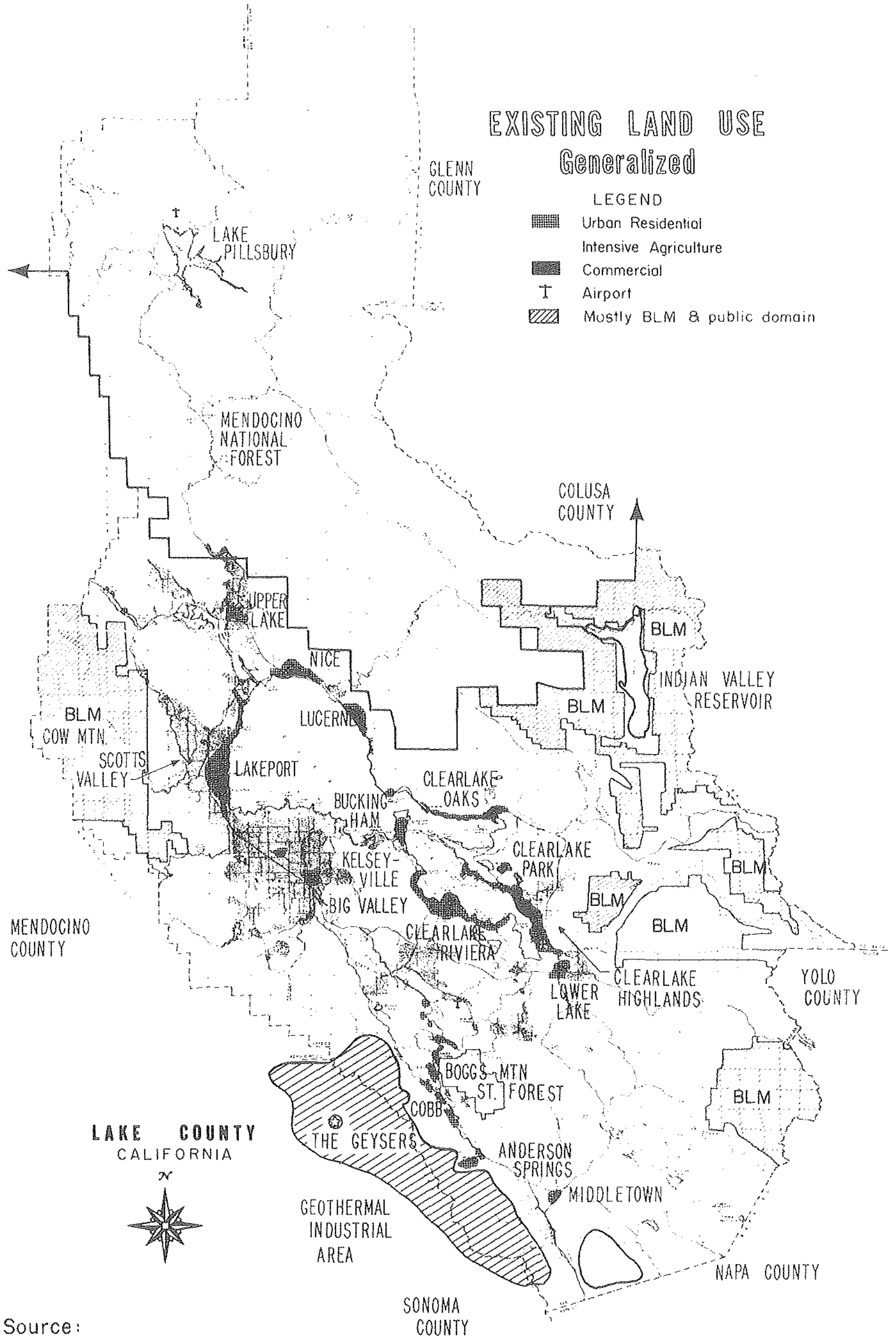

Source:
Lake County General Plan, 1967

Fig. 1. The Geysers geothermal energy development area in Lake, Sonoma, Napa and Mendocino counties. (XBL 774-911)

and transportation, impacts seem to be limited to parts of the county where the development is taking place. However, as development expands, and spreads throughout the southern county, the extent of impacts on these areas may become significant.

Perhaps the most interesting area of geothermal impact is its effect on local government financing. Complications arise due to the California law SB90 limitations on tax rates and school financing, various geothermal assessment procedures, the price of steam, costs of industry's development, and political decisions of the Board of Supervisors. Since Lake County's annual budget is small (approximately $12 million in 1976-77, compared to $86 million for Sonoma County), the potential for significant economic impacts is great. To date, geothermal development has generated significant tax revenues in Sonoma County. Lake County is just starting to experience the effects of its development. Since Lake County's total budget and assessed valuation is much less than Sonoma County's, the relative extent of the future impact would be greater in Lake County than in Sonoma County. As an example, we calculated that PG&E Unit 13 and steamfield (135 MWe) now under construction in Lake County, would pay approximately $600,000 per year in property taxes, or one-third of all local property taxes paid in the Middletown School District.

An often misunderstood factor in the Geysers economic calculations is the price that PG&E pays developers for steam delivered to the power plant. The price is determined by a complicated formula that is based largely on PG&E's average cost of fossil fuels for the preceding year, and slightly modified by their expanding nuclear output and costs. Thus, the price of steam at the Geysers increased sharply following the 1973 Oil Embargo and subsequent price increases. It should be pointed out that this pricing formula serves two important purposes in encouraging geothermal development. First, the formula prices geothermal steam approximately one-half the cost of fossil fuels, thus insuring its continued attractiveness to the utility. Secondly, the tying of the price of steam to the price of fossil fuels insures that runaway oil profits will not siphon away any exploration capital from geothermal projects.

As for the local costs of geothermal development, little analysis has been done. More data needs to be generated and analyzed before accurate estimates can be made of the impacts of geothermal development in the county. Generally speaking, the impacts include: 1) environmental degradation due to the incursion of industrialization into a rural area; 2) local and state governmental response to mitigate adverse impacts; 3) increased local political disharmony; and 4) the depletion of domestic energy resources.

To attempt to calculate the costs and answer the questions of geothermal development, Lake County has initiated a comprehensive and integrated program to gather all existing baseline data for the Geysers, to specify additional needed research, to project the extent and nature of impacts using various scenarios, and to provide access to a centralized data file for all Geysers decision-making agencies and industries. The program, called GRIPS (Geothermal Resources Impacts Projection Study), has been endorsed by all four counties in the Geysers area (Lake, Sonoma, Napa, and Mendocino). It is hoped that a successful GRIPS program will solve some of the institutional and environmental problems that have been constraining the Geysers development.

FOOTNOTE

*Condensed from Lawrence Berkeley Laboratory Report, LBL-5944, The Lake County Economy: Potential Socioeconomic Impacts of Geothermal Development, L. R. Vollintine, L. Kunin and J. Sathaye, September 1977.

A WATER CONSERVATION SCENARIO FOR THE RESIDENTIAL AND INDUSTRIAL SECTORS IN CALIFORNIA: POTENTIAL SAVINGS OF WATER AND RELATED ENERGY*

P. Benenson, R. Clear, B. Greene, Y. Howell,
B. Krieg, H. Ruderman, and L. Vincent

INTRODUCTION

The objectives of this study are to determine the impact of current and potential water conservation efforts for reducing both water consumption and the attendant energy and peak power demand; to pinpoint the water conservation strategies that are likely to have the largest impacts on energy and water demand; and to highlight some of the complementarities between water and energy use.

To accomplish these objectives, a residential and industrial water conservation scenario for California was constructed in which water consumption was disaggregated by residential end-use, industrial sector, and hydrologic study area (HSA). The sector and end-use disaggregations were used to determine the potential for energy and water savings from specific water conservation measures. The geographic disaggregation helps capture the variability across the state in energy requirements for water delivery. These energy requirements vary because, in general, the major sources of water in the state are not located near the major points of use. The hydrologic study areas are shown in Fig. 1.

The energy use associated with this water use was estimated by considering surface and groundwater delivery, distribution, heating, and waste-water treatment. For each end-use and sector, water conservation measures have been delineated, and their potential savings in terms of both water and attendant energy use have been estimated. This material was combined to estimate the total water and energy savings potential by end-use, sector, and HSA. This potential was then compared with the reported water savings to date, and finally, some conclusions and policy implications were drawn from the results. The general findings are discussed first, followed by a listing of the more important detailed results.

RESULTS

There are several important links between water and energy. In California, water is a major source of energy supply; in 1975, 25%

Fig. 1 Hydrologic study area boundaries. (XBL 776-8970A)

of total electric energy was supplied by hydroelectric power. Water is also needed for power plant cooling, and fossil fuel extraction and refining. Energy is required to extract, convey, purify, and heat water prior to use, and to treat wastewater. Thus water conservation results in savings of both water and energy. The estimates from this study indicate that approximately 1.8 million acre feet of water, 2.6 billion kWh of electricity, and 0.5 billion therms of natural gas could be saved in 1977 by implementing the water conservation measures presented in Tables 1 and 2. This constitutes 28% of the estimated residential and industrial water use (approximately 5% of statewide water use), 2% of statewide electricity consumption, and 3% of statewide natural gas consumption. The electricity savings would lead to a decreased consumption of nonrenewable fuels and to decreased pollution emissions.

The estimated savings potential is thought to be conservative because several water districts and industries have already reported far greater savings. However, the lack of data for the industrial sector prevented any further estimates. A comparison of the estimated water savings potential with the savings actually reported shows that while the estimated potential is attainable, and in some cases has been exceeded, only 1/3 of the conservation potential derived in this study has been reached overall. Moreover, the actual gap is probably even greater due to the conservative nature of our estimates.

POLICY IMPLICATIONS

The significant conservation potential can be regarded as an alternative to constructing water supply systems for protection against

Table 1. Residential water conservation by end use.

End Use	Overall Savings from Water Conservation	Derivation and Sources
Toilet	28%	Two quart plastic bottles in 5-gallon Tank (10%). Reduce number of flushes per day from 5 to 4. (20%).
Bathing	57%	Flow control restrictors (40%). Reduce showering time from 5.6 to 4.6 minutes (18%).
Laundry	14%	Existing stock: Wash full loads, check for leaks, and save and reuse cleanest rinse water (5%). Wash on shortest cycle and eliminate prewash.(10%). New machines: Buy the most water-efficient.
Dishwashing	41%	Existing stock: By machine: plug leaks and wash only full loads (5%). By hand: aerators (50%), plug leaks and shut off water when not in use (5%). Dishwasher saturation assumed to be 24% 8, p.18 .
	50%	New stock: Buy the most water-efficient.
Cooking,	5%	Reuse boiling water in soups or other drinking cooking and save unused drinking water (5%).
Bathroom sink	50%	Collect running water while waiting for water to get hot; turn off water while not in use, e.g. while lathering hands and face or brushing teeth; use cup for brushing teeth; install aerators.
Utility sink	50%	Install aerators and apply all relevant measures given for bathroom sink.
Exterior use	50%	Landscape watering: Use household grey-water. Water with soak hose or drip irrigators. Eliminate use of sprinklers. Water during low windperiods. Do not overwater plants. Plant drought-resistant varieties. Collect rainwater in barrels. Sidewalks: Sweep, don't wash. Swimming pools: Cover to reduce evaporation loss. Empty pool. Car wash: Wash and rinse with bucket, not hose.

Table 2. Water conservation measures applicable to industry.

	Food and kindred products	Paper and allied products	Petroleum and coal products	Chemicals and allied products	Lumber and wood products	Stone,clay and glass	Primary metals
Water consumption (10^6 gallons fresh water in 1970)	83852	55646	55043	26185	22013	15167	10335
Percentage of total industrial water use	27	18	18	8	7	5	3
Type of Conservation Measure							
1. Housekeeping							
Leak plugging	x	x	x		x		x
Waste reduction	x	x	x		x	x	
2, Cooling							
Dry			x			x	
Wet	x	x	x	x	x	x	x
Spray ponds							x
3. Effluent reduction for re-use							
Filter	x		x		x	x	x
Reverse osmosis							x
Flocculent						x	x
Counter flow	x				x		x
Re-use as is	x	x		x	x		x
Wetting agents							x
Closed systems			x	x	x		x
High pressure steam	x				x		x
Savings of water and energy from water conservation	5 - 7	10 - 50	24 - 48	*	*	*	*

*Five percent water and energy savings from water conservation is assumed in these industries.

water scarcity. For example, in the San Francisco HSA the estimated annual water savings potential of 410,000 acre feet exceeds the estimated deliveries from the major proposed water supply projects there. In the South Coastal HSA the estimated potential savings of 820,000 acre feet annually is more than twice as large as the current short run overdraft in the Owens Valley. Statewide, the estimated potential savings is approximately 40% of urban fresh water use in 1972.

Therefore, for optimal water supply planning, the pros and cons of both dams and water conservation should be considered. Dams regulate the water supply and provide flood control, hydroelectric power, and lakes for recreation. But they are costly, employ few people relative to other projects of comparable cost, and have many negative environmental impacts (e.g., they destroy natural habitats and accelerate eutrophication). Water conservation eases the water scarcity and has none of the environmental impacts associated with dams. Many measures can be implemented cheaply and quickly.

One of the main difficulties in relying on water conservation is the potential for sustained consumer resistance to behavioral change. The residential and industrial consumer directly perceives the inconvenience of water conservation, but not that of dam construction. In the latter case, local residents absorb most of the inconvenience and the financial cost is borne by the taxpayers. Generally, the costs of these two alternatives are not equally apparent; this hinders the process of evaluation of the alternatives, and hence of rational water supply planning.

Consumer resistance tends to focus mainly on conservation measures that require continuous attention. But large savings are possible from conservation measures that require a one-time installment of a technological device. As savings accrue from these types of measures, the likelihood of reaching full conservation potential will be easier to assess because we will have more experience with conservation.

Presently, although conservation cannot be relied upon with certainty to yield its full potential, it cannot be ignored as it often has been in the past. Although surplus capacity for water supply has large economic and social value, water supply planning based on historic water consumption patterns would result in suboptimal planning. Given the advantages and disadvantages of dam construction and water conservation, a rational water supply planning process requires reassessment of those plans for construction of additional water supply systems that do not take into account recent evidence on water conservation potential.

SUMMARY

The more detailed results upon which these general conclusions are based are summarized below:

- Overall residential water consumption can be reduced by 44% of average use by implementing the measures in Table 1. Electricity and natural gas consumption associated with this water use could be reduced by about the same percentage.

- Exterior water use, toilet flushing, and bathing are the largest residential water uses. Conservation efforts applied to these uses will result in the largest reductions in residential water consumption.

- The highest per capita electricity consumption associated with water use occurs in the South Coastal HSA where 57% of the state's population resides.

- Of the four energy components considered, energy for water heating dominates the energy uses associated with water consumption. Potential natural gas savings are greater than potential electricity savings because gas hot water heaters are more prevalent than electric water heaters in California.

- Bathing and laundry rank first and second for energy consumption among residential water uses because of the high volume of hot water used.

- Accordingly, water conservation measures that reduce water for bathing and laundry, and all measures that reduce water consumption in the South Coastal and San Francisco HSAs (where the energy required for water delivery is relatively high) would have the largest impacts in water-related energy savings.

- Industrial water consumption and the associated energy requirements for water delivery and distribution can be reduced by at least 19% and 23%, respectively. This is thought to be a conservative estimate.

- The conservation measures that can be applied most immediately are housekeeping measures, some closed cycle cooling water reductions, and reuse of process water where extensive retrofitting of equipment is not required.

- The centers of industrial water consumption are the South Coastal and San Francisco HSAs. Water-related energy use also is highest here because of the energy requirements for delivery and distribution. So relatively large and immediate water and energy savings can be made by implementing the above mentioned water conservation measures in these areas.

- So far the largest savings potentials reported are in the paper and petroleum sectors. Food processing should be given special attention because it is the largest industrial water user.

FOOTNOTE

*Condensed from Lawrence Berkeley Laboratory Report, LBL-6817, A Water Conservation Scenario for the Residential Sectors in California, P. Benenson, August 1977.

ELECTRICAL LOAD MANAGEMENT FOR THE CALIFORNIA WATER SYSTEM*

B. Krieg, I. Lasater, and C. Blumstein

INTRODUCTION

To meet its water needs California has developed an extensive system for transporting water from areas with high water runoff to areas with high water demand. This system annually consumes more than 6 billion kilowatt hours (kWh) of electricity for pumping water and produces more than 12 billion kWh/year of hydroelectric power.

From the point of view of energy conservation, the optimum operation of the California water supply system would require that pumping be done at night and generation be done during the day. Night pumping makes it possible for the pumps to be supplied with electricity from "base-load" generating plants. These plants are more efficient (compared with "cycling" and "peaking" units using the same type of fuel), so night pumping saves energy. Night pumping also reduces requirements for capital investment in electric generating capacity since capacity requirements are determined by the peak demand on the electricity distribution system which occurs during the day. (This strategy of shifting electricity use from peak demand periods to off-peak periods is known as "load management.") Daytime hydroelectric generation conserves energy if it can be used to replace generation from inefficient fossil-fuel-fired "peaking" units.

Two important sets of issues govern the feasibility of operating the water system according to this optimum schedule. The first is the technical issues of what facilities (e.g., pumping, generating, water storage) would be needed to adopt this strategy now and in the future, what they would cost, and what benefits they would yield in energy and capital savings. The second set of issues concerns the institutional arrangements between the water projects and the electric utilities who purchase power from the projects and supply energy for pumping. These transactions are governed by contracts which set the prices for electricity and determine what, if any, differential in price exists between peak and off-peak power. The contracts thus determine the incentives for the water agencies to practice load management. Circumstances have changed vastly since most of these contracts were negotiated. Thus, the major institutional question is whether, and in what way, these contracts should be altered in light of the new situation.

This study has examined both the technical and institutional aspects of load management for the water projects. It has attempted to explain some of the actions which might be pursued and to develop recommendations for the California Energy Resources Conservation and Development Commission (CERCDC).

TECHNICAL REQUIREMENTS

Water projects have typically been designed to minimize capital costs for construction. Although reliability and capacity to meet future demands have often been important considerations in design, operating costs have usually been of secondary concern. Since water was free at the source, it was assumed that capital costs would always be the major component of the price of water delivered to the users. Water project planners did not anticipate the energy crisis.

Because of high capital costs associated with their construction, water projects are designed for nearly continuous operation. None of the California projects were planned for pumping exclusively during off-peak periods to reduce operating costs by load management.

In principle, it is possible to redesign existing projects so that pumping can be done offpeak. This does not require that all of the project facilities be sized for off-peak operation; the conveyance facilities (canals, etc.) still can operate continuously. Increased pumping capacity, plus storage facilities before pumping stations (forebays) and after (afterbays), are the essential requirements. With these installations the system would operate in the following way:

- Water would flow continuously into the forebays and out of the afterbays;
- During off-peak periods the pumps would operate, drawing down the forebays and filling the afterbays;
- During peak periods the pumps would shut down, the forebays would fill, and the afterbays would be drawn down.

Thus, storage capacities of the forebays and afterbays would be determined by the volumes needed to hold and supply the flow of the conveyances during peak hours. The pumping capacity would have to be sufficient to lift all the project water during the off-peak period.

This study made an analysis of the potential benefits of pursuing this strategy. Attention was focused on the State Water Project (SWP) since this project is the largest in California and its need for electricity is growing rapidly (at full capacity the project will use about 13 billion kWh/year). The analysis suggested that very substantial investments (perhaps more than $2 billion) might be warranted to modify the SWP so that load management could be increased. However, detailed engineering studies and more sophisticated economic analyses are required before decisions can be made as to whether to pursue this alternative. We recommended that the CERCDC and the California Department of Water Resources initiate a cooperative effort to pursue these studies.

POWER CONTRACTS AND OPERATING SCHEDULES

The primary determinant of the scheduling of operations on the water projects is the demand of water users; however, their needs do not require an entirely fixed operating schedule. Thus, there is flexibility to accommodate, to some extent, the second factor that influences scheduling; the contracts governing prices for the exchange of electricity among the water projects and the electric utilities. Over the years these contracts have developed into a fairly intricate network of agreements. Clearly, the power contracts are critical to load management. Price differentials between peak and off-peak power set by these contracts will be a major determinant of the economic feasibility of load management strategies.

Our study made an analysis of these agreements, particularly as they affect the SWP. It was concluded that the main contracts, dating from the mid-1960's, which govern power sales and purchases by the SWP do not contain sufficient incentives for load management. A number of possible improvements, more or less within the framework of the existing contracts, were examined. However, it was concluded that the best solution would be to depart from the existing arrangements and to establish a more flexible agreement similar to those governing some of the "power pools" which exist in the eastern United States. We recommended that the CERCDC take steps to encourage such an agreement and suggested that the CERCDC could assist in using certain provisions of the proposed National Energy Act to establish a power pool.

FOOTNOTE

*Condensed from Lawrence Berkeley Laboratory Report, LBL-6367, Electrical Load Management for the California Water System, B. Krieg, T. Lasater, and C. Blumstein, 1977. Research sponsored by the California Energy Resources Conservation and Development Commission.

CALIFORNIA'S DISTRIBUTED ENERGY SYSTEMS

P. P. Craig

During the winter of 1977 a group of University of California faculty and staff from Berkeley, Davis, Lawrence Livermore Laboratory and Lawrence Berkeley Laboratory became intrigued by the prospects for alternative energy futures based on renewable energy forms. A major stimulus to this interest was the work of Amory Lovins, especially his article in Foreign Affairs and his more detailed report, presented at the symposium on Future Strategies for Energy Development, held in the fall of 1976 at Oak Ridge, Tennessee, under the sponsorship of Oak Ridge Associate Universities. This project represents the results of two months of effort on an eighteen-month study.[1]

We have focused our attention on the development of distributed energy systems. Since many problems or issues can be evaluated only in comparison with alternative choices, we include as well discussion of alternative "hard" systems. The criteria we have used in defining distributed systems are:

- Renewable
- Environmentally benign
- Local
- Subject to graceful failure
- Foolproof
- Flexible
- Comprehensible
- Matched in energy quality

In practice much difficulty was found in meeting these criteria.

Patterns of energy supply and use in California differ from national averages. On a per-capita basis, California uses only 85 percent as much energy as the national average. Transportation energy use is 8 percent greater than the U.S. average. Residential sector energy use is 68 percent of the U.S. average, a difference which results from the unusually mild climate. Industrial sector use is 65 percent of the U.S. average on a per-capita basis as a result of the dominance of the service sector. Manufacturing industries use less energy in California than the U.S. average. For every 1000 kilowatt-hours of energy used, California produces $158 of value added as compared to only $94 for the nation as a whole. The largest single industry in the state in terms of energy is agriculture, which uses directly about 5 percent of the energy in the state (and several times as much when indirect energy is included). Agriculture also uses about 85 percent of all the water in the state.

Table 1 summarizes our estimates of the likely limits of renewable resources in California.

The fossil resource base of California is declining, and there is no possibility of meeting a significant portion of the state's energy needs in the next century. Fossil fuels will, however, continue to be available at some cost, and we have assumed these will be used to meet needs for petrochemical feedstocks, lubricants, and waxes and greases.

OUTCOME ANALYSIS--CALIFORNIA IN 2025

Initial analyses balancing demand against supply for the year 2025 have been made. The demand analysis was based upon the National Academy of Sciences' Demand/Conservation (1977) report developed by the Committee on Nuclear and Alternative Energy Strategies (CONAES), scaled to California population assumptions and modified in some other respects (especially in the transportation sector). Key demographic and economic assumptions are: 1) population of the state will have nearly doubled from its 1975 level, 2) Gross State Product will have nearly quadrupled from its 1975 level, and 3) the structure of the economy is not significantly changed. In addition it is assumed that there is vigorous emphasis on energy conservation.

In the end use analysis, energy use is divided into electricity, high- and low-temperature requirements, and liquid fuels. Because of a severe liquid fuels problem which developed in the supply/demand integration, transportation assumes electrically-fueled vehicles for urban transport. The electric urban transit assumption decreases liquid fuels requirements at the expense of increasing the demand for electricity.

These energy needs were matched with centralized and distributed supplies. The balance for the two distributed cases considered is shown in Table 2.

Biomass is used to meet liquid fuels needs. On-site solar is used for residential, commercial and agricultural low-temperature needs. Solar-driven cogeneration is used for those industries where it appears appropriate to provide both low- and high-temperature heat, together with some electricity. Geothermal and hydro-power are used almost to the limit. On-site solar electric power is used to meet the remaining electricity needs. In each case energy storage is assumed which is adequate to provide seasonal averaging. In the centralized case liquid fuels are assumed supplied by conversion from oil shale or coal. Electrical needs are met using nuclear power, coal and hydropower. The problems associated with each of these components of the energy system are considerable. If the energy were supplied by coal, California would use about as much coal in 2025 as the entire U.S. uses today.

RESERVATIONS AND OBSERVATIONS

Tentative observations from the work carried out thus far are that: the supply/demand balance presented here requires that great attention be paid to energy conservation; there are severe

Table 1. Summary of California Energy Resource Estimates for the Year 2025

Resource	Annual Energy, 10^{12} Btu Heat	Annual Energy, 10^{12} Btu Electricity or mechanical	Fuels
Solar Energy	Immense	Immense	
Biomass, Land			570-700
Biomass, Ocean			280-540
Wind		2400-9400	
Geothermal	34000	510	
Hydroelectric		230	
Ocean Energy		Nil	
Fossil Fuels			Nil

Table 2. Supply/demand balance--distributed case.

	Scenario A: Extensive Energy Conservation					Scenario B: Moderate Energy Conservation				
	Primary Energy	Electricity	Heat < 350°F	Heat > 350°F	Liq.	Primary Energy	Electricity	Heat < 350°F	Heat > 350°F	Liq.
Biomass[a]										
Wastes	100% collection of available wastes				480	100% collection of available wastes				480
Energy Farms	2.5-5% of non-commercial forest and brushland annually				618	2.5-5% of non-commercial forest and brushland annually				618
Kelp, synthetic fuels or hydrogen	18,000 sq. mi. of kelp or 50 million tons of coal converted to methanol at 60% efficiency				667	34,000 sq. mi. of kelp or 90 million tons of coal converted to methanol at 60% efficiency				1162
On Site Solar										
Residential, Commercial & Agriculture	3300 million sq. ft. of collectors and 330 sq. mi. of land area		616[b]			3500 million sq.ft. of collectors and 350 sq. mi. of land area		657		
Paper Industry	84,500 acres of land for a typical system	40[d] cogeneration	53[c]	11[c]		101,700 acres of land for a typical system	43[d] cogeneration	57[c]	12[c]	
Other industries		132[g] cogeneration	498[e]	383[f]			142[g] cogeneration	531[e]	417[f]	
Geothermal	13 GWe at 85% capacity; 65% of available sites	330				13 GWe at 85% capacity; 65% of available sites	330			
Hydroelectric	9.2 GWe at 50% capacity; 65% of total estimated capacity	137				9.2 GWe at 50% capacity; 65% of total estimated capacity	137			
Wind	19,000 3.5 MWe windmills at 40% capacity[h]	759				22,500 3.5 MWe windmills at 40% capacity[i]	918			
TOTAL		1398	1167	394	1765		1570	1245	429	2260

[a] Biomass supply falls short of demand by about 600 Trillion Btu in Scenario A and by about 1100 Trillion Btu for Scenario B; liquid fuels, kelp, or hydrogens are needed to fill the gap.

[b] On-site solar assumed to match all residential commercial and agricultural low heat energy requirements.

[c] Heat requirement of the paper industry assumed to be supplied partially by solar and partially by wastes from the production process (wastes can supply 56% of the demand).

[d] Cogenerated electricity by the paper industry 183 kwh generated by each 10^6 Btu heat fed into the process.

[e] All industrial low temperature heat demand is supplied by on-site solar.

[f] High temperature heat demand of food, chemicals and construction and 40% of "other manufacturing" is supplied by on-site solar.

[g] Electricity from cogeneration in manufacturing. Typical design assumed which gives 0.15 Btu as electricity for each Btu of heat (McDonnell-Douglas Corporation, 1977).

[h] 4.5 million small wind mills (50 ft high, 60 ft in diameter and spaced every 600 ft). A centralized wind mill system of 3.5 MWe would require 19,000 such wind mills.

[i] 5.4 million small wind mills (50 ft high, 60 ft in diameter and spaced every 600 ft). A centralized wind mill system of 3.5 MWe would require 22,500 such wind mills.

liquid fuel problems; the analysis suggests that an advanced post-industrial state can, at least on technical grounds, be operated using indigenous renewable resources for a population nearly twice the present size and an economy nearly four times the present size; the land-use implications of both centralized and distributed systems are considerable; the environmental impacts of the distributed systems appear less than those of centralized systems;

system reliability questions are fundamentally different in distributed energy systems and in systems based on fossil energy forms. New approaches to and attitudes toward reliability of energy systems may be required for systems based predominantly upon renewable energy forms; the inclusion of relatively small quantities of fossil-based energy forms (hybrid systems) can considerably ease the difficulties of a distributed energy system.

PLANNED ACTIVITIES IN 1978

The study will be expanded to include far more complete analysis, especially in the economic, environmental and technical areas. Major attention will be given to institutional issues and to policies and implementation measures that may be appropriate to support the distributed energy system.

One of the most important features of the first phase of this study was the interaction between participants in the university community (UC Berkeley and UC Davis) and the national laboratories (Lawrence Berkeley Laboratory and Lawrence Livermore Laboratory). Future work will continue to emphasize and strengthen the substantive interaction between researchers in these institutions, with the long-term objective of molding an effective interdisciplinary team. As such, an important element of the 1978 activity will be the integration of the research effort into a volume that can receive wide distribution in the Department of Energy and elsewhere.

REFERENCE

1. Distributed Energy Systems Study Group, Distributed Energy in California's Future: A Preliminary Report, Volumes 1 and 2, Lawrence Berkeley Laboratory Report, LBL-6831, September 1977.

Solar Energy

INTRODUCTION

Solar energy has emerged as a serious alternative for supplying a substantial fraction of the nation's future energy needs. To help fulfill that potential, the Department of Energy (DOE) is supporting activities ranging from the demonstration of existing technology to research on long-term possibilities. At LBL, projects spanning that range of activities are currently in progress.

An important aspect of assessing solar applications is quantifying the solar resource. In one project, completed this year, historic solar data for California were rehabilitated and assembled into a manual. The manual is intended primarily for solar heating and cooling applications. A continuing project has developed special instruments and is now using them to measure the solar and circumsolar (around the sun) radiation. These measurements help to predict the performance of solar designs which use focusing collectors (mirrors or lenses) to concentrate the sunlight.

Several efforts are under way to aid DOE in demonstrating existing solar technology, or in transferring such technology to industry. Technical and management support have been provided to DOE's San Francisco Operations Office (SAN) for its management of two solar energy retrofits of low-to-moderate cost homes, sixteen commercial solar demonstration projects, and seven hotel/motel hot water demonstrations. Design work was initiated this year on a solar hot water and space heating system to be installed on an LBL building. This work will establish model techniques and procedures, and help reduce fossil fuel consumption at the laboratory. In a joint solar technology transfer project with Lawrence Livermore Laboratory, resource handbooks were prepared for seminars presented to professional and trade groups in California. Finally, technical support is being provided for SAN in a DOE small scale technology pilot program. In this program, individuals and organizations will be awarded grants to develop and demonstrate technologies appropriate to small scale use.

Solar heating and, especially, solar cooling are areas in which research is expected to have a substantial impact in the near-term. An absorption air conditioner is being developed that is air cooled, yet suitable for use with temperatures available from flat plate collectors. In another approach, the feasibility of using a "shape-memory" alloy (known as Nitinol) in heat engines is being investigated. Work is proceeding on a prototype Nitinol engine capable of driving a moderate-sized residential air conditioner with solar-heated hot water. The performance of many-component solar heating and cooling systems may be improved by controlling their operation with inexpensive but sophisticated micro-electronics. A program is under way to develop and test such a controller, and to evaluate commercially available units.

Efforts were initiated this year on "passive" approaches to solar heating and cooling, in which careful considerations of architectural design, construction materials, and the environment are used to moderate a building's interior climate. In a collaborative project with Los Alamos Scientific Laboratory, computer programs are being developed to evaluate passive designs. A second "passive" project is investigating specific passive cooling methods. In particular, a process is being studied whereby heat storage material would be cooled by radiation to the night sky, then provide "coolness" to the building the next day. Finally, the laboratory personnel involved in these projects are also providing technical support to the Solar Heating and Cooling Research and Development Branch of DOE in developing program plans, evaluating proposals, and making technical reviews of projects at other institutions and in industry.

Several projects are investigating longer-term possibilities for utilizing solar energy. One project, started this year, is addressing the environmental aspects of Ocean Thermal Energy Conversion (OTEC). LBL is participating in bio-ecological measurement programs at potential OTEC sites, and providing technical support to the Environmental and Resource Assessments Branch of DOE's Division of Solar Energy. Work continued this year on chemical storage processes (such as $2SO_3 \rightleftharpoons 2SO_2 + O_2$) that could play an important role in providing long-term storage for high temperature power generation cycles. Two projects are exploring biological systems. In one, the emphasis is on understanding the biological processes linking hydrogen consumption, nitrogen-fixation, and photosynthesis in blue-green bacteria, with a view towards increasing the productivity of the bacteria. The second project is investigating the possibility of developing a photovoltaic cell, based on a catalyst (bacterio-rhodopsin) which converts light to electrical ion flow across the cell membrane of a particular bacteria.

ANALYSIS OF THE CALIFORNIA SOLAR RESOURCE*

P. Berdahl, D. Grether, M. Martin, and M. Wahlig

INTRODUCTION

Lack of adequate solar data would seriously limit development of solar energy as an alternative energy source. This project was designed to evaluate the current extent of this limitation, and to plan to avert such limitation in the future. More specifically, the objectives of the project were to:

1. Carry out an interim program to meet immediate needs for solar data in California by:
   a. Locating and gathering present and potentially available California solar radiation data,
   b. Evaluating the quality of these data, and
   c. Publishing these data with relevant background information in a solar data manual to be used by Californians.
2. Consider all reasonable options and make a recommendation to the California Energy Commission detailing the role it should fulfill to ensure availability of adequate solar data for California.

The project was essentially completed early in 1977, and draft versions of the California Solar Data Manual[1] and the final report[2] were forwarded to the California Energy Commission and the U.S. Department of Energy. The cycle of reviews and preparation of final versions of these reports is not yet completed.

ACCOMPLISHMENTS DURING 1977

California Solar Data Manual

The Data Manual contains the results of the project's tasks of data collection, data correction and editing, and data processing. The primary raw-data sets consisted of total daily solar radiation values received by a horizontal surface. Data sets for 19 locations in or near California were judged to be of sufficient accuracy and duration of record to be included in the data manual.

The correction and editing process relied primarily upon the comparison of measured clear-day radiation values (over the course of the year for several years) with corresponding theoretically calculated values. This clear-day analysis is documented in the final report[2] and elsewhere in the literature.[3] The analysis revealed that a substantial fraction of the historical data set was erratic or subject to instrumental drift. The data were improved partly by adjusting the instrument calibration constants a posteriori, using the clear-day method, and partly by deleting data which could not be rehabilitated. Fig. 1a shows a plot of solar-radiation values for Riverside derived from the raw data. Figure 1b shows the same plot, derived from the corrected and edited data.

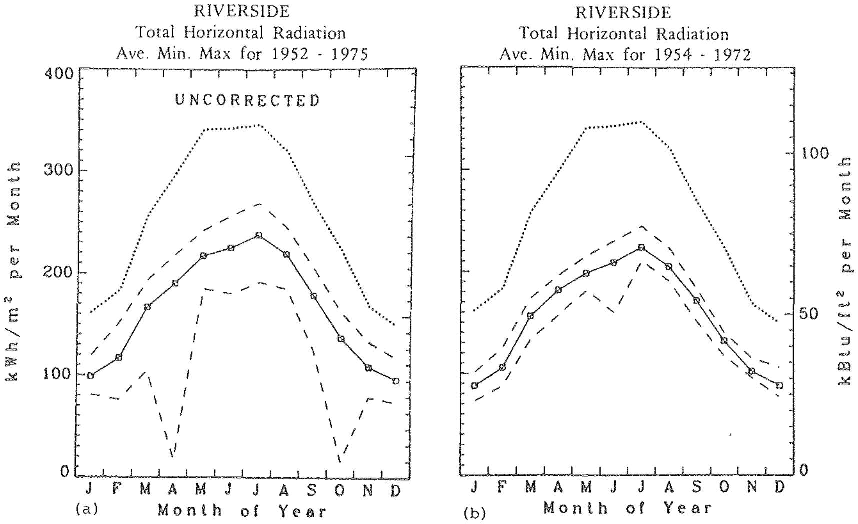

Fig. 1. (a) A figure as it would have appeared in the solar data manual if raw solar radiation had been used. The top curve gives the radiation received by a horizontal surface above the atmosphere (the extraterrestrial radiation). The solid curve shows long-term averages of monthly radiation totals. The dashed curves represent the high and low months of record. (b) Same as Fig. 1(a), but constructed from rehabilitated data.

Elimination of obviously bad data is seen to narrow the upper and lower bounds about the average values.

In addition to the radiation received by a horizontal surface, two other types of solar data were needed by users: direct radiation, and radiation received by tilted surfaces. Direct radiation is that which originates from the disk of the sun; this is the quantity of primary interest for systems which focus sunlight onto a receiver. Radiation received by tilted surfaces is required for many applications, especially solar heating with flat plate collectors, since these collectors are commonly inclined toward the south to increase the seasonal radiation received. Longterm measurements of these needed quantities have not been made in California, so it was necessary to employ a standard climatological method[4] to derive them. These data are presented in the Data Manual, together with explicit estimates of the errors generated by the derivation process. Figure 2 and 3 show examples of these data, again for Riverside, California.

Further information contained in the manual is designed to supplement the basic data and to provide additional information useful for solar collector system design. Subsidiary solar data presented includes (i) charts showing the location of the sun in the sky, (ii) histograms showing the probability of receipt of differing amounts of radiation, and (iii) "string statistics" giving the probabilities of sequences of consecutive cloudy days. Tables of climate data contain monthly averages of cloud cover, percent possible sunshine, temperature, humidity, etc. Finally, a "Guide to Simplified Performance and Cost Methods" is included to assist the reader in choosing a simplified system design method for solar buildings.

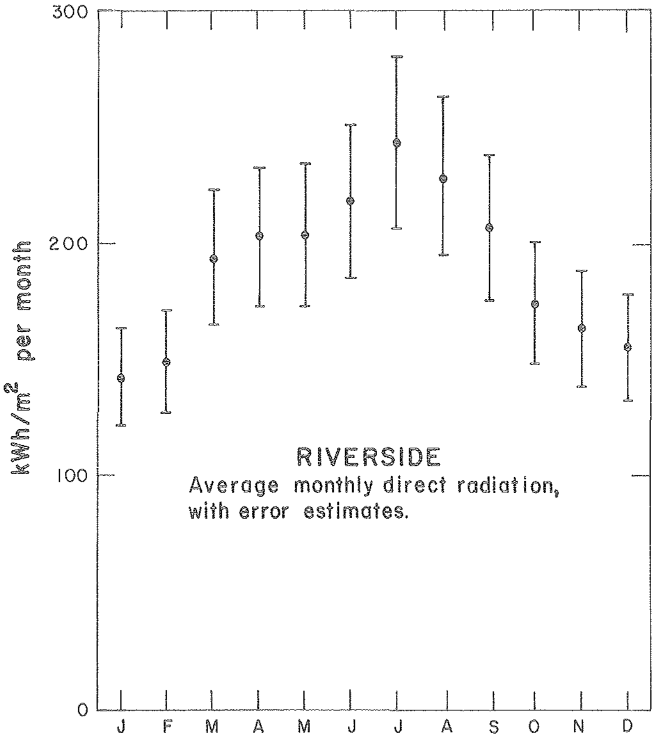

Fig. 2. Monthly averages of direct radiation. (XBL 784-616)

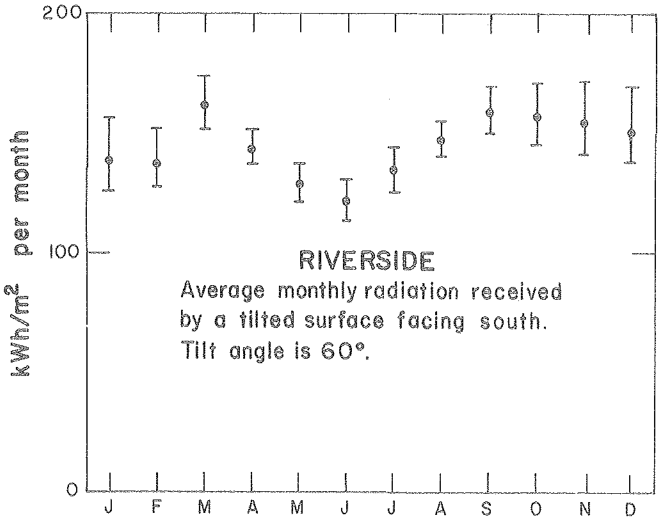

Fig. 3. Monthly averages of radiation received by a south-facing surface tilted 60° from the horizontal. No radiation from ground reflection is included. (XBL 784-615)

Recommendations for the Future

Recommendations for improvement of the quality and quantity of California's solar data are intended to assure the future existence of data for engineering design of solar collector systems and other solar energy applications. Over the near term future (say, 10 years), the types of radiation data needed are the total radiation received by a horizontal surface, direct radiation, and radiation received by inclined surfaces. The time resolution should be 1 hour or better to permit detailed simulation calculations for various systems and to permit modeling (i.e., the approximate calculation of unmeasured radiation quantities).

Both measurements and modeling are essential. Modeling is necessary because it is impossible to make measurements of all solar radiation quantities of interest at all sites. Measurements are necessary to provide basic data and to verify that models produce realistic data. The detailed recommendations[2] provide for measurements of the above-mentioned radiation values at a minimum of 15 California sites. The usefulness of the data should be assured with a regular program for instrument calibration, and routine examination and analysis of the forthcoming data.

Efforts in the area of modeling should be concentrated in two primary areas. First, the standard climatological model[4] for estimating unmeasured quantities from the total horizontal radiation should undergo further verification. Second, spatial interpolation techniques to estimate radiation received at non-instrumented sites should be refined.

FOOTNOTES AND REFERENCES

*Work supported partially by DOE and partially by the California Energy Resources Conservation and Development Commission (Energy Commission).

1. P. Berdahl, D. Grether, M. Martin, and M. Wahlig, California Solar Data Manual, Lawrence Berkeley Laboratory Report UCID-5971 (1978).

2. P. Berdahl, D. Grether, M. Martin, and M. Wahlig, Analysis of the California Solar Resource, Lawrence Berkeley Laboratory Report (1978).

3. M. Martin, P. Berdahl, D. Grether, and M. Wahlig, "Rehabilitation Techniques for Daily Solar Radiation Data," Proc. Amer. Sec. of the Int.Solar Energy Society, (Orlando, Florida, 1977), p. 14-22.

4. B. Y. H. Liu and R. C. Jordan in Solar Energy 4, 1 (1960), and ASHRAE Transactions, 526 (1961).

MEASUREMENT OF CIRCUMSOLAR RADIATION

D. Grether, A. Hunt, and M. Wahlig

INTRODUCTION

Circumsolar radiation refers to light that, to an observer on the ground, appears to originate from the region around the sun. Aerosol particles, with dimensions on the order of or greater than the wavelength of light, cause this radiation by scattering light through small angles. The aerosol particles may be composed of ice crystals or water droplets in thin clouds, dust or sea salt particles, or photochemical pollutants. The amount and character of circumsolar radiation vary widely with geographic location, climate, season, time of day, and observed wavelength.

Many solar energy collectors have been proposed or constructed that focus the solar radiation by means of mirrors or lenses. Types of collectors include the central-receiver and the parabolic trough. Once concentrated,the sunlight is converted to thermal energy (and used, for example, to drive a steam turbine) or directly to electricity by means of photovoltaic cells.

Focusing solar energy systems typically collect the direct beam solar radiation (that coming directly from the sun) plus some fraction (usually small) of the circumsolar radiation. The exact fraction collected depends upon many factors, but primarily upon the angular size (field of view) of the receiver, that blackened surface or cavity that absorbs the sunlight. A somewhat larger receiver will collect more of the circumsolar radiation but will experience somewhat larger radiation losses. A knowledge of the circumsolar radiation can be a factor in optimizing a receiver design, or in choosing between competing designs for a particular application.

The pyrheliometer, the instrument normally used to estimate the direct beam radiation, has a 5°-6° field of view as compared to the 1/2° subtended by the sun. The pyrheliometer thus measures a substantial fraction of the circumsolar radiation as well as the direct beam radiation. For most focusing systems, the pyrheliometer will overestimate the amount of radiation that will be collected. A knowledge of the circumsolar radiation at a given location can thus be used to correct the pyrheliometer measurement.

Four instrument systems have been constructed at LBL to measure the circumsolar radiation. The basic instrument is a telescope that scans through a 6° arc of the sky with the sun at the center of the arc. The output is a digitization of the brightness of the sun and circumsolar region every 1.5 minutes of arc. Auxiliary instruments include a pyrheliometer (see above), and two pyranometers that provide a measure of the direct sunlight plus the diffuse sky light. Additional details of the instrument are given in previous annual reports.

ACCOMPLISHMENTS DURING 1977

Operation of Telescopes

Three of the telescopes were orginally deployed during 1976. In 1977, one of the instruments continued to be operated at the Solar Thermal Test Facility at Albuquerque, New Mexico. A second telescope, originally located at China Lake, California, was moved in May to Barstow, California, the future site of the 10 MWe Central-Receiver pilot plant. Until August, a third telescope was operated at Ft. Hood, Texas, the future site of a Total Energy System employing parabolic trough collectors. The instrument was then moved to Argonne National Laboratory to compare focusing systems with low concentration, non-focusing systems. The fourth telescope was used in several short-term measurement programs, then moved to Atlanta, Georgia in June, to the 400 kW Central-Receiver test facility.

Analysis of Instantaneous Values

A major effort this year was to reduce telescope data to forms suitable for applications to focusing solar energy systems. One approach was to correlate the reading of the pyrheliometer with a measure of the circumsolar radiation known as the circumsolar ratio.

This ratio is given by

$$R = C/(C + S)$$

where S is the intensity of the direct solar radiation (obtained by integrating the telescope measurement from the center of the sun out to one solar radius), and C the intensity of the circumsolar radiation (integral from one solar radius out to 3° from the sun's center). This ratio approximately corresponds to the fractional error in using a pyrheliometer estimate for the energy available to a highly concentrating solar device (that only collects the energy coming directly from the sun).

Figure 1 is a plot of circumsolar ratios vs pyrheliometer readings for the month of February in China Lake, California. The plot shows 1186 points; another 117 points were excluded because the pyrheliometer reading (referred to as "NI" in the figure heading) was too low to be of interest. The figure shows three fairly distinct regions. First, there is a dense clumping of points at high (~1000 W/m^2) pyrheliometer readings and low ($\lesssim$1%) circumsolar ratios. This "clump" corresponds to clear sky conditions during the middle part of the day (defined to be from three hours after sunrise to three hours before sunset). The second region is a "tail" of rapidly decreasing pyrheliometer values accompanied by slowly increasing C/(C + S) values. These points are for clear-sky conditions during the three hours after sunrise and the three hours before sunset. Under these conditions, atmospheric absorption dominates; the relatively low pyrheliometer values corresponding to times relatively closer to sunrise or sunset. The third region is a "crescent" of relatively high C/(C + S) values extending from the clump down to the bottom right-hand corner of the plot. This crescent corresponds to periods when forward scattering dominates, and atmospheric absorption plays a lesser role. A possible origin of the effect is scattering from high, cirrus clouds. If so, the range of values along the crescent would vary with the thickness of the cloud layer and the size of particles it contains. The values in the crescent are only weakly correlated with time of day.

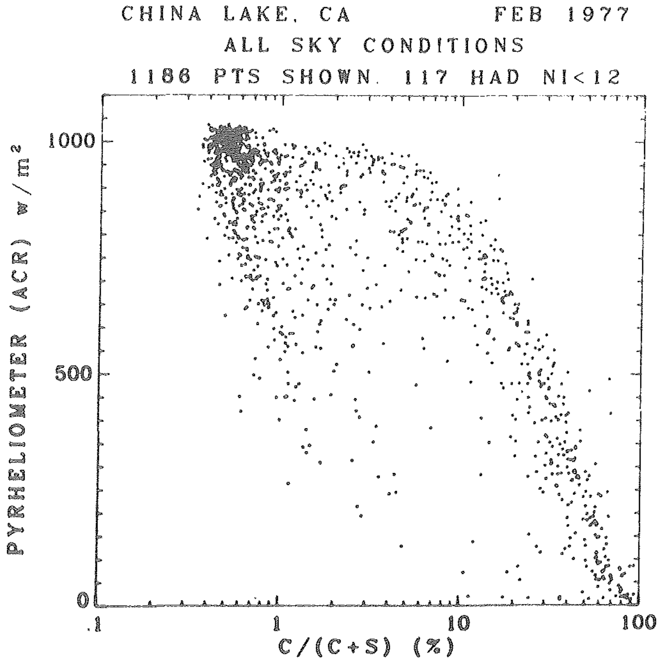

Fig. 1. Plot of the circumsolar ratio vs the corresponding pyrheliometer reading for each of 1,186 measurements made during February in China Lake, California. (XBL 782-7240)

The general features of Fig. 1 (clump, tail, crescent) are present in the data from all telescope locations for all seasons of the year. There are, however, significant variations in detail and in the relative number of points in the three regions. These data show that a pyrheliometer measurement often is not an adequate estimate of the instantaneous energy available to focusing solar-energy systems.

Analysis of Monthly Values

Typically, a focusing solar energy system will be operated during periods of good sky conditions (high values of solar radiation, low circumsolar levels) intermixed with periods of poor conditions (low-to-moderate solar radiation, moderate-to-high circumsolar levels). It is thus of interest to use the telescope data to calculate an average effect over a period such as a month.

Figure 2 shows one approach to presenting such calculations. The data are for May 1976 through May 1977 in Albuquerque. The quantity being plotted is the overestimate made by a certain type of pyrheliometer (referred to in the figure as NIP, for Normal Incidence Pyrheliometer) in predicting the amount of solar radiation available to a focusing solar power plant. In this approach, focusing systems are characterized by two idealized parameters. The first is an "operating threshold." The plant is assumed to be operating whenever the solar radiation is above the threshold, and otherwise shut down. The threshold used in constructing Fig. 2 was 50 watts/m^2. The second parameter is an "effective aperture radius" (half the field of view) of the receiver, expressed as an angular distance from the center of the sun. All solar and circumsolar radiation up to the radius is assumed incident upon the receiver, and none thereafter.

Consider, in Fig. 2, the value for March, 1977 and for an effective aperture radius of 0.28° (slightly larger than the half-width of the sun). For this month a pyrheliometer would overestimate by ≈6% the energy available to a solar plant having a threshold of 50 watts/m^2 and designed essentially to capture only the radiation coming directly from the sun. Current designs typically have apertures on the order of 0.80°. The overestimate then would range from 1% to 2.5%. The overestimate is slightly less at China Lake, a desert location like Albuquerque. For Ft. Hood, a more humid location, the overestimate ranges from 1.5% to 4% for the 0.80° aperture.

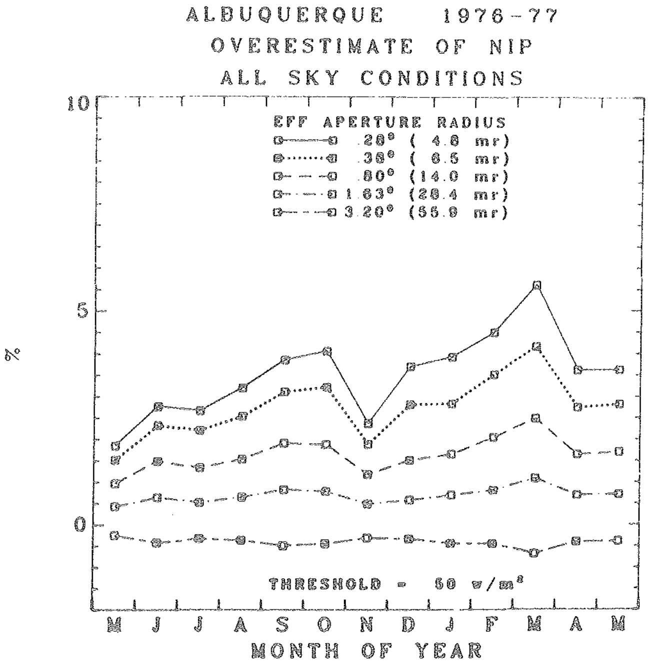

Fig. 2. Plot of the overestimate made by a pyrheliometer in determining the amount of solar radiation available to collectors with different effective apertures. (XBL 782-7241)

Analysis of Specific Designs

Any given focusing solar plant can be described only approximately by the approach discussed above. In cooperation with Sandia Laboratories, Livermore, computer analysis was made of two specific designs for the 10 MWe Central-Receiver pilot plant: the design of McDonnell-Douglas (the selected design) and that of Martin-Marietta (the backup design).

These solar plants are planned so that essentially all of the direct solar radiation that is reflected from a given heliostat (mirror mounted on a sun tracking platform) is incident upon the receiver. Some fraction of the reflected circumsolar radiation will impinge on the receiver, and the rest will be "lost." The analysis indicated that for the Martin-Marietta design typically 60% of the energy content of the circumsolar radiation would be lost. For the McDonnell-Douglas design, which has a somewhat larger receiver, typically about 35% would be lost. The actual energy lost (in percentage of the energy content of the solar-plus-circumsolar radiation) ranges from 1-5% for the Martin-Marietta design, to 0.6-3.7% for the McDonnell-Douglas design, depending on the season and location.

PLANNED ACTIVITIES FOR 1978

The measurement program will continue, with one of the telescopes moved to the Great Plains. The data analysis will proceed on a continuing basis to process and summarize the solar and circumsolar measurements taken during the latter part of 1977 and during 1978.

The correlation studies begun in 1977 will be expanded to investigate whether some combination of conventional solar and/or meteorological measurements can provide an adequate estimate of the circumsolar level.

The results obtained in 1977 suggest that a small but important energy gain would be made by designing plants with relatively large receivers. However, such receivers would have somewhat greater convective and re-radiative losses. In 1978, the analysis of specific designs is to be extended to include consideration of such losses. Furthermore, similar analyses are to be performed for other focusing systems, such as systems for photovoltaics and lower-concentration thermal devices.

CONTROLLER DEVELOPMENT AND EVALUATION OF CONTROL STRATEGIES FOR SOLAR HEATING AND COOLING OF BUILDINGS

M. Majteles, M. Wahlig, and H. Lee

INTRODUCTION

This project has three main objectives: (1) the development of a relatively inexpensive electronic controller that will be capable of operating a solar heating and cooling system in a near-optimized manner; (2) use of this controller and the LBL experimental solar simulation facility to compare experimentally the value of alternative control algorithms under a variety of input meteorological conditions and output load demands; and (3) determination of the relative performances of this controller and more complex control systems.

A prototype of the electronic controller was completed and found capable of carrying out the pre-programmed algorithms as anticipated.[1] The LBL experimental solar simulation facility is being upgraded to allow conduction of more precise and reproducible tests. While the facility is being improved, efforts continue to achieve heat balance accuracies adequate for controller performance evaluation.

ACCOMPLISHMENTS DURING 1977

Activities during 1977 were concerned primarily with the improvements of the experimental test facility. The test facility was equipped with two simulators: one for heat input and one for building load. Both simulators were designed to operate either independently of each other, or in unison by having both driven by the same input-meteorological data set. Instrumentation was added to the facility, and heat balance tests have been carried out. The tests consisted of runs both with solar collectors and with the heat input simulator as well as system heat loss experiments with no heat inputs or loads. In conjunction with these tests, the TRNSYS computer program was employed to predict system performance and to compare such calculations with actual experimental results.

Heat Balance Tests

Precision instrumentation was installed in the experimental facility and calibrated against standards. The instrumentation consists of turbine flow rate meters and temperature sensing devices. A multi-channel data-acquisition system prints instrument outputs at pre-set time intervals. There is an error associated with each measurement and data processing step. It was found that the resultant error in the digital flow-rate readout was less than 1% over the entire range of flows that will be used in the tests. The error associated with the temperature readout was found to be ±0.5°C for thermocouples wired to give direct measurements of each temperature. Wiring thermocouples in pairs produced readouts sensitive to temperature differences between the sensors. This technique lowered the measurement error to about ±0.1°C. Temperature readouts using solid state sensors resulted in errors of similar magnitude.

Efforts were made to control every element of heat flow within the experimental system. The storage tank lids were re-sealed to eliminate vapor losses to the ambient air. The collector draining system was modified to prevent mixing air with the return fluid, so that uniform heat exchange conditions would persist throughout the experimental runs. Detailed analysis of the fluid was performed to assess its thermal characteristics. The storage volume was measured and controlled at the start-up of each experimental run.

Extensive measurements were made of the facility heat losses. An empirical equation was derived using the data obtained during several long experimental runs. This equation computes the rate of heat loss as a function of difference in temperature between the central axis of the storage tank and the ambient air. To compute losses from segments of the facility hardware, weighting factors are used based on pipe lengths and surface areas. When the entire facility was being used, it was found that the storage loss was approximately 50% of the total heat losses.

The heat input and load subsystems were monitored carefully. Precision flow measurements were taken along with temperature differentials. These data were used for the computer calculation of heat quantities, including integration of heat quantities over short time intervals, typically 5 to 15 min.

Table 1 lists values obtained in a typical heat balance experiment. Three methods of temperature sensing are summarized for comparison. Differences in the calculated individual heat quantities using the various sensors are in excess of 10% in some cases. However, the magnitude of the mean error is around 6% for all the sensors, as summarized in Table 2. A slight superiority of the solid-state sensors over the thermocouples is indicated from the statistical summary in Table 2, but this is offset by the fact that the solid state sensors show the widest spread between the magnitudes of the smallest and largest errors.

Heat Input Simulator

A "pseudo-collector" boiler was a part of the initial solar facility design.[2] The boiler output passes through a temperature control valve (TCV) which can be activated to allow precise adjustment, within a wide range, of the output temperature of the pseudo-collector flow loop. In the initial design, the TCV was "slaved" such that the output temperature of the pseudo-collector would duplicate

Table 1. LBL solar system typical heat balance experiment.

Sensor	Heat In[a]	Heat to Load[a]	Heat Loss[a]	Δ Storage[a]	Heat Balance[a]	% Error[b]
Solid State	1.888	6.856	0.559	-5.724	0.189	2.5
Δ Pair of Thermocouples	2.107	7.544	0.557	-5.422	-0.571	-7.6
Thermocouples	1.856	7.201	0.557	-5.422	-0.479	-6.6

[a] In units of 10^8 joules.

[b] $$\% \text{ error} = 100 \times \frac{\text{Heat Balance}}{\text{Heat In} - \begin{Bmatrix} \Delta\text{Storage} & \text{if } \Delta \text{ Storage} < 0 \\ 0 & \text{if } \Delta \text{ storage} \geq 0 \end{Bmatrix}}$$

Table 2. Errors: summary of six heat balance experiments.

Sensor	Smallest[a] Error (%)	Largest[a] Error (%)	Mean[a] Error (%)	Standard Deviation (%)
Solid State	1.9	15.2	5.7	4.5
Δ Pair of Thermocouples	0.9	12.0	7.2	4.6
Thermocouples	2.9	11.9	6.7	3.3

[a] Tabulations based on the absolute values of errors.

that of the roof collectors. Consequently the pseudo-collector acted as a substitute for a large segment of roof collectors and its output temperature fluctuated in accord with the real collector outputs.

Since reproducibility of the experimental heating and cooling system operation is essential for quantitative comparisons of the performance of alternative control strategies, a more reproducible input element than the collectors was needed to control the pseudo-collector output. This was accomplished with an electro-mechanical heat input simulator that tracked a programmed temperature curve, as shown schematically in Fig. 1. This device produces temperature increases across the pseudo-collector in accordance with the curve fed through a strip-chart recorder. A photo-diode is used to trace the curve and mechanically adjust a linear potentiometer. A voltage derived from the potentiometer is used as input to the pseudo-collector controller, in place of the sensor input. By using various curves, heat inputs can be produced that correspond to solar collectors operating under diversified meteorological conditions.

Tests were run to determine errors in the repeatibility of the simulated heat inputs. A typical eight-hour run was reproducible with an error of about 1%. This result was irrespective of the storage tank initial temperature, in the 30°-60°C range. There is an upper limit on the storage tank temperature, at about 80°C, above which the simulator accuracy becomes unsatisfactory because boiling occurs prior to mixing in the TCV. If experiments with storage temperatures above 80°C are to be run, some modifications in the heat input simulator will need to be made to balance the heat quantities under conditions of boiling and water/steam mixtures.

Simulator for Building Load

A "pseudo-load" air flow channel, designed to simulate the flow of air across the heating coil or the cooling coil located in the furnace ductwork of an ordinary residential system, has been partly completed.[3] In its initial design the flow channel was configurated to recirculate inside air and to allow mixing with outside air. This initial design was re-evaluated and modified to allow greater experimental flexibility. As shown in Fig. 2, the new load simulator design relies on digital computational techniques to achieve controlled and reproducible residential loads across both heating and cooling coils.

The purpose of the simulator is to provide residential-building-type loads for the solar energy system. It is necessary to produce the proper residential building air temperature, essentially isolating it from the inappropriate laboratory building environment in which the solar system is actually located. This has been achieved with the duct network shown in Fig. 2a. The temperature within the duct can be carefully controlled through the combination of an electric heater and an air conditioner. Both heating and cooling loads can be simulated, as the duct air temperature is made to vary over a wide range of values independent of the ambient laboratory temperature. Provisions have been made to permit spraying water into the duct. This would provide hot, moist air to simulate a summer cooling load, as necessary for testing the solar-driven air conditioner.

As seen in Fig. 2b, a desktop calculator serves as the central element of the building-load subsystem. The calculator is interfaced with a multi-channel data acquisition instrument.

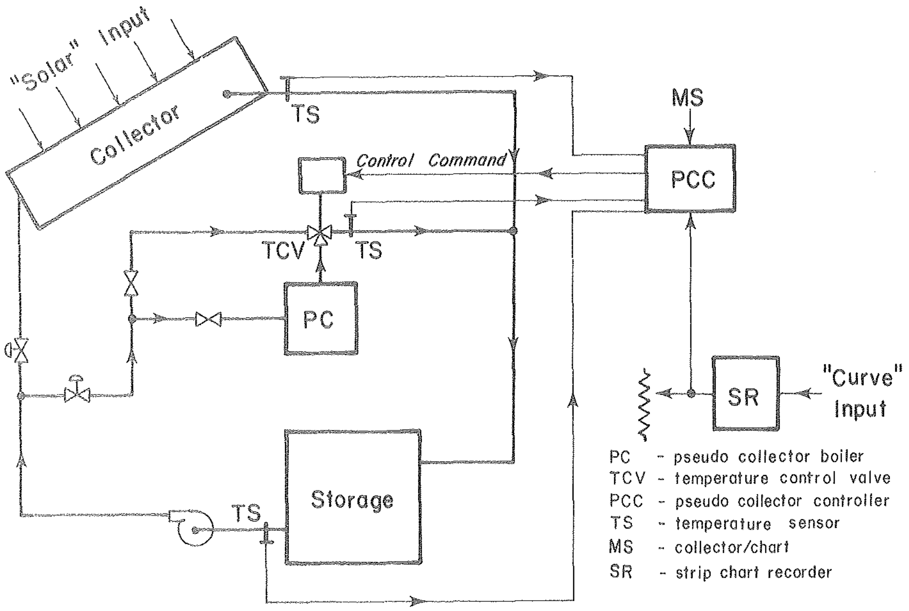

Fig. 1. Heat input subsystem. (XBL 784-618)

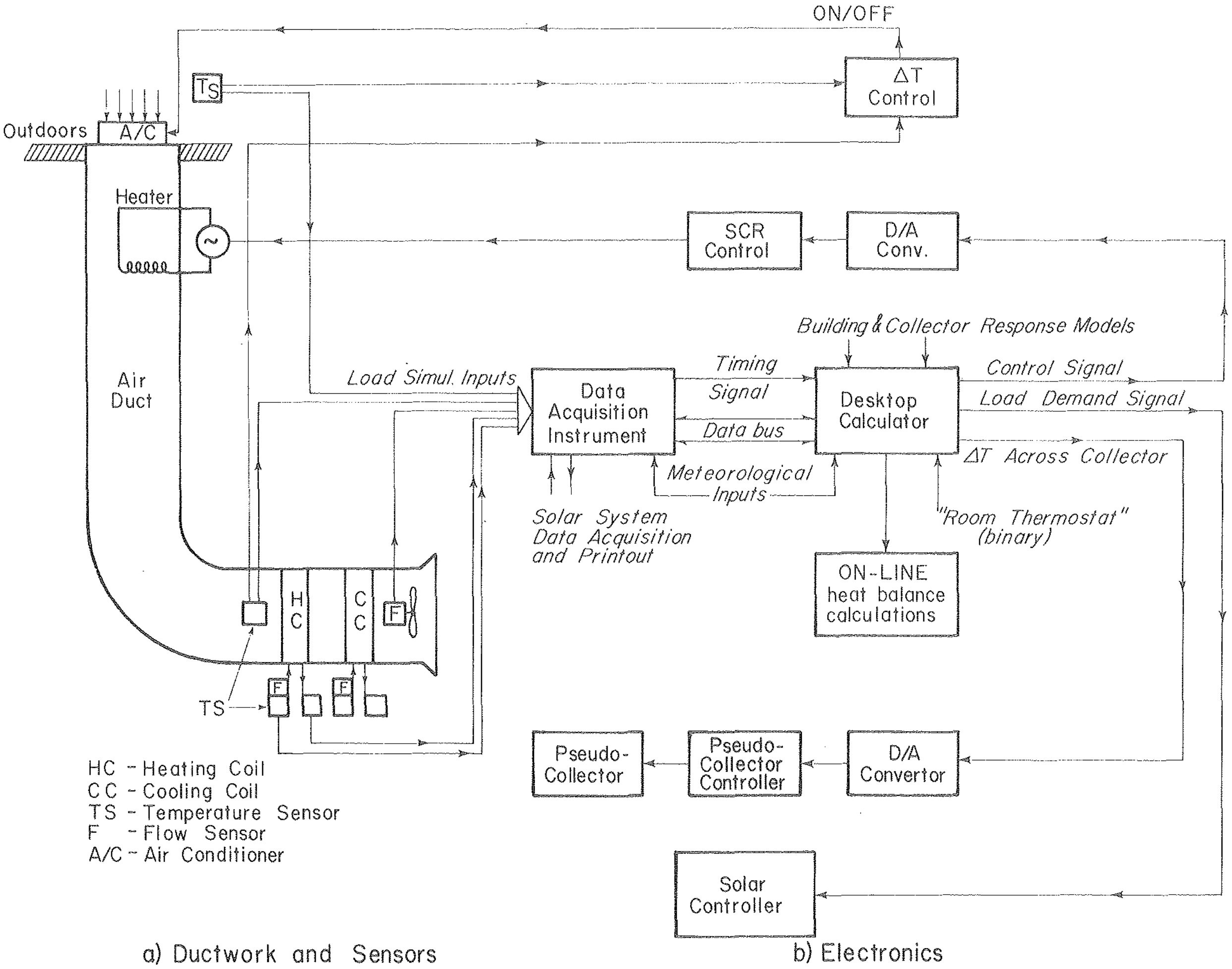

a) Ductwork and Sensors b) Electronics

Fig. 2. Building load subsystem. (XBL 784-620)

This allows the calculator to receive all of the inputs in digital form and process the data either for on-line heat balance calculations or for control purposes.

As a controller, the desktop calculator performs three functions: (1) it reproduces the desired duct air temperatures by controlling the duct-heater current; (2) it provides input to the pseudo-collector controller, thus replacing the "programmed curve" input described above and shown in Fig. 1; and (3) it provides load demand information to the controller of the solar heating and cooling system.

As a computer, the desktop calculator incorporates building and collector response models. The inputs to the calculator consist of meteorological and insolation data required to solve the equations of the models in addition to system parameters. Weather tapes from various regions can be used. Correspondingly, building and collector models can be selected for the geographical region under analysis. Thus, the experimental facility and the solar controller can be tested under diverse and realistic weather and load conditions.

Computer Modeling

It was decided to use the TRNSYS program, the University of Wisconsin-Madison developed model. This model operates on the "component interconnection" principle, well-suited for the multi-component experimental facility at LBL. Each component is described by equations containing physical parameters measured in the system. The equations (component models) are fixed within the program. The solar system controller is treated as one of the components.

After gaining familiarity with the program and updating it to the latest version, the program was set up to run from the storage files at the LBL computer center. The necessary physical parameters were measured, and the solar facility was simulated by completing the layout and interconnection of those components handled by the program.

Validation of the TRNSYS simulation commenced with an effort to compare the calculated system temperatures with the measured ones. Comparisons were made for several different modes of the solar system operation. A typical comparison using the heat inputs simulator is shown in Fig. 3. The agreement between measured and

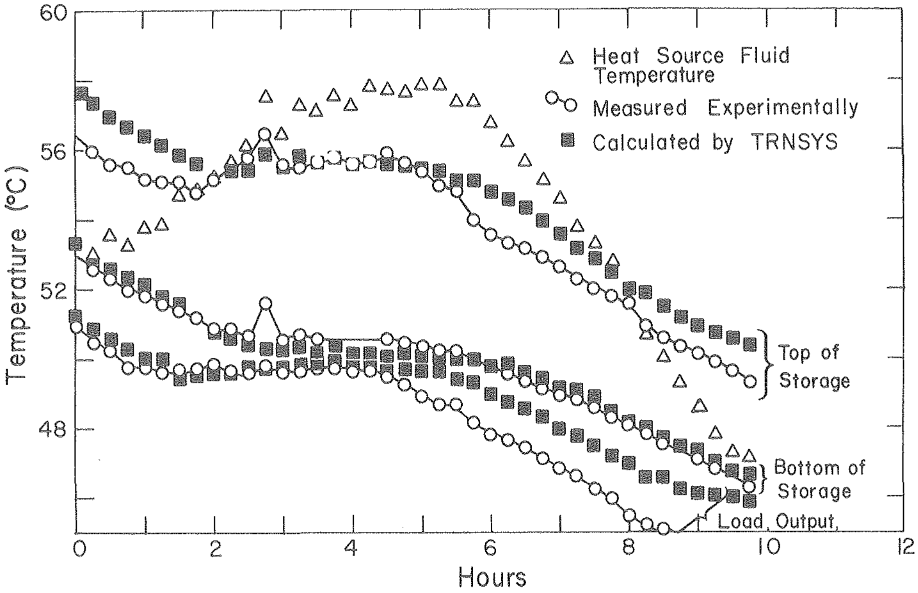

Fig. 3. "TRNSYS" validation experiment with heating and load loops operating. (XBL 784-617)

calculated values is quite close. Somewhat less close agreement was observed in low flow conditions when only the heat input subsystem is involved (no load). Efforts have been made to improve the model for such low-flow modes of operation by revising the method of representing the storage tank.

Simple controllers were also studied with the computer model. A study of ON/OFF controllers with low offset and hysteresis values ran into numerical convergence problems. Similar problems developed in studies involving proportional control schemes. Only ON/OFF controls with fairly high offset (20°C) and low hysteresis (1.5°C) settings ran successfully. Realistic flow-rate values were used throughout the runs. The static equations used to describe components in TRNSYS apparently cause the convergence problem. To study the control algorithms more precisely and realistically, some TRNSYS equations may need to be modified to include short-term dynamic effects.

PLANNED ACTIVITIES FOR 1978

The load simulator is still being synthesized. Upon its completion the operating algorithms will be evaluated experimentally. A modification of key system actuators is planned to enable testing of proportional controllers. The LBL controller may be modified to execute both ON/OFF and proportional-based control algorithms. Commercial controllers will be tested at the LBL facility and will be compared with the LBL controller. Both simple and microprocessor controllers will be evaluated. Optimized control strategies will be compared with simple preprogrammed ones to determine whether optimizing strategies are useful in the operation of fairly simple solar systems scaled for residential buildings. Computational models will be used as an aid in assessing the controller performance, and the experimental effort will verify the model predictions.

REFERENCES

1. M. Wahlig, E. Binnall, J. Dillworth, C. Dols, R. Shaw, W. Siekhaus, Controller Development for Solar Heating and Cooling Systems, Lawrence Berkeley Laboratory report, LBL-5982 (Energy and Environment Division Annual Report, 1976).

2. M. Wahlig, Control System for Combined Solar Heating and Cooling Systems, Lawrence Berkeley Laboratory report, UCID-3716, January 1975.

3. M. Wahlig, E. Binnall, C. Dols, R. Graven, F. Selph, R. Shaw, M. Simmons, Control System for Solar Heating and Cooling, Lawrence Berkeley Laboratory report, LBL-

LBL BUILDING 90 SOLAR DEMONSTRATION PROJECT

T. Webster

INTRODUCTION

This project was one of eleven projects selected to be part of the FY 1977 DOE Facilities Solar Demonstration Program, a portion of the Solar Federal Buildings Program. The objectives of this program are to establish model procedures and techniques for assessing and implementing solar systems for federal facilities, and to assist in energy reduction within DOE facilities.

The following criteria were used to select projects for this initial program:

- Buildings should be suitable for retrofitting; i.e., possessing orientation, location, and configuration amenable to solar.
- Solar space and hot-water heating should be emphasized.
- Buildings should be typical government buildings.
- Design and construction should not cost more than $200,000.

These projects are funded by the DOE Division of Solar Energy through the Construction, Planning, and Support Division. LBL Plant Engineering is responsible for design and construction of the project with assistance provided by the LBL Solar Group.

Building Description

LBL Building 90 was constructed in 1958 and is a typical three-story office building (with forth-story addition and basement) with approximately 88,000 gross ft^2 of floor-space. It houses about 400 people from the Energy and Environment, Earth Sciences, and Engineering and Technical Services Divisions. The building is located in an open hill-top area, has a front wall facing southwest, and has no obstructions to sunlight around it. About 46% of the building walls are single-pane glass; the remainder are 1-in. insulated panels. The roof is tar and gravel on top of 2 in. of insulation supported by corrugated metal decking.

The heating system is a 100% outside-air, hot-water system consisting of three heating elements: intake-air preheating coils, duct heating coils, and perimeter convection coils. The water is currently heated by two gas-fired boilers. Domestic hot water is heated by an indirect heater with hot water supplied by the boilers.

A number of measures have already been taken to conserve energy in the building: time clocks switch fans off at night, automatic dampers reduce the amount of ventilation-air on cold days, controls switch off hot-water circulation when outdoor temperature is above 60^oF, and domestic hot water is set at 110^oF. In addition, a return air system is currently being designed to reduce consumption further.

ACCOMPLISHMENTS DURING 1977

In the preliminary design, the solar heating system consisted of a saw-tooth array of flat-plate solar collectors mounted on galvanized steel trusses on the roof of the building. Because of the design of the existing roof, the support structure must be attached to the building's structural-members through roof penetrations. The collectors were oriented due south (35^o off building axis) and tilted at 48^o (latitude + 10^o) for maximum annual space heating performance. The collectors would drain back to storage when shut off at night to protect against freezing. A high-temperature cut-off would limit maximum storage temperature in the summer. A pressurized, insulated storage tank was to be buried in the back of the building under a roadway. The existing main circulating pumps would supply solar-heated water from storage to the existing heating system. Domestic hot water is heated by the existing indirect heater, utilizing the solar-assisted main heating water.

The preliminary system performance estimates were calculated using the procedure in an early draft of the ERDA Facilities Solar Design Handbook being prepared at Los Alamos Scientific Laboratory (LASL). Assuming the building to be one zone, building loads for this analysis were calculated with the NECAP building-simulation computer program at LASL. Monthly insulation data was obtained from a draft of the LBL Solar Data Manual being prepared by the LBL Solar Group.[2] The cost optimization procedure of the Solar Design Handbook was used to evaluate optimum system size. This analysis, based on the system cost estimate and assuming existing fuel prices ($\$2.86/10^6$ btu fuel oil at LBL), indicated the system would not be cost effective. However, the analysis did indicate what system size would practical for a demonstration project.

The Preliminary Proposal[3] contains estimates for systems of two sizes: 2300 ft^2 with a 53% solar fraction, the maximum collector area that could easily fit on the roof; and 1250 ft^2 with a 33% solar fraction, recommended as a practical minimum for demonstration purposes.

Final Design

The 1250 ft^2 system was authorized by DOE for design in March 1977. A modification of the design to include one bank of on-site-constructed collectors was approved in April. The schematic flow diagram in Fig. 1 shows the 1977 final system design. This system is basically the same as the preliminary design, but a number of changes and improvements were made:

1. The three-dimensional trusses for collector support have been abandoned because of high cost. Prefabricated supports are currently being evaluated.
2. Storage was reduced from 2500 gal to 2000 gal and was relocated above ground.
3. Collector "drain down" was abandoned because of possible operating problems and low incidence of freezing in this locality. Storage water will be pumped through collectors during freezing weather to protect them against freezing.
4. To limit system temperature in summer, water will be circulated through collectors at night when storage is greater than 180^oF.

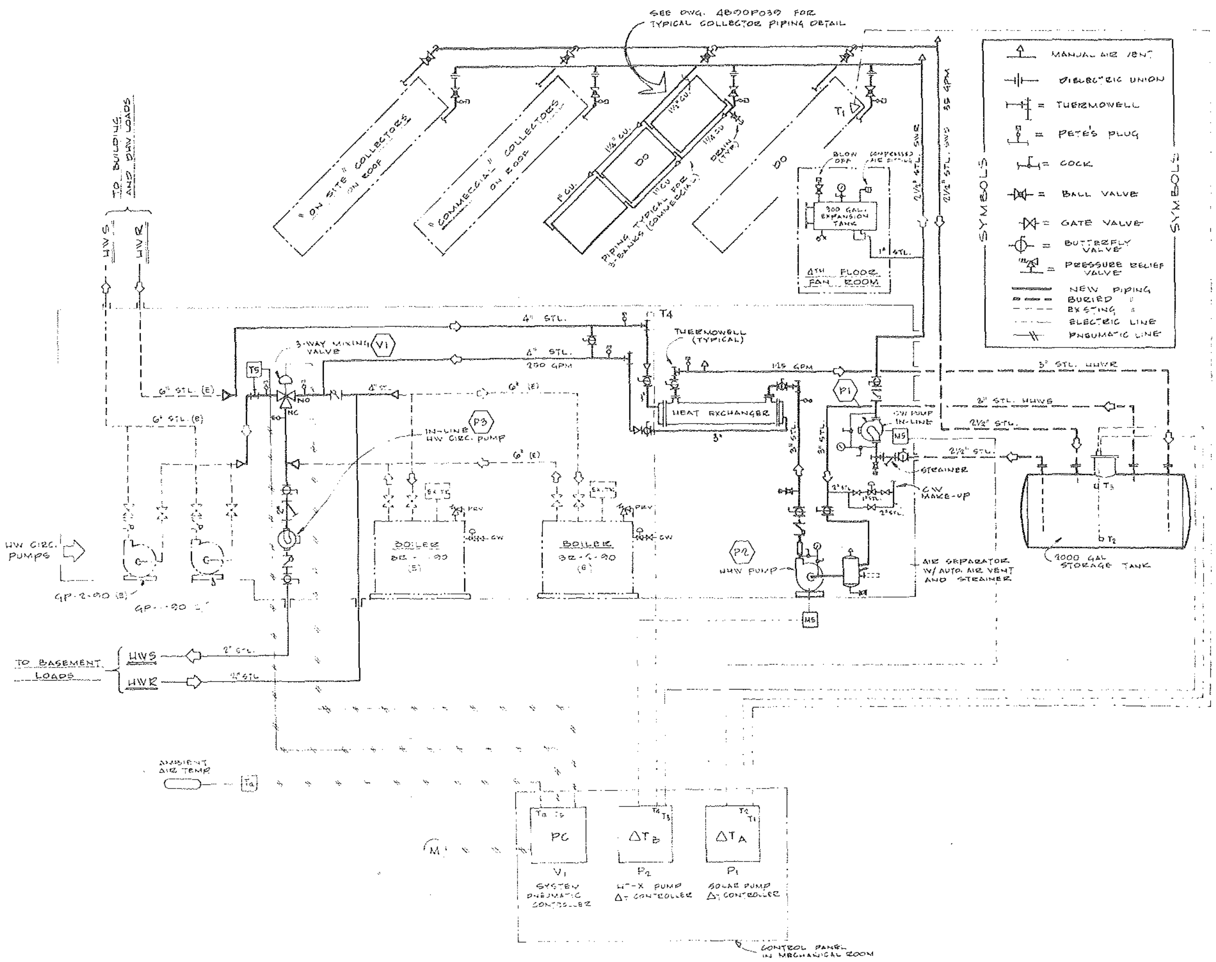

Fig. 1. Bldg. 90 solar heating system schematic diagram. (XBL 781-6781)

5. A heat exchanger was added between storage and the existing heating system because of pressure limitations of the boiler.

6. The expansion tank was relocated to the 4th floor to minimize tank size and cost.

7. A three-way modulating valve will be installed to reset heating-supply water temperature when warranted by outdoor temperature.

8. The basement heating system was arranged to operate independently of the solar system, to reduce complexity of system and controls.

The initial analysis with the CAL-ERDA building-simulation computer program indicates that with loads reduced by addition of a return-air system, the lower temperature (120°F) supply water would meet heating loads with the existing duct-coil system. A final pre-construction cost estimate for the system was $131,000.

PLANNED ACTIVITIES FOR 1978

System performance and system operating parameters will be re-evaluated using a new version of the CAL-ERDA computer program. Collectors will be bid prior to construction bidding so that design details can be completed. Final design drawings and specifications will then be completed and released for bid. Construction should be completed by the fall of 1978. An instrumentation system is planned and will be installed along with the system. The instrumentation data will be transmitted over phone lines to IBM in Huntsville for analysis.

REFERENCES

1. ERDA Facilities Solar Design Handbook, ERDA 77-65, August 1977.

2. California Solar Data Manual, LBL Energy and Environment Division, January 1977 (Draft).

3. Preliminary Design Proposal, LBL, March 1977.

DEVELOPMENT OF SOLAR-DRIVEN AMMONIA-WATER ABSORPTION AIR CONDITIONERS AND HEAT PUMPS

K. Dao, R. Wolgast, and M. Wahlig

INTRODUCTION

The objective of this project is the development of absorption refrigeration systems for solar heating and cooling applications. Absorption cooling has been the leading solar candidate for residential and small commercial applications. However, several liabilities of the present state of this technology have served to inhibit more widespread utilization; namely, the need for water cooling towers (and their associated maintenance problems) as an essential component of the LiBr-H_2O absorption chillers most commonly used, the constant value of the coefficient of performance (COP) with increasing temperature (in constrast to Rankine cycle systems, which have increasing values of COP with increasing temperature), and the high cost of these units.

The approaches adopted by the LBL effort are directly aimed at overcoming these obstacles. Ammonia-water has been selected as the refrigerant-absorbent pair because the condenser and absorber components for these working fluids can be air-cooled rather than water-cooled, thus obviating the need for water cooling towers. Currently under investigation at LBL are advanced absorption chillers whose COP increases with temperature, maintaining an almost constant fraction of the Carnot COP over a wide range of operating temperatures. Reports will be prepared on these cycles when their analyses are completed. The cost problem is being addressed with the assistance of industrial firms. LBL's efforts consist of striving to design prototype chillers that use heat exchangers and other components that can be fabricated at reasonable cost, and continuing to use the resources of industrial consultants who have experience in the practical building and marketing of these units. In addition, the services of industrial firms are being used to fabricate the major components of the chiller and to provide cost estimates for mass produced components.

Finally, it is recognized that these absorption-cycle units may also be operated as heat pumps for solar heating purposes. Designs including provision for operation in both air-conditioning and heat-pump modes are under study. Such dual use is expected to enhance the cost-effectiveness of these absorption-cycle systems.

The first phase of this project consisted primarily of the design and fabrication of a test model,[1] using as a base the condenser, absorber, precooler, evaporator, and solution-pump components from an Arkla gas-fired, ammonia-water absorption chiller. The modifications for operation with solar-heated hot water included the addition of the following components: generator (a packed-tower, counter-flow heat exchanger), preheater and rectifier (both shell-and-tube, one-pass, counterflow heat exchangers), storage tanks, adjustable expansion valves, and measurement instruments.

This version of the air conditioner permitted operation at temperatures near 200°F. This temperature level, coupled with the use of air cooling rather than water cooling for the condenser and absorber coils, meant that the chiller was being operated close to the cutoff point (that low temperature where the generator ceases operation). Calculations had indicated that chiller operation was possible under these conditions. The main objectives of the experimental test program were, therefore, to determine the stability of operation near cutoff conditions and to determine experimentally the accuracy of the calculated values of operating temperatures, pressures, and coefficient of performance.

Completed in late 1976,[2] this first phase of the air conditioner development has demonstrated experimentally that it is technically feasible to use the ammonia-water absorption cycle solar cooling with generator temperatures $\geqslant$195°F (when the condenser and absorber temperatures are $\leqslant$110°F, and the evaporator temperature is $\geqslant$45°F). In addition, it was discovered that several changes should be incorporated in subsequent designs, such as: (a) replacement of the packed-tower generator with a forced-circulation type, thus increasing the heat-exchange effectiveness and reducing the cost of this component simultaneously; (b) use of a combined preheater-rectifier for the vapor path, instead of using separate components for these functions; and (c) reduction of the pressure-drop across the absorber (thereby reducing the evaporator temperature) by the introduction of more parallel flow paths in the absorber stage.

ACCOMPLISHMENTS DURING 1977

The second phase of the project continued the development of the single-effect, ammonia-water absorption air conditioner. A completely new 3-ton unit is being constructed, taking into account all the results and conclusions of the first-phase experimental tests. All parts are designed for solar heat input in the range of 200°F-240°F. The heat exchangers will be tube-in-tube for high effectiveness at low cost. A schematic diagram of the unit being fabricated is shown in Fig. 1. Figure 2 shows the physical lay-out of the unit.

The objectives of this phase of the development are:

(1) to test the effectiveness of the low-cost, tube-in-tube heat exchangers used for the generator and preheater;

(2) to measure the increase in COP due to the use of a combined preheater-rectifier for the vapor and solution paths, instead of using separate com-

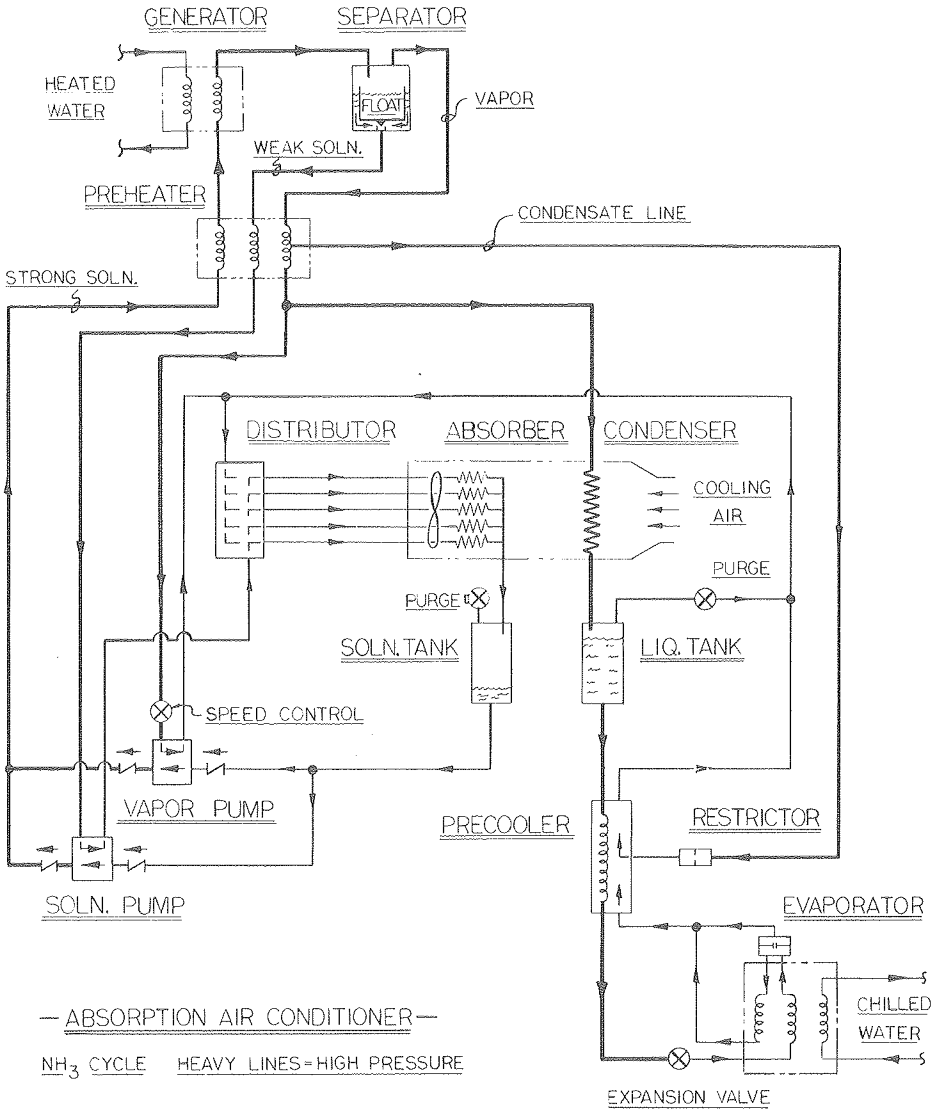

Fig. 1. Schematic diagram of the single-effect absorption chiller being fabricated. (XBL 781-6923)

ponents for these functions (calculations showed an increase of about 7 to 9% in COP);

(3) to test the efficiency of the newly designed pair of reciprocating pumps. One pump uses the pressure drop of the weak solution (otherwise wasted) to pump about 70% of the strong solution from the absorber to the generator. The remaining strong solution will be pumped by the other paired reciprocating pump which is driven by a small flow of high-pressure ammonia vapor from thegenerator These pumps replace the usual electrically driven diaphragm pumps;

(4) to estimate the production cost of the unit. The unit was designed with special attention to reducing the cost of the components and of the overall assembly.

The design, working drawings, and fabrication have been completed for all components except the generator and the evaporator, whose fabrications should be finished by late February 1978. The major components, namely the preheater, the pumps, the condenser-absorber, and the generator are being fabricated by outside manufacturing companies. The remaining components are being fabricated by LBL shops.

The new pumps, called "double-feedback-controlled, tandem, reciprocating pumps" have been fabricated and tested under no-load conditions. The testing used nitrogen gas at 10 to 60 psig as the driving fluid, while ambient air was used as the pumped fluid. The purpose of this initial testing was to confirm the operation of the feedback control of the pumps. Test results showed that the pumps are self-starting and their speeds can be controlled from 0 to about 300 cycles per min. Further tests are under way to determine the performance

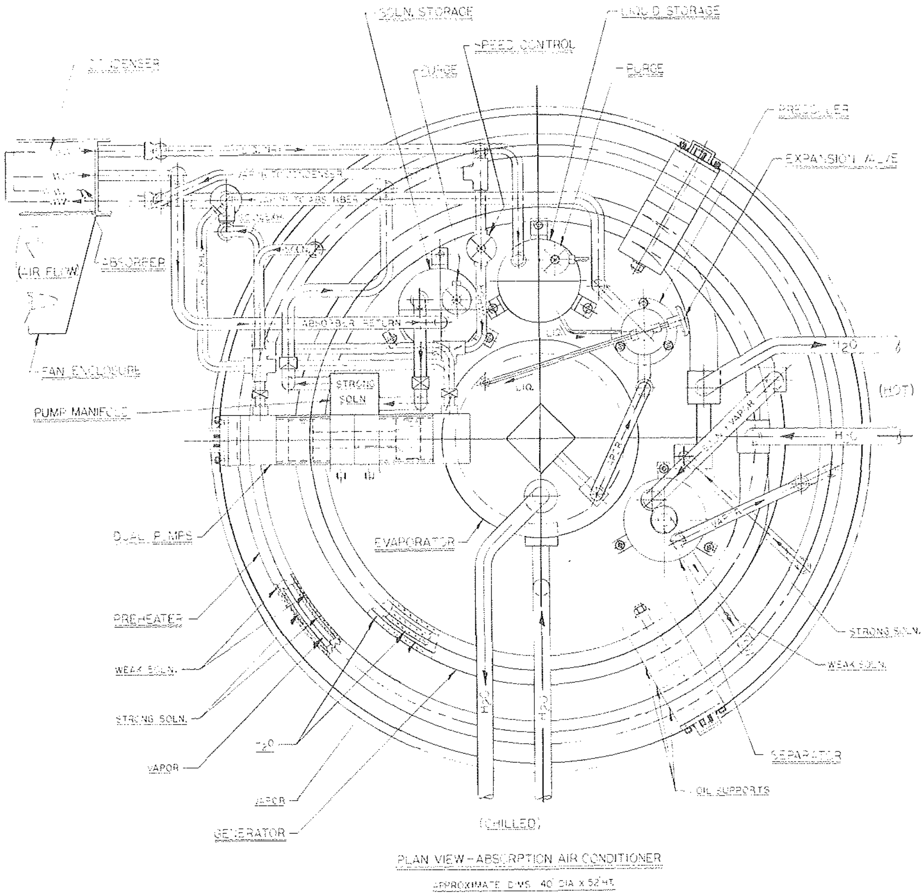

Fig. 2. General lay-out of the unit being fabricated.
(XBL 781-6924)

of the pumps under heavy liquid loads. The assembly and installation of the new chiller are expected to be completed by late April 1978. Testing, therefore, should begin in May 1978.

The expected performance of the new chiller is as follows, taking into account the measure pressure-drop characteristic of the fabricated preheater:

Capacity:	3.5 tons
Coefficient of performance:	0.71
Hot water temperature:	225°F (input to unit)
Condensing temperature:	112°F
Chilled water temperature:	45°F (output to unit)

Preliminary analysis of the "double-effect, regenerative, absorption cycle" has been completed. The performance of this new advanced adsorption cycle was calculated for a fixed condenser-absorber temperature T_O of 110°F, for a fixed evaporator temperature T_E of 40°F, and for boiler temperatures T_B variable from 160° to 300°F. Calculations using ammonia-water as the refrigerant-absorbent pair showed that the COP varied with boiler temperature T_B as follows:

T_B(°F)	160	180	200	220	240	260	280	300
COP	0.05	0.36	0.55	0.74	0.85	0.94	0.99	1.00

The conceptual design of another new, advanced absorption cycle has also been completed. This cycle is called the "single-effect, regenerative absorption cycle." More accurate calculations are needed to confirm the estimated COP of this cycle, which can be in the range of 65 to 80% of the Carnot COP. The Carnot COP for this cycle is defined as:

$$(T_B - T_O)(T_E + 460)/(T_B + 460)\ (T_O - T_E)$$

PLANNED ACTIVITIES FOR 1978

The installation and testing of the new, single-effect absorption air conditioner will occur during the first part of 1978, followed by an evaluation and report of the testing program results. Assuming that test results substantiate the performance goals of this single-effect chiller, as described above in the 1977 program description, commercialization opportunities for this unit will be pursued during the latter part of 1978. This will be accomplished primarily through contacts with industrial consultants to this project, and also through direct contact with other representatives of companies currently active in the air conditioning industry.

The work on the analysis of advanced absorption cycles will continue into the middle part of 1978. At that time a specific system will be designed that will be capable of achieving an approximately constant fraction of Carnot efficiency over the input temperature range of 170°F to 300°F. This unit will then be fabricated and tested, with scheduled completion by the end of 1979.

REFERENCES

1. M. Simmons, R. Wolgast and M. Wahlig, A Solar-Driven Ammonia-Water Absorption Air Conditioner, Lawrence Berkeley Laboratory report, LBL-3293 (August 1975).
2. K. Dao, M. Simmons, R. Wolgast and M. Wahlig, Performance of an Experimental Solar-Driven Absorption Air-Conditioner-Annual Report, Lawrence Berkeley Laboratory report, LBL-5911 (January 1977).

RADIATIVE AND PASSIVE COOLING

M. Martin, P. Berdahl and M. Wahlig

INTRODUCTION

It has long been known that the earth's surface cools more rapidly on cloudless nights than it does under overcast conditions. Infrared radiant energy, emitted from the surface, passes through the clear atmosphere into outer space. Under overcast conditions, the cloud layer itself emits infrared radiation that is in turn absorbed by the earth, thus inhibiting rapid cooling. Even under clear-sky conditions, atmospheric gases (chiefly carbon dioxide and water vapor) emit substantial amounts of infrared radiation, and the radiative balance achieved is popularly known as the greenhouse effect.

The net amount of energy that can be radiated from a surface on the earth depends on both the physical characteristics of the surface, and on the amount of atmospheric back-radiation incident on the surface. A number of correlations have been proposed to relate the total amount of atmospheric infrared radiation to the local air temperature and humidity.[1] However, few measurements have been made in which the spectral details of the atmospheric infrared radiation have been recorded, and these measurements have typically been made on a single night, with no attempt to correlate details of the spectrum with prevailing weather parameters.[2,3]

The objective of this project, which was started in March of 1977, is to assess the radiative cooling resource in order to determine the extent to which radiative cooling can supplement or replace refrigeration systems for the space cooling of buildings. Radiative cooling is known to be quite effective in arid regions, and the most promising areas for application are probably those in which large diurnal temperature fluctuations occur. The extent to which a suitably designed radiator system could contribute to cooling a building in more humid areas has not yet been investigated. Furthermore, the development of selective emitter surfaces, which radiate preferentially in the 8 to 12 micron region of the spectrum (where the atmosphere is most transparent),[4] presents the possibility of extending the use of this technique to climatic regions where it would not previously have appeared feasible.

It is important that radiative cooling not be considered in isolation from the other two important passive cooling methods that have been in use for centuries, namely, convective and evaporative cooling processes. A current example of the application of these techniques is found in the Skytherm system,[5] in which a plastic-covered roof pond forms both the thermal storage system and the radiating, convecting, and possibly evaporating surface. One of the goals of this project is to develop computer subroutines (to be used with a dynamic, building loads program) to predict the performance of a variety of passive cooling methods under various climatic conditions.

ACCOMPLISHMENTS DURING 1977

At the beginning of the project in March of 1977, work was started on two complementary tasks: the development of a computer model to predict atmospheric infrared radiation as a function of wavelength; and the design of a spectral radiometer, four of which are to be installed throughout the United States to collect atmospheric radiation data during the summer of 1978.

An existing computer program (LOWTRAN),[6] which calculates the spectral transmissivity of the atmosphere under a variety of weather conditions, was modified to predict the infrared emittance from the atmosphere as observed at ground level. Input to this program includes temperature and water vapor profiles, aerosol content, cloud cover, and elevation above sea level. A sensitivity analysis was performed to assess the effects of changes in these parameters on the spectral radiance.

The spectral radiance of the atmosphere in the vertical direction is plotted in Fig. 1 under three conditions, to illustrate the effect of water content on the radiation emitted. The solid curve represents the radiance calculated for a precipitable water vapor column of 3 cm. The upper curve shows how the atmospheric radiance increases as the water vapor content is doubled, and the lower curve shows a decreased radiance corresponding to an atmosphere with half the original amount of vapor.

Figure 2 shows four different spectral radiance calculations representing the infrared radiation received from the horizon, from the zenith direction, and from two intermediate

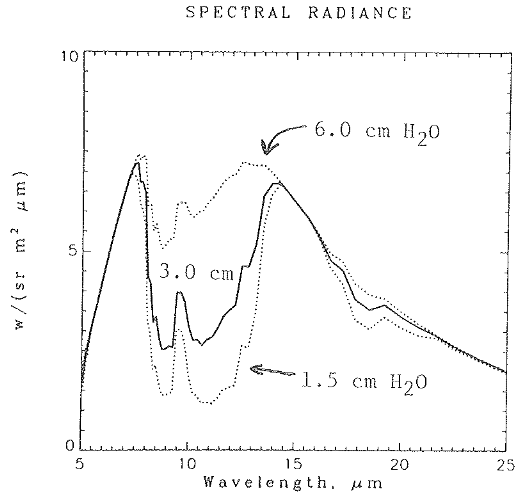

Fig. 1. The solid curve shows the atmospheric radiance from the zenith, (3 cm precipitable water vapor). The upper dotted curve shows the radiance when the water vapor is doubled (6 cm). For the lower curve the water vapor is halved (1.5 cm).

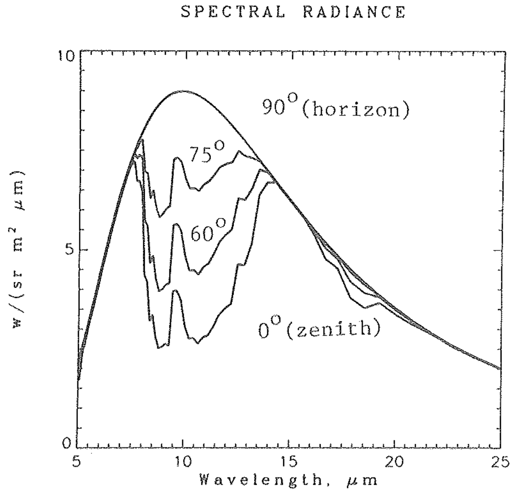

Fig. 2. Spectral radiance of a clear, midlatitude summer atmosphere. Zenith angles (from top to bottom) are: 90°, 75°, 60°, 0°.

angles. Work is under way to obtain the spectral radiance received from a hemisphere incident on a flat surface which is capable of being tilted in an arbitrary direction.

The second task, undertaken simultaneously, was to develop an infrared spectral radiometer suitable for unattended field use. The design is based on the Barnes model 12-880 radiometer equipped with an eight-position filter wheel and pyroelectric detector. The prototype assembly includes a stepping mechanism to allow the filter wheel to be positioned automatically, and a rotating mirror assembly to direct the infrared beam alternately in the vertical direction and into a reference blackbody cavity. The entire instrument will be under microprocessor control and will be accessible to LBL through a MODEM telephone link. The signal received through each of the eight filters will be stored every half hour and transmitted to LBL from the random-access memory of the microcomputer, at intervals of one or two days. Dry-bulb and wet-bulb temperature readings will be recorded with each set of infrared measurements.

PLANNED ACTIVITIES FOR 1978

Four field radiometers, based on the prototype, are scheduled for installation in May of 1978. These instruments will collect data for four months, at locations selected on the basis of summer cooling requirements and climatic diversity. The results will be correlated with temperature and humidity data, and with radiosonde measurements where available.

The experimental data will be used to verify the output from the atmospheric infrared radiance computer program (described in the previous section). In parallel, the subroutine used to calculate the radiance will be integrated into a dynamic building loads program that can be used to predict the performance of a variety of radiative cooling system designs.

REFERENCES

1. W. D. Sellers, Physical Climatology, Chapter 4, University of Chicago Press (1965).

2. E. E. Bell, L. Eisner, J. Young, and R. A. Oetjen, J. Optical Soc. Amer. 50, 1313 (1960).

3. K. Ya. Kondratyev, Radiation in the Atmosphere, Section 9.8, Academic Press (1969).

4. S. Catalanotti, V. Cumom, G. Piro, D. Ruggi, V. Silvestrini, and G. Troise, Solar Energy 17, 83 (1975).

5. H. Hay, "Atascadero Residence" in Passive Solar Heating and Cooling Conference and Workshop Proceedings (Alburquerque, New Mexico, May 18-19, 1976. Available from NTIS.

6. J. E. A. Selby, E. P. Shettle, R. A. McClatchey, Atmospheric Transmittance from 0.25 to 28.5 Microns: Supplement LOWTRAN 3B, Air Force Geophysics Laboratory Report (1976). Available from NTIS.

NITINOL ENGINE DEVELOPMENT

R. Banks, R. Kopa, M. H. Mohamed, and M. Wahlig

INTRODUCTION

The objective of the Nitinol Engine Development Project is to determine the feasibility of using a dynamic phase change in a crystalline solid as the basis for conversion of heat energy to mechanical work. Temperature-dependent changes in the elastic properties of certain Shape Memory Alloys make possible the conversion of relatively low-temperature heat to mechanical work by means of "solid state" heat engines. Such engines show promise of having competitive conversion efficiencies and capital costs when compared to other types of engines for low-temperature energy conversion.

Of the dozen or more binary and ternary alloy systems known to exhibit the Shape Memory Effect (SME), the project has concentrated investigation on the nickel-titanium alloy "55-Nitinol," developed at the U.S. Naval Ordnance Laboratory, Silver Spring, Maryland, in the late 1950's.[1] In addition to its SME properties, Nitinol possesses favorable mechanical characteristics such as high tensile strength and corrosion resistance, as well as potentially lower production costs than most other Shape Memory Alloys now known to exist.

A prototype Nitinol heat engine has been in operation at the Lawrence Berkeley Laboratory since August 1973.[2] Since that time, several iterations of engine design have led to an improved understanding of the important practical considerations in applying this material to energy conversion in continuously cycling heat engines.[3] These studies, as well as experimental and theoretical investigation of the material's thermodynamic and metallurgical properties, have confirmed the potential for developing useful and practical mechines for the recovery of thermal energy from low-grade or waste heat.

ACCOMPLISHMENTS DURING 1977

Work Continuing from 1976

In early 1977, a prototype engine designed to fulfill some of the unique requirements inherent in using a solid, rather than a fluid, as the working medium of a heat engine was completed and submitted to preliminary tests. This prototype, known as the Nitinol Cam-Track engine, was designed to permit wide flexibility in the mechanical cycle to which the Nitinol working elements were coupled, so as to match the mechanics of the device as closely as possible to the dynamic behavior of the Nitinol wire elements;[4] this design is illustrated in Fig. 1. The Cam-Track engine, an experimental mechanism, was configured and scaled so that it could also function as a prime-mover to be integrated into a solar-powered, vapor-compression air-conditioning system, when proven to operate at sufficiently high power-output levels. Figure 2 shows the completed engine.

Preliminary operation of the Cam-Track engine indicated that the mechanical cycle, arrived at empirically in the course of developing and testing the concept, was consistent with enhanced working lifetime of the Nitinol power elements. Problems that were encountered in the areas of mechanical friction losses and engine instrumentation, however, suggested that improved performance of the Cam-Track engine would be most efficiently approached through experimental simulation studies, conducted prior to initiating actual design modifications on the engine itself. Accordingly, program emphasis for the balance of the year shifted towards completion of the design and fabrication of the fully instrumented cycle simulator (described below), and initiation of experimental and theoretical investigations of the Nitinol thermodynamic cycle.

Work Begun in 1977

The design of a new electronically controlled Cycle Simulator for a parametric study of Nitinol characterization was begun early in 1977. In this device, Nitinol materials will be subjected to simulated engine cycles in which a number of test parameters are systematically varied so that a "map" of efficiency values can be obtained as a function of operating (and material) parameters. Such a map can serve as a guide for choosing the optimal design of a Nitinol heat engine, for comparing the theoretical and experimental conversion efficiencies of Nitinol, as well as for further research and development of other promising thermoelastic materials. In addition to conversion efficiency, an important goal is the determination of an engine cycle which offers the lowest progressive degradation and irreversible

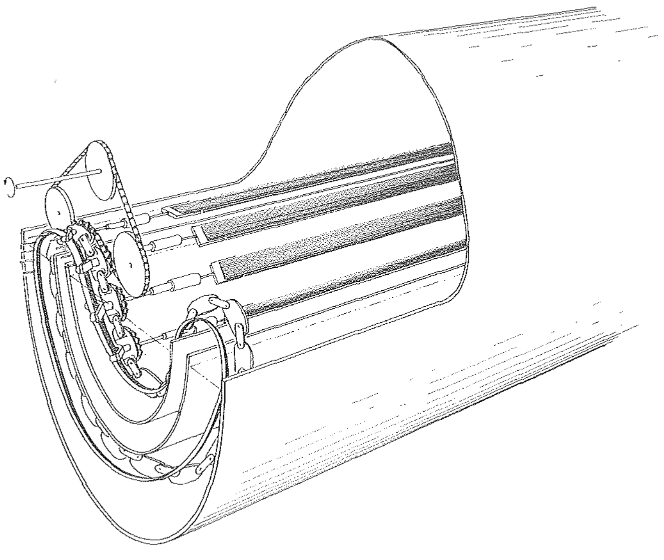

Fig. 1. Cutaway view showing the design of the Nitinol Cam-Track engine. (XBL 767-3131)

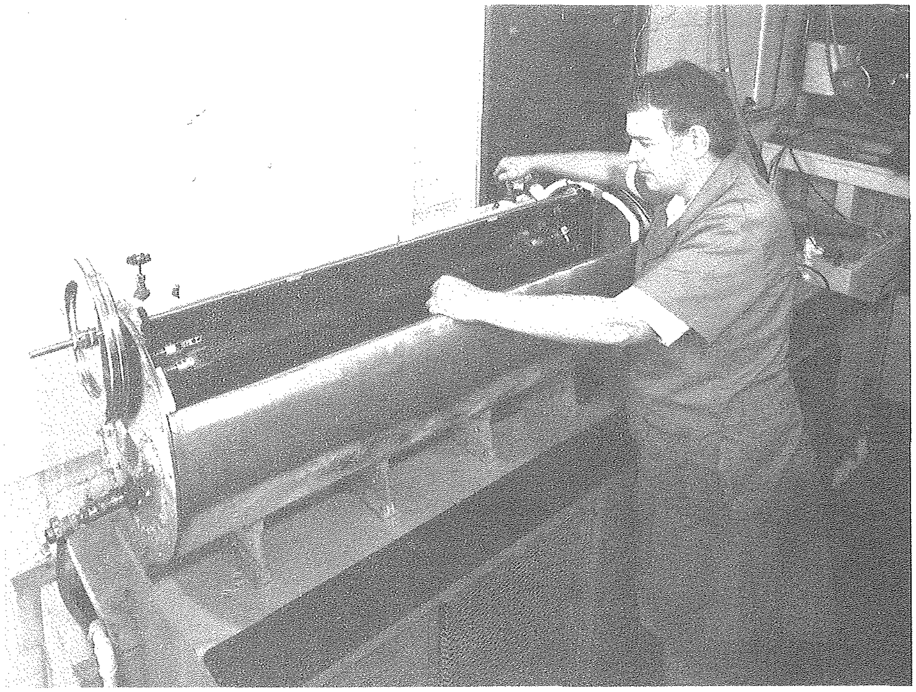

Fig. 2. The Nitinol Cam-Track engine. (CBB 755-4474)

damage, and therefore the longest life of the Nitinol-wire elements.

The objective of the Cycle Simulator design was the realization of a test system in which a single Nitinol wire could be subjected to specific classes of thermodynamic cycles (e.g., isothermal, adiabatic, constant stress, "programmed stress," heat recuperation, etc.) as selected during this investigation. The test parameters, which can be varied singly or in combination, include: stress levels, stress rates, percent of elongation of the wire, temperature levels, heating and cooling rates, cycling speeds, etc. The system is fully automated and capable of continuous operation for millions of cycles. The stress-elongation relationship (work diagram) and all pertinent test data are automatically recorded on a video tape at predetermined intervals.

Materials Studies

The mechanical and thermodynamic behavior of Nitinol in relation to the martensitic transformation of the Shape Memory Effect has been under investigation both theoretically and experimentally. The objective of this investigation is to optimize the performance of Nitinol in energy conversion devices with reference to the thermodynamic conversion efficiency, and the fatigue strength of the material.

Work done so far has concentrated on the thermodynamic conversion efficiency and the parameters that determine this efficiency. For a given alloy composition these parameters are: (1) the transformation temperatures and their functional dependence on external stresses, heat treatment, and thermal cycling; (2) latent heat of transformation, as determined by transition entropy and the equilibrium transition temperature; (3) the recovery stresses developed by Nitinol upon heating (the upper limit of these stresses is restricted by the yield stress of the high-temperature phase); and (4) the specific heat of Nitinol.

Transformation temperatures and their functional dependence on external stress have been measured by means of a specially designed dilatometer. From these data the transition entropy has been calculated using a modified Clausius-Clapeyron equation. A method has been developed by which the equilibrium transition temperature can be determined from experimentally measured transformation temperatures.[5] The recovery stresses of Nitinol have been estimated as a function of strain, temperature, and the yield stress of the high-temperature phase. Experimental work is now in progress to compare the measured and predicted values of the recovery stress.

PLANNED ACTIVITIES FOR 1978

The cycle simulator work and the materials studied will be continued to identify rigorous parameters for the optimally efficient application of Nitinol to energy conversion in heat engines. Depending on the outcome of these studies, the information gained will be applied either to improving the performance of the Cam-track engine, or towards developing new concepts for high-performance Nitinol engines.

FOOTNOTES AND REFERENCES

1. The name of the alloy is derived from the chemical symbols for nickel and titanium, and the abbreviation of the Naval Ordnance Laboratory (now the Naval Surface Weapons Center) in Silver Spring, Maryland, It was here that the alloy's shape memory properties were first observed in the late 1950's.
2. R. Banks, "Nitinol Heat Engines," in Shape Memory Effects in Alloys, J. Perkins, ed. (Plenum Press, 1975).
3. H. P. Hernandez et al., Nitinol Engine Project Test Bed Report, Lawrence Berkeley Laboratory report, UCID-3739 (1975).
4. R. Banks and M. Wahlig, Nitinol Engine Development, Lawrence Berkeley Laboratory report, LBL-5293 (1976).
5. H. Mohamed, "On the Equilibrium Transition Temperature of Thermoelectric Martensitic Transformations," to be published in J. Mater. Sci.

CHEMICAL STORAGE OF THERMAL ENERGY

A. S. Foss and S. Lynn

INTRODUCTION

Economical energy storage is essential if solar power plants are ever to supply a significant fraction of the needs of a power grid. The purpose of this study is to develop technically feasible, efficient flowsheets for the use of the sulfur oxide system,

$$2SO_3 \rightleftharpoons 2SO_2 + O_2 \quad , \qquad (1)$$

and the methane system,

$$CH_4 + H_2O \rightleftharpoons CO + 3H_2 \qquad (2)$$

in energy storage. The forward reactions for these two systems are endothermic and can be used to absorb energy. The reverse reactions are exothermic and release the energy that has been stored. Both the forward and reverse reactions occur at temperatures above 500°C; however, storage can be at ambient temperature so that there is no energy dissipation during the storage period. This method of energy storage is thus suitable for incorporation with high-temperature power generation cycles and for long-term energy storage.

To place the costs of the chemical storage systems developed in this study in perspective, they must be compared with the costs of alternative storage systems. For such a comparison to be valid the assumptions made in costing must be equivalent. For this reason a flowsheet for a sensible-heat storage system is being developed as a part of the chemical-energy storage project.

Funding for this work was initiated in November 1975. During 1976 the major effort in the project was in flowsheet development. The major factors affecting system efficiency were identified, and the primary energy losses were made the subject of further study.

ACCOMPLISHMENTS DURING 1977

Chemical Storage

A major fraction of the effort during this year has been the development of computer simulations of the various steps of the process using the sulfur oxide system. This work has concentrated on the development of storage-process configurations, and on their integration in a manner that maximizes the overall heat efficiencies, with the steam cycle of a parallel solar power plant.

A simplified sketch of a flow sheet for this coordinated system is given in Fig. 1. Major features include operation of the heat-absorption step at 40 atm and operation of the heat-release step at 10 atm. These conditions enhance heat economy, help reduce equipment size, and allow the pumping of only liquids. The coordination of the storage system with the power plant involves SO_3 vaporization by 200-psi steam and the preheating of boiler feedwater in both the heat-absorption and heat-release steps. Estimation of the equipment costs for such a system is still in progress.

In all these evaluations, steam generation conditions have been taken to be 1000°F and 3000 psi; these permit turbine operation at the standard value of 2400 psi. One stage of reheat to 1000°F has also been incorporated. Details of the flowsheet were presented by Dayan et al. (1977).[1]

Calculations to date indicate that overall efficiency for the combined power plant and storage system (new electrical output/total thermal input) is about 30%. The total output of the storage system would be about 18% that of the daytime power plant, and could be delivered at a variable rate to meet the demand. These numerical results correspond to one set of values of a large number of parameters and are not necessarily optimum. Further work will be required to determine where the optimum lies.

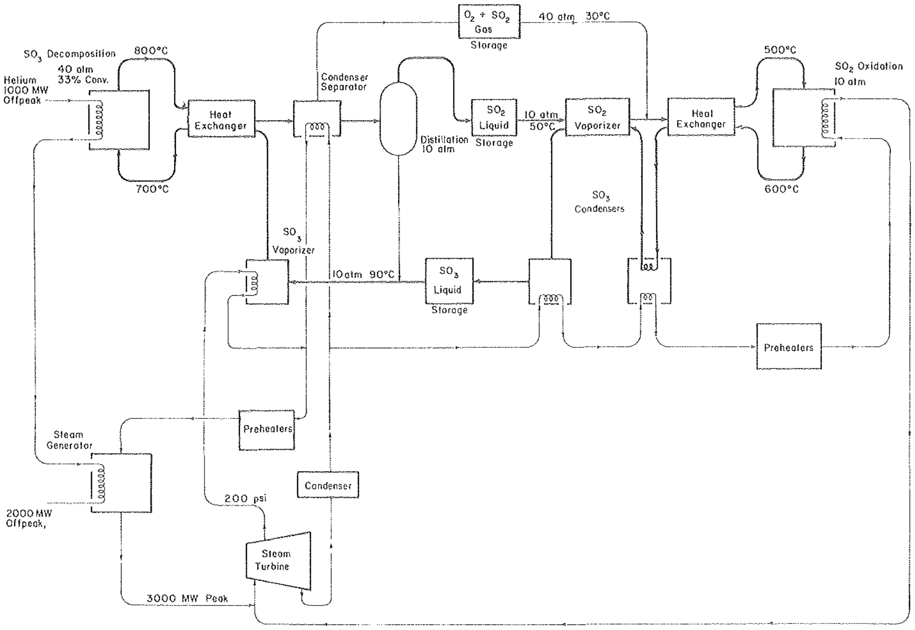

Fig. 1. Simplified flow sheet of sulfur oxide storage system co-ordinated with a steam power plant. (XBL 784-619)

Sensible-Heat Storage

The sensible-heat storage system is based on a design reported by Boeing (1976)[2] for use with a Brayton-cycle power plant. This design has been modified for application to a steam-cycle power plant. Further modification has been introduced to improve the overall thermal efficiency by taking advantage of the difference between the maximum collector temperature and the maximum steam-cycle temperature. When this temperature difference is of the order of 278°K, a thermal efficiency of the order of 95% is possible with the flowsheet that has been developed. The high efficiency results from cycling the sensible-heat storage system over the temperature range between the above limits.

In the Boeing design, helium is proposed for the cycle fluid. Preliminary calculations indicate that, for the flowsheet proposed here, water vapor at a pressure of about 500 psia would have a number of advantages. Lower cost of the heat-transfer medium is only one. The higher molar heat capacity of water vapor permits a lower volumetric flowrate for a given rate of heat transfer. That, in turn, reduces significantly the parasitic power requirement for its circulation. The use of water vapor will also affect the design of the heat-storage system and the power plant in ways that are currently being studied.

PLANNED ACTIVITIES FOR 1978

Comparison of Storage Systems for Solar Electric Power Plants

The work to date has concentrated on the process design and operating details of two chemical storage systems (the sulfur-oxide and methane systems). One major effort for the coming year will be the comparison of the technical features and economics of these two systems for solar heat storage. Points for comparison include the ease of incorporation of the endothermic reactors into the central receiver system, integration of the exothermic reactors with the power generation system, degrees of storage-system interdependence on power plants operating in parallel with storage systems, efficiency differences related to the intrinsic chemical and thermodynamic properties of the chemical reactions, ease of storage of the gases and liquids, materials problems, and strengths and weaknesses of the systems when operating under diurnal cycles.

Cost Estimation of Sensible-Heat Storage

The Boeing sensible-heat storage system was not designed for use with a steam-cycle power plant. Hot helium was used directly in gas turbines operating on a Brayton cycle. It has therefore been necessary to redesign this system, to some extent, to make it compatible with steam-cycle power generation. The overall efficiency of the storage system appears to be improved when this is done. The costs of this redesigned system will be estimated during the coming year. The thermal efficiency will also be calculated. Both will be compared to the respective estimates made in the Boeing design and to alternative storage systems being proposed for steam-cycle power plants.

REFERENCES

1. J. Dayan, A. S. Foss, and S. Lynn, "Evaluation of a Chemical Heat Storage System for a Solar Steam Power Plant," 12th Intersociety Energy Conversion Engineering Conference (Washington, D.C., September 1977).

2. Boeing Engineering and Construction Co., Advanced Thermal Energy Storage Systems, U.S.E.R.D.A. Report, Contract EY-76-C-03-1300 (December 31, 1976).

PASSIVE SYSTEMS ANALYSIS

R. C. Kammerud and T. Borgers

INTRODUCTION

Essentially all buildings are passively heated, and/or cooled to some extent by virtue of 1) insolation on exterior surfaces, 2) insolation entering windows, and 3) controlled and/or uncontrolled ventilation. A substantial fraction of the heating load is met naturally by insolation on the building surfaces, and some portion of the cooling load is often an unfortunate by-product of this same building/environment interaction. In order to meet even greater fractions of the heating and/or cooling loads by passive means, the collection, dissipation, storage, and transfer of thermal energy within the boundaries of the building must be understood and quantified in terms of the building parameters and the climatic and environmental conditions under which the building is used. Additionally, this generalized understanding of thermal performance can lead to improved strategies for control of thermal energy flow and therefore result in improved control of the comfort conditions in the structure.

The objective of this project is to develop and validate the analytic tools on which the generalized understanding of the thermal performance of both residential and commercial buildings can be based. These tools will be utilized in the evaluation of passive solar and large thermal mass designs, and in the definition of design and operating guidelines for passive systems. The analysis capabilities will be provided in existing public domain computer programs (BLAST and Cal-ERDA) for building energy-analysis and will therefore be available to the building designer and engineer, the solar and conservation researcher, and those segments of the community involved in the regulatory processes.

Technical Approach

Over the past year there have been substantial efforts to improve building-energy analysis capabilities. Two new programs have been developed, BLAST and Cal-ERDA. The structures of the programs are very similar in that they have separate Loads, Systems, Plant routines; and both incorporate "simple," user-oriented, building-description language inputs. Both of these programs take into account features such as construction details, surface properties, floor plan, HVAC system and controls, internally generated loads, and occupancy. This project focuses on improving and modifying the two programs in those areas where existing capabilities are expected to be inadequate for passive systems, and adding algorithms and models which describe generic passive systems. The two programs to be modified are not redundant; they complement one another. Both are required to provide analysis capabilities that include commercial buildings.

Primarily, the programs differ in the type of load calculation performed. BLAST uses a thermal-balance technique, in which energy balances on all surfaces and on room air are simultaneously performed in response to excitations such as insolation, lighting loads, etc. It takes into account the radiative, conductive, and convective components of the energy flow at each inside and outside surface. The calculation produces all surface temperatures, the air temperature, and the building (zone) load which is then used as input to the System and Plant routines. The primary limitation of this technique is the number of surfaces that can realistically be balanced simultaneously. Its strength is that it provides a desirable format for model development and validation, because the component models have physical descriptions. The operational parameters and equations of the modeled component and its interactions with the rest of the building elements are described in an intuitive, rather than mathematical, manner.

Cal-ERDA uses an approximate procedure for calculating the envelope and zone loads. To compute the heat gain to a space, and the resulting zone loads on the heating or air conditioning system, weighting factors are used. The weighting factors are a time-series of numbers which characterize the time delay between instantaneous heat fluxes and zone HVAC loads for the structure; they therefore include the effects of the mass and absorptance of the zone furnishings, floors, and partitions. The load is not a simultaneous response to many excitations, as in the thermal balance technique, but is a sum of approximate responses to individual excitations. The advantage of using this technique is the efficiency and speed of the resulting loads calculation; a large set of simultaneous equations need not be solved. An additional simplifying assumption used in Cal-ERDA is that the load calculation is performed at a constant inside-air temperature. The actual temperature and load are then obtained by perturbation techniques. The combination of constant-temperature calculations and the use of weighting factors and perturbation techniques contributes to Cal-ERDA's speed of calculation and makes possible the extensive multizone capabilities required in analyzing commercial buildings.

The weighting factors and perturbation coefficients used in Cal-ERDA have been derived by parametrically studying the load response to various driving excitations, using a thermal-balance approach. It is expected that the existing weighting factors and perturbation coefficients must be modified and/or recalculated for passive-solar and large thermal-mass systems. Therefore, two efforts are required in order to provide passive-analysis capabilities that include commercial buildings. Detailed models must be provided in a thermal-balance program (BLAST) in order to calculate the approximation parameters used in Cal-ERDA for the multizone building.

This project began in November of 1977 as a joint undertaking of LBL and Los Alamos Scientific Laboratory (LASL). In subsequent efforts, LBL will concentrate on model development and incorporation into BLAST; LASL will utilize the results of the LBL effort to identify and implement appropriate approximate methods for modeling passive systems within Cal-ERDA.

ACCOMPLISHMENTS DURING 1977

During 1977 the scope of the project was defined in cooperation with LASL personnel. The efforts were divided such that LBL will be primarily responsible for BLAST modifications and development of passive-system algorithms, while LASL concentrates on incorporating these algorithms into Cal-ERDA.

During the last two months of 1977, algorithm development efforts were begun; convective heat transfer between building zones and natural convective processes which take place in a Trombe-wall system are being emphasized. In both cases, algorithms are being developed based on the fundamental fluid dynamics of air flows driven by differences in temperature. In addition, investigation of the detailed calculation procedures used in the BLAST load-program has been initiated. The goal is to better understand the program methodology and assumptions, and to develop a plan for incorporating the modifications and additions that are envisaged for 1978.

PLANNED ACTIVITIES FOR 1978

The initial emphasis in this project is on identifying those areas in BLAST where the existing, conventional-building analysis capabilities might be inadequate for passive systems, on modifying BLAST as necessary, and on utilizing the modified program to alter the approximate techniques used in Cal-ERDA. In particular, the following areas will be investigated:

1. the relationship of the distribution of thermal mass and the size and location of glazing in direct gain systems;
2. the interaction of the thermally massive, passive structure with the auxiliary HVAC system, including the effects on performance of increased HVAC cycling time;
3. The effects on human comfort of envelope storage and high internal surface temperatures of large thermal mass buildings.

These topics concentrate attention on understanding the basic, large thermal-mass building, both with and without direct gain coupling to the environment. In parallel, the algorithm-development efforts initiated in 1977 will lead to:

1. Trombe-wall analysis capabilities, including both the natural convection and conductive coupling to the occupied space;
2. An algorithm describing the passive coupling of building zones which includes thermal conduction, forced convection, and natural convection.

Finally, algorithm validation efforts will be initiated during 1978. Data from LASL test cells will be used to validate the convection algorithms. A full-scale building validation effort will be planned for implementation in 1979.

FEA/HUD/ERDA REGIONAL SOLAR ENERGY RETROFIT OF LOW AND MODERATE COST HOMES

T. Webster

INTRODUCTION

This project was a cooperative effort undertaken by HUD, FEA, and ERDA within the Region IX area common to these agencies. The general objectives of the project are the same as those of the National Demonstration Program, that is, promotion of solar energy to reduce demand on conventional fuel supplies. However, unlike other programs, this effort is directed to the demonstration of retrofitted solar heating systems on low and moderate cost homes. The basic objectives are (1) to evaluate the social and economic impact of this application of solar technology, (2) to assess the savings resulting from various energy conservation measures, and (3) to publicize the efforts of the participating agencies.

Two houses in each of two locations (Sacramento and Las Vegas) were selected for retrofitting; all houses were well insulated, and one house in each location was equipped with a solar space and domestic hot water heating system. The houses were provided by HUD. The solar systems were funded by DOE and designed by Koepf and Lang under contract to LBL. FEA coordinated the projects, funded the house insulation and weather stripping, and will monitor the houses for three years.

The LBL activities during 1976 consisted of organizing the project technical requirements (which resulted in the issuing of a memorandum of understanding), preparing a conceptual design report and initial cost estimate, and selecting an architect/engineer to prepare detailed design drawings and specifications. The design was completed and issued for construction bidding in December 1976. System design information and a more detailed project description are contained in the 1976 Energy and Environment Division Annual Report.[1] System parameters are shown in Table 1.

ACCOMPLISHMENTS DURING 1977

Activities during 1977 consisted primarily of constructing the two solar systems. Construction bids were received by LBL during January. The low bidder for Las Vegas, Action Air Conditioning, was awarded a contract for $9,567. However, of the four bids received for Sacramento, three were designated non-responsive because affirmative action documents were not completed; the fourth bid was much greater than budget. Therefore, the Sacramento system was re-bid. In addition, Revere collectors were purchased by LBL to expedite the project. A contract was awarded during February to Thor Grendahl and Sons for $12,401.

Sacramento

The following are some of the more notable problems that arose during construction:

a. The Revere collectors were delivered two weeks late. The coverplate seals were inadequate and had to be resealed at the site with RTV caulking compound. The seals are designed for the Revere standard glass coverplate, and had not been changed to accommodate the thinner plastic Kalwall glazing.

b. Collector area requirements were specified incorrectly on the drawings (i.e., 300 gross ft^2 rather than 300 net ft^2) resulting in installation of 16 collectors (277 net ft^2) instead of 18.

c. The Rho Sigma RS500 temperature controller did not work, and was replaced with a standard on-off type (RS 104).

d. Perforated hose clamps were erroneously used to install collector silicone hose and had to be replaced with solid band clamps.

e. The roof structure of the house was not adequate for the added weight of collectors and it required additional supports. Additional supports under affected bearing walls were also required by the building inspector. Most of the structural changes were funded by HUD.

f. Inspectors required backflow preventers in two places.

Las Vegas

The Nevada sites were also not without difficulties, including:

a. Solarmaster brand collectors as submitted by the contractor were rejected because no independent test-performance curves were available. Ying Mfg. brand collectors were finally selected.

b. Seals of Ying collector coverplates (20-mil Lexan) were inadequate, resulting in dust and water leakage into the collectors. The collectors were resealed with RTV, and weep-holes were drilled in the ends to relieve condensation inside the coverplate.

c. The check valve in the vent line did not prevent flow through this line and had to be rearranged to minimize flow. Apparently,

Table 1. Design and performance parameters for solar heating system.

	Latitude	Collector Slope	Collector Area	House Load	DHW Load	Storage Capacity	Solar Fraction
	Deg	Deg	ft^2	Btu/hr-°F	Gal/ Day	Gal	%
SACRAMENTO	38.5°	20°	277	500	60	600	65
LAS VEGAS	36°	7°	200	459	60	450	60

the collector return line had too much resistance because of the long underground run to the storage tank.

d. Two ΔT sensors for the controller (Rho Sigma RS104) and the controller itself, had to be replaced to obtain correct operation.

e. A leak occurred in the union domestic hot water (DHW) heating coil. The leak was discovered because the tank was overflowing. The unions were replaced with hard-soldered couplings.

f. A modified refrigerant coil was used for the solar heating coil. The coil was undersized and did not perform or drain well (drain-down of the coil is used to prevent coil freezing in winter, since the coil is located in an outside duct). A new heating coil, larger and designed for water, was installed. A higher-head pump and a throttling valve on the discharge side of the coil were required to make the new coil operate properly.

g. A new, larger three-speed fan motor was required to overcome the increased resistance of the solar heating coil when the air conditioner was operating. A trial-and-error procedure was necessary to establish proper fan speed for all modes of operation.

In September, both systems were complete and accepted by LBL. Operation and maintenance manuals were submitted to HUD, after drawings were completed by Koepf & Lang, for transfer to the new home owners. The property transfer from LBL to HUD was then completed. These activities marked the end of LBL's involvement in the project except for preparation of a final report.

System costs

Both contractors were required to submit actual cost breakdowns for the system installations. Table 2 summarizes the actual costs for each system.

The high costs for these systems appear to be attributed primarily to the following factors:

a. Site-dependent factors/special construction--plastic glazed collectors for vandalism protection, secure enclosures for storage, HUD requirement precluding use of garage for storage tank, and minimal yard space necessitating unobtrusive location of storage.

b. Retrofitted system--necessity to work in tight spaces and utilize existing utilities systems.

c. High-quality components for long life and reliability. Less expensive components (e.g. pumps, piping, and controls) could be used in a non-demonstration system.

d. On-site construction--few of the components were shop fabricated or modularized.

e. Problems--collector sealing, wrong components installed, control malfunctions. Some of these problems may have been avoided if an on-site inspector had been available.

CONCLUSIONS

A few tentative conclusions can be drawn from the experiences on these projects:

a. The system should be designed with as many shop-fabricated, or purchased, modular components as possible to reduce installation costs.

b. "Standard" retrofit designs are difficult to achieve because of the number of site-dependent factors. Many compromises must be made for each specific installation that affect cost, complexity, and performance.

c. Storage tanks should be located inside an existing enclosure or garage, if possible, to reduce costs.

Table 2. System actual costs.

	SACRAMENTO			LAS VEGAS		
	Materials	Labor	Total	Materials	Labor	Total
Collectors	$3184	$1436	$4620	$1619	$ 240	$1859
Storage Tank	657	151	808	609	360	969
Piping & Mechanical	1423	1638	3061	1250	2136	3386
Installation	561	340	901	185	513	698
Elect. & Controls	760	860	1440	530	600	1130
Site work/enclosures	334	958	1292	--	969	969
Miscellaneous	321	126	447	--	672	672
Overheat & Profit	--	--	3158	--	--	279
TOTALS	$7240	$5329	$15727	$4193	$5490	$9962

d. Special collector construction (e.g., plastic glazing) may add cost and jeopardize performance and durability of collectors.

e. Site-dependent factors should be thoroughly evaluated to determine feasibility of providing solar. Some of these factors may preclude a cost-effective installation (though this depends on future costs of gas or electricity).

REFERENCE

1. Energy & Environment Division, Annual Report (1976), Lawrence Berkeley Laboratory Report, LBL-5982.

SOLAR INFORMATION SUPPORT FOR DOE (LLL) SOLAR TECHNOLOGY TRANSFER PROGRAM

Y. Howell, H. Miller, and M. Wahlig

INTRODUCTION

The Solar Technology-Transfer Program for the Western Region has been presenting seminars coordinated by Lawrence Livermore Laboratory (LLL) to certain multiplier groups (groups that can hasten the dissemination of solar energy technology). LBL has had responsibility for producing resource handbooks for seminar distribution that would facilitate business or design decisions about solar energy systems. The handbooks are tailored to meet the special needs of each seminar audience in its particular geographic region.

ACTIVITIES DURING 1977 AND FUTURE PLANS

Procedure

LBL worked with LLL, each multiplier group, and seminar speakers, to assess the information needs of the target audience and to determine what data would be appropriate to meet those needs. The materials were then written, compiled, and edited at LBL. Draft handbooks were reviewed by the seminar speakers. The handbooks, in their final form, were subject to feedback/evaluation by the seminar attendees. These evaluations have been generally favorable.

Handbook Content

Target audiences for the three handbooks produced by LBL in 1977 were the American Society of Plumbing Engineers (ASPE); the Technology Transfer Society (T^2S), which operates in conjunction with the Los Angeles Office of the Small Business Administration (SBA); and the American Institute of Plant Engineers (AIPE). The handbooks developed for these audiences are described below.

Information in the handbooks, although "customized" for each audience and its geographic region, fell into the following sections:

Mechanics

The design parameters of solar components and systems were described clearly, in appropriate detail. A glossary of terms was included to facilitate further reading.

Solar Data

Insolation and weather data from LBL's "California Solar Data Manual" were presented for the region where the seminar took place. A glossary of descriptive terms and a list of solar data sources for other regions were also included.

Computer Programs for Systems Optimization

Some of the more widely used solar-design computer programs were described and compared. Both detailed programs (Cal-ERDA, TRNSYS) and simplified methods (F-chart, SOLCOST, LASL method, RSVP) were included in this section.

Solar Legislation

Existing and proposed solar legislation, on both the state and federal levels, was listed and summarized.

Standards, Codes and Testing

Applicable standards and codes were listed and compared. A description of the State Energy Commission's Solar Testing and Inspection program was included, with a compilation of collector test facilities.

Solar Buildings

The reader was furnished with a list of a few local buildings using solar energy. Most buildings were demonstration-oriented or, at least, well-instrumented for acquisition of performance data.

Solar Firms

Local solar architects, engineers, installers, builders, manufacturers, and distributors were listed to provide the reader with access to the local solar community.

Information Access

The reader was provided with references to solar information-services, associations, societies, and to colleges offering solar courses. An extensive "customized" bibliography was made available.

Solar Business Development

The subject of solar marketing was covered in the handbook for the SBA seminar, titled "How to Get into the Solar Energy Business." Topics covered included: market projections, solar marketing techniques and tips, and discussions of factors that affect market penetration (economics, consumer acceptance, financing, insurance and liability, etc.).

Future Plans

A continued Solar Technology-Transfer Program will present seminars and provide information to the existing multiplier groups in various geographic locations, and will develop contacts with additional such groups. Bankers, builders/developers, and building officials are likely candidates for future efforts because they will have a direct effect on the rate of solar commercialization.

SOLAR DEMONSTRATION PROGRAM: TECHNICAL REVIEW AND PROJECT MONITORING

F. Salter and T. Webster

INTRODUCTION

The Solar Applications Group at LBL provides technical consulting and management services to support the DOE San Francisco Operation Office's (DOE/SAN) overall management of sixteen commercial-building solar demonstration projects and seven hotel/motel hot water solar projects located throughout the Western States. These projects are part of the National Solar Heating and Cooling Demonstration Program,[1] whose primary objective is to stimulate a solar industry, and to promote the use of solar energy as a means of reducing demand on conventional fuel supplies.

LBL began work on the commercial solar demonstration projects in August, 1977. These projects represent the second cycle of the Commercial Demonstration and were selected from the proposals of the Program Opportunity Notice (PON) DSE 76-2.[2] This PON emphasized solar space-heating projects, but allowed for space cooling, and/or domestic hot water, in conjunction with space heating.

LBL began work on the hotel/motel projects in October, 1977. These projects, although part of the national program, are separate from the yearly cycle of proposals, and were selected from the proposals of the PON EG-77-N-03-1450.[3] This PON was restricted to solar hot water applications, and emphasized stimulating widespread commercial construction of this particular solar application which appears to have the greatest immediate potential for cost effectiveness.

ACCOMPLISHMENTS DURING 1977

Project Monitoring

The LBL Solar Application Group provides day-to-day project monitoring and liaison between solar project contractors and their representatives and DOE/SAN Project Managers. Our monitoring includes review and approval of periodic reports from contractors on such items as cost, schedule, and project technical status. Daily technical problems are resolved as they occur, and frequently relate to system calculations, instrumentation, improvement or changes in system design, review of proposed equipment substitution, costs, and scheduling. Drawing and specification submittals are reviewed, and meetings are arranged as required. LBL is also liaison between the contractors and IBM in Huntsville, Alabama for planning and installation of instrumented systems. In this regard, LBL is attending training programs and meetings with IBM. LBL has obtained an On-Site Monitor and is available for trouble shooting on the instrumented commercial projects.

Technical Reviews

LBL participates in the following technical reviews during the course of a project:

Commercial Projects

1. Final design review
2. Construction progress review
3. Final inspection and start-up

Hotel/Motel Projects

1. Final design review
2. Final inspection and start-up

For the final design reviews, the project solar contractor submits project schedules, design drawings, specifications and an acceptance test plan. These documents are reviewed separately by DOE/SAN Project Managers, PRC Systems Sciences Company (PRC), and LBL. They then are reviewed in common at a meeting with the contractor and his representatives. (PRC is not involved in the hotel/motel projects.) The review includes evaluation of system design and performance, equipment selection, rationale for modifications or deviations from the proposed system, preparations for instrumentation on designated projects, schedules and costs, status and content of the bid documents, review of the acceptance test plan, and usually, a site inspection. Meeting notes and recommendations resulting from the final design review are then written and submitted to DOE/SAN, and are transmitted to the contractor at DOE discretion. The recommendations resulting from the review are not binding for the system designer, except when they concern life-safety items.

LBL holds construction progress reviews when construction is 50% to 90% complete. Construction and construction drawings and specifications are reviewed at the demonstration site for solar subsystems or components which have been delivered or installed. The acceptance test plan is also reviewed at this time. Finally, instrumentation progress is reviewed on appropriate commercial projects.

During final inspection and start-up, LBL reviews the completed solar system for conformance with the contract documents, determines whether the control system performs properly in all modes of operation, examines "as built" drawings, reviews operation and maintenance manuals, and participates in trouble shooting when necessary. On projects where instrumentation is required but is not completed, LBL examines the remaining instrumentation construction schedule and attempts to expedite the process where possible.

Monthly Project Assessment

On each project, LBL prepares a monthly progress report which includes a system description along with basic system data. The report covers design, equipment delivery, and installation progress for the previous month. Significant problems are noted, and job completion and remaining scheduling are discussed.

Proposal Reviews

The LBL Solar Applications Group participates in the technical review of proposals submitted in response to the various Program Opportunity Notices of the National Solar Heating and Cooling Demonstration Program.

REFERENCES

1. National Program for Solar Heating and Cooling of Buildings, ERDA 76-6, November 1976.
2. Commercial Integrated Projects for Use in Demonstrations of Solar Heating and Cooling, PON DSE 76-2, ERDA, 1976.
3. Hot Water Initiative for Hotel/Motel Installations, PON EG-77-N-03-1450, ERDA, 1976.

SUPPORT ACTIVITIES FOR DOE SOLAR HEATING AND COOLING RESEARCH AND DEVELOPMENT PROGRAM

M. Wahlig, M. Martin, and R. Kammerud

INTRODUCTION

This project consists of technical supporting activities for the Solar Heating and Cooling Research and Development Branch of the DOE Office of Solar Applications. These activities include: a) peer review of unsolicited proposals; b) technical evaluation of projects performed by other contractors, including site visits and review of progress reports; c) preparation and evaluation of Program Research and Development Announcement (PRDA) and Request for Proposal (RFP) solicitations; d) program planning, reviews, and summations; and e) interlaboratory coordination of these activities. The LBL effort has been primarily in the areas of controls for solar heating and cooling systems and passive cooling, and secondarily in other solar areas in which LBL has a measure of expertise as a result of ongoing R&D projects (namely, absorption cooling, systems studies, and non-engineering aspects). Most of the staff members of the Solar Energy Group have participated in this effort in some way during 1977.

ACCOMPLISHMENTS DURING 1977

Review of Unsolicited Proposals

LBL solar energy group members participated in one formal review session for unsolicited proposals received by ERDA in the areas of cooling, heat pumps, and controls. In addition, seven other unsolicited proposals were given peer review on an as-received basis, with the reviews being summarized and forwarded to ERDA/DOE Headquarters (the transition from ERDA to DOE was formally accomplished in October 1977) along with recommendations for action. These proposals offered projects dealing with controls or with passive cooling topics.

Preparation and Evaluation of Program Solicitations

A number of PRDA and RFP solicitations were issued by ERDA in 1977 for projects involving R&D activities related to solar heating and cooling. LBL participated in the preparation of these documents, especially the drafting of the Statement of Work for the controls categories in the RFP on Controls and Passive Systems. LBL was responsible for planning, arranging, and managing the Technical Evaluation Committee that evaluated the responses to this RFP. Subsequent to the selection (by ERDA) of the best proposals for awards, LBL staff assisted ERDA/SAN (the San Francisco Office) in formulating the Statement of Work for the ensuing contracts. Several months afterwards, LBL prepared for DOE Headquarters a set of recommended tasks that could be the basis of another round of RFPs that might be issued later in FY 1978.

In addition, LBL solar energy staff members participated in the technical reviews of the PRDA on Collector Materials and Fluids, the PRDA on Passive and Hybrid Systems, and the RFP on Solar Activated Cooling Projects.

Project Monitoring

Project monitoring consists of the continuing technical evaluation of projects being performed by other contractors, including site visits, review of progress reports, and organizing contractor meetings when appropriate. As a result of the PRDA and RFP solicitations, a number of new projects were started in 1977 in those areas where LBL has monitoring responsibility; namely controls and passive cooling. Initial contacts with these new contractors were made late in 1977 through visits to LBL, by phone, and by interactions at meetings. Site visits are scheduled for early in 1978.

Several other controls projects and passive cooling projects were initiated in 1977 as a result of unsolicited proposals to ERDA/DOE, and these are also being monitored by LBL, as is another project that has been ongoing since 1976.

Monthly progress reports and other communications have been received and read for all of these projects. Periodically, status summaries are prepared and sent to DOE Headquarters in Washington, D.C.

Gradually, the contracts for those projects that LBL is reviewing have been transferred to the DOE/SAN Office, for the convenience of having the LBL technical monitors and DOE contract monitors at nearby locations. All except one of the controls and passive cooling contracts are now at SAN.

When requested to do so, LBL personnel have participated in negotiating meetings with contractors, to provide input on the definition, or change in scope, of certain projects.

A meeting of all the contractors engaged in controls projects is scheduled for late February 1978.

Program Planning, Reviews, and Summations

LBL has summarized the status of the overall R&D program in the areas of controls and passive cooling several times during 1977, sometimes for presentation by LBL staff members, and at other times for the use of DOE Program Managers for their presentations.

The National Program Plan for Research and Development in Solar Heating and Cooling, ERDA 76-144, is in the process of being updated and improved, and the DOE Laboratories are providing key support roles in this endeavor. In particular, LBL has participated in numerous working-group meetings during 1977 for the purpose of formulating a comprehensive Passive Solar Systems Program Plan. To a lesser extent, some preliminary work has been done toward the development of a Controls Program Plan.

Several specific topics have arisen that have required special attention within the framework of the overall R&D plan. One is the need for standardization in the collection of operating data from solar energy systems, so that each experimenter will not be repeating mistakes of his predecessors, and so that the results of different operating systems may be fairly compared. Accordingly, efforts to satisfy these needs have led to the scheduling of a Workshop on Instrumentation and Data Acquisition for Solar Systems, now set for April 1978; LBL has participated in the planning for this meeting.

A similar need, the subject of much activity during the latter half of 1977, is to establish performance evaluation factors and data acquisition requirements for passive solar systems. LBL has joined with Los Alamos Scientific Laboratory (LASL), the National Bureau of Standards (NBS), the Planning Research Corporation (PRC) and DOE Headquarters in the development of these passive performance indicators. Several working meetings have been held on this subject, and several task plans have been drafted and reviewed by the various participants in this project, including LBL.

Los Alamos (LASL) carried out preliminary planning for a Workshop on Adaptive Controls, tentatively scheduled for January 1978, and LBL was involved peripherally in this planning activity. It was subsequently decided not to hold this workshop in January; but rather to merge it with another Controls Conference scheduled for May 1978. Planning for this Controls Conference has involved LBL to a small extent during 1977, but will develop into a major activity here in 1978 as the meeting date approaches.

As part of the continuing effort to improve the efficiency of executing the overall R&D program plan, PRC has assisted DOE Headquarters in the drafting of a revised Management Plan for the Research and Development Branch. All of the DOE Support Laboratories, including LBL, have reviewed and provided feedback on the several options for this revised plan.

Inter-Laboratory Coordination

LBL has participated in the two 1977 meetings of the Support Laboratories Coordinating Committee, which meets regularly to discuss the state of implementation of the R&D Program, and to insure that the various Laboratories are acting harmoniously in their performance of the many tasks.

Related Activities

LBL staff members have assisted in the evaluation of proposals submitted to ERDA/DOE in response to PON's (Program Opportunity Notices) issued by the Solar Heating and Cooling Demonstration Branch. These included the review panel at Huntsville for the 2nd-Cycle Commercial Heating and Cooling PON, and the evaluation panel at SAN for the Hotel/Motel Hot Water Initiative PON.

In all, about thirteen LBL staff members were involved in the review of proposals for solar PRDA's, RFP's, and PON's during 1977.

PLANNED ACTIVITIES FOR 1978

Activities in all of the above areas will continue throughout 1978. Unsolicited proposals will be reviewed and evaluated as they are received. It is likely that a new set of RFP's will be prepared and released before the end of 1978. The monitoring of outside projects will continue on an expanded basis, as more projects are started and as the existing projects complete the major part of the tasks they contracted for in 1977. Overview presentations of the Controls Program and the Passive Cooling Program are scheduled for many of the solar energy workshops that will be held in 1978. The Controls Conference in May 1978 will be a major event in terms of LBL participation. At the present time, solar energy R&D Workshops have been scheduled for February, March, April, and May of 1978. The first versions of the Passive Program Plan and the Controls Program Plan should be completed during 1978. Additional meetings of the Support Laboratories Coordinating Committee will be held during 1978. Finally, it is certain that numerous LBL staff members will be called upon to assist in the review and evaluation of proposals submitted to DOE solar energy PRDA's, RFP's, and PON's issued during 1978.

OCEAN THERMAL ENERGY CONVERSION: ENVIRONMENTAL PROGRAM

P. Wilde, J. Sandusky, A. Jassby, and M. Tatro

INTRODUCTION

In cooperation with the Atlantic Oceanographic and Meterological Laboratory, Miami, and under Dr. Lloyd Lewis, F. A. Koomanoff, and Sigmund Gronich of DOE's Solar Energy Division, LBL will be providing management assistance, technical monitoring, analytical support, and methodological development capabilities for the environmental aspects of the Ocean Thermal Energy Conversion (OTEC) program. The OTEC program is an attempt to generate useful power using the temperature difference between the warm surface waters of the ocean and the uniformly cold waters of the deep ocean. For a proposed engine using ammonia as the working fluid, the minimum temperature difference required is 20°C. Practically, OTEC sites must be in tropical and subtropical oceanic areas, and in water depths between about 800 to 1000 meters.

At present, two types of operations are being considered: 1) the electric option, in which generated power is transferred from a moored, floating OTEC platform into the electrical grid system of the United States; and 2) the manufacturing plant-ship option, in which the power is used at sea to manufacture some product such as ammonia, hydrogen, or aluminum for shipment to shore. Proposed sites for the electric option are off Hawaii and Puerto Rico and in the Gulf of Mexico. The initial thermal region deemed suitable for plant-ship operations is in the South Atlantic just south of the Equator, off Brazil.

ACCOMPLISHMENTS IN 1977

The OTEC program started at LBL in the summer of 1977 with the occupation of the first environmental "benchmark" site in the Gulf of Mexico near New Orleans, at 29°N 88°W. This site was reoccupied in November 1977. LBL, in co-operation with the Gulf Coast Research Laboratory, is taking bio-ecological/chemical measurements at this site. These are trial operations to develop techniques and methods to be used at subsequent sites. The overall purpose of these measurements is to provide background environmental data, to aid in actual site selection for an operating OTEC plant, to alert engineers and designers to design parameters potentially affected by the environment, and to catalogue information required by regulatory agencies for operating permits.

In addition, LBL is assisting DOE headquarters by monitoring contracts on general environmental assessment of proposed OTEC systems, and providing technical review for other OTEC program areas studying physical modeling, fouling, and corrosion.

PLANNED ACTIVITIES FOR 1978

The environmental-benchmark program will be expanded to include bi-monthly occupations of five sites: three in the Gulf of Mexico, one off the southeast coast of Puerto Rico, and one off the island of Hawaii. The bi-monthly surveys in the electric-option areas are part of a one-year study. In the summer of 1978, the thermal region suitable for plant-ship operations off Brazil will be visited during a regional oceanographic survey. Initial operating OTEC test-systems are scheduled to occupy the sites in early 1979.

APPROPRIATE ENERGY TECHNOLOGY

C. W. Case, H. R. Clark, B. A. Greene, and F. B. Lucarelli

INTRODUCTION

During the summer of 1977 the Director of the DOE/ERDA Division of Buildings and Community Systems commissioned the DOE/ERDA San Francisco Operations Office (SAN) to establish a pilot program for appropriate energy technology grants. The program is designed for individuals, small businesses, state and local agencies, local non-profit groups, and Indian tribes residing in Federal Region IX, which includes Arizona, California, Nevada, Hawaii, and the Pacific Trust Territories. DOE/ERDA set aside $500,000 exclusive of operating costs, to be distributed in small grants of around $10,000, although grants can be for as much as $50,000. These grants will be for small scale energy innovations and demonstration projects which fall within the guidelines of appropriate energy technology. These guidelines encourage projects which make the best use of available renewable energy resources, are labor intensive, utilize locally available materials, emphasize decentralized technologies, are environmentally sound, and increase community energy self-reliance.

The SAN Office established a three-step procedure for reviewing the proposals and granting the awards:

a) Prescreening and reviewing the proposals to make sure the applications are properly completed and to see if any of the proposals require special handling;

b) Reviewing the proposals for technical and economic merit;

c) Reviewing the proposals by Peer Review Committees appointed through the governor's office of each state. These Committees, along with DOE/SAN, will make the final decisions concerning the allocation of the grants.

LBL's role in the process is as follows:

a) Perform the prescreening for all proposals received from the various states;

b) Review the proposals from Arizona, Nevada, and the Pacific Trust Territories for technical/economic merit (the applications from California will be reviewed by the California Office of Appropriate Technology, while those from Hawaii will be reviewed by the University of Hawaii);

c) Perform various program management functions, which include establishing the procedures used during review processes, as well as compiling and analyzing data from these processes.

ACCOMPLISHMENTS DURING 1977

The grant-solicitation phase started on September 21, 1977 and lasted until November 21, 1977. The San Office compiled a mailing list of prospective applicants and sent out program announcements and about 12,000 short, easy-to-read applications. Radio and newspapers gave the program extensive exposure. By the November 21 deadline, the SAN Office had received back 1116 applications. Table 1 shows the applications allocated by state, and Table 2 shows them by applicant group.

After sending out receipt cards to the applicants, SAN forwarded the proposals to LBL. During the first two weeks in December, we prescreened the applications to make sure they were complete and came from eligible applicants and states, as well as to see if any of the proposals required special handling. (Proposals which required special handling, about 10%, include those which we sent to other government agencies for funding.) When the prescreening was completed, we sent the California applications to the California Office of Appropriate Technology and the Hawaii applications to the University of Hawaii. Tables 3-5 show additional data taken from the prescreening operation.

Table 1. Applications and funding levels by state.

Area	Number of Proposals	% of Total Received	Funding Request ($K)	% of Total Request	% of Total Population
Arizona	119	11	$ 2,199	10%	8%
California	845	76	16,654	77	87
Hawaii	70	6	1,019	5	3
Nevada	67	6	1,444	7	2
Pacific Trust	15	1	271	1	NA
Total	1116	100%	$21,587	100%	100%

Table 2. Number of applications by applicant type.

Group Type	AZ	CA	HI	NV	PTT	Total
Individual	55	398	43	33	5	534
Small Business	36	261	15	14	6	332
Local Non-profit	13	106	4	8	1	132
State Agency	7	19	7	6	3	42
Local Agency	5	37	0	2	0	44
Indian Tribes	2	14	0	4	0	20
Total	118	835	69	67	15	1104

PLANNED ACTIVITIES FOR 1978

During the first few weeks in January, we will review for technical and economic merit the 201 applications from Arizona, Nevada, and the Pacific Trust Territories. A number of individuals and groups from the University of California, and from LBL's Energy and Environment Division, Earth Sciences Division, and Engineering and Technical Services Divison, are participating in the review. The active and passive solar groups from the Solar Energy Program are reviewing the majority of applications. The ecosystem stability group, various LBL mechanical engineers, personnel from some of the geothermal groups, and the windows and lighting group are reviewing a significant number of the applications.

By mid-January, when the review is finished, we will send the review sheets to the various Peer Review Committees of each state. The review sheets for each application will contain a total point score based on the project's technical and economic merits as set forth by the small-scale energy guidelines referred to above. DOE anticipates that the Peer Review Committees will be finished with their reviews by mid-February, and that awards will be made by about March 1. This is approximately a 90-day turn-around for the total review process, from the November 21, 1977 application cutoff date to the March 1 award date.

During 1978 LBL also plans to help SAN with the monitoring of the DOE-funded projects, and to help with Phase II of the program. Phase II will include the same features as the pilot program, but will expand to include the other western states.

Table 3. Funding request by applicant type ($K).

Area/ Group Type	AZ	CA	HI	NV	PTT	Total
Individual	$ 961	$6,455	$ 434	$ 584	$ 42	$ 8,476
Sm. Business	840	6,264	328	396	179	8,007
Local Non-Profit	186	2,997	72	152	14	2,421
State Agency	85	483	185	91	36	880
Local Agency	77	1,218	0	58	0	1,353
Indian Tribes	50	237	0	163	0	450
TOTAL	$2,199	$16,654	$1,019	$1,444	$271	$21,587

Table 4. Average funding request by applicant type.

Area/ Group Type	AZ	CA	HI	NV	PTT	Total
Individual	$17,480	$16,219	$10,084	$17,700	$ 8,391	$15,873
Small Bus.	23,318	23,999	21,875	28,263	29,879	24,116
Local Non-profit	14,325	18,866	17,866	19,015	14,160	18,218
State Agency	12,120	25,425	26,439	15,152	11,833	20,938
Local Agency	15,426	32,920	0	28,881	0	30,748
Indian Tribes	25,000	16,923	0	40,739	0	22,494

Table 5. Funding requests by technology.

Technology	No. of Applications	% of Total	Total Funding	% of Total	Average Funding
Agriculture Related	24	2%	$ 601,854	3%	$25,077
Bioconversion	51	5	1,076,589	6	21,011
Solar Heating & Cooling	214	19	3,493,189	20	16,323
Solar Passive	43	4	686,224	4	15,959
Solar-Photovoltaic	8	1	150,287	1	18,786
Solar-Other	68	6	1,440,191	8	21,179
Transportation Related	80	7	1,988,603	11	24,858
Energy Conservation-Building	68	6	1,303,773	7	19,173
Energy Cons.-Appliances	80	7	1,422,418	8	17,780
Energy Cons.-Recycling	44	4	975,043	6	22,160
Wind	90	8	1,692,087	10	18,801
Ocean	17	2	284,646	2	16,744
Hydroelectric	19	2	533,913	3	28,101
Education	20	2	319,196	2	15,960
Other	83	7	1,594,009	9	19,205
Subtotal	909	82%	$17,562,002	100%	$
Solar-Combined with Other Tech.	127	11	NA		NA
Other Combinations	80	7	NA		NA
GRAND TOTAL	1116	100%	$21,587,000	100%	$

FUNCTIONAL LINKING BETWEEN H_2 CONSUMPTION, N_2 FIXATION, AND PHOTOSYNTHESIS IN BLUE-GREEN BACTERIA

L. Packer, L. W. Luijk, R. Cammack and R. Ohki

INTRODUCTION

Blue-green bacteria (also designated as blue-green algae or cyanobacteria) are unique photosynthetic organisms because in certain species a single organism is capable of carrying out both an oxygen-evolving type of photosynthesis and fixation of atmospheric nitrogen. Large-scale, mass-culture projects to produce biomass from these organisms have been established in Mexico and Africa. These organisms have also been used to process organic wastes, and are being considered for use in producing ammonia fertilizer. Hence it is of considerable interest to determine ways to increase bioproductivity, particularly photosynthesis and N_2 fixation, of these organisms. N_2-fixing species of blue-green bacteria can produce considerable quantities of H_2 gas through energetically wasteful "leak" in some of the steps in the reduction, catalyzed by nitrogenase, of N_2 to ammonia.

Indeed, the loss of H_2 during the process of N_2 fixation is widespread amongst symbiotic bacteria, which provide a major source of combined nitrogen for higher plant species. In a survey of many symbiotic N_2-fixing species, Shubert and Evans have reported that the average loss of energy due to this process is from 30% to 50%. The presence of a hydrogenase enzyme in such organisms is believed to increase the efficiency of N_2 fixation by providing a mechanism for recovery of the lost H_2.[2-7] This appears to be the case in two species of heterocystous blue-green bacteria, Nostoc muscorum and Anabaena cylindrica, which are under study in this laboratory.[5-7] These species, when grown in the presence of H_2 gas, have an increased activity of the enzyme hydrogenase which actively consumes atmospheric H_2.

Our studies have demonstrated that in such cultures N_2 fixation and photosynthesis are significantly enhanced by H_2 consumption. Because of the obvious importance of this observation to the enhancement of bio-productivity of these organisms, we are investigating the functional linking between H_2 consumption, N_2 fixation, and photosynthesis.

Figure 1 shows schematically two vegetative cells and a heterocyst in a N_2-fixing, filamentous, blue-green bacterium. On the left, a vegetative cell is shown to carry out O_2-evolving photosynthesis, producing carbohydrates (CH_2O) and biomass. Some products of photosynthesis can be translocated into adjacent heterocysts, there serving as reducing power for nitrogenase-catalyzed reduction of N_2 to ammonia. The wasteful unidirectional leak of H_2 by nitrogenase may be partially overcome by recapture of lost H_2 by hydrogenase-catalyzed H_2 consumption. Energy for N_2 fixation is provided by cyclic photophosphorylation and/or by adenosine triphosphate (ATP) production from the oxidation of molecular H_2 by O_2 (oxyhydrogen or Knallgas reaction) using reducing power derived from the unidirectional consumption of H_2 gas via hydrogenase.

On the right a vegetative cell is shown to carry out hydrogenase catalyzed H_2 consumption; two possible linkings between CO_2 fixation and H_2 consumption are shown; i.e., H_2 as a source of reducing power to CO_2 reduction and/or for the oxyhydrogen or Knallgas reaction which enhances energy levels by ATP synthesis. Present evidence favors the latter route.

ACCOMPLISHMENTS DURING 1977

H_2 Consumption and N_2 Fixation

When we began this research about two years ago, we were investigating whether heterocysts and vegetative cells of two species of blue-green bacteria, *Nostoc muscorum* and *Anabaena cylindrica*, possessed a hydrogenase which consumed H_2 gas with a Km of about 50 μmoles. This catalyst could also produce H_2, but only if the cell preparations were fortified with an artificial, low-potential mediator like methylviologen. Hence we concluded that H_2-production activity by hydrogenase was not physiologically significant and that no net production of H_2 occurs by this pathway.

During 1977 we pursued these studies and were able to demonstrate that hydrogenase activity is inducible by H_2 in growing cultures of both organisms. When cultures were grown under N_2-fixing conditions in the presence of a gas mix (N_2:CO_2:H_2 = 75:5:20) H_2-consumption activity increased by tenfold compared with the activity of the original aerobically grown cells. This N_2-fixing growth condition also increases nitrogenase activity. Using H_2-and-hydrogenase induced cultures, we were able to show that the basic level of nitrogenase activity was enhanced twofold. Moreover, in the presence of H_2, the activity could be increased two-to-threefold further, yielding N_2 fixation at a rate of five μmoles N_2 fixed per mg chlorophyll per hr (16 μmoles ethylene formed from acetylene per mg chlorophyll per hr).

Pathway of H_2 Consumption

H_2-induced cells of *N. muscorum* consume H at a rate between 20-40 μM per mg chlorophyll per hr under anaerobic conditions in the light. In the dark, the activity was 5-10 times lower than that in the light. An inhibitor of photosynthetic oxygen evolution, dichlorophenyl-dimethylurea, DCMU (10^{-5} M), inhibited H_2 consumption in the light by 40-50%; if 2-12% O_2 was added, a twofold stimulation in H_2 consumption occurred in the light. In the dark, oxygen had the effect of increasing the rate of H_2 consumption tenfold so that the final activity was similar to that

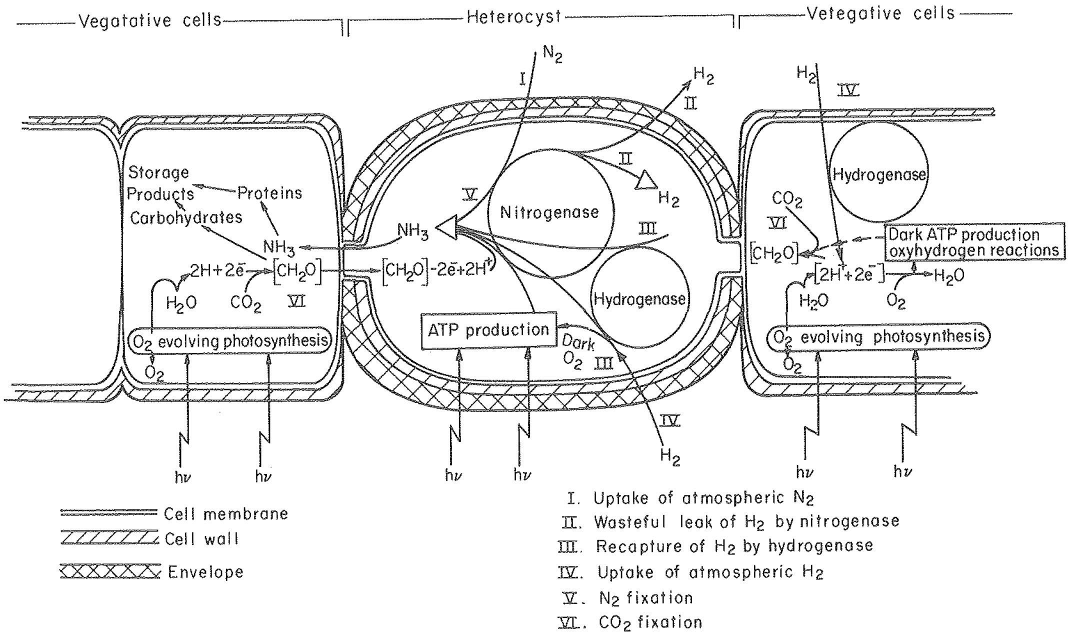

Fig. 1. Relation of pathways of H_2 metabolism to N_2 fixation and photosynthesis in heterocystous blue-green bacteria. (XBL 781-2712)

seen in the light. These observations were interpreted to indicate that O_2 is probably an efficient and final electron acceptor for H_2. Our interpretation also explains the DCMU inhibition in the light, which could be ascribed to the elimination of O_2 evolved by water photolysis.

H_2 consumption in the presence of O_2 both in the light and the dark was inhibited 90% by 1 mM KCN, but was unaffected by DCMU. When H_2-consumption activity was assayed in the presence of phenazine methosulphate and methylviologen, which act as artificial electron acceptors for H_2 via hydrogenase,[8] the same level of H_2 consumption activity was observed as in the presence of O_2. However, the fact that 1 mM KCN did not inhibit this activity indicates that KCN does not inhibit hydrogenase itself, but probably inhibits H_2 consumption by blocking the respiratory chain. Bothe et al.[9] have reported similar effects of O_2 on H_2 consumption in aerobically grown A. cylindrica. The results of both laboratories support the view that electrons from H_2 are transferred to O_2 via an oxyhydrogen reaction in aerobically grown and hydrogenase-induced cultures.

H_2 Consumption and Photosynthesis

To study the relationship between H_2 consumption and CO_2 incorporation in hydrogenase-induced cultures, we followed H_2 consumption in the presence of $NaHCO_3^-$ (8 mM). H_2 consumption increased twofold. The $NaHCO_3^-$-stimulated activity was inhibited 90% by the oxygen-evolution-inhibitor dichlorophenyl-dimehtylurea. We also measured CO_2 incorporation under the same conditions. H_2 did not stimulate CO_2 incorporation as much as HCO_3^- stimulated the H_2 consumption. The stimulation of CO_2 incorporation was variable, up to 30% in aerobic, and 10% in H_2-induced cultures. The reason for this variability is still not understood.

Our present studies suggest tht the stimulation of H_2 consumption by $NcHCO_3$ is probably due to enhanced photosynthesis which produces molecular oxygen by water photolysis. O_2 then serves as the final electron acceptor for H_2. Enhanced photosynthesis in hydrogenase-induced cultures is probably the result of increased energy synthesis through the oxyhydrogen reaction, which provides an alternative mechanism for the synthesis of ATP (Fig. 1).

Having observed that HCO_3^- stimulates H_2 consumption and that H_2 consumption stimulates CO_2 incorporation, it was decided to determine if some of the carbon products of photosynthesis were modified by H_2 in hydrogenase-induced cultures. Initial experiments with cultures exposed to $H^{14}CO_3^-$ indicated that the products of photosynthetic CO_2 fixation, observable by two-dimensional chromatography,[10] differ qualitatively more than quantitatively. We have not yet determined if these differences are due to aerobic-versus-anaerobic culture conditions or to an increase of H_2 consumption. Although the results are preliminary, they are of sufficient interest for follow-up studies to reveal the physiological pathways involved in H_2 enhanced photosynthesis.

Photosynthesis and N_2 Fixation

In hydrogenase-induced cultures the addition of 8 mM $NaHCO_3$ resulted in a 50-80% inhibition of nitrogenase activity. This inhibition was reversed by dichlorophenyl dimethylurea, the inhibitor of CO_2 fixation. This reversal indicates the possibility that CO_2 incorporation and N_2 fixation compete for energy supplied as ATP. Further experiments are in progress to elucidate more details of this relationship between N_2 and CO_2 fixation in regard to H_2 consumption.

Identification of Oxidation-Reduction Catalysts by Low Temperature Electron Paramagnetic Resonance (EPR) Studies

During the past year we[11] have been developing a method for suitably concentrating samples of blue-green bacteria cells for low temperature EPR spectroscopy. First, we removed some of the non-specific iron and manganese that interfere with observation of EPR centers of metalloproteins. Removal involved growing cultures in media which are deficient in iron and other metals, freezing and thawing samples in the presence of a metal ion chelator (ethylene diamine tetracetate) and then concentrating the samples by centrifuging them in EPR tubes before observation. Intact filaments and cell preparations from two blue-green bacteria species prepared in this manner yielded clear EPR spectra down to 5°K without manganese interference. The following two components have been tentatively identified: a heme protein at $g = 6.0$ and a new type of iron-sulfur protein at $g = 1.92$. The following two soluble components were detected in intact cells: ferredoxin; an iron superoxide dismutase; and a large amount of an Fe-containing component, mainly in the soluble fraction, which may be a storage form of iron. Under Fe-limited conditions of growth, we detected a diminished response from the A and B centers of photosystem I, the $g = 1.92$ signal, and the soluble ferrodoxin signal; the center X was undetected. All of these signals could be restored by reintroduction of iron into the culture medium. This provides important evidence that iron has a role in the synthesis and/or structure of these components. We found all of the above components to be present in heterocyst and vegetative cell preparations from aerobically grown cells. This preparation method should afford a means of characterizing electron transfer components in intact cell preparations. In future studies it will be used for characterizing pathways of H_2 consumption.

Ammonia Excretion by N_2-Fixing Filaments

Blue-green bacteria have been employed for many years as a nitrogen source for growing rice, being particularly useful for this purpose because this plant grows in moist paddies. Blue-green bacteria might, however, become an important ammonia producer for dry-land crops if a mechanism could be found, either through chemical or genetic manipulation of the growing microorganisms, such that ammonia utilized for assimilation into proteins might be partially excreted into the surrounding environment. It was recently reported that the glutamine-synthetase system plays a role in nitrogenase induction.[12-13] Initial studies have employed oxalyl diaminopropionic acid, a glutamate analog mainly found in the seeds of the legume Lathyrus sativus (a powerful neurotoxin in man).[14-15] Two species of N_2-fixing cultures grown in the presence of micromolar quantities of this analog were found to excrete relatively large quantities of ammonia.

Higher concentrations of the analog inhibited differentiation of heterocysts. This represents an exciting finding. It may provide a means to investigate regulatory pathways of ammonia assimilation into protein in these organisms, and the pathway relation to heterocyst differentiation.

PLANNED ACTIVITIES FOR 1978

To elucidate more fully the functional linking between H_2 consumption, CO_2 fixation and N_2 fixation, it is intended that:

1. We will identify pathways of H_2 consumption. The oxidation-reduction catalysts that accept electrons from H_2 will be investigated in hydrogenase-induced cultures by low temperature EPR and spectrophotometric methods.

2. We will investigate whether H_2 provides electrons or increased adenosine triphosphate (ATP) levels for nitrogenase-catalyzed N_2 reduction in heterocysts and for CO_2 reduction in vegetative fragments. These experiments will involve assays of nitrogenase and of CO_2 incorporation in the presence of known inhibitors of photosynthetic electron transfer, of dark electron transfer to O_2 (oxyhydrogen or Knallgas reaction), and of ATP synthesis.

3. The competition between N_2 fixation and CO_2 fixation will be further investigated, and the influence of H_2 consumption on the competition will be examined.

4. We will continue our studies to identify products of photosynthesis in H_2-induced cultures after exposure to $H^{14}CO_3^-$ by established techniques of two-dimensional paper chromatography.

5. The regulatory mechanisms of hydrogenase and nitrogenase induction are an interesting problem, one in which certain aspects can be readily investigated in blue-green bacteria. We shall study nitrogenase induction using an inhibitor of glutamine synthetase, oxalyl diaminoproprionic acid. We have found that this substance, even at very low concentrations, markedly stimulates ammonia excretion in two species of N_2-fixing blue-green bacteria. We intend to explore whether such chemical analogs involved in the assimilation of ammonia may be useful for ammonia production by growing microorganisms.

REFERENCES

1. R. Shubert, and H. Evans, "H_2 Evolution: A Major Factor Affecting the Efficiency of N_2-Fixation in Nodulated Symbionts," Proc. Nat. Acad. Sci. (U.S.A.) 73, 1207 (1976).
2. H. Bothe, J. Tennigkeit, G. Eisbrenner, and M. G. Yates, "The Hydrogenase-Nitrogenase Relationship in the Blue-Green Alga Anabaena cylindrica," Planta 133, 237-242 (1977).
3. K. Schneider, and H. G. Schlegel, Biochim. Biophys. Acta 452, 66-80 (1976).
4. R. O. D. Dixon, Arch. Mikrobiol. 85, 193-201 (1972).
5. E. Tel-Or, L. W. Luijk, and L. Packer, "An Inducible Hydrogenase in Cyanobacteria Enhances N_2 Fixation," FEBS Letters 78, 49-52 (1977).
6. L. Packer, E. Tel-Or, and L. W. Luijk, Fed. Proc. 36, 881 (1977).
7. L. Packer, E. Tel-Or, and L. W. Luijk, "H_2 Increases N_2 and CO_2 Fixation in Hydrogenase Induced Cyanobacteria," 4th International Congress on Photosynthesis Research (Reading, England, September 4-9, 1977).
8. E. Tel-Or, L. W. Luijk, and L. Packer, "Hydrogenase in N_2-Fixing Cyanobacteria," Archives of Biochemistry and Biophysics, January, 1978, in press.
9. H. Bothe, J. Tennigkeit, and G. Eisbrenner, "The Utilization of Molecular H_2 by the Blue-Green Alga Anabaena cylindrica," Arch. Microbiol. 114, 43-49 (1977).
10. T. Kanazawa, M. R. Kirk, J. A. Bassham, "Regulatory Affect of Ammonia on Carbon Metabolism in Photosynthesizing Chlorella pyrenoidosa, Biochim. Biophys. Acta 205, 401-408.
11. R. Cammack, L. Luijk, J. Maguire, and L. Packer, 1977, in preparation.
12. R. S. Tubb, "Glutamine Synthetase and Ammonium Regulation of Nitrogenase Synthesis in Klebsiella," Nature 254, 481-485 (1975).
13. S. L. Streicher, K. T. Shanmugam, F. Ausubel, C. Morandi, and R. B. Goldberg, "Regulation of Nitrogen Fixation in Klebsiella pneumoniae: Evidence for a Role of Glutamine Synthetase as a Regulator of Nitrogenase Synthesis", J. Bact. 120, 815-821 (1974).
14. S. L. N. Rao, and P. S. Sarma, "The Isolation and Characterization of -N-Oxaly-L- , -diaminoproprionic Acid," Biochem. Pharm. 16, 218 (1964).
15. M. C. Duque-Mugalhues, and L. Packer, "Action of the Neurotoxin B-N-Oxaly-L- , -Diaminoproprionic Acid on Glutamate Metabolism of Brain Mitochondria," FEBS Letter 23, 188-190 (1972).

PHOTOVOLTAIC EFFECTS OF BACTERIORHODOPSIN AND STUDIES ON ITS MECHANISM OF ACTION

L. Packer, R. Mehlhorn, P. Shieh, T. Konishi and S. Tristram

INTRODUCTION

We have been developing a photovoltaic cell that utilizes catalytic conversion of light to energy electrical ion flow across a cell membrane. The protein catalyst bacteriorhodopsin, isolated in purple patches from the cell membrane of the halophilic bacterium Halobacterium halobium,[1] is well suited to the device because its energy transduction is a direct process unlike the complex system of pigments, proteins, and hydrophobic cofactors that are employed for light-energy transformation by photosynthesis in higher plants.

Because of its potential for photovoltaics, the mechanism of light-energy transformation by bacteriorhodopsin is presently one aspect of our studies. The possibility of using these proteins in laboratory-scale photovoltaic devices was first demonstrated in the laboratory of Skulachev in Moscow,[2] where it was shown that proton pumping vesicles of lipid and bacteriorhodopsin could be induced to adsorb to the surface of planar membranes formed across a small orifice in a TEFLON vessel. Unfortunately such membrane films are not stable for more than an hour under optimum conditions.

The planar membrane technique was improved when the structural matrix of a Millipore filter was used to provide long-term mechanical stability for membranes with diameters in the centimeter range.[3-6] Using the Millipore-filter system, we are attempting to optimize photocurrent and voltage and to increase stability of the membrane photocell under conditions of continuous illumination.

ACCOMPLISHMENTS DURING THE CURRENT CALENDAR YEAR

Structural Elements of the System

Photovoltaic assay parameters of membrane composition and procedures for attaching bacteriorhodopsin onto the planar membrane have been varied to achieve maximum possible photocurrents and voltages. The two structural elements of the system are (a) the lipid-impregnated filter membrane, and (b) the bacteriorhodopsin-containing spherical lipid vesicles. Each of these structural elements was studied with the following results:

(a) Optimal lipid impregnation of the filter membrane was observed to require considerable time. The resistance of the filter membrane and the subsequent photovoltages increased over a period of hours, reaching a plateau after immersion for 15 hours in a decane solution of soybean lipids.

(b) Bacteriorhodopsin was incorporated into lipid vesicles using a standard ultrasonic irradiation procedure. We found that maximum photovoltages could be achieved by forming lipid vesicles with prolonged (30 min) sonication of the lipids alone, followed by a brief (3 to 5 min) sonication of purple membrane sheets mixed with the vesicles. Photovoltages were affected by the bacterial strain from which BR was obtained (R1 was better than S9), and the lipid-to-protein ratio of the vesicles. Maximum photovoltages were realized when the lipid-to-protein ratio was 30:1, a surprisingly high value compared to the low ratios found in the purple membrane patches isolated from the bacteria. In principle, photovoltages should be higher when lipid-to-protein ratios are smaller because of higher bacteriorhodopsin concentrations at the filter interface and also because back-leakage of pumped protons would thus be diminished.

To form a photocell, we have combined the Millipore filter and the bacteriorhodopsin-containing vesicles under conditions which promote adsorption. Maximum photovoltages have occurred in the presence of calcium ions that caused attachment of the vesicles to the filter membrane. The maximum photopotential reached a steady-state value after about 40 min. Once the vesicles were tightly attached to the filter, washing the aqueous compartments on either side of the filter membrane more than ten times with calcium-free media reduced the maximum photovoltage by only 30%.

Specific purified lipids (e.g. phosphatidyl choline) impregnated into the Millipore filter gave poorer results than a relatively crude fraction of soybean lipids. Although some of these lipids conferred a higher-resistance across the filter membrane, no straightforward relationship between membrane resistance and photopotentials could be demonstrated. The highest photovoltages obtained, 350 millivolts for a single membrane, compare well to the maximum-possible-value suggested by an analysis of current-voltage curves.[3]

The photovoltaic cell, optimized as described above, was illuminated continuously, and its open-circuit voltage and short-circuit current were measured over time to assess its stability. A decline in the photovoltage and current leading to a complete cessation of activity after 90 min was observed. Since it has been shown earlier[4,5] that the system is stable for months in the dark, the destruction is light activated. It is also noteworthy that the isolated purple membrane patch is considerably more stable (more than 6 hrs),[4] suggesting that the reconstitution technique had enhanced the system's susceptibility to photodestruction.

There is considerable interest in technological applications of the bacteriorhodopsin membrane including, possibly, coupling the system to specific ion-exchange membranes for specific ion accumulation. We have been interested in utilizing the electrical output of the membrane to electrolyze water. To this end, we have connected several Millipore filter membranes in series. As shown in Fig. 1, a maximum voltage of 1.55 V is achieved when five membranes are illuminated.

Proton Translocators in Lipid Vesicles

In order to develop practical photochemical cells based on bacteriorhodopsin or analogous molecules, it will be important to understand bacteriorhodopsin's mechanism of action (Fig. 2). Chemical modification is a good approach to gaining some understanding because bacteriorhodopsin is the only protein in the purple membrane preparation and is extremely stable.[4-7] As shown in Fig. 2, both catalysts of primary energy-transducing membranes are involved in proton translocation. Bacteriorhodopsin carries out light-energy transformation by proton translocation across the cell membrane and is comprised of a single protein. One portion of the protein, in the vicinity of the retinal chromophore, is involved with photoexcitation events and the photoreaction cycle which initiates the vectorial movement of the proton. This section of the molecule appears to be concerned with proton pumping activity. Aromatic amino acid residues, like tyrosine and tryptophan, are important for the proper environment of the chromophore. The remainder of the molecule efficiently channels the vectorial translocation of the proton by a mechanism which is not yet well understood.

Mitochondiral ATPase is a large complex catalyst consisting of about twelve polypeptides. The F_1 portion is the site of hydrolysis and ATP synthesis. The hydrophobic membrane proteins which are associated with it appear to be involved in proton translocation. One of these, the 7,500-dalton, subunit-9 proteolipid, passively catalyzes proton translocation in model membrane systems. Hence, in this molecule, two regions may be visualized: the pump region (F_1 portion) and the channel region (hydrophobic proteolipid portion). The gate that controls coupling the proton between these two regions may be in the vicinity of the oligomycin sensitivity-conferring protein (OSCP).

During the past year, we have studied the effects of chemical alteration induced by both monofunctional and bifunctional reagents on photocycling of the bacteriorhodopsin molecule.

Cross-linking bacteriorhodopsin with a bifunctional reagent, dimethyl adipimidate (8.5Å), has shown that the protein exists in a dark-adapted conformation that is distinct from its light-adapted conformation. The more compact light-adapted conformation may facilitate interacting the retinal chromophore with nearby amino acid residues.[8] These two conformations differ in their exposure to the aqueous medium (as shown with ^3H_2O and D_2O), displaying a 5-7% difference in tritium exchangeability.[9]

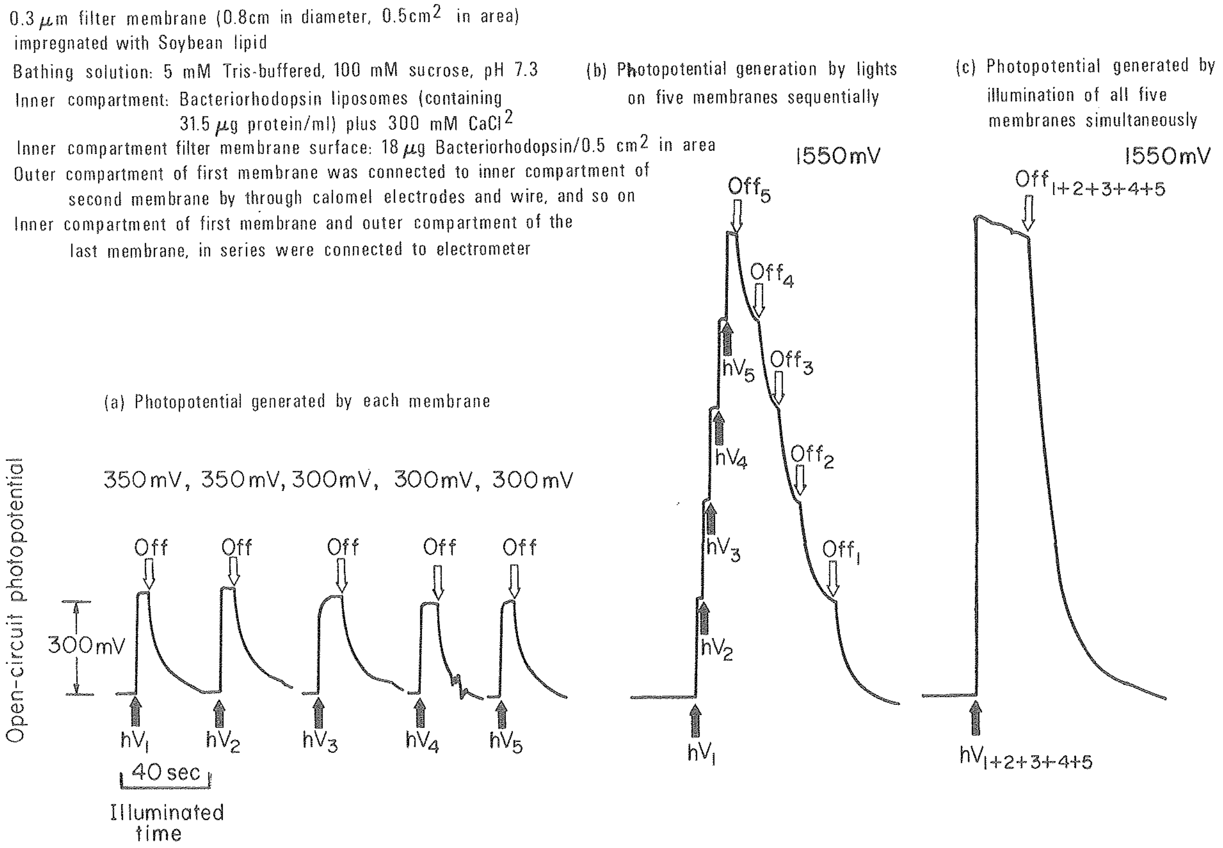

Fig. 1. Open circuit photopotential of a series connection of five lipid-impregnated millipore filter membranes with adsorbed bacteriorhodopsin lipid vesicles. (XBL 774-3312)

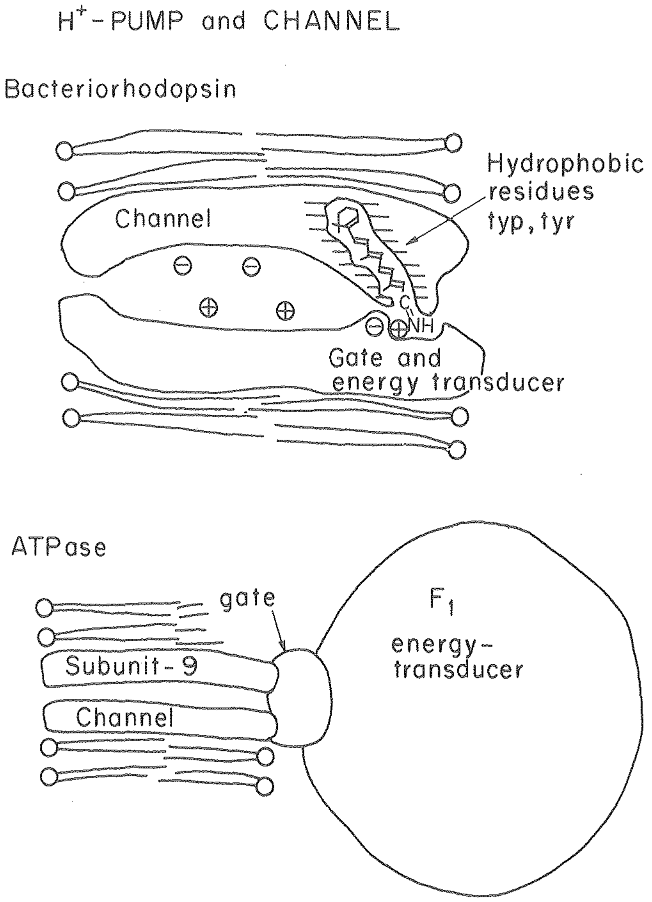

Fig. 2. Mechanism of the proton translocators, bacteriorhodopsin and the proteolipid subunit-9 polypeptide of the mitochondrial adenosine triphosphatase. (XBL 781-2711)

Treatment with dimethyl suberimidate (11.5Å) causes intermolecular cross-linking of bacteriorhodopsin, as shown with gel-electrophoresis, yet does not impair proton pumping activity.[10,11] This implies that mobiity of bacteriorhodopsin molecules relative to one another is not required for activity. Why this protein is arranged in crystalline membrane arrays is thus still an open question; we believe the cluster arrangement of three molecules may facilitate light absorption and help properly orient the protein in the plane of the membrane. Intramolecular cross-linking with a shorter bifunctional reagent, dimethyl adipimidate, inhibits light-driven proton translocation.[10]

Modification of tryptophan[12] and tyrosine[13] with monofunctional reagents showed that at least some of these amino acids are located in close proximity to the retinal chromophore of bacteriorhodopsin. Such modification was associated with alterations in proton translocating activity, suggesting that these amino acids participate in coupling light energy to proton-pumping process.[12]

How bacteriorhodopsin's structure is related to its function as a unidirectional, light-activated proton gate has generated worldwide interest and research. Our present findings contribute important information about the role of protein conformational changes in the vicinity of the retinal chromophore and about how hydrophobic amino acids of the protein environment affect activity.

Another proton-translocating protein, subunit-9 isolated from the yeast mitochondrial-ATP-synthetase complex (Fig. 2), was also studied as part of our overall effort to understand how membrane pumps, ionophores, and channels function. Our assay involved collapsing a light-induced proton gradient formed by bacteriorhodopsin in liposomes attached to a planar membrane.[14] We were able to demonstrate unequivocally that in lipid vesicle systems these proteins act as proton ionophores and are specifically inhibited by the inhibitor of the native membrane enzyme ATPase, oligomycin. Confirming evidence was provided with subunit 9 preparations isolated from an oligomycin-resistant mutant.[14,15] These studies indicate that the subunit 9 protein lipid may form the link between proton gradients, formed by the mitochondrial respiratory chain, and synthesis of chemical energy as adenosine triphosphate by the membrane ATP synthetase.

FUTURE PLANS

(1) To study the structure of the bacteriorhodopsin-containing Millipore filter membranes. The intent of these studies is to understand the present requirement for high lipid-to-protein ratios and also to prolong the active lifetime of the photocell. Preliminary evidence suggests that lipid oxidation is a major factor in the deterioriation of the system, and thus that observed instability will be decreased by free radical scavengers in the lipid phase and by lipid-soluble singlet oxygen quenches and superoxide free radical traps in the membrane interface region.

We also plan to make planar membranes without lipid to avoid photo-induced lipid damage. Searching for ways to orient sheets of purple membranes and to anchor them to a planar membrane surface, we will explore chemical cross-linking and embedding within a polymer matrix.

(2) To continue with studies on the mechanism of bacteriorhodopsin function. Some of the strategies we will employ are:

(a) To pursue further chemical modification studies to identify how amino acid residues are involved in photoexcitation of the chromphore (photocycling).

(b) To design experiments that will reveal which amino acid residues of the molecule are involved in proton translocation. These will include cleavage of the retinal pigment and tests of the bleached protein's ability to manifest proton ionophore activity in reconstituted liposomes or the Millipore filter assay system.

Both studies will help clarify what regions of the bacteriorhodopsin molecule are distinctly involved in light-induced, proton-pumping activity and how the photoexcitation events are coupled to the vectorial proton transport. The studies may help us understand how the molecule has evolved to function so efficiently as a light energy converter and how the structure of the molecule prevents the backflow of protons.

A longer-range goal is to mimic the mechanism of light energy transduction by bacteriorhodopsin and to construct a biosolar cell based upon a simpler synthetic system.

REFERENCES

1. O. Oesterhelt and W. Stoeckenius, "Rhodopsin Like Protein from Halobacterium halobium", Nature New. Biol. 233, 149 (1971).
2. L. A. Drachev, A. A. Jasaitis, A. D. Kaulen, A. A. Kondrashin, E. A. Liverman, L. B. Nemecek, S. A. Ostroumov, A. Somehov, A. Yu and V. A. Skulachev, "Direct Measurement of Electric Current Generation by Cytochrome Oxidase, H^+-ATPase and Bacteriorhodopsin," Nature 249, 321 (1974).
3. V. P. Skulachev, "Conversion of Light Energy into Electric energy by Bacteriorhodopsin," FEBS Letters 64, 23 (1976).
4. L. Packer, T. Konishi and P. K. Shieh, "Model Systems Reconstructed from Bacteriorhodopsin" in Living Systems as Energy Convertors, R. Buvet and M. J. Massue, Eds., (North Holland Publ.) p. 119.
5. P. K. Shieh and L. Packer, "Photoelectrical Potential and Current Generation by Bacteriorhodopsin Across Lipid Impregnated Millipore Filter Membranes," Biophys. J. 17:2, 257a (1977).
6. L. Packer, P. K. Shieh, J. K. Lanyi and R. S. Criddle, "Use of Lipid Impregnated Millipore Filters for the Direct Measurement of Photopotentials Across Envelope Vesicles of Halobacterium halobium and for Assay of Ionophere Activity of the Oligomycin Binding Subunit 9 of the Yeast Mitochondrial ATPase," in Bionergetics of Membranes, L. Packer et al., Eds. (Elsevier/North-Holland Biomedical Press, 1977), p. 149.
7. L. Packer, T. Konishi and P. K. Shieh, "Conformational Changes in Bacteriorhodopsin Accompanying Ionophore Activity," Fed. Proc. 36, 1819 (1977).
8. T. Konishi and L. Packer, "Light-Dark Conformational States in Bacteriorhodopsin," Biochem. Biophys. Res. Comm. 72, 1437 (1976).
9. T. Konishi and L. Packer, "Hydrogen Exchange of Dark-Adapted and Illuminated Bacteriorhodopsin," FEBS Letters 80, 455 (1977).
10. T. Konishi, S. Tristram and L. Packer, "Photocycling Activity of Cross-Linked Bacteriorhodopsin," in Abstract of U.S.-Australian Joint Seminar on Evolution of Light Trapping Systems (Hawaii, Dec. 12-15, 1977).
11. L. Packer, T. Konishi and R. Criddle, "Proton Pumps and Channels: Studies with Bacteriorhodopsin and a Proteolipid of the Mitochondrial ATPase" in Evolution of Light Trapping System, D. W. Deamer et al., Eds., (Academic Press, N. Y. 1978), in press.
12. T. Konishi and L. Packer, "Chemical Modification of Bacteriorhodopsin with N-Bromosuccinimide," FEBS Letters 79, 369 (1977).
13. T. Konishi and L. Packer, "pH Titration and Tyrosine Modification of Bacteriorhodopsin," in Abstract of Biophysical Society Meeting (Washington, D. C. March 26-30, 1978).
14. R. Criddle, L. Packer and P. Shieh, "Oligomycin Dependent Ionophoric Protein Subunit of Mitochondrial ATPase," Proc. Nat. Acad. Sci. (U.S.A.) 74, 4306 (1977).
15. T. Konishi, L. Packer and R. Criddle, "Purification and Assay of a Proteolipid Ionophore from Yeast Mitochondrial ATPase," in Methods Enzymol, S. Fleischer and L. Packer, Eds., in press 1978.

Energy Efficient Buildings

INTRODUCTION

Research in the Division's energy use and conservation program addresses a broad range of technical and institutional issues that influence the pattern of energy use. These include research into energy use in buildings, and the analysis of energy conservation strategies and measures.

Work on energy use in buildings has concentrated on the following areas:

- Research on the thermal performance of building envelopes. This work includes <u>in-situ</u> studies of heat transfer through building components, as well as measurements of air infiltration. Research on the effectiveness of various retrofits is also being carried out.
- Research on building ventilation and indoor air quality as it affects health. Particular attention is paid to the effects on air quality of energy-saving decreases in ventilation rates.
- Development of CAL-ERDA (DOE-1), a computer program for energy analysis of buildings, which is a tool for design, research, and the evaluation of compliance with building codes.
- Development of a national plan for windows and lighting. Several research projects are underway at LBL, including beam daylighting, window thermal performance, and state-of-the-art fluorescent lighting.
- Demonstration programs that focus on energy conservation in schools, colleges, hospitals and homes.
- Conservation education programs to increase public awareness of conservation strategies.
- Provision of data and recommendations to enable governmental agencies to establish energy-conserving standards for buildings and appliances.

BUILDING ENVELOPES PROGRAM

P. Condon, D. Grimsrud, R. Kammerud, A. H. Rosenfeld
and R. Sonderegger

INTRODUCTION

The Building Envelopes Program began during the second quarter of calendar year 1977 as part of a broad based conservation program titled Building Envelopes and Ventilation (BEV). The program was initiated in response to a need for a systematic study of the building as a whole rather than as a sum of component parts.

The objective of the Building Envelopes portion of the Program is to develop energy-efficient envelope systems through RD&D which will lead to a fundamental understanding of the thermal operation of buildings. The program is divided into two project areas: infiltration of outside air and system thermal performance.

The infiltration projects have the following goals: (a) to identify and determine the magnitude of infiltration sources, (b) to identify and demonstrate retrofit measures, component designs, and fabrication techniques which effectively limit infiltration, and (c) to develop simple measurement techniques appropriate for widespread application. The first goal, source identification, is geared specifically to improving our understanding of the impact on energy consumption of infiltration; computer modeling is an inherent part of this effort. The second goal, infiltration reduction, is closely related to air quality studies which are part of the Ventilation program. Substantial reductions in infiltration rates must be accompanied by increased rates of controlled ventilation. The third goal is directed toward demonstrating techniques of infiltration measurement that would be appropriate for application in code compliance checks or broad-based conservation inspection services.

The system thermal performance projects have the following goals: (a) to correlate field performance, predictive methodologies, and laboratory thermal measurements of envelope systems, (b) to define and/or develop parameters which quantify the thermal performance of envelope systems, (c) to foster the development and acceptance of innovative system designs which effectively improve the thermal performance of the envelope. The first two goals are closely related. They address the need to provide appropriate tools and data to the building designer so that the performance of the completed structure can be reliably predicted. Field performance must be related to laboratory-measurable quantities through methodologies which are applicable at the design and engineering stage. Design and construction guidelines must be developed to insure that the performance of the structure will correspond to the predictions. The final goal is not independent of the first two, but is distinct in implementation. It is expected that this goal can best be met through a combination of design/demonstration competitions and a thorough research program directed at understanding the advantages and limitations of existing building envelope systems.

ACCOMPLISHMENTS DURING 1977

The infiltration projects began with the creation of an annotated bibliography from an extensive literature search of previous work. Emphasis was placed on determining the relative merits of various measurement techniques, on determining the extent of existing infiltration data, and on assessing the state-of-the-art of computer modeling of infiltration. Based on the search, two measurement techniques were selected for the experimental efforts--tracer gas measurements and building pressurization. Subsequently, the measurement systems were specified, hardware fabrication took place, and data analysis software was developed. In cooperation with Department of Energy personnel, the information gathered in the literature search was summarized and presented to the International Energy Agency in the form of a proposed research agenda for their future attention. This research program was directed towards improved techniques for modeling infiltration.

At LBL, residential and small commercial building infiltration projects were chosen for study. These projects have been coordinated with parallel efforts at the National Bureau of Standards, whose research will be concentrating on the commercial building sector. The LBL efforts are oriented towards low-rise buildings where infiltration is driven by both pressure and temperature differentials (wind and stack effects respectively). Infiltration source identification and repair, applicability of simplified measurement techniques (pressurization) and modeling will be emphasized.

The thermal performance projects have been planned and implementation begun. These efforts focus on research and development which will initially lead to a detailed understanding of the heat transfer through conventional building systems (stud walls). A coordinated set of field experiments and testing laboratory measurements have been identified. The goal is to explore the degree of correlation between laboratory measurements of building components and field performance of structures. The in-situ experiments will be used to lead to an understanding of the deleterious effects of air leakage into uninsulated and insulated walls, and also to study the three-dimensional heat flow effects caused by wall studs and by convection in the stud spaces. Additionally, the field data will be utilized in validating a simplified, engineering oriented, one dimensional dynamic model for heat flow in wall systems.

The laboratory measurements are being used to determine the micropatterns of heat flow in stud wall construction. Data from laboratory tests will be used to calibrate a detailed three-dimensional heat flow thermal modeling computer program. The analysis will be important in the development of recommendations for the test procedures to be used in measuring wall systems. Current standard procedures are inadequate and not sufficiently specific to insure unambiguous results. In the long term, a data base of thermal performance properties of multicomponent wall systems must be made available to the building design/engineering community; the measurements obtained in the laboratory experiments will aid in defining the types of data to be included in the data base and will identify the best methods to be used in obtaining the data.

It is anticipated that both the laboratory and field experiments out lined above can be extended in the future to other types of construction (masonry, wall/window/door combinations, etc.). The attention to conventional construction types will be supplemented by demonstrations of innovative construction and by the utilization of unconventional materials and fabrication techniques. The results from this work will be included in the overall data base.

PLANNED ACTIVITIES FOR 1978

During the early weeks of 1978, both the infiltration and in-situ thermal experiments will begin. Detailed studies of the infiltration properties of a single house will be undertaken. There will be three goals: (a) correlation of the measured infiltration rate with measured weather conditions, (b) correlation of the infiltration rate as measured by tracer gas techniques with the leakage rate measured by building pressurization, and (c) identification and quantification of the sources of infiltration, and identification of repair procedures. The detailed studies of infiltration in a single residence will be complemented by a survey of several other buildings so that the generality of the results can be investigated.

The thermal experiments will begin with an examination of the variability of the conductive properties of the envelope of a single building. This will indicate the magnitude of the effects on the performance of the as-built structure due to variations in workmanship. These experiments will be followed by detailed examination both of the effects of convection within stud walls, and of the effects of the studs themselves. The data obtained will be compared to that obtained in laboratory tests.

Laboratory measurements will begin in mid-1978. They will be performed under contract with one of the existing testing laboratories. In early 1978, an assessment of the capabilities, past experience and testing procedures of the testing laboratory will be conducted. Standard procedures for the types of tests to be performed do not currently exist and will be specified by LBL. The data gathered will be analyzed using a three-dimensional finite difference heat transfer code. The calibrated/validated code will be used, together with the experience obtained in the measurement program, to develop recommendations for industry-wide testing procedures of built walls.

VENTILATION PROGRAM

C. D. Hollowell, J. V. Berk, R. G. Langenborg,
C. Lin, and J. H. Pepper

INTRODUCTION

The Ventilation Program, which is funded by the Department of Energy's (DOE) Division of Buildings and Community Systems, is a major component of Lawrence Berkeley Laboratory's (LBL) Energy Efficient Buildings Program. The objective of the Ventilation Program is to conduct indepth research and development on existing and proposed ventilation requirements and mechanical ventilation systems in order to provide recommendations for the establishment of energy efficient ventilation standards and ventilation designs for residential and commercial buildings. LBL will provide both technical and management support to DOE headquarters for ventilation research and development projects.

Approximately 20% of the nation's yearly energy use is for heating, cooling and ventilating buildings. It is expected that energy savings will be realized after implementation of energy-efficient ventilation standards. These standards and design criteria will be based upon a comprehensive analysis (including health and comfort of occupants) of the data base established by this ventilation program. The goal is to minimize the energy needed to provide ventilation while at the same time not compromising human health and comfort. One of the main components of this data base will be data gathered by LBL on indoor air quality. Previous research at LBL concerning combustion generated indoor air pollution indicated that it is essential to consider the impact of reduced ventilation on indoor air quality.[1]

ACCOMPLISHMENTS DURING 1977

Work began on the Ventilation Program in April, 1977. In order to meet the objectives of the program, tasks were carried out both in-house at LBL and, to a large extent, by outside contractors who are supervised by an LBL management team.

A mobile laboratory for research and development studies of ventilation requirements and energy utilization in residential and commercial buildings was designed and fabricated by the Ventilation Group in 1977 (Figs. 1 and 2). In support of the field monitoring projects, laboratory and small scale field studies are being carried out to achieve a methodology for characterization and measurement of indoor air pollution. The variables to be measured are:

1) temperature, relative humidity, and air velocity

2) odors

3) toxic chemicals

4) biological species.

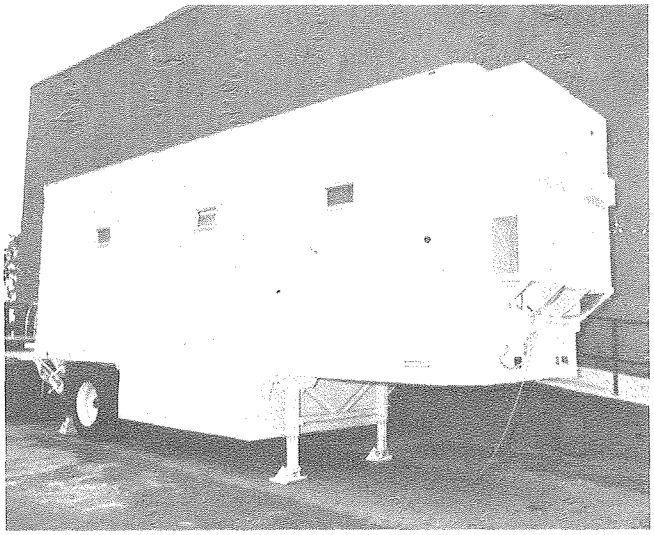

Fig. 1. Exterior view of the EEB Mobile Laboratory. (CBB 770-13104)

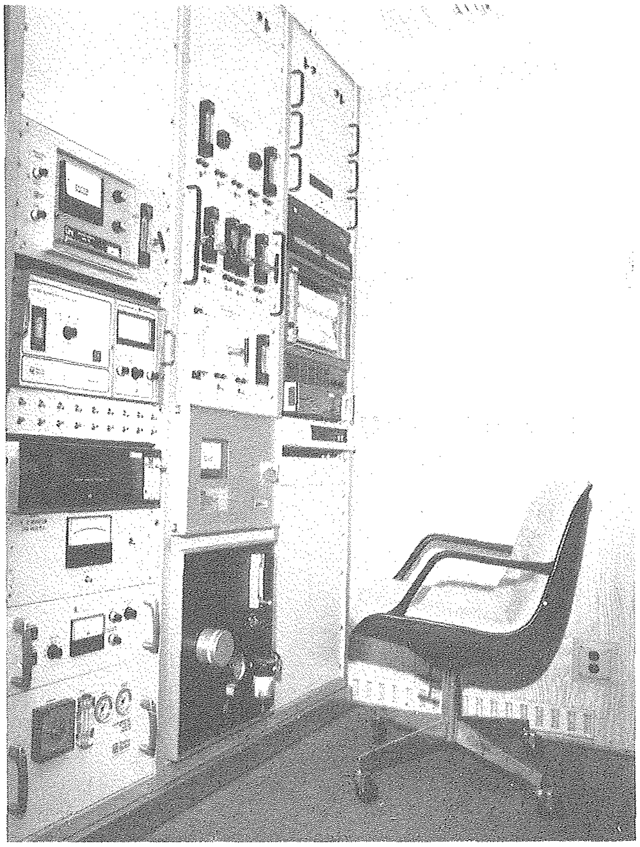

Fig. 2. View of air quality measurement and data acquisition systems in the EEB Mobile Laboratory. (CBB 770-13108)

The Energy Efficient Buildings (EEB) Mobile Laboratory will initially be used in studies of indoor air quality for the establishment of energy efficient ventilation requirements in several types of buildings. These include buildings before and after energy conservation retrofits and new buildings incorporating energy efficient designs.

The EEB mobile laboratory will be located outside the building to be studied and air from various locations within the structure will be drawn through teflon sampling lines into the trailer for analysis. By extending sampling lines (one of which will be used to monitor ambient air) from four different locations into the trailer and sequentially sampling these lines, the air quality can be simultaneously monitored in several rooms.

The mobile laboratory contains sampling, calibration, and monitoring systems (Fig. 3) to measure the concentration of several pollutant gases. Table 1 lists the air quality monitoring capability of the EEB mobile laboratory. The gas parameters, as well as indoor comfort parameters such as temperature, relative humidity and air velocity at the sampling sites, and outdoor meteorological parameters (temperature, relative humidity, wind speed, wind direction and solar radiation) are monitored continuously. Infiltration rates will also be monitored continuously using a tracer gas system developed at LBL in which ethane is injected and monitored under controlled conditions at the sampling site. All of these continuously monitored parameters are recorded on a microprocessor-controlled floppy disk. This information can be transmitted from the field back to LBL via telephone or by physically sending the floppy disk to LBL where it may be read into the LBL system.

In addition to the parameters discussed above, there are several others for which continuous monitoring is not feasible. Some of the contaminants must be collected with gas bubblers and other sampling techniques requiring subsequent laboratory analysis. These contaminants include radon, aldehydes, ammonia, and selected organic compounds. They will require the use of laboratory techniques such as UV spectrophotometry, gas chromatography, liquid chromatography, etc.

The size distribution of the particulate matter in the air will be measured using both an optical scattering instrument and automatic dichotomous air samplers; the latter are also used to collect particulate matter for chemical analysis. The dichotomous air samplers, developed at LBL, separate the aerosols into respirable and non-respirable fractions (below and above 2.5 micron size) using a flow-controlled virtual impaction system which deposits the particulate matter on teflon filters. The particulate matter collected on the filters is analyzed at LBL using beta ray attenuation to measure mass concentration, and x-ray fluorescence to determine chemical composition for 27 elements.

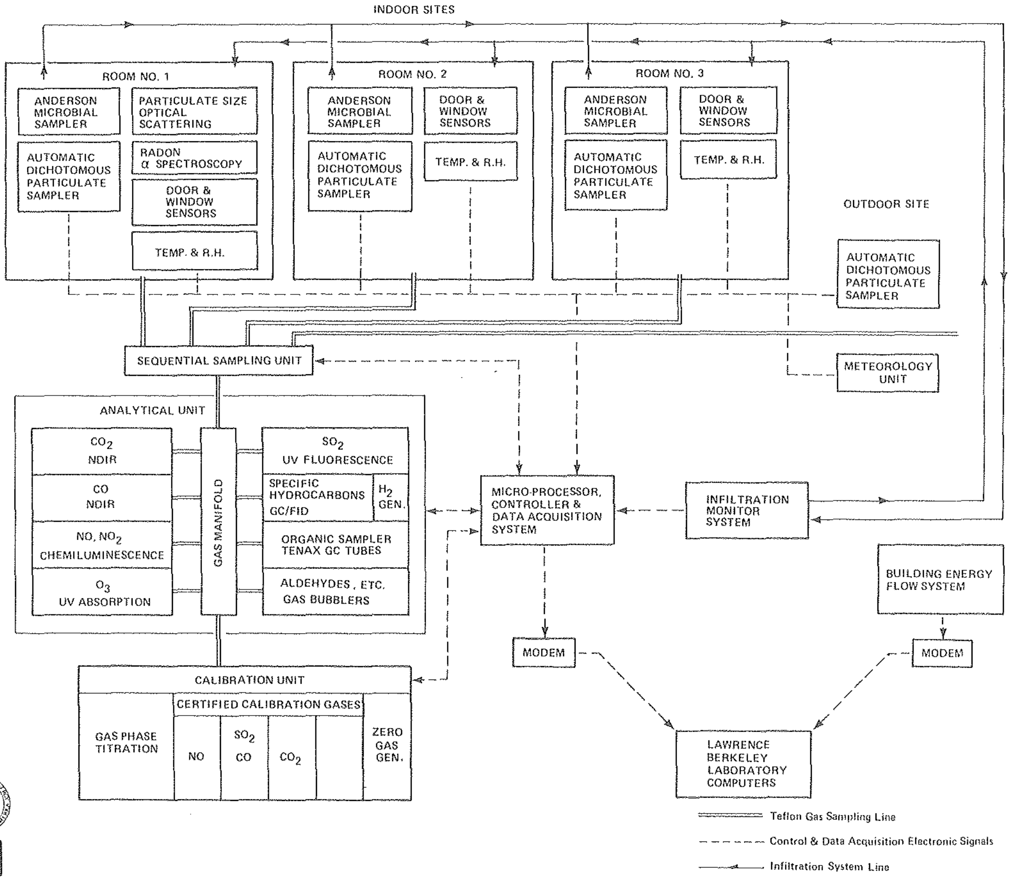

Fig. 3. Energy Efficient Buildings Mobile Laboratory System. (XBL 7712-11471)

Table 1. Instrumentation for Lawrence Berkeley Laboratory Energy Efficient Building Mobile Laboratory.

Parameter	Principle of Operation
FIELD	
Continuous Monitoring Instruments:	
Infiltration	
Ethane (Tracer Gas)	IR
Indoor Temperature, Moisture and Air Movement	
Dry-Bulb Temperature	Thermistor
Relative Humidity	Lithium Chloride Hygrometer
Air Velocity	Anemometer
Outdoor Meteorology	
Dry-Bulb Temperature	Thermistor
Relative Humidity	Lithium Chloride Hygrometer
Wind Speed	Generator
Wind Direction	Potentiometer
Solar Radiation	Spectral Pyranometer
Gases	
SO_2	UV Fluorescence
NO, NO_x	Chemiluminescence
O_3	UV Absorption
CO	NDIR
CO_2	NDIR
Radon	Alpha Spectroscopy
Particulate Matter	
Size Distribution	Optical Scattering
Radon Progeny	Alpha/Beta Spectroscopy
Sample Collectors:	
Gases	
Aldehydes, NH_3	Chemical Reaction/Absorption (Gas Bubblers)
Selected Organic Compounds	Absorption (Tenax GC Adsorption Tubes)
Particulate Matter	
Aerosols (Respirable/Non-respirable)	Virtual Impaction/Filtration
Bacterial Content	Inertial Impaction
LABORATORY	
Gases	
Aldehydes, NH_3	UV-Visible Spectroscopy
Selected Organic Compounds	Gas Chromatography (GC-FID/EC/MS)
Particulate Matter	
Mass Concentration (Respirable/Non-Respirable)	Beta Ray Attenuation
Chemical Composition	
Inorganics	X-Ray Fluorescence (XRF), Photoelectron Spectroscopy (ESCA)
Organics	Gas Chromatography-Mass Spectroscopy (GC-MS) Liquid Chromatography
Bacterial Content	Colony Counting

The bacterial content of the air is measured with inertial impaction devices that deposit particles in specific size intervals on petri dishes. The dishes are incubated for 48 hours and their bacterial colonies are counted. This microbial sampler was developed by the University of California Naval Biosciences Laboratory under contract to LBL.

During 1977 LBL began conducting a literature and equipment survey of existing and advanced contaminant control systems. The specific tasks in progress are:

1) Development of a contaminant control equipment file, edited and categorized by product type for each of 500 suppliers contacted in Fall 1977. A follow-up survey of non-respondents will be initiated in early 1978.

2) Development of an annotated bibliography on ventilation contamination control systems.

3) Installation of a comprehensive data base and numerical data bank utilizing the Berkeley Data Base Management System. Preliminary feasibility has been established, and construction of a pilot bibliographical data base is in progress.

LBL was managing two subcontracts in 1977, both of which will continue into 1978. The University of Minnesota, under a sole source subcontract, is performing a critical literature assessment to establish the current practice and state of the art in hospital ventilation requirements. The intent is to recommend an R&D program for development of a data base adequate to establish energy efficient hospital ventilation standards.

The Naval Biosciences Laboratory (NBL), under a subcontract, has developed a field sampling unit for measuring the microbial burden of air in hospital and educational facilities. This apparatus will aid LBL in evaluating the effects of ventilation and energy conservation measures on the levels, characteristics, and control of the microbial burden of air in hospitals and educational facilities.

PLANNED ACTIVITIES FOR 1978

In 1978 the following sites will be included in the field monitoring study of indoor air quality:

LBL Research House, Walnut Creek, CA
Educational Facilities Buildings,
  San Francisco Bay Area
Minimum Energy Dwellings, Mission Viejo, CA
Naval Regional Medical Center, Long Beach, CA
Iowa State University Energy Research
  House, Ames, IA
Iowa State University, Carver Hall Classroom
  Building, Ames, IA
Fairmoore School, Columbus, OH

In 1978 LBL will continue to manage subcontracts already let in 1977 (University of Minnesota and NBL) and also several new ones. The University of Minnesota will hold an International Working Conference in the winter of 1978 on Hospital Ventilation Standards and Energy Conservation.

It is intended that several new subcontracts will be initiated in 1978. These will be in the areas of odor control and ventilation requirements in hospitals and educational facilities, energy conserving mechanical ventilation systems, and variable ventilation control systems with occupancy/activity sensors.

Work will begin in 1978 on the development and demonstration of variable ventilation control systems using sensors which measure parameters sensitive to building occupancy and activity loads (e.g., sensors for CO_2, CO, enthalpy). The following tasks will be pursued in this project:

1) Estimate the magnitude of energy savings through national implementation of variable ventilation control systems.

2) Determine the cost-effectiveness of variable ventilation control systems with occupancy/activity sensors.

3) Establish the relationships between building occupant/activity loads, ventilation rate, and ventilation requirements.

4) Design and fabricate a variable ventilation control system with occupancy/activity sensors.

5) Demonstrate variable ventilation occupancy/activity-based control systems in various commercial building types.

A detailed study of the mechanical methods of providing ventilation to buildings will reveal areas in which better design can conserve energy. Research, design and development will begin in 1978 to provide innovative, cost-effective, and readily acceptable mechanical ventilation systems for the retrofitting of existing buildings and for application to new buildings.

Mechanical ventilation systems of the simple mechanical exhaust type (with air replacement by infiltration) and the balanced type (with both mechanical supply and exhaust) will be investigated for residential buildings in 1978. A major task will include studies of heat recovery devices as integral components of mechanical ventilation systems in residential buildings.

A ventilation data base will be initiated in 1978 to contain bibliographic and numeric entries, compiling existing data bases from LBL, Naval Biosciences Laboratory and the University of Minnesota. In 1978 it is expected that the logical and physical program design will be completed and that LBL data bases on infiltration and contaminant control will be entered.

Present recommended standards for natural and mechanical ventilation of buildings of various types are contained in the American Society of Heating, Refrigeration and Air Conditioning Engineers (ASHRAE) Standard 62-73. One of the tasks of the Ventilation Program is to examine and coordinate, on an interagency basis, guidelines for the updating of ventilation standards which could be applied to retrofit and new building applications. It is anticipated that ASHRAE will assist LBL in the development of recommended ventilation standards.

The impact on human comfort and health of energy efficient heating, ventilating and air conditioning systems in buildings will be studied by LBL with the cooperation of government agencies, professional societies and academic institutions. These studies will consider the effect on humans of various physical, physiological and psychological factors.

The culmination of the program activity described above will be a set of recommendations for the ventilation requirements needed in retrofit applications and new construction. It is expected that these requirements will subsequently be included in the standard building codes issued by local, state and federal agencies.

REFERENCES

1. C. D. Hollowell, R. J. Budnitz, and G. W. Traynor, Combustion-Generated Indoor Air Pollution , presented at the 4th Intern. Clean Air Congress, Tokyo, Japan, May 16-20, 1977.

CAL-ERDA (DOE-1): A COMPUTER PROGRAM FOR ENERGY ANALYSIS OF BUILDINGS*

W. F. Buhl, J. J. Hirsch, M. Lokmanhekim,
H. C. Mitchell, A. H. Rosenfeld, and F. C. Winkelmann

INTRODUCTION

The analysis of energy use in buildings has been facilitated by the development of a new, public domain computer code, Cal-ERDA (to be known as DOE-1 in 1978). Its purpose is to provide both a comprehensive tool to aid in the design of energy conserving buildings, and to analyze existing buildings for opportunities for cost-effective energy-saving modifications. Cal-ERDA (DOE-1) differs from earlier programs in two major respects: (1) it executes faster in the computer, and (2) where earlier programs read data cards filled with numbers punched in fixed format from forms filled in by the engineer, Cal-ERDA (DOE-1) reads a new "Building Design Language" (BDL) designed to increase speed, flexibility, and reliability of input. Special commands and key-words permit the user to specify building properties and parameters such as geometry, construction materials, schedules, heating-ventilating-air-conditioning systems, etc. Environmental data is provided via standard meteorological tapes of hourly weather conditions. Figure 1 is an example of part of a BDL input deck.

ACCOMPLISHMENTS DURING 1977

Cal-ERDA became operational this year and was released for public use in December as Version 1.3. The program is still under development, and additional features are planned to be added in 1978. It consists of four simulation programs:

1. LOADS--Computes hourly heating and cooling loads.
2. SYSTEMS--Simulates the operation of HVAC distribution systems.
3. PLANT--Simulates the operation of the primary heating, cooling, and electrical generating plant.
4. ECONOMICS--Calculates the life-cycle costs of equipment (first cost and operating costs) with account taken of likely energy pieces.

Three applications of the program were completed in 1977:

a. The analysis of the International Energy Agency (IEA) Standard Test Building. This was in support of the IEA effort to compare the results of a number of computer programs for building energy analysis. The results of the intercomparison were inconclusive and a large scatter in the output data was observed.

b. The analysis of nine different non-residential buildings for the State of California. The intention was to determine building energy-use budgets for use by the State Energy Resources Conservation and Development Commission. The analysis was undertaken by Consultants Computation Bureau.

c. A third application was with another IEA test building. Five variations of the test building specifications were used in new comparisons, but a scatter of results still persisted when different computer codes were intercompared.

The first of a series of Cal-ERDA workshops was held on December 7-10, 1977, for 50 managers of facilities connected with the Department of Energy. Some of these people are now using Cal-ERDA by remote operation of the LBL computers.

PLANNED ACTIVITIES FOR 1978

A new version of DOE-1 will be produced to reflect extensive testing of the input language and calculational routines, with improvements in the output reports and error diagnostics. A step-by-step guide to using the program will be written.

Later in 1978 improvements will be made to the PLANT, SYSTEMS, AND ECONOMICS programs. Work will begin on a package to deal with residential analyses.

Although DOE-1 already has solar-energy features (collectors, thermal storage, and heat recuperation), these will be extended during 1978 to include the popular passive solar techniques. The effects of Trombe walls, water walls, and direct gain of sunlight by heavy floors and walls will be included in the package to be developed.

FOOTNOTE AND REFERENCES

*Argonne National Laboratory and Los Alamos Scientific Laboratory are working in collaboration with Lawrence Berkeley Laboratory on this project.

```
*  84 *  INF-2           =DAY-SCHEDULE        (1,24) 0.0                                      ..
*  85 *
*  86 *  INF-WEEK        =WEEK-SCHEDULE       (MON,FRI) INF-1    (WEH) INF-2                  ..
*  87 *
*  88 *  INFIL-SCH       =SCHEDULE            THRU DEC 31 INF-WEEK                            ..
*  89 *
*  90 *                            /*SET-DEFAULT VALUES*/
*  91 *
*  92 *                   SET-DEFAULT         FLOOR-WEIGHT = 70.0
*  93 *                                       GLASS-HEIGHT = 4.0
*  94 *                                       GLASS-WIDTH = 5.0
*  95 *                                       GLASS-TYPE = W-1                                ..
*  96 *
*  97 *                            /*BUILDING-SHADE INSTRUCTIONS*/
*  98 *  BUILDING-SHADE TR=0 H=3.5 W=47 XB=2 ZB=7 SAZ=180 T=180                               ..
*  99 *  BUILDING-SHADE TR=0 H=4 W=5 XB=59 ZB=8 SAZ=180 T=180                                 ..
* 100 *
* 101 *                            /*GENERAL SPACE DEFINITIONS*/
* 102 *
* 103 *  PLENUM          =SPACE-CONDITIONS    FLOOR-WEIGHT = 5       TEMP = 70                ..
* 104 *
* 105 *  SPACE-1         =SPACE-CONDITIONS
* 106 *                                       PEOPLE-SCHEDULE       =OCCUPY-1
* 107 *                                       NUMBER-OF-PEOPLE      =50
* 108 *                                       PEOPLE-ACTIVITY       =400.0
* 109 *                                       LIGHTING-SCHEDULE     =LIGHTS-1
* 110 *                                       LIGHTING-TYPE         =2
* 111 *                                       LIGHT-TO-SPACE        =80
* 112 *                                       LIGHTING-W/SQFT       =3
* 113 *                                       EQUIPMENT-SCHEDULE    =EQUIP-1
* 114 *                                       EQUIPMENT-W/SQFT      =1
* 115 *                                       INF-METHOD            =2
* 116 *                                       NEUTRAL-ZONE-HEIGHT   =6
* 117 *                                       INF-SCHEDULE          =INFIL-SCH                ..
* 118 *
* 119 *                            /*SPECIFIC SPACE DETAILS*/
* 120 *
* 121 *  PLENUM-1        =SPACE               SPACE-CONDITIONS=PLENUM
* 122 *                                       VOLUME=10000           SPACE-HEIGHT=2           ..
* 123 *
* 124 *      WALL-1PF    =EXTERIOR-WALL       HEIGHT = 2             WIDTH = 100
* 125 *                                       AZIMUTH = 180
* 126 *                                       CONSTRUCTION = WALL-1                           ..
* 127 *
* 128 *      WALL-1PR    =EXTERIOR-WALL       HEIGHT = 2             WIDTH =  50
* 129 *                                       AZIMUTH =  90
* 130 *                                       CONSTRUCTION = WALL-1                           ..
* 131 *
* 132 *      WALL-1PB    =EXTERIOR-WALL       HEIGHT = 2             WIDTH = 100
* 133 *                                       AZIMUTH =   0
* 134 *                                       CONSTRUCTION = WALL-1                           ..
* 135 *
* 136 *      WALL-1PL    =EXTERIOR-WALL       HEIGHT = 2             WIDTH =  50
* 137 *                                       AZIMUTH = 270
* 138 *                                       CONSTRUCTION = WALL-1                           ..
* 139 *
* 140 *      TOP-1       =ROOF                LENGTH = 100           WIDTH = 50
* 141 *                                       X=0   Y=0   Z=10       AZIMUTH = 180
* 142 *                                       TILT=0                 GND-REFLECTANCE=0
* 143 *                                       CONSTRUCTION = ROOF-1                           ..
* 144 *
* 145 *  SPACE1-1        =SPACE               SPACE-CONDITIONS      =SPACE-1
* 146 *                                       AREA   =    1056       VOLUME = 8448
* 147 *                                       NUMBER-OF-PEOPLE   =   10.56                      ..
* 148 *
```

XBL 783-7896

Fig. 1. Example of part of the input deck for Cal-ERDA Version 1.3 using the Building Design Language (BDL).

Consultants Computation Bureau (Oakland, CA) is the major sub-contractor to LBL.

"Cal-ERDA Users Manual", ANL/ENG-77-03, October, 1977 (Cal-ERDA/77-1)

"Cal-ERDA Program Manual", Los Alamos Scientific Laboratory, October, 1977 (Cal-ERDA/77-2)

"Sample Cal-ERDA Runs of a 31-Story Office Building and a Medical Center" (Draft), LBL, UCID-3969, UCID-3970, September 30, 1977 (Cal-ERDA/77-3, 77-4)

"A Technical Guide to Energy Computer Programs for Buildings", E. Stamper, E. Smithberg, and R. Jourdain, LBL-6862, December 1, 1977 (Cal-ERDA/77-5)

"Cal-ERDA, A New Program for Building Energy Analysis", LBL-6331 (Cal-ERDA/77-6), to be published in the Proceedings of the First International Conference on Energy Use Management, Tucson, Arizona, October 24-28, 1977.

SAVING ENERGY IN SCHOOLS

A. Heitz and H. Sigworth

INTRODUCTION

This program was initiated by the American Association of School Administrators (AASA) and was funded by the Federal Energy Administration (FEA). Educational institutions are users of considerable amounts of energy, amounting to 5% of the national energy consumption for heating and cooling. Reduction in this energy use would be a significant contribution to a national program for energy conservation. In addition, school districts will benefit by keeping down energy costs. On a per pupil basis these costs have increased by nearly 50% between 1973 and 1975 with continued increases thereafter. School districts have large fixed costs due to the intensity of labor used and so even small savings in operating costs are very desirable.

In 1975 an energy audit and monitoring program was developed to study the energy consumption of schools in the United States. The American Association of School Administrators, with funds from FEA, proposed a demonstration project involving ten schools representative of climatic regions of the United States; the school locations are shown on the map, Fig. 1. Cost effective retrofit measures were selected for these schools with suggestions made for a demonstration project of the effectiveness of such measures.

An effective energy conservation program can be divided into four phases:

1. Conduct an effective energy audit and define energy conservation opportunities with an attractive rate of return on investment.

2. Select and design modifications.

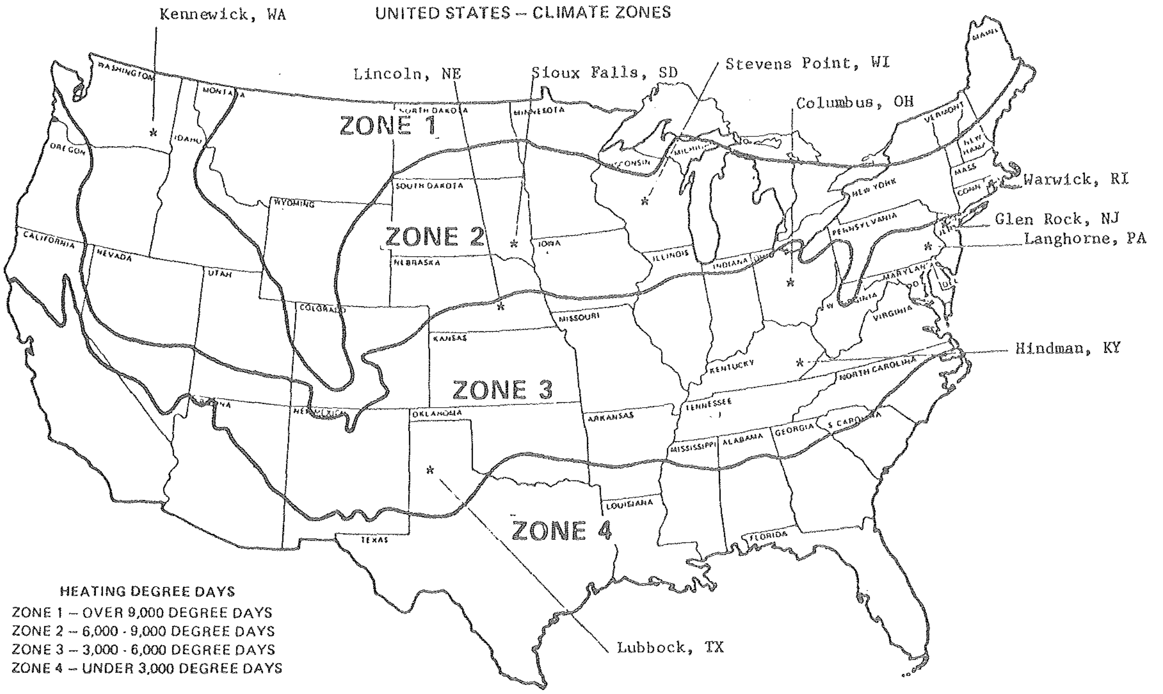

Fig. 1. Demonstration Sites.

3. Install modifications according to engineering designs.

4. Monitor the energy use of the buildings after retrofit and compare with the energy use prior to the modifications.

Phases 1 and 2 of this project had been completed when LBL became involved with the project. The laboratory was given the responsibility of administering the remainder of the project, that is, 3-4. The AASA, which is in close contact with the ten schools, was subcontracted to supervise the engineering work. The Lawrence Berkeley Laboratory has the responsibility of designing and deploying a monitoring system to produce data with which to validate the effectiveness of the retrofit measures. The overall management of the project is also the responsibility of the Laboratory.

The Laboratory involvement in this project provided a means whereby other ongoing programs at the laboratory could benefit from the availability of test sites in diverse climatic regions. In particular, the data expected from the project is being used as source material in verification tests of the Cal-ERDA (DOE-1) program developed to estimate the energy use of buildings. Another group who will benefit from a study of schools are those who are investigating levels of ventilation, and health, in buildings which are to be made energy efficient.

ACCOMPLISHMENTS DURING 1977

A tour of the schools was made to evaluate the results from the first phase of the project, and to collect design criteria for the monitoring systems which would be installed. The ten schools had heating plants utilizing either hot water or steam. Most of the schools used unit ventilators, which were often found to be operating improperly. Many thermostats were found to be functioning poorly. Many districts were short of maintenance support. The modifications which were selected to be implemented at each school are shown in Table 1. Costs, both estimated and actual, are shown for those schools where modifications have been completed.

While these modifications were being implemented, work was continuing at LBL on the design of the monitoring systems. The system selected utilizes a small computer chip to interrogate 32 to 60 input signals which will record such information as air temperatures, flow of water, gas, and steam, and other data relevant for the determination of the energy utilization pattern in the school. Additional binary circuits are used to detect opening and closing of doors or windows. Two classrooms, representative of those in the school, are thoroughly monitored, as is the operation of the central heating plant. Data from the computer system is transmitted over telephone lines to receiving stations at LBL, for storage and subsequent analysis by a computer, and to the AASA district offices for print-out. The whole package has been designed for ease of service in the field by persons not familiar with all the intricacies of the package.

Cost considerations have necessitated the manufacture of two types of instrumentation systems, one being more elaborate than the other. The more complex system is capable of monitoring air quality. It involves chemical and biological measurements in addition to heat and temperature data. The analysis of the air quality data will be the responsibility of the ventilation group whose work is described elsewhere in this report.

In December 1977, it was decided in conjunction with the Department of Energy that a large fraction of the information needed to evaluate the effectiveness of the retrofit proposals could be obtained by installing monitoring systems in three of the ten schools. Energy use in the remaining seven schools will be monitored by a manual system developed by LBL involving careful analysis of meterological and school fuel consumption records.

It was further agreed that there is a need to study an additional school that utilizes air conditioning. This school will be chosen from zones 3 or 4 of Fig. 1.

PLANNED ACTIVITIES FOR 1978

In mid-January, the first monitoring system was installed at the school in Lincoln, Nebraska. The installation of monitoring equipment at Kennewick, Washington and at Columbus, Ohio is expected to be completed by June 1, 1978. The summer will be used to de-bug these systems so that they will be ready for use at the start of the following school year in September.

Selection of the additional school with air-conditioning will be made in the early part of 1978 and a monitoring system will be designed and installed before the start of the school year.

In January data analysis began with information from the school in Lincoln, Nebraska. Energy use patterns for this school are being modelled using the Cal-ERDA (DOE-1) program. The computer runs are being compared with actual energy use in the school before and after the energy saving modifications were made. Similar computer runs and comparisons are being made for all of the other schools in the project.

Table 1. Schools program modifications and costs.

No.	School/Location	Reduce Outside Air	Night Thermostat Set-Back	Roof Insulation	Replace Boiler	Lower Stat Setting	Close Exhaust Dampers	Weather Strip	Increase Boiler Eff.	Reduce Glass %	Summer Equip. Shut Down	Auto-Boiler Control	Improve A/C Use	Improve Indoor Lighting	Reset Air Temperature	Est. Mod. Cost	Act. Mod. Cost
1	Scott/Warwick, RI	X	X	X												42,800	44,885
2	Central/Glen Rock, NJ	X		X	X	X	X	X								43,550	NA
3	Everitt/Langhorne, PA	X			X											21,200	23,320
4	Hindman/Hindman, KY								X	X						13,659	NA
5	Fairmoor/Columbus, OH	X	X						X		X					25,700	NA
6	P. F. Brown/Lubbock, TX											X				1,000	496
7	Eastridge/Lincoln, NB	X	X				X					X			X	10,000	8,577
8	Garfield/Sioux Falls, SD	X	X						X							20,000	23,946
9	Plover-Whiting/Stevens Pt., WI	X											X	X	X	3,900	4,320
10	Washington/Kennewick, WA		X	X					X	X				X		80,425	88,254

COMMUNITY COLLEGES PROJECT

P. C. Rowe and C. M. York

INTRODUCTION

A potential exists for saving energy on community college campuses with the additional advantage of influencing a large number of people through outreach activities. A plan of work has been prepared to implement a program to be carried out in conjunction with community colleges and public utilities.

ACCOMPLISHMENTS DURING 1977

The program got underway at a meeting in December between the Presidents, Business Managers and Physical Plant Managers of five community colleges, together with representatives of LBL and the Pacific Gas and Electric Company. The program plans were met with enthusiasm: colleges have fixed costs which amount to 85% of their operating budgets; of the remaining 15%, 4% goes to fuel bills. Therefore, any savings in this 4% would be very worthwhile financially. Additionally, schools and colleges account for about 5% of the national energy demand and demand reductions of 20% or more would certainly help in our attempts to curtail the total energy demand. We hope that savings of energy of at least 20% at each college should be possible without the outlay of capital funds.

PLANNED ACTIVITIES FOR 1978

Simple energy audits will be carried out at each college and the results shared with the energy teams that will be established at each campus. These teams will represent all of the major constituencies at each campus and will be wholly responsible for the implementation of the conservation strategies that have been suggested either by LBL or by the teams themselves.

Later in the program more extensive technical assistance will be given and comprehensive computer audits made at selected campuses. The usefulness of the Cal-ERDA (DOE-1) program for field use at colleges will be assessed at this time.

The plan of work will be extended later in 1978 in anticipation of a statewide program. We hope to be able to help draw up guidelines with the State Community Colleges Chancellor's Office to enable them to choose between retrofit options that may be funded with federal monies. Both the Association of Physical Plant Administrators and the American Association of Community and Junior Colleges will be kept closely informed of our activities as liaisons with these organizations strengthen.

HOSPITALS PROGRAM

C. D. Hollowell and M. Chatigny

INTRODUCTION

The Hospitals Program which is funded by the Department of Energy's (DOE) Division of Buildings and Community Systems is a major component of Lawrence Berkeley Laboratory's (LBL) Energy Efficient Buildings Program.

It has been estimated that, in the United States, hospitals consume approximately 15% of all energy used in commercial structures. Approximately 50% of this energy is used for heating, ventilation and air conditioning systems. Hospitals have been selected for special study because of their relatively large energy use and also because of the widely varying ventilation standards used in these institutions. It is expected that the establishment of a consistent set of ventilation standards in hospitals will lead to significant energy savings.

The Hospitals Program includes research and development in evaluation and control of the hospital air environment; assessment of the effects of energy conservation measures on the patient care environment; identification of hospital activity areas which are most suitable for introduction of cost-effective conservation measures that will not compromise the patient care environment; and collaboration with ongoing energy conservation efforts of other government agencies and professional organizations to permit rapid dissemination and acceptance of the recommendations of this program. Pertinent knowledge gained in other areas of the LBL Energy Efficient Buildings Program, e.g. ventilation, lighting, and building envelopes, will also benefit the hospitals program. With recognition of the primary need for a strong multi-agency coordinating role by DOE, this program is seen as filling a need for rapid development, testing, and application of new and existing technology to hospital energy conservation.

The project areas of the Hospitals Program may be described as follows:

(1) Assessment of the effects of energy conservation measures on environmental quality including air chemical content, microbial burden, odors, and comfort in existing, retrofitted, and new "energy efficient design" hospitals.

(2) Development, review and acceptance by user and regulatory agencies of augmented, cost-effective energy conservation measures that may have an impact on hospital design and operating procedures.

(3) Rapid transfer of advanced energy conservation technology in practical format to users.

ACCOMPLISHMENTS DURING 1977

Work began on the Hospital Program in August, 1977. The Energy Efficient Buildings Mobile Laboratory, which is described elsewhere (see "Ventilation Program") has been designed and fabricated by LBL for studies of indoor air quality in hospitals and other buildings. The first hospital to be studied with this mobile laboratory will be the Naval Regional Medical Center at Long Beach, California.

LBL was managing two subcontracts in 1977 which involved energy conservation research and development in hospitals. The University of Minnesota, under a sole source subcontract, is performing a critical literature assessment to establish the current practice and state of the art in hospital ventilation requirements. The intent is to recommend an R & D program for development of a data base adequate to establish energy efficient hospital ventilation standards.

The University of California Naval Biosciences Laboratory (NBL), under a subcontract, has developed a field sampling unit for measuring the microbial burden of air in hospitals. This apparatus will aid LBL in evaluation of the effects of ventilation and energy conservation measures on the levels, characteristics, and control of the microbial burden of air in hospitals.

PLANNED ACTIVITIES FOR 1978

The work proposed for 1978 is grouped in the three general areas described above.

(1) Efforts in 1978 will include a DOE-1 computer program energy utilization study of the Naval Regional Medical Center, Long Beach, California. In addition, LBL will be collaborating with the Navy in the design of an in-situ system for monitoring energy flow in selected functional areas of the hospital. The monitoring of existing indoor air quality in several functional areas (e.g., wards, pediatrics, kitchens, etc.) in this hospital is also planned in order to provide baseline data for comparison with subsequent data in 1979 following retrofit.

(2) Efforts will include preparation of a report summarizing a meeting of an "international experts" group to be held by a subcontractor, the University of Minnesota. The University of Minnesota will review current hospital HVAC standards and practices of the U. S. Department of Health, Education and Welfare (HEW), the American Hospital Association (AHA), and other groups, and will develop recommendations for energy conservation measures compatible with both good patient care and good engineering practice. This meeting will be followed later in 1978 by an LBL/DOE-sponsored working group meeting of HEW, AHA, the Department of Defense, the Veteran's Administration and other hospital operators or regulators, where the recommendations and practical aspects of their implementation will be considered. Concurrently, LBL will subcontract a study to examine energy conservation practices in hospital water usage (kitchens,

laundries, boilers, etc.) and the cost-benefits limitations imposed by sanitation requirements.

(3) Efforts in 1978 will be directed towards the establishment of LBL as a coordinating and information disseminating center for energy conservation practices in hospitals. We will establish a permanent working group, consistent with meeting schedules of pertinent national societies (American Hospital Association, American College of Physicians and Surgeons, American Institute of Plant Engineers, etc.), and co-sponsor at least one short symposium on energy conservation. It is anticipated that the major effort in this area for the remainder of 1978 will be to develop a technology transfer program on energy conservation in hospitals.

500 HOMES: THE ENERGY INSPECTION SERVICE

A. Meier and A. H. Rosenfeld

INTRODUCTION

A number of reports from LBL and other institutions have estimated the potential energy savings through residential retrofit measures. We have carried this research two steps further. First, we determined the conservation potential in real homes. Then we attempted to persuade the occupants that such measures were indeed worth doing. At the same time, we sought the most effective means of conveying energy conservation information to the occupants. A trained inspector can often find opportunities while conducting a 90 min energy audit to reduce the home's energy use (typically 700-1100 therms/year) by as much as 80 therms/year with no investment. Most homes inspected could reduce their energy use from 10-40% by investing in conservation measures with a return greater than 20%. Several new conservation measures were discovered during the inspections.

The Energy Conservation Inspection Service was a collaborative effort involving LBL, Pacific Gas and Electric Co. (PG&E), the California Energy Commission and the University of California (UCB). Ten conservation inspectors were trained at UCB during the spring quarter, 1977. They were the top 10 out of 30 students enrolled in a course entitled Energy and Resources 199. An intensive publicity campaign solicited homes for inspection in the early summer. Over 50 Berkeley homes requested inspections by the cutoff date. Half were actually inspected while the remaining half received a literature packet which included a "do-it-yourself conservation guide." PG&E, the local utility, gave us the past (and will provide the future) energy consumption for the homes; this will enable us to determine the relative effectiveness of the inspection versus the informational materials alone. Including a control group, more than 750 homes are involved in the study.

A typical inspection lasted 1-1/2 hr. The inspector usually discussed the resident's energy use over the last year for 10-45 min. Many of the unique social aspects of that household, which were important in understanding its energy use, surfaced in this conversation. The inspection then followed. Back at the office, the inspector prepared a "conservation prescription." This included suggested conservation measures, their cost, expected annual savings and payback time. The prescription also included local stores and contractors where the devices or services were available.

In many cases the inspector, at the request of the occupant, turned off the furnace pilot light, closed ducts to unused rooms and set back the hot water heater thermostat by as much as 40°F. These combined no-cost measures often saved the residents an estimated 80 therms (about $20) a year.

We found that conventional degree-day calculations vastly overestimated savings from insulation and storm windows. In many homes, the mild Berkeley winters and the residents' minimal heating habits made these conservation measures not cost effective. Other measures, such as weatherstripping, insulation blankets for hot water heaters and reduced or fluorescent lighting often appeared more attractive in terms of return on an investment. We were surprised to discover that over half of the fireplaces lacked dampers. This could result in winter heat losses of up to one therm per day.

If the measures recommended in the prescription were followed, the houses would probably reduce their total energy use by 10-40%. Most houses' savings were on the lower end but this may be due to the self-selection of the sample; we suspect that we inspected homes whose occupants had already adopted many more conservation measures than in average San Francisco Bay area homes.

In 1978, we shall monitor the control group's energy use to determine the most effective techniques of implementing energy conservation.

Fig. 1. Many Berkeley homes are heated with gas floor furnaces, which when they are not in operation (most of the time) are sources of considerable quantities of cold outside air. (XBB 783-3191)

Fig. 2. An open damper in the chimney permits a draft which sucks $25 to $40 worth of the hot air out of the home each season. Accordingly the students were instructed to label the damper position--open vs closed, so that the homeowner would be reminded to close the damper after the fire is out. But of the first 60 homes inspected, 48 had no dampers at all. A retrofit damper can be made for about $10. There seems to be the possibility of a small industry here. (XBB 783-3188)

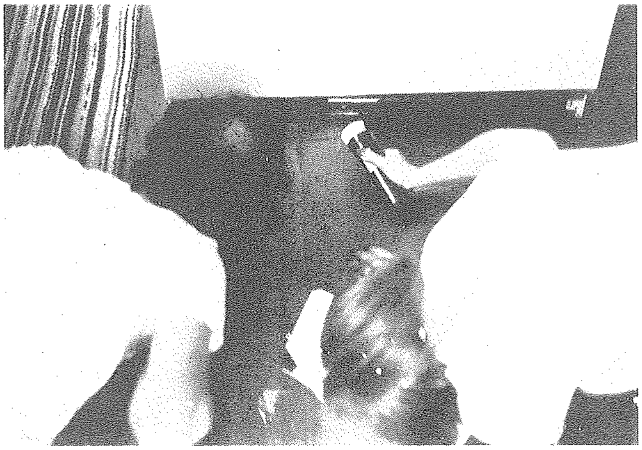

Fig. 3. Doors and gaskets on a refrigerator can easily be adjusted to seal properly. (XBL 783-3190)

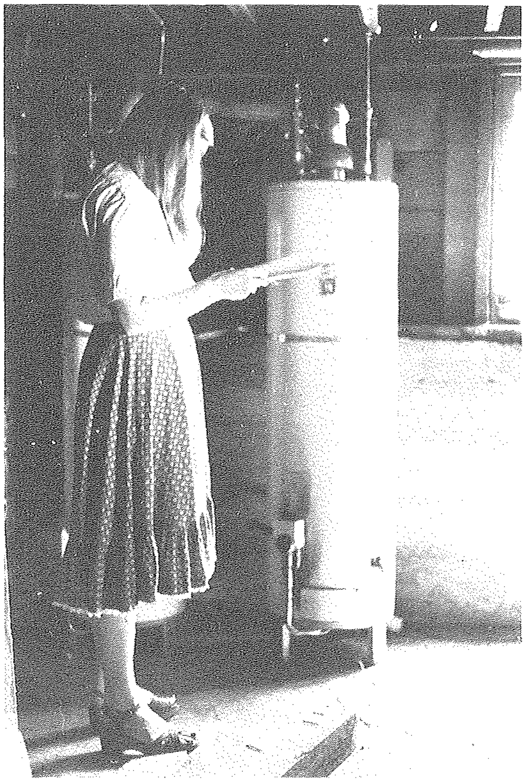

Fig. 4. Reducing the water heater thermostat setting from 150°F to 120°F can save \$10 of gas each year. Or \$6 of insulation will accomplish the same thing. (XBB 783-3189)

Photo credit to be given to Jean-Claude Dercle

ENERGY EFFICIENT WINDOWS PROGRAM

S. Berman, S. Selkowitz, R. Verderber, and J. Klems

In the latter quarter of 1976, we initiated a program to plan, manage, and conduct an Energy Efficient Windows Research Program at LBL. Funding was provided from the Consumer Products and Technology (CPT) Branch of the Department of Energy. This branch is charged with supporting research, development, and demonstration (RD&D) activities in energy conservation that will:

- accelerate the efforts of private industry
- complement the efforts of private industry
- foster the acceptance of energy saving technology
- maximize the effectiveness of energy use
- minimize adverse socio-economic and environmental impacts.

The Energy Efficient Windows Program at LBL is designed to further these CPT goals. The potential impact of this program on total national energy consumption is large. Approximately 20% of annual consumption is used for space conditioning of residential and commercial buildings, and about 25% of that figure is required to offset loads resulting from windows. Thus 5% of national energy consumption, 3.5 quads annually, or 1.7 million barrels of oil per day equivalent are tied to the thermal performance of windows. Although the conservation potential is enormous, there are significant obstacles to achieving that potential. Recent studies of problems concerning diffusion of innovation into the building industry suggest that in the area of energy conservation, the development of technically usable, energy conserving products and design practices will not necessarily be sufficient to guarantee their acceptance, their utilization, or their effective impact in reducing energy consumption. The Energy Efficient Windows Program has initiated efforts that not only will develop and commercialize innovative and effective window designs, materials and accessories, but will also ensure that they are recognized, accepted and utilized by design professionals and the public at large. The LBL role encompases overall program planning and assessment of research priorities, technical management of research activities subcontracted to private sector firms, and an in-house LBL windows research program.

ACCOMPLISHMENTS DURING 1977

Program accomplishments have been divided into two major areas: (1) program planning, management and support activities, and (2) materials, processes and prototype developments.

In its Program Planning and Management role, LBL plays a vital integrative and catalytic role. The process of formulating short and long term goals and building an RD&D program around them is complicated by the nature of the "window" industry. Although a small number of large firms manufacture glass, aluminum- and wood-framed windows are sold by a vast number of small businesses, most of whom service local markets. Some progress has been made in constructing a model of the structure of the window industry. On the manufacturing end, we have gathered information on sales volumes, mark-up patterns, and distribution networks in the glass/window industry. At the user end, we have developed data to characterize residential and commercial buildings by window area and type as a function of climatic region.

A further characteristic of the window industry is that significant product developments can be generated by small firms with minimal resources. We have endeavored to assist this process by developing a Windows Review which will be circulated widely through the professional community (architects, engineers, manufacturers, inventors, suppliers, code officials, researchers, etc.) to report on latest developments, patents, new materials and products, legislation, publications, etc. Initial response to the concept has been positive and a first issue will be published at LBL in Spring, 1978.

A Building Technology Laboratory has been set up in the College of Environmental Design of the University of California, Berkeley, to support research and development activities, to provide independent tests and evaluations of materials and products submitted by subcontractors, and to permit evaluation of new products being introduced to the marketplace. Window measurement apparatus and capabilities, in place or under construction, include: a calibrated hot box, an infiltration test station, emittance measurements, a solar calorimeter, and spectrophotometers for measurements of solar optical properties of glazing materials. A wide range of commercially available windows have been purchased for demonstration, inspection, and test.

Laboratory testing capabilities described above are all steady state measurements of static materials and devices. A major philosophical thrust of our program is the use of managed window systems, windows whose thermal/optical properties are changed (manually or automatically) over time. To test the performance of such devices, we have designed a Mobile Window Testing Facility. This unique facility will allow us to test net window thermal performance (combined infiltration, conduction/convection, radiation effects) as a function of climate and window orientation over many daily test periods. The four test cells can be configured to simulate a range of building insulation levels as well as a range of building thermal capacities. Results from this test facility should provide good comparative results on which to base assessments of window performance, and against which analytical models can be validated.

Two analytical efforts are underway and will be completed in 1978. The first is a detailed model of the resultant net heat transfer through a window assembly composed of an array of glazing elements and optical coatings. This model will be used to characterize the performance of window components. In order to determine the effectiveness of window management strategies, the performance of the windows must be assessed in the context of the performance of the remainder of a building. For these studies, we have utilized the CAL-ERDA Building Energy Analysis Program (DOE-1) and are modifying the program to incorporate a variety of window management strategies and to allow us to model new window designs and materials.

The development and commercialization of new materials, production processes and window prototypes is being supported through a variety of subcontract and in-house research efforts. These include:

Heat Mirror Commercialization. A heat mirror is an optical coating, applied to a glass or plastic glazing material, which transmits the full solar spectrum but reflects long wave infrared emitted by room temperature surfaces. By reducing the radiative component of thermal losses, the heat transfer coefficient of a single or double glazed window is approximately halved. Heat mirror coatings with good optical/IR performance have been produced by Suntek Research Associates by production techniques which appear to be cost effective if the material is produced in large volume. The abrasion and corrosion resistance of the coatings is not yet sufficient to guarantee long life in an exposed position. Subcontracted work is now underway to produce durable overcoats which do not degrade the IR reflectivity of the heat mirror coating.

The cost and performance of several large scale, high volume, thin film deposition techniques were examined in a small subcontract with Sputter Films, Inc. An existing electrically conducting polymer utilizing a thin gold coating was examined by its manufacturer, Sierracin Corporation, to determine its suitability and cost effectiveness as a heat mirror. Contacts have been made with a number of other firms with interests in producing or utilizing heat mirror films in energy conserving window products. Several efforts are in progress to assess marketing approaches which are most likely to lead to early consumer acceptance. Heat mirror may ultimately be sold in a tinted or reflective form to provide some glare and solar control, with the additional advantage of building upon consumer experience with solar control films. Performance of several different heat mirror configurations combined with solar control properties will be studied to determine the relative benefit of summer cooling load reduction compared to some loss of winter passive solar gain.

Optical Shutter. An ideal window should have optical properties which change in response to environmental stimuli based upon requirements for thermal and visual comfort within a given building. A variety of mechanical optical shutter devices are available (blinds, shades, shutters, etc.) to perform such functions. The availability of a glazing coating or glazing material which incorporates thermotropic or thermophototropic qualities would be a useful extension of the range of optical shutter mechanisms. A chemical gel which is transparent in its "cool" state and a milky white with high reflectivity in a "hot" state has been developed by Suntek Research Associates and was the subject of extensive testing and development under an LBL subcontract. A manufacturing facility for volume production was conceptualized and product costs were estimated. Although measured performance and durability were good, estimated production costs were sufficiently high to cast doubt on its marketability in its present state. After a review of other candidate optical shutter mechanisms in 1978, LBL will initiate further development efforts in this program area.

Selective Reflectance Coatings. Reflective and/or tinted glass is widely used in many commercial buildings to reduce solar impact and thus energy requirements for air conditioning. Glazing with very low shading coefficients may reduce the opportunities for utilizing available daylight and thus increase electrical lighting energy requirements.

Since approximately one half of incident solar radiation is short wave infrared which contributes nothing to illumination, an optical coating with selective reflectance properties could ideally reduce cooling load by 50% without reducing available illumination. Such coatings are being developed under subcontract by Kinetic Coatings, Inc., using novel ion beam sputtering techniques which produce very durable, weather resistant coatings. This will allow the coating to be applied to the outside of a window where it will function more effectively in a solar control mode. A wide range of selective reflectance coatings and protective layers have been produced and tested for both optical performance and weatherability. In 1978, efforts will be supported to investigate deposition techniques which will allow the sputtering system to be scaled up to a viable production process. Sample preparation and weathering tests will continue throughout the year.

Convection Suppression Window Prototypes. Double glazed windows frequently incorporate venetian blinds or similar devices between the glass planes for light and glare control and to provide privacy. They also reduce heat loss although the design of the devices has not been optimized for that purpose. It is possible to produce double glazed windows with heat transfer rates approaching those of insulated walls by the use of a mechanism in the air space which segments the airspace in such a way as to suppress convective transport. The Mechanical Engineering Department at the State University of New York, Stonybrook, is investigating the design and performance of such mechanisms. Prototypes have been built and tested with a thermal resistance of R5 in an open mode and R10 in a closed mode. Energy loss measurements are being made using a novel heat transfer gage and in 1978 interferometric techniques will be used to visualize convective transfer patterns. Candidate mechanisms will also be studied in 1978 to predict solar gain and an assessment will be made of the impact of these devices on the view from a window.

PLANNED ACTIVITIES FOR 1978

Most existing projects will be continued in 1978 and expected activities have been summarized. A major new program solicitation entitled "Innovative Window Systems" will be initiated in 1978. Unlike the more sophisticated materials development efforts described previously, this program will support development and demonstration of near term, low risk, innovative, energy efficient window systems.

ENERGY EFFICIENT LIGHTING PROGRAM

S. Berman, S. Selkowitz, R. Verderber, J. Klems,
and R. Clear

Lighting now accounts for 20% of the electrical energy generated in this country every year or about 5.5% of total U.S. energy consumption. This amounts to some 400 billion kilowatt-hours of electricity, broken down by end use sector as follows:

Residential Use	20%	Schools	7%
Stores	19%	Streets and Highways	3%
Industrial Use	19%	Other Indoor Uses	14%
Offices	10%		
Outdoor Uses	8%		100%

A comprehensive conservation program for research, development and demonstration to improve lighting efficiency, while maintaining desired visibility, could have immediate and lasting benefits in terms of reductions in the energy consumption of our nation's building stock, and in the costs to building owners and users incurred by this consumption.

We estimate that approximately 40% of the electrical energy consumed by lighting, or about 8% of total electrical sales, could be saved by a concerted near-term conservation effort. Additional peak power savings of a large, but undetermined, magnitude will accrue. These results could be expected from a program based upon (1) cost effective substitution of currently available, energy efficient design practices and products in place of less efficient choices, (2) operation and maintenance of lighting systems consistent with sound energy conservation practices, (3) provision of the appropriate design guidelines for increased use of natural lighting where applicable to displace electrical consumption, and (4) rapid commercialization of new energy efficient products now entering the marketplace. The LBL lighting research program is designed to generate additional conservation options in all of these areas. More detail on the philosophical foundations of this conservation commercialization program is provided in the description of the Energy Efficient Windows Program.

ACCOMPLISHMENTS DURING 1977

Daylighting Studies

Electric lighting represents 25% to 50% of the total energy consumption in many major office buildings. Many office spaces within fifteen feet of an exterior window could be partially or wholly daylit for a significant number of working hours per year. A photocell controlled fluorescent fixture was installed in a small perimeter office and initial observations indicate that the lights are off approximately 80% of the working hours. There has been a renewed interest in promoting the use of daylighting practices to reduce lighting energy consumption. The efforts are frustrated in part by 1) the lack of daylighting availability data, i.e., what are the sky luminance characteristics at a particular location over a year's time, 2) the lack of widely accepted simplified design methods, 3) the lack of widely accepted methods to assess annual energy savings, and 4) uncertainty in the integration of conventional lighting system design with daylighting practice. These issues were addressed by three related activities at LBL. A comprehensive literature search and review of existing data and design methods was completed. An attempt is underway to correlate solar radiation data with illumination values. If this is successful, solar data accumulated at numerous stations would become available for use in daylighting design and assessment. Simultaneous readings of illumination and solar radiation will be taken atop the Pacific Gas & Electric Building in San Francisco to validate analytically derived relationships. Finally, a very comprehensive set of experiments was planned to test various switching control strategies and hardware designs, using the dimmable high frequency ballast experiment in San Francisco. This is discussed in more detail in the section which describes the solid state ballast program.

Beamed Sunlight Project

Conventional daylighting techniques which rely on incident diffuse light are of limited usefulness more than ten or fifteen feet from an exterior wall. Direct sunlight represents a collimated, intense source of high quality light which can be controlled and redirected to interior spaces deep inside a room. This project, undertaken with the assistance of the University of California at Berkeley Department of Architecture, has focussed on the development of sunlighting control devices, to be mounted on the upper portion of windows, which are designed to reflect beam sunlight to a diffusely reflecting ceiling surface deep within a room. Several fixed and moveable devices have been designed and built, both as prototype and full size models. A test apparatus has been designed and built to model the performance of several scale model prototypes and the full size device will be installed in Building 90 at LBL to assess its performance. A survey of a typical office block in downtown San Francisco was completed and preliminary results indicate that there may be very few opportunities to retrofit such devices in existing buildings. Based on current testing, the most promising prototype will be developed in 1978 to the stage where an assessment can be made of its marketability and cost/benefit performance.

High Frequency, Solid State Fluorescent Ballast Program

Fluorescent lighting systems are the dominant form of lighting in the commercial and industrial sectors. A ballast is required in most fluorescent fixtures to first start the lamp, and then regulate current and voltage to maintain light output. Conventional ballasts, which drive the lamps at line frequency of 60 cycles, typically consume 20% of the total lighting system power. Solid state electronic ballasts have been shown to improve system efficiency by 1) reducing ballast losses, and 2) increasing lamp efficacy by driving the lamp at higher frequencies, 20,000-30,000 cycles. High frequency ballasts have been used in space vehicles, in emergency lighting systems and other DC driven applications. In order to be used in AC circuits in buildings, they must have long life, no adverse effect on lamp life, acceptable power factor and low RF noise. Finally, these capabilities must be provided at a price that is cost effective to the building owner.

A development and demonstration program was initiated in 1977. Two subcontractors were selected to complete prototype development of two ballasts with differing capabilities. Ballasts produced by Iota Engineering Inc., were tested by an independent test laboratory and showed efficiency improvements of 20%-30% compared to conventional units. Their design is a low cost approach intended to produce paybacks of the incremental first cost in one to three years, depending upon light output level and energy costs. A ballast developed by Stevens Luminoptics, Inc., is continuously dimmable by manual or automatic means but is somewhat more complex and costly. These units will be delivered for test and evaluation in early 1978.

The true test of the viability of these products is not their performance on a laboraotry bench but rather in a typical office environment where the unit must survive a variety of thermal and electrical stresses. Our commercialization strategy is based on a demonstration of these units which will be credible to the architectural and engineering design community which ultimately must accept and specify them. A very comprehensive and heavily instrumented demonstration has been planned utilizing solid state ballast retrofits on three floors of the Pacific Gas & Electric headquarters building in downtown San Francisco. An instrumentation system was designed, built and will be installed in early 1978 to monitor all electrical and thermal parameters of interest (approximately 60 channels of data). In addition, eight roof mounted sensors will report solar radiation and illumination levels as part of related daylighting experiments.

This demonstration will provide an opportunity to assess ballast reliability and potential effects on lamp life. A parallel effort is underway at LBL, in conjunction with the fluorescent lamp manufacturers, to assess impact on lamp life. A complete lamp life test capability (aging racks, integrating sphere and associated electrical and photometric measurement capabilities) is under construction at LBL and testing will be initiated in early 1978. A variety of related ballast commercialization activities were conducted. A study was completed of the chronology of developments efforts of high frequency fluorescent lighting systems, a history which spans thirty years. The market potential, from the point of view of both fixture manufacturers and ballast manufacturers, was explored. Power semiconductors are essential elements in the solid state ballast and discussions with manufacturers of state-of-the-art devices were continued. In two to five years, we expect to see integrated circuits and hybrid chips replacing the discrete component devices under development now. We have begun our examination of the impact of these trends on product cost and performance. Finally, we have played a crucial role as a credible source of information concerning ballast development to potential users and developers of this energy saving device.

Other Lighting Activities

Polarized lighting panels have been promoted as a product that provides good visibility with reduced energy consumption when compared to standard non-polarized lenses on light fixtures. A very exhaustive study of published research was undertaken to determine the utility of the panels in a variety of lighting design situations. The tentative conclusion reached was that when used as a direct replacement for a standard fixture lens, the polarized panels do provide greater visibility for most tasks and thus provide opportunities for reduced power output and energy savings.

Fluorescent lighting has never made a very deep penetration into residential applications for economic and aesthetic reasons, and in the past units were not available as replacements for a wide variety of common lamps and fixtures. In the last two years, screw-in fluorescent adapters utilizing small circular lamps have appeared on the market and expanded the range of consumer options. Although their initial cost is considerably higher than incandescent bulbs, because of their long life and improved efficiency it can be shown that they will frequently be more cost effective on a life cycle cost basis. A document has been prepared for consumers containing comparative life cycle cost data to allow them to make intelligent purchasing decisions.

PLANNED ACTIVITIES FOR 1978

Planning was initiated in late 1977 to extend lighting program activities into three new areas:

1) High intensity discharge (HID) lighting systems represent a fast growing sector of the lighting market for both indoor and outdoor applications. All HID systems require ballasts and some appear to offer opportunities for electronics ballast operation which would result in improved energy efficiency and other operational advantages.

2) Switching and control hardware and strategies for lighting systems offer substantial opportunities for both immediate and longer term savings. Development and demonstration of approaches offering improved energy efficiency will be supported.

3) The incandescent bulb is the dominant light source in the residential sector and parts of the commercial sector. Though it is versatile and cheap, it is not very energy efficient. Contract activity will be initiated to support commercialization of one or more energy efficient replacements for incandescent bulbs.

REFERENCES

See review article in the special Berkeley issue Vol. 1. No. 1 of the Journal "Energy and Buildings".

CONSERVATION EDUCATION

C. Blumstein, P. Rowe, L. Schipper, W. Wilms and C. York

INTRODUCTION

The Conservation Education Program of the Lawrence Berkeley Laboratory (LBL) was established in the summer of 1977 to communicate the results of the research and development program in Energy Conservation to those who can utilize and apply those results. When a new technology or idea has been developed, the first step in transferring it into a commonly accepted practice is to disseminate information about it to appropriate audiences. The way in which the new technology works in the field and its subsequent improvements require additional information flow between the developers, the user, potential users and the general public. In the area of energy conservation, when common practice in the use of existing equipment can be changed to produce energy savings, the flow of information is especially important.

It is the purpose of the Conservation Education program to coordinate and expedite this information flow.

The program is organized according to the specific audience to whom the information is directed. In addition to the set of audience-directed programs, there is an analysis program which correlates and generates new information needed for dissemination by the other programs.

PROGRAM ORGANIZATION

1. Teachers' Program

There is a tried and true approach to information transfer which employs the simple device of inducing teachers in the school system to include new ideas and material in their courses. There is an immediate multiplicative factor in the number of people who are aware of the new information when this is done. This program will be divided into several project levels, not only to match the formal structure of the country's educational institutions, but also to reflect the differences in technical detail which the information must contain in order to be communicated to the various audiences.

A summer school for community college faculty has been planned for 1978.

A project to develop "Energy Conservation Strategies on Community College Campuses" has begun.

2. Public Utilities' Customers Program (in collaboration with Pacific Gas and Electric Co.)

Both the '500' Homes Demonstration Project and the Community College Project are collaborative programs with local public utilities.

3. Professional and Skilled Workers Program - Licensure Project

An attempt to modify the state licensing requirements for architects, contractors, accountants, etc. by introducing questions on energy conservation into licensing exams has been successfully started. W. Wilms of UCLA is in charge of this project, which has been supported by the California Energy Commission. The first phase of the project has been completed and the following licensing boards are actively engaged in modifying their examinations to include appropriate energy conservation measures: Accountants, Architects, Contractors, Engineers, Landscape Architects, and Structural Pest Controllers.

4. Television Project

In collaboration with the LBL Public Information Office, a script for a television film strip has been produced. The long-range objective is to produce a pilot series of public service announcements on energy conservation. Louie Robinson has written the script, and Jim Halverson will collaborate in the filming and production.

5. Analysis Program

This part of the program is devoted to special studies needed both to evaluate various conservation education strategies and to analyze energy conservation problems which may require improved educational programs as part of their solution.

Manpower for Energy Conservation. This study, a collaborative effort between LBL and W. Wilms at UCLA, will assess the need for training and retraining professionals and skilled laborers to carry out proposed conservation measures. It will, in a sense, provide a "marketing study" for the Teachers Program, above, to focus the classroom training on the correct audiences in order to upgrade and modify their skills. The work has been planned in 1977 and will be concluded during the summer of 1978.

Overcoming Institutional Barriers to Energy Conservation. Many of the problems associated with increasing the efficiency of energy use are institutional rather than technical. Examples of such problems are: obsolete building codes, lack of methods for re-training already skilled workers in new methods, and misallocation of conservation's costs and benefits (builders vs. buyers, landlords vs. tenants, etc.) While the literature on energy policy is filled with references to such problems, there has been surprisingly little systematic work in this area.

This project, sponsored by the U.S. Council on Environmental Quality, is making a systematic examination of institutional barriers to energy conservation with the aim of contributing to the development of methods for formulating conservation policy. The initial stage of the project has been devoted to the preparation of a bibliography by E. Krieg. Future efforts in the project will be devoted to an analysis of issues which are especially important to understanding the nature of barriers to energy conservation. Special attention will be paid to problems which might be resolved by improved educational programs. The project team includes C. Blumstein, E. Krieg, L. J. Schipper, and C. York.

LONG-RANGE BUILDING AND APPLIANCE STANDARDS

P. P. Craig, D. B. Goldstein, A. J. Lichtenberg,
and A. H. Rosenfeld

We have been stressing the need for a comprehensive approach to saving energy in buildings. To illustrate this approach, we mention a recent study supported by the California Policy Seminar. Entitled "Saving Half of California's Energy and Peak Power in Buildings and Appliances via Long-Range Standards and Other Legislation," the study concludes that savings in space heating can be implemented by upgrading existing California building standards and "sweetening" them with incentives. We would then reduce energy for space heating of homes to less than what is presently required for hot water (270 therms) or consumed by the electric utility to power the refrigerator-freezers in the home (210 therms[1]). Another opportunity for saving energy in the home is increasing the efficiency of refrigerators. Figure 1 is taken from the Policy Seminar paper, and shows that it is possible to reduce refrigerator energy use by one third (from an average of 150 to 100 kWh/mo.) just by comparison shopping. A final gain (from 100 to 50 kWh/mo) will require research, development, and retooling by the manufacturers. According to a survey by A. D. Little,[2] this will add only $50 to the retail cost. Table 1 shows the cummulative peak power savings attributable to eventual "saturation," through normal attrition and replacement with the new optimized refrigerators, would save 2500 MW statewide. This is the reliable output of three 1000 MW power plants, which now cost $1 billion each. But the cost of the 16 million improved appliances is only $750 million! This is another example of the dramatic cost-effectiveness of energy conservation.

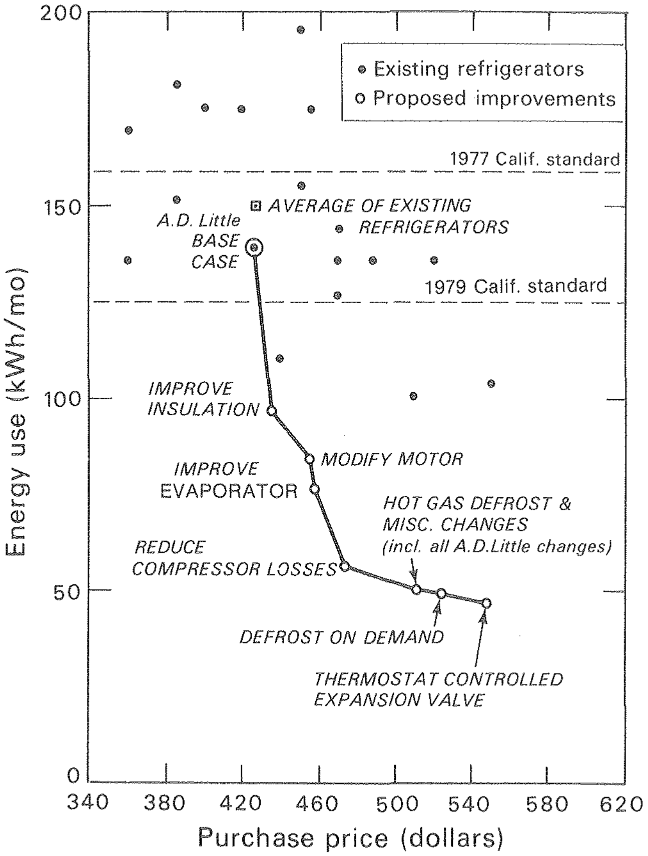

Fig. 1. Energy use vs purchase price for a number of existing and proposed refrigerators. The closed circles in the upper half of the figure represent 16.0-17.5 cu. ft. top-freezer, frost-free refrigerators sold in California in 1976. The open circles in the lower half represent proposed redesigned refrigerators. California standards for maximum energy use allowable for refrigerators of this type shown. (XBL 7712-11464)

FOOTNOTES

[1] The average refrigerator-freezer uses 1,600 kWh/year, and there are 1.2 units per household. If the heat rate of the powerplants supplying electricity is taken to be 11,000 Btu/kWh, then the resource energy required is: (1600 kWh/year) x (11,000 Btu/kWh) x (1 therm/10^5 Btu) x (1.2 units/household).

[2] Study of Energy-Saving Options for Refrigerators and Water Heaters, Volume 1: Refrigerators. Prepared for The Office of Tranportation and Appliance Programs, Federal Energy Administration, Washington, D.C. by Arthur D. Little, Inc. Cambridge, Mass., May, 1977.

REFERENCES

1. "Some Potentials for Energy and Peak Power Conservation in California", LBL-5926, October 1977.

2. "Conservation Options in Residential Energy Use: Studies Using the Computer Program Twozone", LBL 5271, August 1977.

3. "Saving Half of California's Energy and
   Peak Power in Buildings and Appliances via
   Long-Range Standards and other Legislation",
   California Policy Seminar, January 1978.

Table 1. Peak power savings in California resulting from improvements in refrigerator efficiency, after twenty years of normal replacement.

Action Taken	Statewide Power Savings Resulting From Given Action, MW	Cumulative Savings, MW
1. Chose most efficient model presently on the market	1000	1000
2. Redesign for optimum efficiency	1200	2200
3. Optimize freezer design	300	2500

(Note that the California Energy Commission 1979 Standards will result in statewide power savings after twenty years of 600 MW)

Chemical Process Research and Development

SELECTIVE HYDROGENATION OF COAL

A. T. Bell, E. A. Grens, E. E. Petersen, T. Vermeulen, T. T. Derencsenyi, G. P. Dorighi,
E. C. Harris, D. A. Lindsay, J. B. McLean, D. P. Mobley, S. Salim, J. H. Shinn,
C. G. Smith, K. I. Tanner, N. D. Taylor, J. A. Wrathall, G. H. Zieminski

INTRODUCTION

Existing technology for coal liquefaction is based on thermal decomposition (pyrolysis) of the coal with subsequent hydrogenation of the initial pyrolysis products. Such non-selective thermal bond breaking yields a wide range of products, including light hydrocarbon gases, and is therefore not efficient in hydrogen utilization. This project seeks to establish a basis for conversion of coal to liquids, with minimum hydrogen addition, by selective scission, below pyrolysis temperature, of certain bond types in the coal structure. Bonds linking conjugated hydroaromatic groups in the coal, including aliphatic bridges and noncarbon links (e.g., ether, carboxylic, and disulfide bridges), are being attacked by hydrogenolysis or hydrolysis in the presence of homogeneous catalysts. The use of these dissolved catalysts in a liquid reaction medium permits access to reaction loci on the extensive interior surface of the coal.

The investigation involves studies of the interaction of coals with inorganic and organic reaction media; the effects of homogeneous catalysts in promoting reactions in such media at moderate temperatures; and the action of catalyst materials on specific bond types in model compounds representative of certain aspects of coal structure. The interaction of the pore structure of the coal with the progress of reactions and the influence of transport phenomena in this structure on reaction rates are also considered in this study.

The project was initiated in January, 1974. During the first three years of the program, equipment and laboratory procedures were developed and studies undertaken of interaction of subbituminous and bituminous coal with several organic solvents and with zinc chloride melts, phosphoric acid, and sodium hydroxide. Hydrogenolysis of model compounds with Lewis-acid catalysts was also investigated as were the changes in coal pore structure caused by interactions with organic solvents and inorganic melts.

ACCOMPLISHMENTS DURING 1977

The project activities planned for 1977 included investigation of coal interaction with additional polar, organic solvents, and with mixtures of organic solvents. The investigation of organic melts was extended to include examination of eutectic mixtures of zinc chloride with other halides. Catalysis of the hydrogenation of model compounds by homogeneous catalysts, in particularly strong Lewis acids and transition metal carbonyls, was further investigated, and study was undertaken of the removal of heteroatoms (S,O) for coal and model compounds by these treatments. In addition, since solvent refined coal (SRC) represents an initial product of coal hydrogenation, the further hydrogenation of SRC in the presence of solid Lewis acid catalysts was examined.

INTERACTION OF COAL WITH ORGANIC SOLVENTS

(Grens, Dorighi, Lindsay, Zieminski)

Earlier studies of the interaction of subbituminous (Wyodak) coal with polar, nitrogen-containing organic solvents were extended to other solvent systems at 250°C. The coal was extracted, nearly to completion, in pure refluxed solvents, and the extracts were analyzed for elemental composition, average molecular weights, aromaticity of their hydrogen content (by proton NMR), and fractional solubilities in standard solvents (cyclohexane and benzene at their normal boiling points). Not only did the yield of soluble material (at 250°C) increase dramatically with the nitrogen-base character of the solvent (from 8.4% in tetraline to 64.3% in ethylenediamine), but so did the estimated aromaticity of the extracted material as shown in Table 1.

This result, coupled with relatively low hydrogen/carbon atomic ratios found for the dissolved material (0.46 - 1.35), indicates that the more powerful amine solvents are able to separate fairly large (number average MW is about 1800) multi-ring hydroaromatic groups from the coal structure at a temperature below that at which pyrolysis can take place. Solvents without amine bases, such as tetralin, dissolve much less of the coal, and the dissolved material is much more aliphatic although it average molecular weight is only moderately smaller.

Extraction of Wyodak coal, using two-component mixtures of organic solvents, was carried out in a system where the coal was successively contacted with fresh solvent batches at controlled temperature, until further dissolution was not significant. The first investigations were made with mixtures of specific (nitrogen base) and non-specific solvents at 250°C to determine the effect of solvent composition. For these systems, which include pyridine/toluene and pyridine/tetralin,

Table 1. Characteristics of material extracts from Wyodak coal at 250°C - 4 hr.

Solvent	Yield of Dissolved Material (DAF)	H/C Ratio	H_{arom}*	H_α*	f_a**
Tetralin	8.4%	1.35	7.6%	9.5%	0.38
Quinolin	25.0%	0.99	12.9%	12.4%	0.57
Piperidine	35.4%	0.91	3.8%	24.0%	0.56
Ethylenediamine	64.3%	0.46	21.4%	31.0%	0.82

*H_{arom} and H_α are fractions aromatic and α aliphatic protons from proton NMR spectra.

**f_a is the aromaticity (fraction aromatic carbons) estimated from proton NMR data by the method of Brown and Ladner (Fuel 39, 87 (1960)) with aliphatic H/C = 2.

the extent of coal dissolution is found to vary almost linearly with solvent composition between the solubilities in the pure solvents. This result is somewhat surprising, since a large excess of solvent is used, and indicates that local continuum properties of the solvent in contact with the coal, rather than specific chemical (e.g., acid-base) interactions of solvent species with the coal, determine the extent of dissolution of the coal.

The mixed solvent investigation is now being extended to other systems and mixtures with more than two components. In addition studies of the rate limitations in coal/solvent interactions are being undertaken.

TREATMENT OF COAL WITH ZINC CHLORIDE MELTS

(Vermeulen, Shinn)

Experimental work with zinc chloride continues. Early this year we found that tetralin, added to mixtures of Wyodak coal with $ZnCl_2$, served as a co-reactant, rather than merely as a hydrogen donor. Tetralin greatly aids the conversion of coal to preasphaltenes and beyond, but it participates more by adding chemically to the coal than by donating hydrogen to the coal (and forming naphthalene). Later we determined that methanol is equally effective as a co-reactant.

Many inorganic additives (halide salts) investigated earlier proved either to have no effect, or to detract from the activity of zinc chloride alone. In an effort to reduce the water content required to "melt" the zinc chloride, eutectic mixtures (60-20-20- mole-%) of $ZnCl_2$ with NaCl and KCl, and $ZnCl_2$ with KBr and NaI, melting near 210°C, were investigated for their catalytic activity. In one hour of treatment at 250°C, under 20 atm of H_2, the pyridine extractibility of each product was much less than the value given by zinc chloride alone, and in fact only as much as the value for untreated coal.

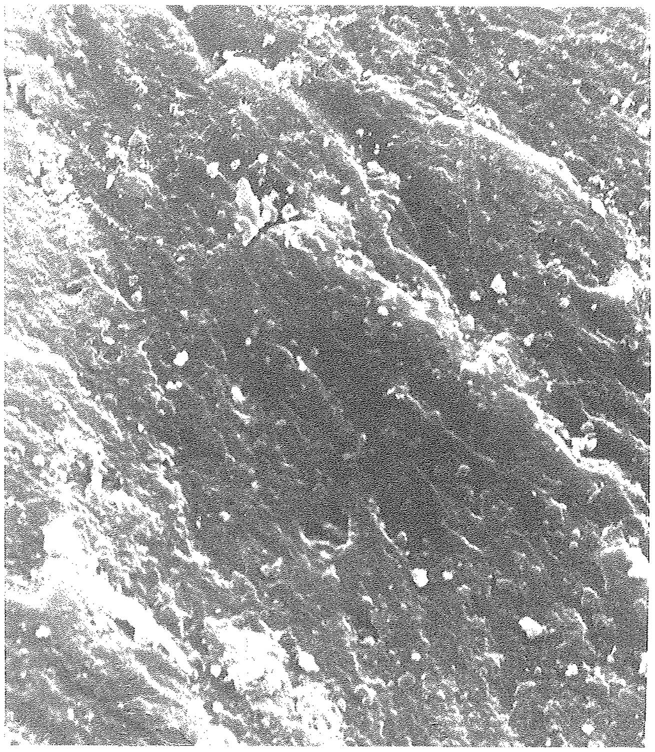

Fig. 1. Electron photomicrograph of untreated Wyodak Mine coal; magnification 3000x. (XBB 777-6714)

A separate study was made of calcium chloride as an additive for zinc chloride. When pure zinc chloride is used, some calcium is extracted from the mineral part of the coal (and some zinc is transferred into the coal). It was therefore encouraging to find that the presence of added $CaCl_2$ does not alter the conversion to pyridine-extractibles given by $ZnCl_2$ alone.

A physical examination of the surface structure of untreated and treated coals was conducted with a scanning electron microscope. At 1000 to 10,000 diameters, the untreated Wyodak coal revealed very little microstructure (Fig. 1). Zinc chloride treatment created some pitting and cracking, but no large-scale structural changes. Pyridine extraction of the melt-treated coal somewhat smoothed the surface of each of the two foregoing samples.

Treatment of coal with zinc chloride and tetralin together yielded a surface appearance much like that from zinc chloride alone. However, when this product was extracted with pyridine, removing over 60% of the carbonaceous material of the original coal, a markedly involved microstructure was observed (Fig. 2). The irregular cellular or honeycomb-type structure is suggestive of a biological origin but has not yet been fully explained.

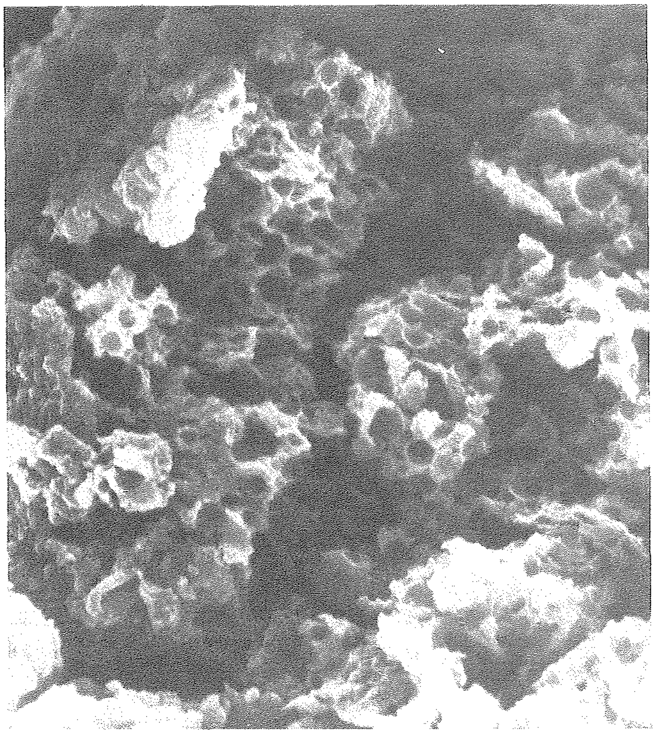

Fig. 2. Electron photomicrograph of Wyodak coal residue from treatment with $ZnCl_2$ and tetralin at 250°C for 1 hr., followed by Soxhlet extraction with pyridine; magnification 3000x.

(XBB 777-6715)

SELECTIVE HYDROGENATION OF FUSED-RING AROMATICS

(Vermeulen, Derencsenyi)

In this study, ligand-substituted metal carbonyls were found to be more stable than the precursor carbonyls at moderate temperatures (up to 300°C) and CO pressures (15 atm or less). Under such conditions the substituted carbonyls remain effective as hydrogenation catalysts, while the precursors lose their activity. As reported last year, iron carbonyl substituted with alkylphosphines is more stable than cobalt carbonyl.

Further study has shown a lack of reproducibility in the catalytic conversion of anthracene to dihydroanthracene when substituted iron carbonyls are used. The activity is nearly doubled by adding NaOH in quantities up to one molecule per iron atom. The alkalized catalyst also promotes the water-gas shift reaction, converting Co and H_2O to near-equilibrium amounts of CO_2 and H_2, at 175°C and 70 atm H_2/CO pressure for two hours.

For iron carbonyls, it appears that the catalytically active species may contain two atoms of iron. By analogy, dimanganese decacarbonyl was investigated using tributylphosphine as a complexant. At 200°C with 20 atm each of CO and H_2, in one hour of contact, the following conversities of dihydroanthracene were obtained:

Ligand molecules/Mn	0	0.5	1.0	2.0	4.0
% conversion	6	25	33	25	15

The substituted carbonyls appear promising as co-catalysts in zinc chloride melt systems. When Fe, Co, or Mn carbonyls, stabilized with tributylphosphine in decane solution, were augmented by a small amount of $ZnCl_2$ (1g/100g solution), higher conversions to dihydroanthracene were obtained than with $ZnCl_2$ absent, in runs at 600 psi and 180°C.

When a model compound, dibenzyl ether, was studied in place of anthracene under the above conditions (with $ZnCl_2$), a polymer was the only product if cobalt carbonyl and ligand were omitted. With these materials present, some toluene was recovered, and there was evidence of toluene inclusion in the condensation products. These results indicate that the carbonyl is able to introduce hydrogen as a replacement for aromatic carbon in the incorporation reactions. This effect is very desirable and needs further study.

TREATMENT OF SRC WITH SOLID AND LEWIS ACID CATALYSTS

(Bell, Tanner)

The hydrogenation and hydrogenolysis of SRC with solid acid and Lewis acid catalysts was investigated in a high-pressure autoclave. To disengage the reaction products from the unreacted SRC, a solvent, either benzene or cyclohexane, was used. The addition of isopropanol was investigated to determine its ability to enhance the solubilization of SRC.

Exploratory experiments conducted at 300°C and 2000 psi of H_2 showed that Al_2O_3, Cr-Al_2O_3,

$Fe-Al_2O_3$, $Co-Al_2O_3$, $NiMo-Al_2O_3$, $NiW-Al_2O_3$, $CoMo-Al_2O_3$, and zeolite cracking catalysts had little effect in increasing the extent to which SRC could be solubilized in benzene. Characterization of the dissolved product by elemental analysis and ^1H-NMR showed that none of the catalysts significantly altered either the ratio of hydrogen to carbon (H/C) or the ratio of aliphatic to aromatic hydrogen (H_{al}/H_{ar}), relative to what was observed in the absence of the catalyst.

Initial investigations with Lewis acid catalysts showed that at 2000 psi of H_2 and 300°C, none of the catalysts ($AlCl_3$, $FeCl_3$, $SbCl_3$ and $HgCl_2$) caused an increase in the degree of SRC solubility in benzene, over that which could be obtained without a catalyst. Zinc chloride did not alter the benzene solubility of SRC, but produced a product characterized by significantly higher H/C and H_{al}/H_{ar} ratios. A similar product was obtained using $SnCl_2$, but in this instance a greater percent of the SRC could be dissolved. In addition to promoting the hydrogenation of SRC, both $ZnCl_2$ and $ZnCl_2$ were found to cause a significant reduction in the nitrogen content of the dissolved product. Based upon these results, it was concluded that $ZnCl_2$ and $SnCl_2$ were suitable catalysts for the liquefaction of SRC and, therefore, warranted further investigation.

The choice of solvent used with either $ZnCl_2$ or $SnCl_2$ has a strong effect upon the extent of SRC dissolution and the characteristics of the dissolved product. As seen in Table 2, solubility of SRC was significantly smaller in cyclohexane than in benezene. However, reactions carried out in cyclohexane produced a product characterized by higher ratios of H/C and H_{al}/H_{ar} and a lower ratio of N/C.

Measurements of the molecular weight distribution of the dissolved products, performed by gel permeation chromatography, revealed that the average molecular weights were the same in both solvents, about 200 gm/mole. This molecular weight was about half of that measured when no catalyst was used.

The addition of isopropanol to the solvent was found to increase substantially the solubility of SRC, as shown in Table 2. This effect is particularly striking in the case of $SnCl_2$ used together with benzene, where it is possible to achieve a nearly complete

Table 2. Effects of solvent and isopropanol on reactions of SRC.

Reactions Conditions:
T = 300°C
P = 2000 psig H_2
t = 90 min.
ω = 1250 RPM

Catalyst mass = 5 gm
SRC mass = 5 gm
Additive mass = 5 gm Isopropanol
Solvent volume = 70 ml

Run No.	Catalyst	Additive	Solvent	Sol. (%)	Filtrate Formula	H_{Al}/H_{Ar}*	Isopropanol Alkylated (%)	Comments on Filtrate**
-	SCR	-	-	-	$C\,H_{0.77}N_{0.022}S_{0.0023}$	1.07	-	Dark Brown - Black Solid
6	None	No	Benzene	46.7	$C\,H_{0.85}N_{0.018}S_{0.0022}$	1.33	-	Dark Brown Solid
37	None	Yes	Benzene	65.0	$C\,H_{0.90}N_{0.018}S_{0.0025}$	1.56	0	Black Solid
29	$ZnCl_2$	No	Benzene	46.8	$C\,H_{1.01}N_{0.0023}S_{0.0021}$	2.54	-	Dark Brown Caking Solid
43	$ZnCl_2$	Yes	Benzene	60.4	$C\,H_{1.04}N_{0.0048}S_{0.0017}$	2.71	6	Black Caking Solid, 10 mole % Cumene formed, some Cumene incorporation
31	$SnCl_2$	No	Benzene	57.9	$C\,H_{0.97}N_{0.0105}S_{0.0020}$	2.22	-	Dark Brown Solid
45	$SnCl_2$	Yes	Benzene	99.4	$C\,H_{1.06}N_{0.012}S_{0.0025}$	3.07	8	Black Solid, 5 mole % Cumene formed, Propane formed, some Cumene incorporation
59	None	No	Cyclohexane	15.1	$C\,H_{0.91}N_{0.014}S_{0.0020}$	1.50	-	Brown Solid
68	None	Yes	Cyclohexane	25.3	$C\,H_{0.89}N_{0.017}S_{0.0022}$	1.34	0	Brown Solid
61	$ZnCl_2$	No	Cyclohexane	35.4	$C\,H_{1.06}N_{0.0013}S_{0.0016}$	3.38	-	Dark Brown Viscous Oil, 0.6 mole % Methylcyclopentane formed
65	$ZnCl_2$	Yes	Cyclohexane	57.5	$C\,H_{1.14}N_{0.0053}S_{0.0021}$	5.27	10	Black Solid, 1.2 mole % Methylcyclopentane formed, Propane formed
63	$SnCl_2$	No	Cyclohexane	29.8	$C\,H_{1.00}N_{0.0051}S_{0.0017}$	2.68	-	Dark Brown Solid
67	$SnCl_2$	Yes	Cyclohexane	54.5	$C\,H_{1.11}N_{0.0069}S_{0.0025}$	4.82	12	Brown Solid, Propane formed

*NMR Solvent: $CDCl_3$, except SRC and Run 37 done in Pyridine - d_5.
**Approx. 10 mole % Isopropanol charged in reaction.

conversion of SRC to a soluble product. From ^1H-NMR spectra of the dissolved product it was established that between 5 and 10% of the isopropanol had been alkylated onto the aromatic portions of the product. It is believed that alkylation enhanced the solubility of the reaction product, permitting a larger fraction of the SRC to be brought into solution.

The effects of reaction temperature and pressure were also investigated. It was observed that the extent of SRC solubilization increased from 250 to 375°C and then remained constant. Between 250 and 400°C the H/C and H_{al}/H_{ar} ratios of the product were found to reach maximum values near 350°C. The significant decline in these characteristics at higher temperatures suggests that rearrangement of the product to a more aromatic form takes place when the temperature becomes high enough for pyrolysis to occur. The effects of pressure were investigated at 350°C over the range of 0 to 4000 psi of H_2. In the absence of a catalyst it was observed that H_2 pressure had no effect on either the extent of SRC solubilization or the composition of the dissolved product. By contrast, in the presence of $ZnCl_2$, the extent of SRC conversion increased monotonically with H_2 pressure, as did the hydrogen content of the product.

The present results have demonstrated that $ZnCl_2$ and $SnCl_2$ are effective catalysts for the liquefaction of SRC. Preliminary tests using an Illinois #6 bituminous coal also show promising results. Future studies will further emphasize the effects of solvents and alkylating agents such as low molecular weight alcohols.

CATALYTIC HYDROGENATION AND HYDROGENOLYSIS OF ORGANIC STRUCTURES RESEMBLING THOSE FOUND IN COAL

(Bell, Salim, Taylor)

Strong Lewis acid catalysts such as $AlCl_3$, $ZnCl_2$, and $SnCl_2$ are being investigated to establish their ability to promote the cracking, hydrogenolysis, and hydrogenation of organic structures similar to those found in coal. Model compounds were used in this work to facilitate product identification and to elucidate reaction pathways.

The cleavage of aliphatic linkages between aromatic nuclei was studied using the following model compounds:

1

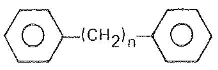

n = 0, 1, 2, 3, 4

2

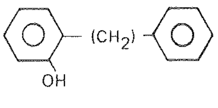

Reactions were carried out in a stirred autoclave at temperatures of 225 to 325°C and H_2 partial pressures of 1000 to 2000 psi.

Using $AlCl_3$ as a catalyst it was found that **1** (n = 1 to 4) could readily be cleaved at temperatures as low as 250°C. The initial reaction products were always benzene and an alkyl-benzene, indicating that cleavage had occurred between the benzene ring and the first carbon atom of the aliphatic bridge. The alkylbenzene product was not stable, however, and was observed to isomerize or crack to shorter chain alkylated compounds. In the cases of **1** (n = 3) and **1** (n = 4), indane and tetralin were observed, respectively, as the major reaction products. Only **1** (n = 0) showed relatively little tendency to react, even when the temperature was raised to 325°C. The observed reaction patterns can be interpreted by a carbonium ion mechanism as shown below:

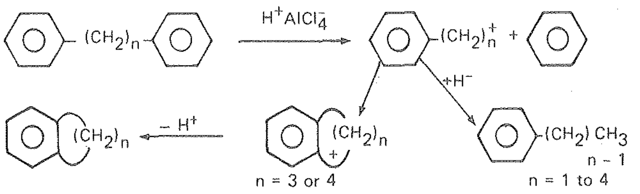

The reduced reactivity of **1** (n = 0) relative to other members of the series can be attributed to the fact that the phenyl carbonium ion is far less stable than any of the alkyl-benzene carbonium ions, and thus is less likely to be formed.

The presence of a hydroxyl group on one of the phenyl rings of **1** contributed an inductive effect, leading to a more ready cleavage of the aliphatic linkage. Thus the reaction of **2** was found to occur more readily than that of **1** (n = 1). Furthermore, cleavage was observed to occur preferentially at the ring containing the hydroxyl group.

Attempts were also made to establish whether $ZnCl_2$, a weaker Lewis acid than $AlCl_3$, could cleave aliphatic bridges. No products were observed when **1** (n = 1 to 4) was contacted with $ZnCl_2$ at 325°C. However, when a hydroxyl group was present on one of the benzene rings, $ZnCl_2$ was observed to catalyze the cleavage of the aliphatic bridge, again indicating the induction effect caused by the hydroxyl group.

The cracking and hydrogenation of fused ring aromatic systems was investigated using naphthalene (**3**) and phenanthrene (**4**) as model compounds. In the presence of $AlCl_3$, **3** first hydrogenated to form tetralin which then cracked to benzene. Initial investigations of the reactions of **4** suggest that this substrate also first hydrogenates and then cracks, forming naphthalene and benzene in this case.

CATALYTIC REMOVAL OF HETEROATOMS FROM ORGANIC STRUCTURES RESEMBLING THOSE FOUND IN COAL

(Bell, Mobley)

This investigation was undertaken to determine the ability of $ZnCl_2$ and $SuCl_2$ to remove oxygen and sulfur from organic structures resembling those found in coal. Reactions were carried out in a stirred autoclave both in the presence and absence of H_2.

It was found that both $ZnCl_2$ and $SnCl_2$ readily catalyzed the removal of oxygen from dibenzyl ether at 225°C. Diphenylmethane or benzyltetralin was formed as the product depending upon whether benzene or tetralin was used as the solvent. Identical results were obtained in the presence and absence of H_2, suggesting that molecular H_2 was not involved in the removal of O atoms from the ether. The nature of the products suggests that the reaction proceeds through a benzyl carbonium ion, which then rapidly benzylates the solvent, following a Friedel-Crafts type of mechanism.

Attempts to catalyze the reactions of diphenyl ether and phenol with $ZnCl_2$ and $SnCl_2$ were unsuccessful, even when the temperature was raised to 325°C. The stability of these reactants relative to dibenzyl ether can be understood in terms of the relative stabilities of the carbonium ions, formed during the first step of the reaction. Both diphenyl ether and phenol would be expected to produce a phenyl carbonium ion, which is far less stable than the benzyl carbonium ion produced from dibenzyl ether.

The reactions of sulfide and disulfide linkages between aromatic nuclei were also studied. $ZnCl_2$ was found to readily catalyze the desulfurization of dibenzyl sulfide dissolved in benzene. The only liquid product formed was diphenyl methane. An identical product was obtained using dibenzyl disulfide as the reactant. Here again, it would appear that the reactions proceed through a benzyl carbonium ion.

At 325°C both dibenzyl sulfide and dibenzyl sulfide with dibenzyl disulfide were observed to undergo thermal reactions in the absence of a catalyst. Both substrates produced a mixture of toluene, diphenyl methane, bibenzyl, and stilbene.

Attempts to remove sulfur from aromatic rings were not successful. Thus, neither thiophene nor dibenzothiophene reacted in the presence of $ZnCl_2$ at temperatures up to 325°C.

LOW TEMPERATURE PROCESSES FOR COAL DESULFURIZATION AND CHANGES IN PORE STRUCTURE OF COAL WITH CHEMICAL PROCESSING

(Petersen, Harris, Wrathall, Smith)

Coal desulfurization processes are needed in most cases to prepare coal so that it can be burned directly and meet air pollution standards. Some coals meet these standards after a physical separation of pyrites; others require the removal of pyrites (i.e., the inorganic sulfur). An appreciable number of higher sulfur coals require the removal of pyrites plus a significant part of the organic sulfur. Two processes were studied here: one based upon sodium hydroxide as a leachant, and the other based on ferric sulfate. Both processes are effective in removing inorganic sulfur from Illinois #6 coal at low temperatures and pressures. Neither process was effective in removing a significant fraction of the organic sulfur. The costs of treatment by each of the above leachants has been reported to be high enough to limit their application.

Alternate methods of treatment were sought that would be specific for organic sulfur removal. The use of metallic sodium proved to be extremely effective in sulfur removal from model organic compounds characteristic of the molecular structures found in coal (structures such as dibenzothiophene). Metallic sodium was dispersed in inert organic solvents. At temperatures below 200°C and at moderate pressures, the conversions in excess of 99% could be attained with reaction times on the order of a half hour.

Experiments are now being conducted to use metallic sodium for treatment of solvent refined coal. The residual sulfur in this material is believed to occur largely in multiring thiophenic form. Preliminary results appear to verify the effectiveness of the metallic sodium treatment in removing sulfur. Ultimately, this technique will be adapted to the treatment of raw coal.

Another desulfurization study concerns the distribution of sulfur between liquid products and char during rapid pyrolysis of coal. The expectation in this work is that organic sulfur will tend to remain with the liquid products, and the inorganic sulfur will tend to remain with char. To the extent that this is true, char desulfurization may become feasible by aqueous leaching to produce an acceptable solid fuel. Existing methods based upon cobalt-molybdenum catalysts, or the previously described metallic process, would be applicable to the desulfurization of the liquid products.

In another aspect of this investigation, surface area and pore volume changes found with progressive reaction and extraction of Roland Seam coal, reveal that solvents and catalysts have access to the micropore structure of coal (although the rate limiting steps may be limited by diffusion into the interior of the coal particles). The pores in coal appear to be slot shaped, becoming wider and wider with progressive treatment.

REFERENCES

1. M. Seth and T. Vermeulen, Interaction of a Sub-Bituminous Coal with a Strong Acid and a Strong Base, Lawrence Berkeley Laboratory Report LBL-5997 (1977).

2. G. P. Dorighi, Interaction of Organic Solvents with a Sub-bituminous Coal Below Pryolysis, Temperature, Lawrence Berkeley Laboratory Rpt LBL-6335 (1977).

3. J. B. McLean and T. Vermeulen, Coal Liquefaction Studies using Phosphoric Acid at Moderate Temperatures and Pressures, Lawrence Berkeley Laboratory Rpt LBL-6638 (1977).

DEASHING OF SOLVENT REFINED COAL

R. J. Steininger, II, C. J. Radke, D. N. Hanson

INTRODUCTION

Solvent-refined coal (SRC) is an attractive possibility to enable the direct utilization of high-sulfur coal. However, filtration of the resulting ash has proved to be a highly difficult and expensive component of the process. Because of the extreme fineness and apparent stability of the suspended ash particles, filtration rates observed in pilot plant operation (Tacoma, WA and Wilsonville, AL) are on the order of 140 $cm^3/sec\ m^2$ (10 gal/hr ft^2). Such low filter rates result in high filter capital costs and unacceptable filter precoat costs, and are a major detriment to the success of SRC.

Past work on improvement in the de-ashing step has taken various directions, but no highly effective improvement has yet been found. High gradient magnetic separation has been investigated.[1] Experiments have been made on replacing the expensive diatomaceous earth precoat with ground coal added directly to the unfiltered oil.[2] Investigations of the parameters of filter operation (temperature, pressure, body feed of precoat, solvent concentration, and rate of advancement of blade) have been investigated, but no particularly beneficial combination has been found.[3] The use of antisolvents which result in precipitation of a portion of the SRC, which is then settled so that it acts as a sweep to collect the ash particles, has been studied.[4] Cross-flow filtration[5] and electro-cross flow filtration[6] have been proposed. Studies have also been made on agglomeration of the particles as a means to improve directly particle filterability.[7]

ACCOMPLISHMENTS DURING 1977

Initiated in July 1976, work at the Lawrence Berkeley Laboratory has been exploratory in nature, attempting to determine the most promising route for ash removal. Except for initial studies on the feasibility of AC-field agglomeration, the work has concentrated on processes that alter the surface properties of the particles, and thereby effect agglomeration. Three means of altering the surface properties of the ash particles are being investigated:

1. Alter the particle surface to allow scavenging by an aqueous phase
2. Add dilute high molecular weight materials to flocculate the particles by bridging
3. Neutralize the surface charge to permit coagulation.

Progress in each of these areas and a brief review of the initial work is outlined below.

Initial Work

Initial work on SRC, from the Tacoma, WA plant, attempted to neutralize ash particle charges by changing the solvent character. Henry and Jacques[8] have reported positively charged particles, and this finding has been confirmed in our work. These charges apparently prevent the formation of strong coagulums under electric fields, since we have observed only weak agglomeration. Based on the assumption that the surface charge stems from hydrogen ions produced by dissociation of SRC phenolics, experiments were performed to basify the solvent, but at the same time, not precipitate the SRC. The experiments consisted of initial microscopic screening followed by high temperature settling studies. Dioxane, tetralin, pyridine, and hexylamine all showed promise as basic additives to neutralize particle charge. Settling curves as a function of additive concentration did show significant particulate removal at high additive concentrations, compared to the unmodified SRC. Further quantitative analysis of the results, however, revealed that the increased settling rates were attributable to lowered viscosity due to the additive liquids. Hence dilution of the SRC with basic liquids does not appear warranted, in view of the increased complication and cost of the SRC process. Almost identical results were noted with dilution by natural process solvent, which was obtained by vacuum distillation of a portion of the original unfiltered oil. This initial work, besides indicating the impracticality of solvent alteration for agglomerating the ash particulates, also showed that the high temperature settling studies were quite time consuming. Therefore, a more expedient method for investigating possible particle coagulation was demanded.

The procedure now established involves resuspension of the ash particles in pyridine, or the natural process solvent. These liquids do not precipitate SRC, and their lack of color allows quantitative zeta potential measurements through microelectrophoresis. Further, the low viscosity permits simple room temperature filtration studies. Hence rapid and meaningful screening of coagulating agents can now be accomplished by correlating particle surface charge measurement (i.e., zeta potentials) vs filtration rate.

Water Scavenging

Attempts were made to transfer the ash particles to a bulk aqueous phase from which they can be separated by ordinary means: filtration, centrifugation, or evaporation. Particles might be introduced into an aqueous phase by using the particles as condensation nuclei: saturating the oil phase with water at a higher temperature, followed by sudden cooling and the formation of a water-in-oil dispersion. The resulting dispersion, depending on the relative amounts of water and particles, would consist of either particles with an adsorbed layer of water on the surface, or water drops in which the particles were attached or embedded. The liquid dispersion could then be coalesced by various techniques, such as AC coalescence or flotation, in order to isolate the particles.

Experiments in the SRC natural solvent confirmed that the ash particles could be effectively coated with water by employing them as condensation nuclei. However, when actual SRC was added to the clear natural solvent and the experiments performed again, considerable SRC came out of solution. Apparently, even at room temperature, sufficient water dissolves to precipitate the SRC. Under the high temperatures of plant operation, the higher solubility of water would cause unacceptable product loss. Thus the possibility of water scavenging of the ash particles does not appear feasible.

Bridging Flocculation

The addition of very small amounts of high-molecular-weight polymers to solid particulate dispersions causes agglomeration in aqueous media. The polymeric species appear to adsorb in a dangling, stringlike fashion, and permit bridging between the particles. Such an aggregation mode is highly attractive because of the extremely small chemical requirements, and because the particle aggregates are strongly bound but loose in structure. Hence high filtration rates can be maintained. Utilization of this idea for SRC, however, requires considerable development; little is known about bridging flocculation in non-aqueous media. The polymeric additive must be oil soluble, or high molecular weight with active groups to promote adsorption, and stable at high temperatures. Initial studies include oil soluble dispersants and latex emulsifiers such as polystyrene, octylphenoxyethanols, acryloid dispersants and naphthalene sulfonic acids. Standard filtration studies are now underway to test these possible flocculating additives.

Charge Neutralization Coagulation

Agglomeration can be promoted by the addition of small amounts of surface-active agents which reduce or eliminate the effective particle charge (i.e., zeta potential) and hence allow inherent dispersion forces to dominate. This type of agglomeration has been observed to produce large aggregates in both polar and apolar media. Further, since very small material amounts are required, the idea appears economic. However, the surfactant additions for use with SRC must be oil soluble, and in addition must dissociate in organic media. Initial candidates for such surfactants include aerosol OT, Cu and Zn oleate, Ca dodecylsulfate, and Ca salicylate.

Quantitative zeta potential measurements, ζ, have been obtained for ash particles resuspended in pyridine, as shown in Fig. 1. Note first that the zeta potential is positive. This establishes quantitatively, for the first time, that the particles are positive. Second, as small amounts of copper oleate are added to the pyridine, the ash particle zeta potential falls dramatically because of charge neutralization and compression of the electrical double layer. Also shown in Fig. 1 is the specific resistance of the ash particle cake, α, obtained from simple room temperature filtration experiments. As the copper oleate concentration is increased, the cake resistance dramatically decreases. Thus the conclusion that as the particles are neutralized, the filtration rate increases. These results are extremely significant because minute amounts of copper oleate cause a 25-fold increase in filtration rate. No attempt was made to establish the most effective neutralization additive.

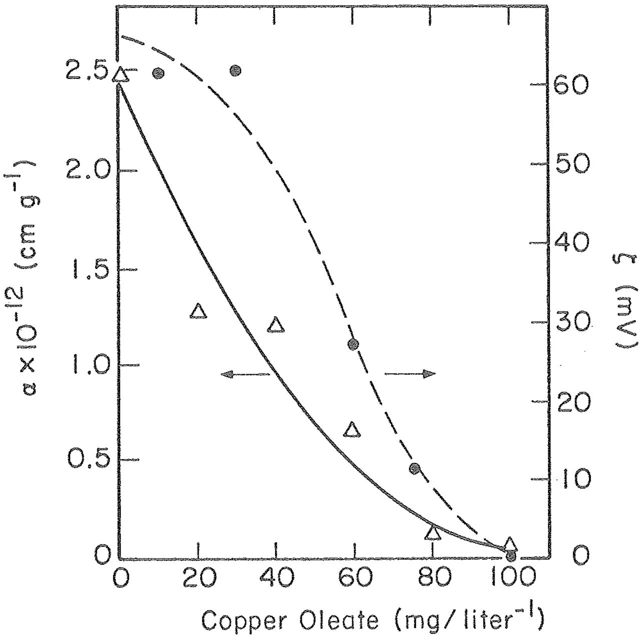

Fig. 1. Effect of particle charge neutralization on filtration rate.

PLANNED ACTIVITIES FOR 1978

The results on filtration rate increases from the addition of copper oleate to pyridine-suspended particles are particularly promising. Filtration rate increases of a factor of 25 have been found. Other coagulants will also be examined, together with the possible addition of polymeric flocculants.

The studies will be extended to coagulation and filtration in the SRC natural solvent, and finally, directly to SRC filter feed at high temperatures.

REFERENCES

1. E. Maxwell, Massachusetts Institute of Technology, ERDA/NSF/EPRI Principal Investigators' Conference - Coal Research, Sept. 3-4, 1976.
2. B. R. Rodgers, and P. R. Westmoreland, ORNL Preprint, 81st National AIChE Meeting, april 13, 1976.
3. G. R. S. Smith and R. C. Himes, Johns-Manville Corp., FE-2007-20, September 1976.
4. G. J. Snell, and A. A. Simone, EPRI AF-234, September 1976.
5. Walden Research, Massachusetts, Contract MER/2245.
6. D. Wasan, Illinois Institute of Technology, Personal Communication.
7. J. D. Henry, West Virginia University ERDA/NSF/EPRI Principal Investigator's Conference-Coal Research, September 3-4, 1976.
8. J. D. Henry and M. T. Jacque, AIChE Journal 23(4), 607 (1977).

COAL LIQUEFACTION BY CATALYTIC HYDROGENATION IN ORGANIC-INORGANIC LIQUID MIXTURES

E. A. Grens, T. Vermeulen
F. Hershkowitz, J. L. Maienschein, J. H. Shinn

INTRODUCTION

The use of inorganic melts, such as zinc chloride, as media for coal hydrogenation has been under investigation by several agencies for a number of years. Our research has shown that the utilization of two-phase reaction media composed of inorganic melts mixed with organic solvents can give considerably greater conversions of coal to liquid products under relatively mild reaction conditions (250°C) than can inorganic melts or solvents by themselves. At the same time, use of the two-phase media helps overcome important problems associated with processing in inorganic melts, such as control of the extent of reaction of initial liquid products dissolving in the melt and recovery of product liquids from the melt. This project is intended to establish the basis for possible new coal-liquefaction processes using such mixtures and to investigate the nature of the interactions occurring in these systems.

In mixed reaction media, coal is preferentially wetted by the inorganic phase, and hydrogenated to initial products in the presence of the organic phase. This hydrogenation at low (below pyrolysis) temperature can be promoted by homogeneous (liquid phase) catalysts, which have access to reaction sites in the solid coal. The inorganic media being studied are either catalytic or contain dissolved catalytic materials. The initial reaction products are expected to be extracted continuously into the organic phase, reducing undesired further hydrogenation of these materials, and could be recovered from that phase.

This project was initiated in January 1976. During the first year of the program, equipment and laboratory procedures were developed for determination of interactions of organic phases with zinc chloride melts. Preliminary coal hydrogenation experiments in two-phase mixtures were undertaken, which established the general feasibility of the approach. As of October 1977, this project was consolidated into a related ongoing LBL project, "Selective Hydrogenation of Coal," concerning the interaction of coal with inorganic melts and the promotion of coal hydrogenation by homogeneous catalysis.

ACCOMPLISHMENTS

The project activities planned for 1977 included study of the interactions of organic and inorganic phases, and confirmation and extension of the favorable results of initial coal-treatment experiments. In particular, we investigated the use of organic systems that could be "activated" by zinc chloride melts to serve as hydrogen donors in breaking down coal to pyridine-soluble products.

The interaction of zinc chloride (with small amounts of water) with a large number of organic materials was examined at temperatures to 200°C. Polycyclic aromatic and hydroaromatic hydrocarbons were found to give clean phase separations with very little mutual solubility when agitation ceased. Phenols (and their polycyclic derivatives), aromatic ethers, and aliphatic alcohols above pentanol gave similar behavior with somewhat increased solubility in the inorganic phase. Lower alcohols, dioxane, THF, and some ketones were soluble in the melt. Most organics involving basic nitrogen (e.g., aniline, pyridine) form high melting complexes with the zinc chloride.

The treatment of sub-butuminous coal in zinc chloride combined with a number of organic phases has been studied. The experiments were conducted with excess $ZnCl_2$ at 250°C for one hour in a stirred autoclave, usually in the presence of hydrogen at 35 atmospheres. The yields of pyridine-soluble materials (preasphaltenes plus asphaltenes and oils) for several of the combinations employed are shown in Table 1. The high yields obtained when zinc chloride is used in combination with tetralin, isopropanol, and methanol suggest that these phases serve as donors of hydrogen, or other active species, which promote extensive decomposition of the coal structure at temperatures well below its pyrolysis temperature. It is noteworthy that small amounts of tetralin (or anthracene oil) in methanol greatly enhance the effectiveness of that treatment. The importance of the coal being wetted by the inorganic phase is illustrated by the fact that, when equal weights of coal and $ZnCl_2$ are used with excess tetralin, the yield of pyridine solubles is only 34% in contrast to 75% in excess $ZnCl_2$.

PLANNED ACTIVITY FOR 1978

Our research will concentrate on evaluation of additional organic-phase compositions (including mixtures), determination of the influence of the phase ratios used, and investigation of the effects of additives in the inorganic phase.

Table 1. Yield of pyridine-soluble material obtained from contacting Wyodak coal (50 g) with inorganic/organic mixed media at 250°C for 1 hr.

Inorganic Phase	Organic Phase	Gas Phase	Yield[a] of Pyridine Solubles (DAF)
None (Untreated Coal)	None	None	10.1%
$ZnCl_2(+H_2O)$ - 300 g	None	None	11.5%
$ZnCl_2(+H_2O)$ - 300 g	None	H_2 - 35 atm	27.3%
$ZnCl_2(+H_2O)$ - 300 g	Tetralin - 50 g	None	65.1%
$ZnCl_2(+H_2O)$ - 300 g	Tetralin - 50 g	H_2 - 35 atm	75.4%
$ZnCl_2(+H_2O)$ - 25 g[b]	Tetralin - 150 g	H_2 - 35 atm	33.7%
$ZnCl_2(+H_2O)$ - 300 g	Isopropanol - 50 g	H_2 - 35 atm	70.9%
$ZnCl_2(+H_2O)$ - 300 g	t-butanol - 50 g	H_2 - 35 atm	29.2%
$ZnCl_2(+H_2O)$ - 300 g	Anthracene Oil - 50 g	H_2 - 35 atm	32.8%
$ZnCl_2$ - 300 g	Methanol - 100 g	H_2 - 15 atm	14.2%
$ZnCl_2$ - 300 g	Methanol - 50 g	H_2 - 15 atm	41.2%
$ZnCl_2$ - 300 g	Tetralin - 10 g Methanol - 50 g	H_2 - 15 atm	65.2%
$ZnCl_2$ - 300 g	Anthracene Oil - 10 g Methanol - 50 g	H_2 - 15 atm	68.1%
$ZnCl_2$ - 300 g	n-Decane - 100 g Methanol - 25 g	H_2 - 20 atm	8.6%

[a] Corrected for any solvent incorporation occurring.

[b] 25 g of Wyodak Coal used.

PROCESSING OF WASTEWATERS FROM COAL CONVERSION PROCESSES

C. J. King, S. Lynn, D. N. Hanson, J. M. Prausnitz,
S. Lubic, D. Greminger, A. S. Newton

INTRODUCTION

Coal gasification and liquefaction processes produce a process condensate wastewater which contains large amounts of phenolic, ammonia, sulfides, dissolved and/or reacted carbon dioxide, other organic acids and bases, and, in some cases, inorganic salts.[1,2] There are often suspended particulates which bind carcinogenic polynuclear aromatics (PNA). For environmental reasons it is desirable to achieve as complete a recycle of this water as possible, minimizing both the amount and the pollutant content of water released to the environment. Biological treatment is suitable only for final clean-up of the most concentrated waters, because of the required large hold-up volumes and because of the refractory nature of some constituents. There is considerable economic incentive for recovery, rather than degradation, of at least phenol and ammonia.

The objective of this project is to devise, explore, and assess appropriate treatment methods for these waters. These methods will combine solvent extraction and stripping, along with other appropriate operations, such as ion exchange or evaporation. Direct extension of the technology established for coke-oven effluents is precluded by the large scale of operation which discourages addition of chemicals, and by the presence of large amounts of CO_2 and quite variable proportions of different acids and bases. The acidic components complicate stripping of ammonia, and the basic components reduce the extractability of organic acids.

One of the novel approaches in the project is the development of testing of improved organic-base solvents with low water solubility. These react chemically with the acidic components, thereby competing more effectively with the ammonia. This extends earlier research on solvent extraction of wastewaters from aceticacid manufacture. Another novel aspect is the development of vacuum stripping as an improved method of removing residual solvents from water. The availability of vacuum stripping for this purpose interacts with the choice of solvent. We are also seeking more energy-efficient designs for ammonia stripping, including better integration of the extraction and stripping steps. Means of recovering and isolating particulates during processing are also being investigated.

ACCOMPLISHMENTS DURING THE CURRENT CALENDAR YEAR

Since the project began, in October of 1977, we have obtained samples of actual wastewaters, preserved at different pH values, from the Synthane gasification process (PERC), the Lurgi gasification process (MERC), and the solvent-refined-coal liquefaction process (Pittsburgh-Midway Coal Co.). These are being analyzed by gas chromatography, coupled with mass spectrometry. The analyses have been directed toward identification and quantification of phenolic, carboxylic-acid, and organic-base constituents, as well as degradation products formed during storage.

Calculations have been made with reported analyses of similar waters to assess both the relative amounts of different acids and bases plus the expected influence of various acid-base equilibria on stripping and extraction operations.

Theoretical and experimental tests of vacuum stripping have demonstrated its capability of removing residual solvents effectively, and have identified the volatility range of interest for solvents.

PLANNED ACTIVITIES FOR NEXT YEAR

We shall obtain additional samples of waters and complete the identification and quantification of the various acid and base components. Equilibrium data will be obtained for extraction of phenolics and carboxylic acids with various solvents and solvent mixtures of interest at different pH values. Similar measurements will be made for vapor-liquid equilibria of ammonia. Vacuum stripping studies will be continued, with the goal of quantifying the factors with paramount influence on solvent selection. Rough conceptual designs and economic analyses will be made to identify the most promising avenues for improvement, and miniplant testing of one or more of these approaches will be initiated.

REFERENCES

1. C. H. Ho, B. R. Clark and M. R. Guerin, J. Environ. Sci. Health A11(7), 481 (1976).
2. P. Milios, Chem. Eng. Prog. 71(6), 99 (1975).
3. N. L. Picker and C. J. King, paper presented at AIChE Annual Mtg., New York, November 1977 (AIChE Symp. Ser., in press).

COMPOSITION AND ENZYMATIC HYDROLYSIS OF CELLULOSIC AGRICULTURAL RESIDUES

M. Riaz, A. F. Sciamanna, R. D. Yang and C. R. Wilke

In the continuing study of the production of ethyl alcohol as a liquid fuel and of other chemicals from agricultural residues, it was found there was a scarcity of data on the composition of these residues. Therefore, a system of analysis applicable to these residues was devised.[1] Published methods of analysis on wood and food grains were adapted or modified to suit these residues.

The composition of certain agricultural residues generated in California are given in Table 1. The main emphasis is on the carbohydrate composition because of the concern for sugar production.

A series of chemical pretreatments were studied to see if sugar production by enzymatic hydrolysis might be improved.[2] The results of these studies showed that pretreatment with 1% sulfuric acid was effective in extracting pentose sugars and improving subsequent enzymatic hydrolysis. Carbohydrate yields obtained in this manner are shown in Table 2. A tentative processing scheme based on the forgoing procedures is shown in Fig. 1.

Efforts are in progress to optimize the production of enzyme, which is the major cost factor in the hydrolysis operation. During the past year, experimental studies on cellulose production were focused on the development of a multistage fermentor with a cell-recycle system providing for maximum cell growth in the first stage and enzyme induction in subsequent stages (along with minimal cell growth). Two-stage and three-stage systems were tested. Maximum enzyme productivity thus far has been obtained with the two-stage system.

In the two-stage system, the first stage was operated on Solka Floc as the carbon source followed by a single induction stage to which cell recycle was directed. The temperature was maintained at 30°C, and the pH was 4.8 for both stages. The data obtained during a five-week experimental run indicated that

Table 1. Assay of residues in wt%.[a]

	CARBOHYDRATES[b]									
Material[c]	Gluc	Mann	Galac	Xyl	Arab	Lign	Ash	Aceo. Bz/EtoH Ext.	Acid Insol.	Other
Ground Wood	40.0	12.1	1.1	3.8	1.4	31.10	0.2	1.8	-	-
Barley Straw	37.5	1.26	1.71	15.0	3.96	13.8	10.8	9.7	2(±1)	-
Corn Stover	35.1	0.25	0.75	13.0	2.8	15.1	4.3	5.5	1(±1)	4 Protein
Cotton Gin Trash	18.0	1.9	0.1	4.0	2.0	17.6	14.8	8.3	2(±1)	3 Amine/Protein
Rice Hulls	32.5	2.7	0.1	12.3	2.6	19.4	20.1	2.0	2(±)	-
Rice Straw	36.9	1.6	0.4	13.0	4.0	9.9	12.4	4.4	2(±)	-
Sorghum Straw	32.5	0.8	0.2	15.0	3.0	14.5	10.1	6.2	1(±1)	1 Protein
Wheat Straw	32.9	0.72	2.16	16.9	2.11	14.5	9.6	7.2	3(±1)	3 Protein

[a] Average of 3-5, Det'm.

[b] Gluc = Glucan, Man = Mannan, Galac = Galactan, Xyl = Xylan, Arb = Arabian, Lign = Lignin, Azeotropic Benzene Alcohol Extractives, Acid Insoluble Material.

[c] 2 MM Wiley milled, 40-60 mesh fraction, and 100% dry.

Table 2. Total yield summary of liquor and enzyme hydrolysis of acid treated material basis: 100 lb original material.

Material	Glucose	Poly Glucose	Pentoses	G&PG Conversion %	Pentose Conversion %
Barley Straw	14.2	2.5	8.7	40.4	40.4
Corn Stover	17.6	2.1	15.5	50.8	86.3
Cotton Gin Trash	5.8	1.2	1.0	35.3	14.7
Rice Hulls	6.7	2.1	9.7	24.7	57.3
Rice Straw	20.3	4.7	14.8	61.6	76.6
Sorghum Straw	15.0	2.6	10.9	49.1	53.3
Wheat Straw	15.0	2.4	15.4	47.9	78.3
Ground Wood	9.3 and 7.9 Mannose	1.0	3.5	23.5	59.2

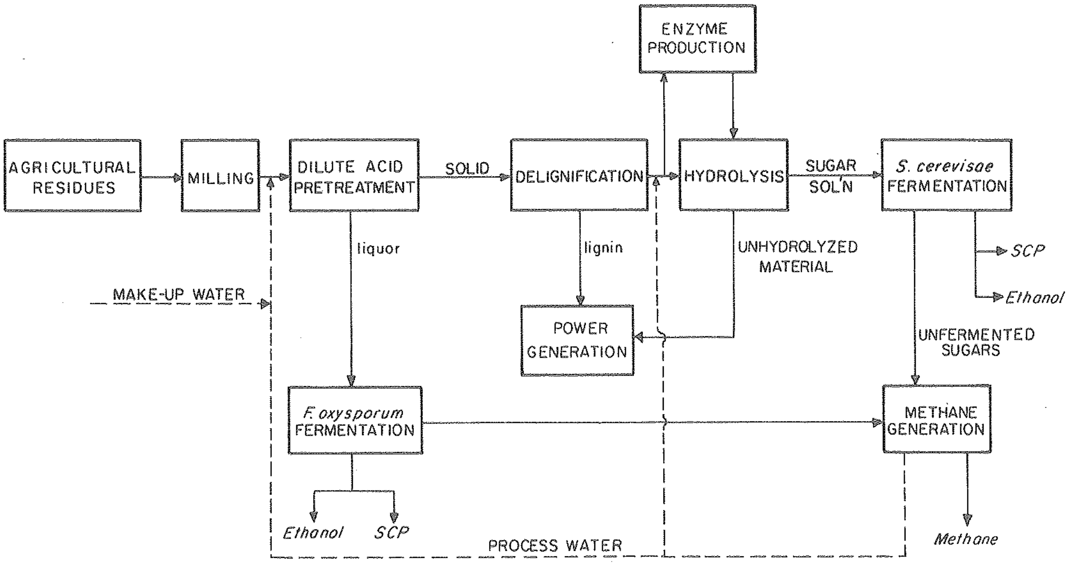

Fig. 1. Flow diagram of the process to produce ethanol from agricultural residues. (XBL 775-5463)

optimum enzyme productivity occurred at an overall dilution rate of 0.029 hr^{-1}, with product enzyme concentration of 3.7 FPA. This productivity is compared with that of previous experiments in Table 3. The two-stage process shows an average 30% increase over the single stage with recycle, and the single stage with recycle shows a 70% increase over the single-stage fermentor without cell recycle.

When insoluble cellulose is contacted with enzyme solution, about seventy-five percent of the enzyme is strongly adsorbed (Fig. 2), and at present is not recoverable by simple means such as washing. The adsorption of the cellulase complex is presently poorly understood and may involve chemical or physical binding of the enzyme molecules of the surface of the cellulosic fiber. Our study has been aimed at disrupting or weakening either type of binding by employment of various agents for washing or pretreatment, in order to displace active enzyme, or to reduce the strength of adsorption. Attempts were made to bring partial denaturation of the enzyme molecule in order to unfold the peptide chain and release it from its cellulosic matrix.

Urea was found to be an effective desorbing agent in this context. Figure 3 shows the enzyme activities removed by treatment of partially

Table 3. Comparison of enzyme productivities.

Fermentation System	(1/hr)	S_R (G/L)	FPA*	Productivity (I.U./ML-DAY)	Cell Density (G/L)	Specific Productivity (I.U./MG-DAY)
Single Stage No Recycle	0.020	7.5	2.7	0.192	2.3	0.0084
	0.030	7.5	1.9	0.169	2.0	0.085
	0.043	7.5	1.6	0.198	2.2	0.09
	0.053	7.5	1.50	0.22	2.0	0.11
	0.063	7.5	1.25	0.21	2.1	0.10
	0.073	7.5	0.85	0.15	2.0	0.075
	0.093	7.5	0.20	0.035		
	0.03	15.0	1.4	0.113	4.0	0.028
	0.04	15.0	0.8	0.075	3.7	0.020
	0.06	15.0	0.7	0.10	3.0	0.033
Two Stage No Recycle	0.02	15.0	2.5	0.17	4.6	0.037
	0.03	15.0	2.0	0.18	3.9	0.046
Single Stage with Recycle	0.02	10.0	3.7	0.32	7.0	0.046
	0.02	7.5	3.61	0.30	6.9	0.043
	0.03	5.0	2.6	0.27	10.0	0.027
	0.032	5.0	3.2	0.40	8.5	0.047
	0.038	5.0	1.4	0.14	9.0	0.016
Two Stage with Recycle	0.021	10.0	4.25	0.43	5.0	0.086
	0.029	10.0	3.7	0.46	8.7	0.053
	0.029	7.5	3.7	0.46	7.0	0.066
	0.029	5.0	3.45	0.41	5.8	0.070
	0.034	5.0	2.9	0.37	6.3	0.058
Three State with Recycle	0.022	10.0	3.8	0.36	4.5	0.080

*FPA = Filter Paper Activity.

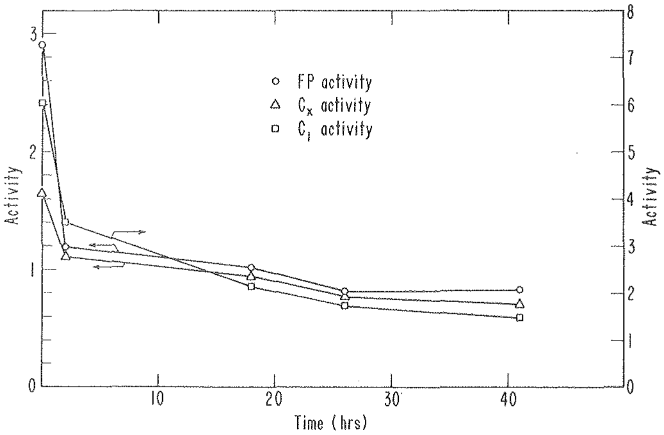

Fig. 2. Enzyme activity remaining in solution during hydrolysis as a function of time. (XBL 7673204)

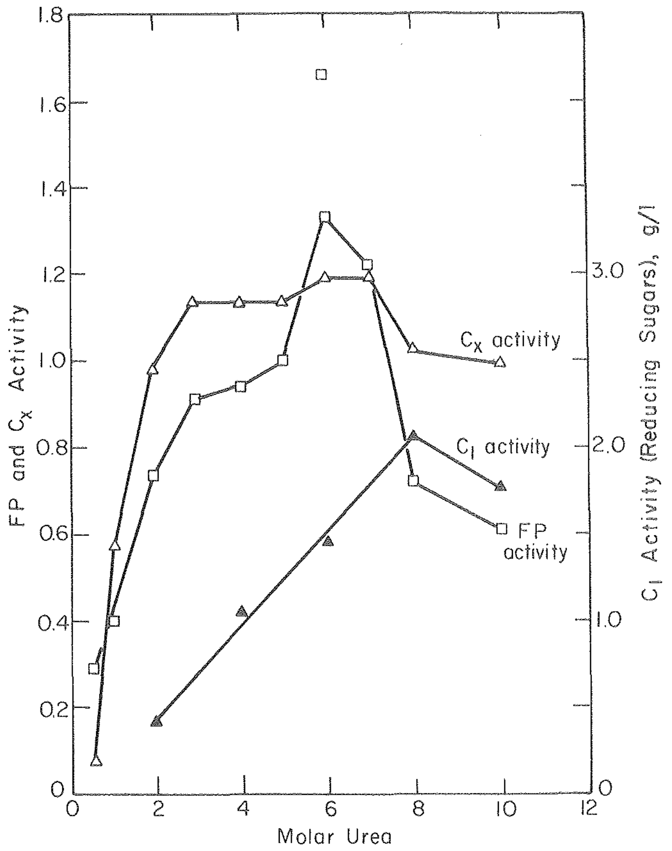

Fig. 3. Recovery of cellulase from cellulose by deportation into urea solutions. △△C_x(1-4 β glucanase), □□filter paper saccarification and ▲▲C_1 cellobiohydrolase. (XBL 774-5285)

hydrolyzed cellulose with urea solutions in 5% solid-liquid suspensions. A single washing with 6 molar urea removed 27-36% of the original enzyme activity. Results of recombining wash solutions and hydrolyzate suggest that about 70% of the original enzyme might be removed in this manner.

Reversible denaturation of cellulose by urea suggested that it may be possible to modify the enzyme molecules by bringing a minimal configurational change in the tertinary or quaternary protein structures. Such change may prevent it from becoming adsorbed on cellulosic matrix without exerting any effect on the active site for its catalytic function. Various amounts of urea were introduced to the hydrolysis vessels prior to the addition of substrate. 0.9 M urea had the optimal effect to retain 67% of the original C_1 component (cellobiohydrolase) in liquid phase, compared with 17% where no urea was added (Fig. 4). Eighty-seven percent of the C_x component (1→4βglucanase) was retained in the solution. 0.9 M urea showed no inhibitory effect and rather increased the overall hydrolysis by 8%. Figure 5 illustrates the rate of hydrolysis of Solka Floc without and with 0.9 M urea added to the hydrolysis reactor. Treatment with urea has increased thermal stability of the enzyme molecules.

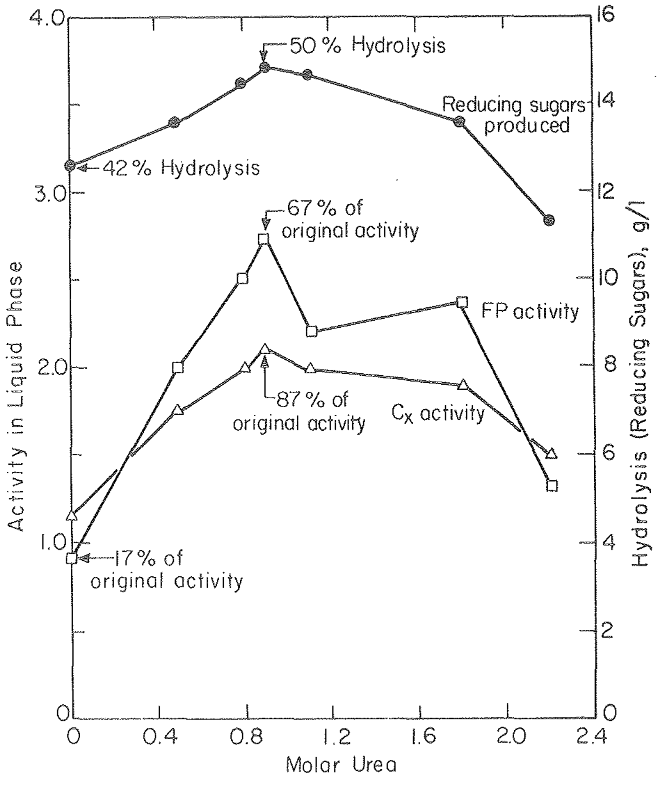

Fig. 4. Enzyme activity remaining in solution during hydrolysis in the presence of various concentrations of urea. Filter paper saccharification. ●● C_x(1-4β glucanase). (XBL 774-5284)

As an alternative approach, experiments were conducted to see if phosphate ion adsorbed on cellulose prior to hydrolysis might provide a weakened adsorption linkage for the protein polar groups of the enzyme and permit enzyme removal by subsequent washing. Pretreatment of Solka Floc with 0.5 M sodium phosphate permitted recovery of 62% of the C_1 component (cellobiohydrolase) and 95% of the C_x component (β-1-4 glucanase) through washing with water after hydrolysis.

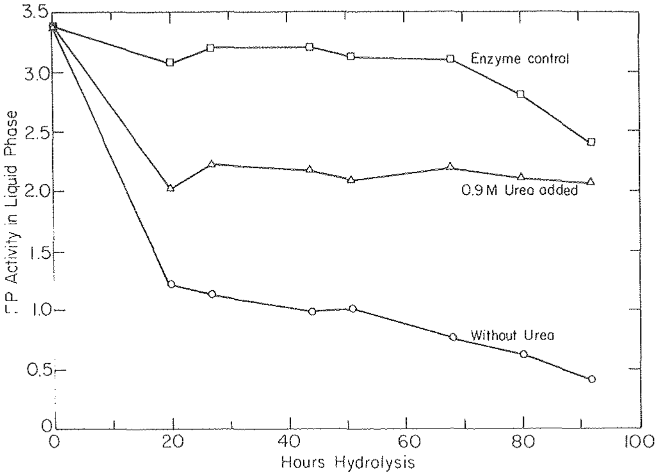

Fig. 5. Enzyme activity remaining in solution during hydrolysis in the presence 0.9 M urea as a function of time. (XBL 774-5281)

REFERENCES

1. R. Freitas, B. Long, A. Sciamanna and C. R. Wilke, Procedures for Analysis of Solids and Liquors from Cellulosic Sources. Lawrence Berkeley Laboratory Report, LBL-5967, 1978.

2. A. Sciamanna, R. Freitas and C. R. Wilke, Composition and Utilization of Cellulose for Chemicals from Agricultural Residues, Lawrence Berkeley Laboratory Report, LBL-5966 (in press).

DESIGN AND ECONOMIC STUDIES OF ALTERNATIVE FERMENTATION METHODS FOR ETHANOL

G. R. Cysewski and C. R. Wilke

Basic fermentation studies have been reported[1,2] in which the productivity of ethanol fermentation systems has been improved by (1) employment of vacuum to remove ethanol as it is formed and thus minimize product inhibition and (2) employment of cell recycle to obtain a high concentration of yeast cells in the fermentor. Some of the most significant conclusions of this work are summarized in Table 1.

Using the results of Table 1 as a basis, optimized process designs and cost estimates were prepared for the processing of molasses solutions containing 50% cane sugar employing each of the four modes of operation. The most productive process employing vacuum and cell recycle will be outlined briefly as an example. Details of all the processes are presented in our report, LBL-5963 (to be published in Biotechnol. Bioeng.).

Figure 1 shows a schematic flow diagram of a process to produce 78,000 gal/day of 95% ethanol. Full strength molasses is first mixed with mineral supplements. The medium is sterilized by steam injection and fed to a single 1.89×10^5 liter vacuum fermentor operating at a total pressure of 55 mmHg and 35°C. Pure oxygen is sparged through the fermentor at a rate of 0.1 vvm at S.T.P. to satisfy the trace oxygen requirement of the yeast. As the fermentation proceeds, ethanol and water are boiled away from the fermentation broth. The vapor from the fermentor is compressed to 340 mmHg and condensed in the fermentor reboiler to supply the energy for the vaporization of ethanol and water in the fermentor. After the vapor recompression cycle, the uncondensible gases (carbon dioxide and oxygen) are compressed to 760 mmHg and cooled to 35°C to condense additional ethanol and water. The fermentation gases are finally fed to an absorber where the last traces of ethanol are removed. The fermented beer is pumped to atmospheric pressure and fed to two continuous centrifuges where the yeast concentrate is removed. A portion of the yeast concentrate is returned to the fermentor. The remaining yeast is spray dried and packaged for sale. The clarified beer from the centrifuges and the condensation products are fed to a distillation column where the ethanol is concentrated to 95%. A portion of the bottoms product from the distillation column is cooled and fed to the absorber.

Costs of conducting the fermentation, exclusive of raw materials, by the alternative methods are summarized in Table 2. From these data it may be concluded that a major economic gain may be achieved by using continuous rather than batch fermentation. A further significant cost reduction is possible by incorporating vacuum and cell recycle in the process. Use of vacuum is most advantageous for highly concentrated sugar solutions for which product inhibition precludes simple continuous fermentation with prior dilution.

Table 1. Some results of the Laboratory fermentation systems. (Optimum pH = 4.0 and optimum temperature = 35°C in all cases.)

Fermentation System	Optimum Oxygen Tension, mmHg	Optimum Sugar Concentration, %	Cell Mass Concentration at Optimum Conditions, g Dry wt, Liter	Maximum Ethanol Productivities, g/ -hr
Batch	a	-	5.6[d]	2.2[c]
Continuous	0.07	10.0	12.0	7.0
Continuous with Cell Recycle	0.07	10.0	50.0	29.0
Vacuum with Cell Recycle	b	-	124.0	82.0

[a] Optimum procedure was to initially air saturate broth and use an aerobically grown 2.0% inoculum with no air sparging during fermentation.

[b] Oxygen tension could not be determined. Optimum procedure was to sparge pure oxygen through the fermentor at a rate of 0.10 vvm at STP.

[c] Assumes 6 hr fermentor down time between 16 hr batch fermentation.

[d] At end of batch fermentation.

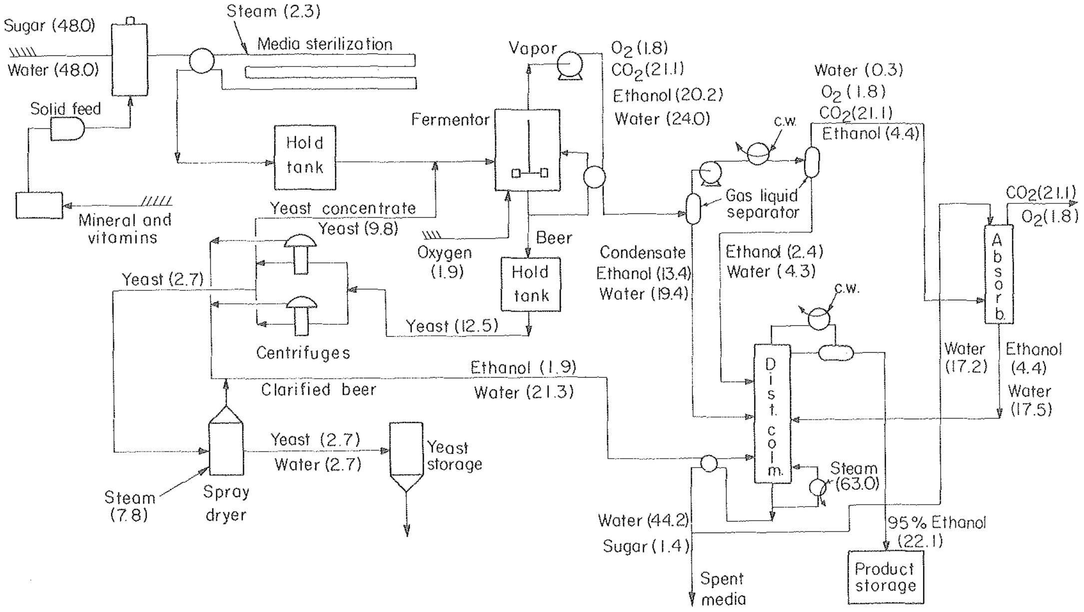

Fig. 1. Flow diagram and mass balance for continuous vacuum fermentation with cell recycle. Capacity 78,000 gal/day of 95% ethanol (flows in 10^3 lb/hr) cw = cooling water.

Table 2. Ethanol production costs for different modes of operation plant capacity 78,000 gal/day of 95% ethanol from 50% "cane" molasses sugar solution.

	Production Cost Cent/Gal			
	Batch	Continuous	Continuous Cell Recycle	Vacuum Cell Recycle
Investment Related Costs	10.3	4.9	4.0	3.5
Operating Labor	3.2	0.9	0.5	0.4
Supervision & Clerical	0.2	0.1	0.1	0.1
Utilities				
Water	0.6	0.6	0.6	0.4
Power	1.2	0.6	0.9	0.6
Steam	10.1	9.5	9.5	6.8
Oxygen	--	-	-	0.5
Laboratory Changes	0.1	0.1	0.1	0.1
Plant Overhead	1.8	0.6	0.4	0.3
TOTAL	27.5	17.3	16.1	12.7

REFERENCES

1. G. R. Cysewski and C. R. Wilke, Rapid Ethanol Fermentation Using Vacuum and Cell Recycle, Biotechnol. and Bioeng. 19, 1125 (1977).

2. G. R. Cysewski and C. R. Wilke, Fermentation Kinetics and Process Economics for the Production of Ethanol, Lawrence Berkeley Laboratory report, LBL-4480, 1976.

FERMENTATION OF HEMICELLULOSE SUGARS TO ETHANOL

T. R. Batter, B. A. Brandon, S. L. Rosenberg and C. R. Wilke

Hemicelluloses, which are pentose and hexose polymers soluble in dilute acid and alkali, comprise a significant fraction of cellulosic biomass. Xylose, a pentose, is usually the major hemicellulose sugar.

Because of the substantial xylose fraction in most cellulosic materials, recovery and utilization of this sugar are being studied in addition to the work on glucose. During the past year, a study on the fermentation of xylose to ethanol was completed.[1]

Xylose can be fermented almost quantitatively to ethanol and carbon dioxide by the mold Fusarium oxysporum. Our work has focused on determining optimum fermentation conditions for maximum production of ethanol from xylose.

Temperature and pH optima for growth have been found to be 30°C and 5.0, respectively. Yield data for the fermentation have been obtained and are shown in Table 1.

Table 1. Yield of products from Xylose fermented by Fusarium oxysporum.

Component	Yield Factor gm/gm Xylose
Cell Mass	0.12
Ethanol	0.41
Carbon Dioxide	0.32
Acetic Acid	0.04

The enthanol yield is 87% of the theoretical value.

Kinetic studies indicate that growth is linear rather than exponential and occurs in two phases. A high linear rate is exhibited during the first 2/3 of the fermentation, and this is followed by a declining rate until the substrate is exhausted.

Studies on the effect of increasing ethanol concentrations on the growth of the organism show that decreased growth rates are apparent at concentrations of ethanol greater than 1.5% by wt. Growth is completely halted at ethanol concentrations greater than 4.1% by wt.

Fermentations have also been carried out using as substrates sugars extracted by the dilute acid hydrolysis of wheat straw. Preliminary results indicate that the organism can grow in these neutralized crude hydrolysates and produce ethanol from glucose, xylose and arabinose.

At the present time, the main problem associated with this fermentation is the slow rate of growth and ethanol production. In batch cultures ethanol productivity is approximately 0.04 g/l-hr. In continuous culture, with a cell-recycle system, ethanol productivity can be increased to 0.07 g/l-hr.

Growth experiments have been conducted in a number of different mineral media in an effort to find nutritional conditions that would permit significantly higher growth rates. Only minor increases have been achieved.

In the future the growth and fermentation rate of this organism will be examined using other sugars as substrates. If faster growth is evident the potential for genetically improving the xylose fermentation by Fusarium oxysporum exists, and experiments to select "fitter" mutants will be conducted. If no higher growth rates can be demonstrated, a comprehensive literature search will be conducted to identify other xylose-fermenting micro-organisms.

REFERENCE

1. T. R. Batter and C. R. Wilke, A Study of the Fermentation of Xylose to Ethanol by Fusarium oxysporum, Lawrence Berkeley Laboratory Report, LBL-6351 (1977).

Environmental Research

ENVIRONMENTAL ASSESSMENT OF SOLAR ENERGY CONVERSION

M. Davidson and D. F. Grether

INTRODUCTION

The objective of this project is to examine the implications of widespread application of solar energy technologies. The approach is to take present concepts of a technology, which are typically in the design study or pilot plant stage, and to investigate the socioeconomic and environmental consequences of the technology, should it supply a substantial fraction of the nation's energy requirements.

ACCOMPLISHMENTS DURING 1977

The principle activity for this year was the completion of a detailed study of the Central Receiver power plant.[1] The study covered three major areas.

Socio-Economic Implications

An economic input/output (I/O) model, described in the previous annual report, was further developed. In particular, EPA effluent data were added.

As a first step in applying the model a "bill-of-goods" was constructed, which estimates the demands on each of 93 industrial categories from building a Central Receiver plant of 100 MWe in size of the intermediate load type. The model is then used to obtain a "cumulative" demand on the 93 industrial categories that includes the effect of multiplicative factors in the economy. The results are tabulated in Ref. 1. As an example, suppose one envisioned a vigorous construction rate of 100 standard size (100 MWe) plants per year. The tables can then be used to obtain the increase in output of the various industries. Industries especially affected include: primary iron and steel (11% increase), heating, plumbing, and structural (19%), glass and glass products (8%), stone and clay products (4%), and iron/ferroalloy ores mining (10%).

The model was also used to calculate the increase in manpower requirements caused by the plant construction. The cumulative increases were largest in categories such as manager and other administrators, assemblers, machine operators, and welders. In all, some 10,000 man years would be required for a 100 MWe plant, assuming current industrial practices (no mass production especially tailored to central receiver plants).

Over the lifetime of the central receiver plant (assumed to be 30 years) a total of about 1.0×10^7 MWh of energy would be generated. The model was used to estimate that to generate the equivalent amount of energy from coal, the labor requirements (including construction of the plant and the coal mining) would be about 3,900 man years. Thus, the solar plant may be considered to be more labor intensive. However, if mass production techniques are introduced into the construction of central receiver plants then the manpower requirements would be reduced.

Finally, the effluents from the manufacturing of the solar plant were estimated, based on 1990 EPA standards. A comparison was made to the effluents for different types of fossil fuel plants generating the energy equivalent of the solar plant. Table 1 (reproduced from Ref. 1) shows this comparison. Surprisingly, the natural gas fired plant is superior in many categories. However, the central receiver (generally) has lower emissions than coal fired plants, which are the fossil plants most likely to be constructed in the future.

Two comments on Table 1 are in order. First, the particulates charged to the central receiver are primarily from the cement industry and tend to be large compared to those from fossil plants. Large particles are generally considered less hazardous and thus the Table is probably biased in favor of fossile plants. The second comment is that the Table excludes CO_2 emissions, which are not considered a pollutant by EPA. There is no doubt that the solar plant would be responsible for far less CO_2 release than fossil plants.

Environmental Implications

The one inescapable consequence of solar electric power plants of the central receiver type is that large land areas in arid or semi-arid areas would be partially covered with heliostats (mirrors mounted on sun tracking platform). A 100 MWe intermediate load plant would require about 3 km^2 of land. There are a number of additional effects, the nature and severity of which will be highly dependent upon specific siting and construction methods. Reference 1 details a number of possible problems. These include destruction of habitat from off-road vehicle use, either during construction or from recreational activities of the increased human population; change of the hydrological cycle; and impact on endangered species.

Climatological Implications

The solar plants will alter the pre-existing radiative and water balance between the ground

Table 1. Comparison between central receiver and various fossil for major air emissions. (Units are tons of effluent per 1.0×10^7 MWh, the total energy generated by a 100 MWe intermediate load central receiver plant operating over a 30 year lifetime.)

	Plant Type				
Emission Type	Coal fired	Residual fuel oil	Natural gas	Oil fired combined cycle	Central receiver
Particulates	$1.5\text{x}10^3$	$1.9\text{x}10^3$	$5.2\text{x}10^2$	$1.7\text{x}10^3$	$1.0\text{x}10^3$
SO_x	$5.1\text{x}10^3$	$1.4\text{x}10^4$	$3.1\text{x}10^1$	$0.9\text{x}10^4$	$1.1\text{x}10^3$
NO_x	$3.8\text{x}10^4$	$1.5\text{x}10^4$	$1.0\text{x}10^4$	$1.4\text{x}10^4$	$9.\ \text{x}10^2$
CO	$2.7\text{x}12^3$	$1.0\text{x}10^3$	$8.0\text{x}10^2$	$5.1\text{x}10^3$	$5.2\text{x}10^3$
Hydrocarbons	$8.0\text{x}10^2$	$6.8\text{x}10^2$	47	$1.0\text{x}10^3$	$9.3\text{x}10^1$

and the atmosphere. The local (at the plant site), regional (many plants in one area) and global (many plants world-wide) climate will be affected to some extent. A study of possible climate modifications, begun in 1976, was extended in 1977 and reported in Ref. 1. Briefly, climate models were applied at the local and global level. Finite changes were observed, but none that (within the context of the models) would indicate a cause for serious concern.

REFERENCE

1. M. Davidson and D. Grether, The Central Receiver Power Plant: An Environmental, Ecological and Socioeconomic Analysis, Lawrence Berkeley Laboratory Report, LBL-6329 (1977).

MICROCOSMS AS A TOOL FOR AQUATIC ECOSYSTEMS ENVIRONMENTAL IMPACT ASSESSMENT

J. Harte and D. Levy

INTRODUCTION

Continuing social concern over the effects of energy production and conversion on aquatic systems demands strategies whereby our needs for new energy sources can be reconciled with the necessity for preserving our dwindling aquatic resources. Part of the solution lies in choosing sites for energy facilities where the environment is sufficiently robust, or buffered, to absorb the impact of energy related processes. In order to aid in site selection we have been working towards the development of practical methods for predicting the robustness or, conversely, sensitivity, of aquatic systems.

The specific problem with which we have been concerned is the effluent waste water from coal conversion processes. This water contains substances known to be toxic to many organisms, including humans. The usual approach to this kind of problem has been to study the direct effect of these substances on specific organisms. We are convinced that species-specific toxicological studies, while most valuable for protecting against critical intoxications, do not provide enough information to assess potential ecosystemic impacts, which can arise from exposure to toxic substances. The effects of certain substances may be mitigated during transit through an active and rich aquatic system, while the effects of others may be amplified. The problem is further aggravated by the fact that many substances, each at low concentration, interact synergistically to produce large net effects. Studies of entire systems obviously cannot be conducted with the same facility as can toxicological laboratory studies. For this reason we have chosen to evaluate freshwater microcosms as a means to test the stability, or sensitivity, of a given aquatic system.

Our long-term objective is to develop predictive indicators that can reveal the sensitivity of a system to disturbance, prior to the imposition of the disturbance. The attainment of this objective would be greatly facilitated if microcosms could be used to generate the data necessary for the development and testing of such indicators. An increasing number of research groups have employed microcosms in recent years, but few standard methods for the design, installation and operation of microcosms have resulted from this expanded interest. Our first priority, therefore, has been to consider the conditions under which microcosms can be used to understand system behavior in natural bodies of water; and to develop an effective protocol that would result in reproducible microcosm behavior. We have sought:

- To characterize the difficulties in obtaining replicate microcosms that simulate natural systems.
- To explore the use of microcosms for simulating perturbations of natural aquatic systems by coal conversion effluents.
- To identify those biological and chemical parameters most useful for evaluating the responses of microcosms to stress.
- To test the use of microcosms in evaluating a hypothetical stability indicator derived from theoretical studies.

Prior to 1977, we had undertaken a wide range of microcosm studies[1] in order to look for those properties of microcosms that may be common to a large number of freshwater lakes. The breadth of our observations was motivated by the need to identify and correct problems that are specific to laboratory systems and thus obscure fundamental properties. We have found, for example, that the exceptionally high underwater surface (sides and bottom) to volume ratios in small laboratory systems results in a disproportionately high percentage of sessile biomass. Long-term operation of microcosms will be possible only if means are found to control this problem. We also have demonstrated that it is unrealistic to attempt to maintain fish, even one fish, in any but exceptionally large laboratory systems.[1] On the other hand, our work showed that patterns of seasonal succession of phytoplankton and zooplankton in microcosms closely parallel in many important ways those observed in natural lakes during the period of spring bloom.

ACCOMPLISHMENTS DURING 1977

Experimental

We conducted our experiments in 1977 with four sets of microcosms that correspond to four different types of trophic conditions in natural systems. This helped us identify not only general problems in microcosms design, but also phenomenological parameters common to diverse systems. One of our initial hypotheses, which we have tested using the microcosms, was that the decomposition process could be analyzed to predict the sensitivity to perturbation of the system. A parameter, K_D, reflecting the carrying capacity of the system for decomposition, was identified from theoretical studies previously conducted. We measured this carrying capacity and assessed its relationship to the sensitivity of each system, as determined by subsequent perturbation, in order to test its value as a predictive indicator.

Each of the three rounds of principal experiments lasted four months, and involved replicate 50 liter microcosms for each condition. The composition of the nutrient enrichment media used to establish the microcosms in correspondence with different trophic types of natural systems has been described.[1]

Each replicate set consisted of two triplets of 50 liter microcosms; one triplet of each set was eventually subjected to contamination by one of the pollutants to be tested while the other remained as a base line, or control, for comparison.

Each experiment was divided into two 2-month phases. During the first two months of each experiment, data were collected and used to assess reproducibility in the microcosm systems for the purposes of locating problems particular to microcosm operation, and to provide trend lines with which to evaluate sensitivity indices. At the end of the first two months of each experiment, sub-experiments were conducted to measure the carrying capacity of the decomposers. Immediately following the commencement of each sub-experiment, a common constituent of coal conversion was added to half the microcosms and all systems were monitored for an additional two months.

The pollutants added in each of the three experiments were chosen because of their prevalence in coal conversion effluent water, their ready availability, and their relatively low hazard to laboratory personnel. They were added at concentrations chosen to simulate possible levels in actual receiving waters. We chose 1.6 mM (28.8 ppm) NH_4, 0.12 mM (6.5 ppm) Fe(III), and 5.3 μM (0.5 ppm) phenol. Ammonium was added as a mixture of NH_4Cl and $(NH_4)_2SO_4$, to minimize pH modification of the ammonia compound as a source of nutrient. Iron was added as $FeCl_3 \cdot 6H_2O$. In this experiment we decided to allow the pH to respond to the imposition of the acidic chloride salt in order to observe the response of the system to the coupled imposition, and because to maintain artificially the pre-perturbation pH, would have resulted in a loss of much of the iron as $Fe(OH)_3$ precipitate. Phenol was added from aqueous solution.

The predictive indicator, K_D, was determined from measured changes in the rate of decomposition in a system when its level of detritus changes. Prior to the disturbance of the microcosms, by the introduction of a toxic substance, we removed aliquots from the microcosms in order to increase their detrital levels, and thus quantify the effects of such an alteration upon their decomposition activity. By using small aliquots taken from the systems under study, we were able to accomplish this without altering the systems. It is necessary to conduct the experiment in this manner since any predictive indicator, if it is to be of value in field application, must be determinable without modifying the natural system.

One method of quantifying the response of decomposers to the addition of detritus is to measure the variation in respiratory gas exchange following the addition. In all of these experiments we monitored altered and control respiration rates in every aliquot.

In the first beaker experiment, which accompanied the ammonia perturbation experiment, we also monitored bacterial plate counts as well as many of the parameters monitored in the basic microcosm experiments. In the beaker experiments related to the iron and phenol perturbation experiments, we closely examined changes in phytoplankton and zooplankton in selected aliquots, primarily to determine if our experimental approach has further application in understanding the mechanisms of planktonic systems.

CONCLUSIONS

An evaluation of the use of microcosms for the assessment of energy conversion impacts on aquatic systems has indicated that microcosms have the potential of being convenient experimental tools for intermediate term (less than three months) studies, provided that standard procedures for design and operation are established. Key problems in the development of these procedures have been identified in this study, and the use of microcosms is recommended, contingent upon the resolution of these problems.

A hypothetical stability indicator, derived from theoretical studies and related to decomposition activity, was measured and its values were compared to empirically derived quantitative indices of the sensitivities of the microcosms to perturbation by coal conversion byproducts. Correlations between the stability indicator and the response of the microcosm systems were only marginally suggestive of a predictive capability. If this indicator has any applicability, it would be over a period of time too long to permit its evaluation by microcosm studies.

Direct observations of the effects of three different constituents of coal conversion effluent water on microcosm systems, corresponding to four different trophic types of natural systems, revealed significant responses to the perturbation in all experiments. The specific responses of the individual systems depended upon the nature of the perturbation. For most measurements the phosphorus-rich, nitrogen-limited systems were most affected by the additions of ammonia and phenol; the phosphorus-rich systems were most affected by the addition of iron.

Interpretation of the results of these studies led to the following conclusions:

- Microcosms can simulate the behavior of natural systems for periods generally not exceeding three months. Longer term studies will require solution to the problem of side growth.
- Microcosms are most useful during a dynamic growth phase, in contrast with the common viewpoint that microcosms become useful when reaching a static phase in their succession.
- A progressive decrease in the replicability of the microcosms in successive experiments suggests a systematic problem that correlates with the age of the parent microcosm from which all inocula were derived. This suggests that microcosms become conditioned by laboratory environments.
- The relatively high proportion of surface to pelagic activity in microcosms diminishes the singular importance of water column nutrieent studies. Quantification of pelagic biota is indispensable. The need for determination of pelagic biota is reinforced by experiments in which nutrient levels as well as IC and OC were similar over time in different systems, but the biota were quite different.
- The means by which microcosms are initiated affects replicability and community structure. Further study of initiation procedures is required.
- Microcosms can be used to simulate specific trophic types of natural systems in order to assess the effects of particular perturbations on a given system. Because they provide a diverse assemblage of interacting biota, upon which a perturbation can be tested, phenomena are observed that would be missed in single-organism studies.
- The most significant effects of the ammonia perturbation were lowered inorganic carbon and zooplankton levels as compared to the controls. This is consistent with the ammonia stimulating primary production while being toxic to the zooplankton.
- In the iron addition experiment, the most significant effects were the decrease in phytoplankton and zooplankton populations. The formation of insoluble iron-phosphate complexes and the chelation of algal surface compounds, resulting in flocculation, were primarily responsible for this effect.
- The addition of phenol to the microcosms resulted in suppression of zooplankton in all systems and of Anabaena in the nitrogen-limited systems.

Further studies to determine the factors influencing tracking of natural systems by microcosms are indicated. Objects for immediate study, suggested by the preceding experiments, include:

- Optimization of initiation strategy.
- Control of surface activity and/or optimal use of microcosms in the presence of surface activity.
- Determination of the effects of size, nutrient levels and temperature on replicability among microcosms, and between microcosms and natural systems.
- The behavior of microcosms during blooms and the effects of perturbation during this dynamic phase, prior to the onset of laboratory conditioning.

Many of the problems impeding the use of microcosms for short and intermediate term simulations of natural systems appear to be readily resolvable. Our experiences indicate that efforts to obtain steady state conditions in microcosms are of marginal value and that the greatest utility of microcosms may well be the opportunity for studying the sensitivity of aquatic systems during dynamic phases.

THEORETICAL CONSIDERATIONS

A shortcoming of much theoretical work in ecology is that results often are not expressed or expressible as relations among readily measureable quantities. The relevant question in much environmental impact assessment work is not whether or not a system is stable, but rather how stable it is. Mathematical tools used in ecology are not well suited to answering this latter question.

Our work in this area was motivated by the need to make theoretical stability analysis accessible to experimental constraints and practical needs. Our objective was to introduce a definition of stability which offers a useful quantitative measure of ecosystem response to stress. Although the definition of stability we developed appears to be mathematically ungainly, it has the advantage of quantifying the most significant responses of ecosystems to environmental stress. Moreover, with rigorous analytical methods, we have now been able to show how the value of this stability measure depends upon certain potentially measureable parameters characterizing the undisturbed system.

The definition of stability we employ provides a measure of the deviation between a disturbed system and a control. In most general form it is given by:

$$S^{-1} = \Sigma\, c_i \int dt\; f[x_i(t)\ ,\ \bar{x}_i(t)] \quad , \quad (1)$$

where the x_i are the variables that describe the disturbed system, the $\bar{x}_i$ describe the undisturbed or control system, $t = 0$ is the time at which the disturbance begins, and $t = T$ is the duration of the perturbation experiment. The c_i are weight constants, and f is a non-negative function that vanishes when $x_i = \bar{x}_i$ and is a monotonically increasing function of $|x_i - \bar{x}_i|$. Note that these properties of the function, f, ensure that our stability measure, S, is greatest when the time-integrated deviation of the perturbed system from the control system is least. A particular form for f that we have used in our data analysis is described in Ref. 2.

While Eq. (1) provides an index or measure of stability which is empirically convenient (or can be made so by appropriate choices of the c_i and f) and has the flexibility to reflect many realities of environmental impact concerns, it does not connect in any obvious way with methods of system analysis other than computer simulation. If S is more than just an empirical property of stresses ecosystems, and can be related in some way to properties of the pre-stressed system, then methods of mathematical analysis of this measure would be useful.

In a recent article,[3] we have developed an analytic approach to the study of this stability index. We picked a reasonable choice for the form of f in Eq. (1), and performed a random average over all initial stresses. Our analysis showed that S, the stability measure, correlates unexpectedly well with two parameters (the mean and the variance) characterizing the distribution of residence times in the ecosystem. Because it may be possible to measure these parameters by means of a tracer experiment, we are encouraged that predictive indicators for the stability measure will be obtainable.

PLANNED ACTIVITIES FOR 1978

Four research areas will be pursued during 1978:

1. Further exploration will be made of optimal ways of using aquatic microcosms. Because of the necessity of controlling either side growth or limiting experiments to an undesirable short time period, strategies for control of side growth will be evaluated. In addition, the influence of alternative modes of microcosm initiation on the replication and development of microcosms will be explored.

2. Microcosms will be used to study some aspects of detrital degradation in aquatic ecosystems. By observing the responses in decomposition activity to prepared additions of organic materials, information can be obtained that will assist in elucidating the relative roles of the various system components that are active in detrital degradation.

3. A method for measuring denitrification rates will be explored. Using optoacoustic detection, we plan to build, and calibrate in our microcosms, a gas flux detection system that can be used to monitor N_2O transfer from aquatic systems to the atmosphere.

4. The development of biological or biochemical methods for the removal of heavy metals from coal conversion plant waste water would be desirable. Studies of certain aquatic plants suggest that heavy metal concentration through biouptake could provide a basis for such a method. The culturing of suitable organisms and biochemical analyses of concentration mechanisms will be undertaken in 1978.

REFERENCES

1. A. Jassby, M. Dudzik, J. Rees, E. Lapan, D. Levy, and J. Harte, Production Cycles in Aquatic Microcosms, Lawrence Berkeley Laboratory Report LBL-5965 (1977); A. Jassby, J. Rees, M. Dudzik, E. Lapan, D. Levy,

and J. Harte, Tropic Structure Modifications by Planktivorous Fish in Aquatic Microcosms, Lawrence Berkeley Laboratory Report LBL-5978 (1977).

2. J. Harte, A. Jassby, E. Lapan, and D. Levy, Aquatic Microbiomes for Assessment of Effluent Effects, Draft Final Report for EPRI, Palo Alto, CA (1978).

3. J. Harte, Ecosystem Stability and the Distribution of Community Matrix Eigenvalves, Lawrence Berkeley Laboratory Report, LBL-6361 (1977) (to be published in Systems Theory and Ecology, Academic Press, E. Haflon (ed.).

ESTUARINE TRACE ELEMENT INVESTIGATIONS IN SAN FRANCISCO BAY

D. C. Girvin, A. T. Hodgson, M. E. Tatro, and
R. N. Anaclerio

INTRODUCTION

Extensive chemical investigations are required in order to adequately assess the potential impacts of new and expanding power plants and petrochemical complexes that will discharge cooling and process waters into sensitive estuarine environments, such as San Francisco Bay. As these facilities can discharge significant quantities of toxic trace elements, it is essential to determine the existing levels of trace elements in the estuary, to understand the physical and chemical processes that control these levels, and to develop models that will provide insight into the biological significance of increased trace element loading.

No reliable trace element data existed for San Francisco Bay waters prior to the initiation of this research program. Therefore, our primary objective in 1976-77 was to determine the large-scale spatial and temporal variations in the levels of both dissolved and suspended particulate-associated Ag, Cd, Cu, Ni, Pb, and Zn. A major portion of this effort was concentrated in the northern San Francisco Bay and Delta where energy-related development is likely to occur. Using our compiled data base, we have begun an investigation of the processes that control trace element levels in the estuary. Three major questions have been addressed:

1. Are anthropogenic discharges of trace elements from power plants, oil refineries, and sewage treatment plants significant relative to the inputs of trace elements from the principal natural sources of fresh water to the estuary?

2. Do trace elements bound to river-borne suspended particulates desorb when river water mixes with ocean water?

3. Are the horizontal down-estuary profiles of dissolved trace elements governed by the simple dilution of river water by ocean water, or are the profiles significantly affected by desorption from particulates and discharges from anthropogenic sources?

ACCOMPLISHMENTS DURING 1977

Beginning in March 1976 and continuing through July 1977, water and suspended particulate samples were collected from a depth of 2 m at 20 stations throughout San Francisco Bay and Delta, and at several offshore stations in the Gulf of the Farallones. The Bay and Delta stations were reoccupied at approximately 4 month intervals. Dissolved Ag, Cd, Cu, Ni, Pb, and Zn in shipboard filtered (0.2 μm pore size) and acidified samples were preconcentrated by solvent extraction techniques and analyzed by flameless atomic absorption spectroscopy. Suspended particulates were collected on filter membranes (0.2 μm pore size) and analyzed by x-ray fluorescence spectroscopy and Zeeman atomic absorption spectroscopy.

In addition, salinity, temperature, pH, total carbonate alkalinity and the concentrations of dissolved oxygen, dissolved organic carbon, nutrients, chlorophyll a, sulfate, hydrogen sulfide, Mn, Fe, and suspended particulates were determined for most samples. This detailed characterization of samples is essential for our anticipated modeling of the chemical forms (i.e., speciation) of dissolved trace elements in the estuary. Sampling and analytical work were done in collaboration with Dr. E. A. Jenne of the U. S. Geological Survey, Menlo Park, California. Chemical modeling would also be done in collaboration with Dr. Jenne.

Representative distributions of dissolved Cu and Cd are shown in Figs. 1 and 2, respectively. These distributions are plotted vs salinity (S), since salinity provides a measure of dilution of outflowing river water (S = 0 ^{o}/oo) with intruding ocean water (S = 34 ^{o}/oo). The distribution of a dissolved constituent in an estuary is termed conservative if it is linearly related to salinity.

The nonconservative nature of dissolved Cu in northern San Francisco Bay is shown in Fig. 1 by the positive inflections of the distribution profiles above the hypothetical conservative mixing line drawn between the end members of the estuary. The observed distribution of Cu suggests that industrial and municipal

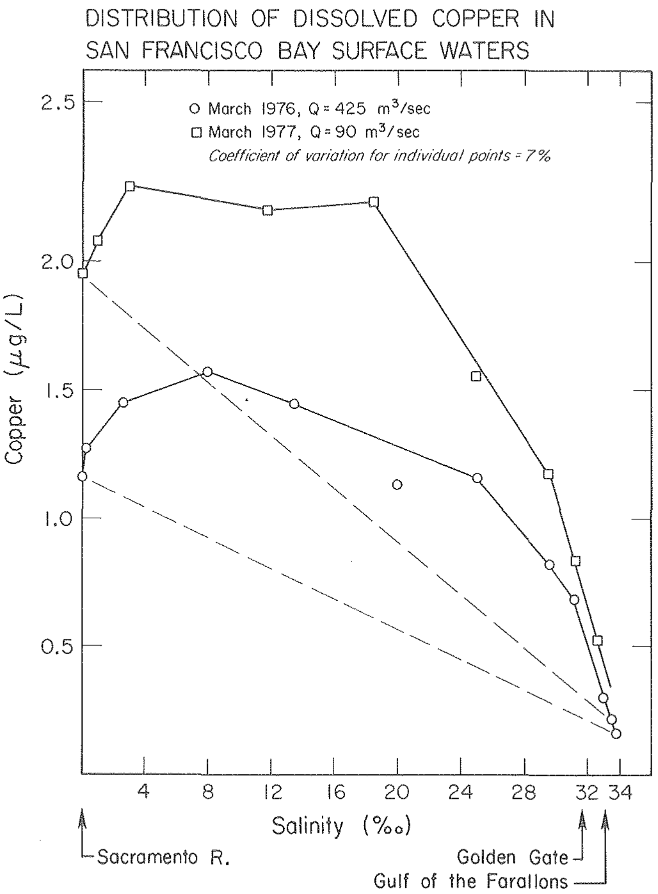

Fig. 1 Dissolved Cu profile in the surface waters of San Francisco Bay from the Sacramento River to the Gulf of the Farallones. Hypothetical conservative mixing is indicated by a straight line for each sampling period. (XBL 782-220)

sources discharged significant quantities of Cu and/or desorption of Cu from river-borne suspended particulates occurred as the particulates moved down the estuary into higher salinity waters. During the study period, the highest Delta outflow (Q = 425 m^{3}/sec) and, therefore, the highest concentrations of suspended particulates occurred in March 1976. An analysis of the March 1976 suspended particulate data showed that for salinities ≤20 ^{0}/oo, desorption could account for approximately 50% of the difference ($\Delta_{\text{Dissolved}}$) between the observed dissolved Cu concentrations and those predicted from the conservative mixing line. However, for salinities >20 ^{0}/oo desorption could not account for a significant percentage of the difference. Industrial and municipal sources also undoubtably affected the distribution of dissolved Cu in the estuary. More than 70% of the Cu from anthropogenic sources in the northern Bay was discharged south of the Carquinez Straits into water that had salinities >20^{0}/oo.[1] In March 1976 the flux of anthropogenic Cu into the estuary approximately equaled the flux of dissolved plus particulate Cu brought into the estuary in this month by freshwater discharge from the Delta. Although upstream transport of anthropogenic Cu by turbulent tidal diffusion could only have accounted for a small percentage of the March 1976 $\Delta_{\text{Dissolved}}$ at salinities <15^{0}/oo, the observed $\Delta_{\text{Dissolved}}$ in each sampling period at salinities >20 ^{0}/oo was probably almost entirely due to industrial and municipal wastewater discharges.

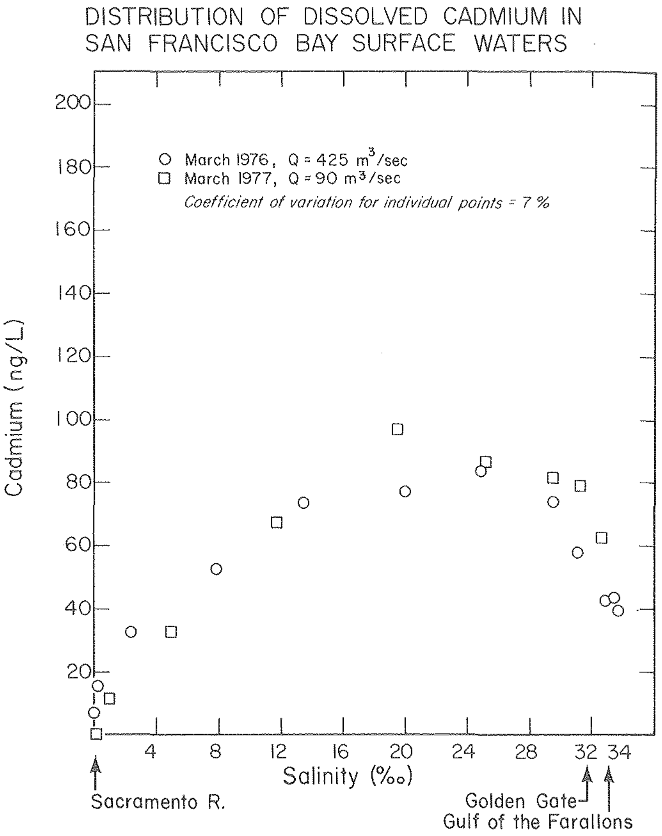

Fig. 2 Dissolved Cd profile in the surface waters of San Francisco Bay. (XBL 782-221)

The distribution of dissolved Cd in the estuary, shown in Fig. 2, is distinctly different from the distribution of dissolved Cu, since the Sacramento and San Joaquin Rivers are major sources of Cu, but not of Cd. In fact, the average concentration of 10 ng/liter of dissolved Cd in these rivers is as low or lower than values recently reported for open ocean surface waters. Therefore, the lowest Cd concentrations occurred in the upper portion of the estuary. The observed increases in concentrations with increasing salinity can not be accounted for by desorption of Cd from river-borne suspended particulates. However, the discharge of Cd from industrial and municipal sources was sufficiently large to have produced the elevated concentrations at salinities >20 ^{0}/oo. In addition, upstream transport of this anthropogenic Cd by turbulent tidal diffusion processes might have contributed as much as 50% of the dissolved Cd in the 1 ^{0}/oo to 20 ^{0}/oo region of the estuary. Thus, we can conclude that the distribution of dissolved Cd in the northern Bay was dominated by anthropogenic sources.

PLANNED ACTIVITIES FOR 1978

As drought conditions and abnormally low Delta discharge rates persisted throughout the 1976-77 study period, additional northern Bay samples must be collected during a year that has a more typical range of Delta discharge rates (e.g., $Q = 200\text{-}6000\ m^3/sec$). Under these conditions we can examine the more general relationships between trace element concentrations in the estuary and the inputs of dissolved and suspended particulate trace elements from the Delta. For example, the difference in the Cu profiles (Fig. 1) for March 1976 ($Q = 425\ m^3/sec$) and March 1977 ($Q = 90\ m^3/sec$) suggests that the distribution of dissolved Cu is altered by variations in Delta outflow. Verification of the dependence of dissolved trace element profiles on Delta outflow requires collection and analysis of initial and sustained high flow samples. The apparent desorption of some trace elements from river-borne suspended particulates as a function of salinity can also be examined during high Delta outflow.

Using existing samples collected over the salinity range of the estuary and geochemical extraction techniques, we plan to determine the quantities of particulate trace element sinks (e.g., organics and amorphous Fe and Mn oxides and organics), as well as the quantities of Ag, Cd, Cu, Ni, Pb, and Zn associated with each of these sinks.

A modified version of the U. S. Geological Survey Chemical model, WATEQ II can be used to model dissolved trace element speciation in the estuary. Initially, the data from a few representative, well characterized, northern Bay samples should be examined. The performance of the model can then be evaluated, and additional thermodynamic data added if necessary. Ultimately, this modeling effort would enable us to predict which dissolved trace element complexes predominate in Bay and Delta waters and how variations in chemical parameters alter speciation.

FOOTNOTE

1. The inputs of Cu and Cd from industrial and municipal sources were obtained from discharge monitoring reports submitted to the Regional Water Quality Control Board, San Francisco Bay Region under the National Pollutant Discharge Elimination System.

WATER CONSERVATION WITH *IN-SITU* OIL SHALE DEVELOPMENT

J. P. Fox, W. G. Hall, E. A. Ossio, G. Amy,
P. Russell and J. F. Thomas

INTRODUCTION

The objective of this program is to identify the impacts of *in-situ* oil shale processing on the water resources of the Upper Colorado River Basin, and to determine control measures to mitigate these impacts. These broad goals were to be achieved by a combination of engineering planning and basic research. The engineering planning phase of the program was completed in 1977 and included evaluations of *in-situ* oil shale technologies, the water resources of the Upper Colorado River Basin, and the existing water quality standards in the oil shale region. The planning phase also provided a detailed characterization of process effluents and an identification of water quality impacts from various disposal options. The basic research phase of the program is continuing and includes programs in six areas. The six subprograms are as follows: (1) biological treatment of retort waters, (2) partitioning of trace elements during *in-situ* retorting, (3) continuous flow bioassay studies of process effluents, (4) organic leaching studies, (5) mathematical modeling of abandoned *in-situ* retorts and (6) characterization of process effluents. The program, which initially was jointly funded by the Departments of Interior and Energy, was initiated in July 1976 and is continuing under DOE sponsorship.

ACCOMPLISHMENTS DURING 1977

The engineering planning phase of this program was completed during 1977. This portion of the work is summarized below in a four paragraph narrative, which seeks to put into perspective the water-related impacts of *in-situ* oil shale processing. This is followed by a brief listing of accomplishments of the basic research phase of this program.

The effect of *in-situ* oil shale processing on the water resources of the Upper Colorado River Basin was evaluated in a series of engineering planning studies. In *in-situ* oil shale processing, the resource is left in place and approximately 20-30% is mined to create void volume. The fractured in-place material is ignited and oil extracted via combustion and/or pyrolysis. The potential impact of this type of processing on the water resources in the Upper Colorado River Basin is primarily related to two factors: water use characteristics of the technology, and groundwater hydrolygy in the vicinity of the oil shale deposits.

The water-use characteristics are dominated by the fact that *in-situ* processing of oil shale produces a minimum of one barrel of water for each barrel of oil. The water coproduced with shale oil is referred to as retort water, and originates primarily from the combustion of organics, from the release of free and bound water present in the oil shale matrix, and from ground water intrusion into the formation. When retorting occurs in the presence of oxygen, in a water-tight system, the retort water to oil volume ratio is about 1. This is equivalent to 2.1 MGD of retort water for a 50,000 barrel per day oil shale plant, and is comparable to the volume of wastewater produced by a town with a population of 14,000. The composition of retort water is characterized by a pH range from 8.5-9.6 and high levels of a number of inorganic and organic constituents.

Water management will be difficult for the oil shale industry due to the scarcity of water in the region, the uncertain regulatory climate, and the complicated nature of retort water. Retort water will be required to meet the water needs of an oil shale complex, and will be upgraded for on-site use. Potential uses, arranged in increasing order of requisite quality, include: spent shale compaction (poor quality water is suitable), dust control, mining, prerefining, agriculture, and cooling tower makeup (good quality water is required). Any excess water will be stored for future use, evaporated or discharged to surface or ground waters. Stringent water quality regulations, combined with the shortage of water in the region, will limit direct discharge to surface or ground waters, and thus promote reuse combined with evaporation of residuals.

Many of the rich oil shale deposits are located in the Piceance Creek Basin of Colorado. In this area, the deposits of interest are sandwiched between two groundwater aquifers. Pressure differences between the lower and upper aquifers will result in the movement of ground water from the lower aquifer through the abandoned in-situ retort chambers and into the upper aquifer. The waters passing through these retorts may leach out organic and inorganic compounds. Some of these constituents will be transported through the upper aquifer where they may ultimately be discharged into surface waters or withdrawn from wells.

Within the above broad areas identified in the water resources planning phase of the project, several areas of basic research were identified and pursued to answer some of the questions raised. Accomplishments from these basic research programs are as follows:

1. The effect of retort operating conditions on the chemical composition of retort waters was investigated using the Lawrence Livermore Laboratory (LLL) pilot-scale retorts. This work indicated that retort operating conditions can be varied to control the quality of retort waters produced. Generally, high temperature combustion runs produce the poorest quality effluents, while most gas runs produce a better quality effluent.

2. The partitioning of some 50 major and minor elements, including Hg, As, Se and Zn between the spent oil shale, shale oil, retort water and offgas was studied using several runs of pilot-scale retorts. This work indicated that most inorganic constituents remain with the spent oil shale, where they may be leached by groundwaters. The exceptions are Hg, As, F, Sb, and Se. These volatile elements are released during retorting and incorporated into the oil, retort waters, and offgas.

3. Continuous flow and batch laboratory studies were conducted to determine the quantity and type of organics leached from spent shale. This work indicated that the concentration and nature of leached organics is controlled primarily by retorting temperature and atmosphere.

4. Biological treatability studies of retort water were completed. These studies demonstrated that 60-70% of the organics present in retort water can be removed with the anaerobic fermentation process. Subsequent treatment by activated sludge can produce a high quality effluent. This, then, is one viable process for upgrading these waters for reuse, thus decreasing the demand for new water supplies from the Colorado River system.

5. A hydraulic model of the aquifer system connected by in-situ retorts was developed, and used to predict flow conditions through abandoned in-situ retorts. This work demonstrated that the residence time of water within an in-situ retort would be on the order of 10 years, and that it would take this water well in excess of 100 years to reach the nearest stream. Any ground water degradation (and attendant surface water disruption via base flow) would occur over a very long period of time. Therefore, an in-situ monitoring program will be required to assure the integrity of water resources in the area.

6. Several new analytical methods were developed. These include a method to continuously monitor Hg in oil shale offgases, and wet chemical techniques to measure several anions and cations of environmental interest.

7. An interlaboratory multi-instrumental study of elemental abundances in oil shale reference materials was completed. The work presented comparisons of several different x-ray fluorescence and neutron activations analysis methods, as well as a comparison of conventional atomic absorption spectroscopy with Zeeman atomic absorption spectroscopy. Agreement among the different techniques and laboratories for the 52 elements measured was typically within two standard deviations of reported errors.

PLANNED ACTIVITIES FOR 1978

The partitioning of 52 major and minor elements during simulated in-situ shale retorting will be investigated using LLL's 125-kg and 6000-kg retorts and Laramie Energy Research Center's (LERC) 20-kg controlled-state retort. Six different runs of the LLL retorts and 20 different runs of the LERC retort will be studied.

These runs will cover the range of retort operating conditions that are presently being evaluated by industry for commercial development. Inputs and products, including raw and spent oil shales, oil, process water and gases have been collected from each run, and will be analyzed for 52 elements using neutron activation analysis, x-ray fluorescence and Zeeman atomic absorption spectroscopy. New analytical methods will be developed during this work to continuously monitor in-situ the volatile elements Hg, As and Se. The partitioning of 15 trace elements including Hg, As, Se and Cd, between dissolved and particulate phases in process waters, will be investigated using scanning electron microscopy coupled with x-ray fluorescence. Elemental distributions in oils, waters, gases and spent shales will be analyzed as a function of retort operating conditions and extrapolated to field operating conditions. Trace element speciation in the waters and oils will be investigated using high pressure liquid chromatography coupled with Zeeman atomic absorption spectroscopy.Mechanisms responsible for the volatization of mercury from oil shale will be investigated, and gas solid phase reactions within the retort studied.

A STUDY OF BRINE TREATMENT

S. L. Phillips and A. K. Mathur

INTRODUCTION

Increasing utilization of geothermal energy resources has resulted in a need for better understanding of the associated corrosion and scale problems. Scale incrustation is a fairly common occurrence that arises mainly from the deposition of soluble or suspended constituents of geothermal brines in piping and other components of power plants. The interest in controlling scaling stems from two major concerns: (1) plugging of well casings and pipes transporting geothermal hot water, and (2) decrease in the efficiency of heat exchangers.

The other main problem related to geothermal hot water utilization covered here is corrosion of metal that is in contact with the fluid. The corrosion process is complicated and related to a number of parameters, including the following: material of construction, chloride concentration, pH, CO$_2$ partial pressure, H$_2$S partial pressure, and temperature of the brine. Current methods of dealing with corrosion center around either scheduled replacement of plant components or the selection and choice of suitable replacement of plant components or the selection and choice of suitable resistant materials. Table 1 lists the principal parameters affecting geothermal scaling and corrosion.

The purpose of this study was to critically evaluate information on brine treatment technology for use by the geothermal power industry. The

Table 1. Important parameters affecting scaling and corrosion in geothermal plants.

SCALE AND INCRUSTATION

Fluid phase (steam or water)
Brine composition
Temperature and temperature changes
Pressure changes, including partial pressure change in CO$_2$, H$_2$S, NH$_3$
Velocity and turbulence
Residence time in each part of plant
Surface effects and surface to volume ratio effects
Geometry of power plant components
Salt carryover in steam phase

MATERIALS CORROSION

Fluid phase (stream or water)
Brine composition
pH of fluid
Temperature and temperature changes
Moisture and soluble salts carryover in steam phase
Partial pressures of CO$_2$, H$_2$S, NH$_3$, H$_2$
Atmospheric O$_2$ leakage into plant system (e.g., piping, condenser, heat exchanger)
Power plant material
Stress levels in materials and especially cyclic stresses
Crevices
Presence of scale deposits
Passive or active state of metal protective films
Velocity of fluid
Suspended solids content
Ionic strength of water
Galvanic coupling of dissimilar metals

literature on treatment of geothermal brines to control scaling and corrosion is sparse, with information widely scattered and incomplete. For this reason, relevant data from other industries (e.g., boiler water, oilfield brines) was also collected and evaluated to provide additional information of use to geothermal brine treatment methodology.[1,2]

This study considers current, developing, and suggested means for the control of scaling and corrosion caused by geothermal waters. These problems arise with both the fresh fluid used for electric power production, and the spent fluid, destined for injection wells or holding ponds.

Table 2 lists methods of scale formation control, while scale removal methods are given in Table 3.

Our study of brine treatment centers around the three principal forms of deposits that are commonly found in geothermal scales: silica, carbonate, and sulfide. It is recognized that a geothermal scale is likely to be composed of a mixture of these main deposits as well as metals (e.g., Fe, Pb) so that brine treatment methods specific to calcite, silica, or sulfides may have to be modified for application to mixed scales. The corrosion section covers mainly deaeration and materials selection, which are the principal methods used or suggested to control the rate of corrosion of geothermal brines.

SUMMARY AND RECOMMENDATIONS

Present methods for controlling scale deposition and materials corrosion in the geothermal industry are mainly cleanup and replacement of pipes and other components on an as-required basis. Incrustations due to deposition of scales (e.g., silica, sulfide) from hot brines are usually removed from boreholes by acidizing or reaming; those in piping are mechanically removed by wire-brushing scrapers or hydroblasting. Materials rendered unserviceable by corrosion are replaced.

Table 2. Typical treatment methods to control scale formation.

Scale Type	Treatment Method	Comments
	Treatment methods for fresh geothermal fluids	
Silica	pH adjustment (acid injection)	Tested at Magmamax No. 1 well, Niland, California
Silica	Injection of base (NH_3 or NaOH)	Sinclair wells, California
Silica	Dilution of the unflashed geothermal fluid	Namafjall, Iceland
Mixed	Application of electrical potential	Sinclair Well No. 4, California
	Treatment methods for spent fluid disposal	
Silica & Arsenic	Sedimentation and coagulation (addition of slaked lime, hypochlorite, and flocculant)	Used at Wairakei and Broadlands, New Zeland
Silica	Plain sedimentation; retention tank	Used at Otake, Japan and Ahuachapan, El Salvador

Research and development activities centered around geothermal scale and corrosion control by treatment of brines have been increasing within the past 2 years. A brine treatment research program should include the following:

1. Characterization of brine chemistry and deposited scales in order to determine the causes and possible means of control. The scale and corrosion products reflect the variable brine composition for different geothermal areas. Brine treatment methods can then be devised for the particular method of disposal under consideration.
2. Basic laboratory data are needed on the mechanisms and rates of scale formation due to corrosion or scale deposition. Basic data are transferable to all geothermal sites and will be needed to select, for example, additives and materials that would control scaling and corrosion.
3. Development of instruments to monitor the important geothermal brine scale and corrosion parameters (e.g., silica, pH, H_2S). The instrument sensors should be sufficiently rugged to monitor geothermal fresh fluids in a reliable manner.
4. Correlation of laboratory test results with actual tests under field conditions. In this way, feedback of the predictions based on laboratory results can be quickly verified and incorporated into brine treatment programs.
5. Development of laboratory screening methods for commercially available scale and corrosion inhibitors for the purpose of evaluating their effectiveness under geothermal conditions. The inhibitors should be effective at the elevated temperatures and pressures encountered in geothermal systems and should not react with brine constituents either to form harmful products or to reduce the effectiveness of the additive.

REFERENCES

1. S. L. Phillips, A. K. Mathur and R. E. Doebler, A Study of Brine Treatment, Electric Power Research Institute, Palo Alto, CA, EPRI ER-476, Nov. 1977.

2. D. W. Shannon, Economic Impact of Corrosion and Scaling Problems in Geothermal Energy Systems, Battelle Pacific Northwest Laboratory Report, BNWL-1866-UC-4 (1975).

Table 3. Typical treatment methods for scale removal.

Scale Type	Treatment Method	Comments
CURRENT METHODS		
$CaCO_3$ (calcite) in borehole	Pump inhibited HCl into the well	Acidizing used at East Mesa Well 5-1 and Otake, Japan
Calcite in well casings	Wash with inhibited HCl	Used in Hungary and Kawerau, New Zealand
Silica in flow control equipment and heat exchangers	Wash with ammonium bifluoride	Acidizing, used at Hveragerdi, Iceland
Silica in borehole	Pump NaOH solution into the well	Used at Matsukawa, Japan
Calcite in borehole	Reaming or redrilling	Used in New Zealand, Hungary, and Mexico
Mixed scales in turbine components	Spaced injection of heavy diesel oils	Used at Larderello, Italy
Mixed scales in injection and brine drain lines	Hydroblasting followed by water flush	Used at Niland Geothermal Test Facility, California
DEVELOPING METHODS		
Mixed scales in heat exchanger tubing and piping	Cavitation descaling	Laboratory experiments
Calcite scale (test probe)	Application of thermal shock	Laboratory experiments

POPULATIONS AT RISK TO AIR POLLUTION

C. D. Hollowell, S. T. Sacks, S. Selvin, W. Winkelstein, Jr.,
D. M. Austin[*] and D. W. Merrill, Jr.[*]

INTRODUCTION

A project to assess the populations at risk to various air pollutants was initiated in July 1976, under funding from the U. S. Environmental Protection Agency (EPA). This research project is divided into three main tasks to be completed by October 1978.

Task One involves the creation of a set of integrated primary data bases containing data on socioeconomic and demographic characteristics, air pollution levels for several important pollutants, and the development of mortality statistics for the United States on a county basis. Task Two involves the determination of the populations at risk to various air pollutants; and Task Three involves the analysis of associations between air pollutant levels and various indices.

The set of data bases to be created in Task One will be interfaced to efficient and sophisticated computer information storage, retrieval, and display systems (including computergenerated color maps, charts, and graphs).

The three categories of data bases to be created are as follows.

Socioeconomic and demographic data base

The extensive Socioeconomic Environmental Demographic Information System (SEEDIS)[1] has been developed at Lawrence Berkeley Laboratory (LBL) and is available for use. The components of SEEDIS required for this project include portions of the 1970 Census of Population (by county and census tract), estimates of U. S. population by county for 1975, and geographical coordinates of centroids and boundaries of states, counties, census tracts and Standard Metropolitan Statistical Areas (SMSA's).

Air Quality and emission data bases

Selected portions of the SAROAD (air quality) data base of EPA for 1975 will be obtained in machine-readable form for total suspended particulates (TSP), sulfur dioxide (SO_2), sulfates ($SO_4^=$), nitrogen dioxide (NO_2), photochemical oxidants (O_x), ozone (O_3), carbon monoxide (CO), hydrocarbons (HC), and nonmethane hydrocarbons (NMHC). Mathematical approximations may be required to fill gaps in the air quality data. It is expected that only straightforward techniques consistent with established EPA procedures will be applied, without recourse to auxiliary data sources.

The machine-readable EPA SAROAD Site Director, which contains geographical coordinates of air quality monitoring stations, will be used to correlate air quality measurements with socioeconomic and demographic characteristics of the population, and with mortality data.

Health statistics data base

Complete U. S. mortality data for the period 1968-1972 will be acquired from the National Center for Health Statistics. These data will be summarized by county for correlation with the air quality.

The geographical subunits to be used in the initial populations at risk assessments of Task Two will be counties of the entire United States. Whenever there are multiple sampling sites in the vicinity of a given county, optimum data utilization will require knowledge of the geographical coordinates of individual monitoring sites, and approximate population centroids of sub-county census units (census tracts). Data and computer programs developed at LBL will be used for the necessary geographical correlations. Air quality estimates will be calculated at the positions of population centroids, taking into account the measurements from nearby monitoring stations and the relative distances to those stations. An important part of the calculation is the estimation of statistical errors, which will be necessarily large for major portions of the U. S. population.

When all of the geographical subunits have been identified and estimates of air-pollutant concentration have been assigned to each subunit, it will be possible to estimate the populations exposed to various air pollutants. A weighting procedure will be used to effectively discard those population subunits for which precise air quality estimates cannot be determined. The air-pollutant concentration will be broken down by a variety of census-determined characteristics, including such parameters as age, sex, indices of economic status, occupational history, and ethnicity. Having identified the population subunits and air pollution characteristics, we will then identify various high-risk groups by geographical area for the entire country.

Task Three will entail the analysis of the disease effects of air pollution. The analysis of the data will be conducted in two stages.

The first stage will consist of essentially descriptive statistics such as tables, graphic representation and typical summary statistics, e.g., means, medians, ranges and contingency coefficients. No attempt to evaluate statistical significance will be done in this phase.

An often overlooked technique of analysis is simple pictorial representation of the relationships between variables. This type of graphic approach is easily implemented in conjunction with the LBL computer system, since one of the most advanced graphics hardware and software systems is available at the Laboratory. An attempt will be made to adjust the death rates simultaneously for differences in both age and socioeconomic status (SES). These rates, once adjusted for age and SES, will provide a comparison of the relationship between air pollution and cancer rates across areas of the U. S. These comparisons will be in terms of simple descriptive statistics and graphical representations.

In the second phase of the analysis, inferential statistics will be developed along two lines. A regression will be used for testing for trends in death rates with increasing population within each socioeconomic status level. That is, a weighted least squares regression line (dependent variable = cancer rate; independent variable = level of pollution) for groups of counties with homogeneous socioeconomic status levels will be used to analyze possible relationships between air pollution and cancer incidence rates. This methodology is a widely used approach in dealing with multivariate data.

The second analytic approach will employ disease multivariate statistical methodology of the type developed for the National Halothane Study.[2] This approach is based on fitting log linear or logistic models to the data under a variety of hypotheses. A chi-square criterion is used as a measure of goodness of fit to assess the competing hypotheses. Among the various hypotheses to be tested, the differences among communities will be specifically investigated. The analysis will identify any inter-community differencees in cancer rates that remain once the influences of SES and air pollution are taken into account. The proposed use of log linear and logistic models makes this aspect of the analysis particularly straightforward since these models are designed to partition and adjust for the separate influences of air pollution on dependent variables such as cancer incidence rates. Such an approach enables the identification of the direct effects of socioeconomic status, habitat, and most importantly, air pollution. The interaction effects of these independent variables can also be evaluated by means of these multivariate models. This type of methodology is analagous to the analysis of variance situations in which the dependent variable under consideration is continuous. Computer implementation of log-linear statistical techniques is accomplished with the program described in Ref. 3. The methodology of discrete multivariate analysis is comprehensively described in Ref. 4. In general, these methods provide the flexibility to investigate complex and possible nonlinear relationships.

ACCOMPLISHMENTS DURING 1977

The initial effort has focused on Tasks One and Two, the creation of an integrated set of data bases.

The data base is self-documenting; that is, it contains considerable descriptive information, and the necessary instructions to enable the user to retrieve desired data without the aid of supplementary printed material.

Complete instructions are included for either listing or interactively accessing, from a remote terminal, the current version of the data base, which is being continuously updated. All potential users of the data have been encouraged to experiment with it at an early date, and to make suggestions.

The present version of the data base contains data on the locations of California air quality monitoring stations measuring eight pollutants (total suspended particulates, carbon monoxide, nitrogen dioxide, sulfur dioxide, sulfates, ozone, total oxidants, and hydrocarbons). The data were obtained from the EPA Energy Data System (EDS), the SAROAD (Storage and Retrieval of Aerometric Data) Monitoring Station Site Directory, and SAROAD yearly summaries.

The decision to install the data base in BDMS, the Berkeley Data Management System, has important implications. Although the computer costs involved in building the full nationwide data base will be high, it is believed that these costs will be more than offset by the savings in human effort, and by the reduced costs of randomly retrieving data at a later date.

The present version of the data base contains several kinds of records or "relations," which are analogous to repeating groups in SYSTEM 2000 terminology. The data stored in any single record (relation) may be randomly accessed, for efficient comparison with the data in any other record (relation).

For example, in order to estimate 1975 nitrogen dioxide concentrations for all counties in California, the following steps will be executed:

1. Scan a California state record for a list of counties (census county codes) in California.
2. Access in turn each county record, extracting from each the latitude and longitude of its population centroid.
3. Access in turn each monitoring station record whose latitude and longitude place it within a specified distance (say 100km) of the county population centroid.
4. For each monitoring station within the 100 km radius, access the record (if present) containing 1975 nitrogen dioxide measurements for that station. Assign to that station a weight depending upon the number of measurements, the percentage of possible measurements taken, the measurement method, the distance of the station from the county population centroid, and (perhaps) other factors to be decided later. The exact form of the weighting function will be described in conjunction with EPA after experimenting with several possibilities. A suggested form is the following:

   $$w(i,j) = v(j)e^{-(d(i,j)\cdot d_0)^2} ,$$

   where w(i,j) is the weight of station j to be used in calculating a composite geometric means for county i; v(j) is the intrinsic weight assigned to station j, which depends upon the number of measurements, the percentage of possible measurements taken, the measurement method, and (perhaps) other factors; d(i,j) is the difference between statio j and the population centroid of county i; d_0 is a distance scaling factor, probably of the order of 5-20 km. Various values will be tried. Too small a value (too conservative) will result in large "gaps" between stations, where concentrations cannot be estimated; too large a value will result in the combination of measurements from neighboring stations that are seen to be statistically inconsistent.
5. Estimate a composite geometric mean concentration at the position of the county population centroid, and a composite geometric standard deviation, as weighted averages of the values observed at all stations within a specified distance; estimate also the statistical uncertainty of the composite geometric mean and of the composite standard deviation. Large statistical errors, which result from sparse or unreliable measurements in the vicinity of this county population centroid, will cause a small (or zero) weight to be assigned to this county in further analysis.

The LBL method disregards the county assignments of the monitoring stations, considering only their geographic coordinates (latitude and longitude). Thus the problem of resolving conflicting county definitions (because EPA county boundaries do not correspond to census county boundaries) is completely avoided.

In the LBL approach, passing to the subcounty (e.g., census tract) level would be a trivial modification, apart from the expense of increasing the size of the data base. To take into account the geographical population distribution within a county, one would use 1970 Census data at the census tract level rather than the county level, and substitute tract centroids for county centroids in the above calculation. Complete census data at the tract level, as well as tract centroids (and boundaries) for the 35,000 census tracts within standard metropolitan survey areas, are presently available at LBL. Such an analysis would be most fruitful in small area studies such as the Third National Cancer Survey.

During March 1977, LBL completed the implementation of software to read and write tapes in the ERDA/ANSI (Energy Research and Development Administration/American National Standards Institute) standard data exchange format. This capability will facilitate the transfer of the data base, at a later stage of completion, to EPA and to other installations wishing to make use of the data. Implementation of the data base in other data base management systems, for example SYSTEM 2000, will be straightforward, though not necessarily inexpensive.

The loading of the prototype California data base is essentially completed. The writing of certain software interfaces to the necessary statistical analysis programs and to LBL's map generation program CARTE (Task Three) is underway. Some of the items in the prototype California data base include:

(1) County geographic boundary points.

(2) Improved geographic centroids calculated from (1) above.

(3) Population centroids of counties.

(4) Several socioeconomic and demographic variables.

(5) 1968-1972 mortality rates for 53 causes of death.

(6) Yearly county averages for 1975 for all pollutants being considered for the data base.

The data presently in the prototype data base are being used to generate maps showing the density (number per square kilometer) and point locations of air quality monitoring stations, as well as county mortality rates for California. Sample maps are shown in Figs. 1 and 2.

PLANNED ACTIVITIES FOR 1978

The experience gained with the prototype data base will permit firm decisions to be made regarding the scope and design of the final data base. At this point, demographic, mortality, and air quality data for the entire U. S. will be loaded into System 2000 in the EPA computer, with the user software already developed during the first year of the project.

Documentation and a streamlined user interface for the data base will be prepared, permitting maps to be easily generated by users at remote terminals. A substantial number of black-and-white and color maps will be produced to aid in the analysis of Tasks Two and Three. These maps, which will provide the necessary basic guidance in planning detailed studies of the project, include:

a. Maps of 1975 SAROAD air quality data, for examining the completeness of data and the measurement methods. For example, it would be useful to prepare maps of SO_2 obtained with the EPA reference method (pararosaniline 24-hour manual method) and equivalent instrumental methods (flame photometric detection (FPD), ultraviolet fluorescence, coulometric) in order to estimate the recently recognized temperature dependence of the EPA reference method.[5] Black-and-white maps will be used extensively in making decisions regarding the adequacy of air quality estimates.

b. Maps of mortality data for 1968-1972 by county, as an initial examination of the patterns of disease-specific mortality.

c. Maps by county of 1970 census variables, including age, sex, race, education, income, housing characteristics, and occupation.

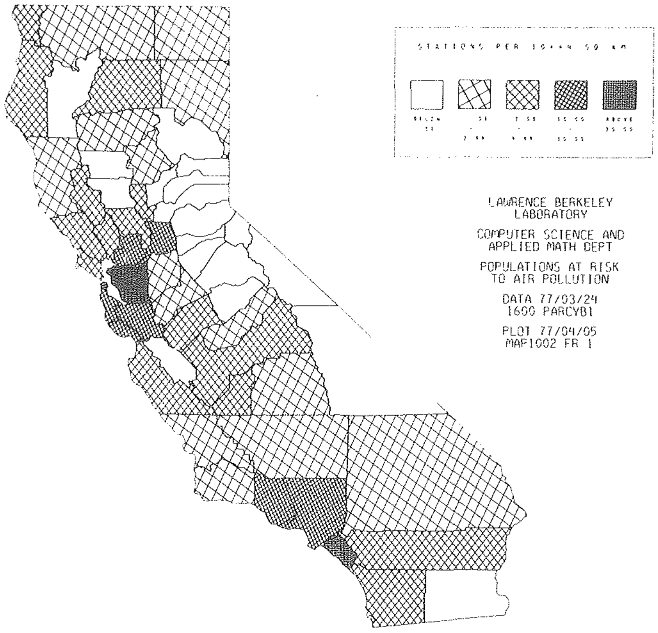

Fig. 1. Air quality monitoring stations per 10^4 square kilometers in any year, 1971-75, California. (XBL 774-8327)

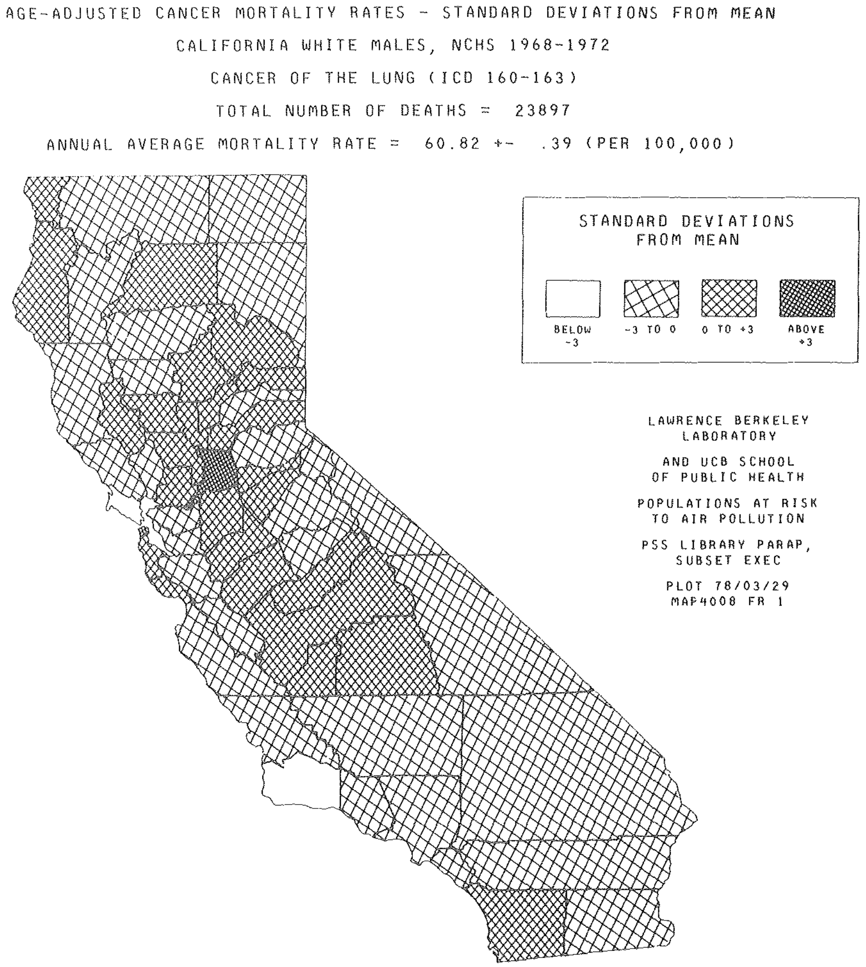

Fig. 2. Mortality rate for lung cancer in white males by county for California. (XBL 784-7986)

Upon request, the data base will be made available in tape form, a format that can easily be loaded into EPA's SYSTEM 2000 or other data base management systems. EPA may wish to continue to use the LBL version directly, thereby profiting from later updates, and also gaining access to LBL's graphics system and complete 1970 census data, neither of which can be economically transported to another computer.

Completion of Task Two, the estimation of populations at risk, is a relatively straightforward calculation, once the estimates of pollutant concentrations (and the associated statistical errors) have been assigned to each county. The values of composite county pollutant concentrations depend upon subjective decisions that are likely to change. For this reason, the calculation of populations at risk (Task Two) will be implemented as a computer subroutine that will be invoked as required by the statistical analysis programs of Task Three. The later inclusion of subcounty geographic detail (e.g., census tract data), if desired, will be a trivial modification, apart from the expense of increasing the size of the data base.

Certain statistical analyses (Task Three) as discussed in the Introduction are planned, but may be revised depending upon the content of the final data bases. Examples of possible analyses include:

1. Examination of mortality data for every city with a population of 250,000 or greater, and relation of these data to the pollutant concentration data available for these urban areas.

2. Calculation of correlations between specific causes of death and various pollutants. High correlations will initiate further investigation of subsets of these data.

3. Comparison of mortality rates in rural areas. Important variables such as age, race, sex, and socioeconomic status, as well as estimated pollutant levels, will be taken into account.

FOOTNOTE AND REFERENCES

*Computer Science and Applied Mathematics Department.

1. D. M. Austin, S. G. Kranz, and C. Quong, An Overview of the LBL Socioeconomic Environmental-Demographic Information System (SEEDIS), Lawrence Berkeley Laboratory Report, LBL-3699 (1975).

2. Y. M. Bishop and F. Mosteller, "Smoothed Contingency Table Analysis," in J. P. Bunker, et al. (eds), Report of Subcommittee on the National Halothane Study of the Committee on Anesthesia, Division of Medical Sciences, National Academy of Sciences, National Research Council, NIH, National Institute of General Medical Sciences, Bethesda, MD, GPO, Washington,DC, 1969, Chapter IV-3, pp. 237-286.

3. L. Goodman and R. Fay, Log-Linear Contingency Tables Analyses, Version 2, ECTA, University of Chicago, 1974.

4. Y. M. Bishop, S. E. Feinberg and P. W. Holland, Discrete Multivariate Analysis, MIT, Cambridge (1975).

5. G. Fuerst, P. Scaringelli, and John H. Margeson, Effect of Temperature on Stability of Sulfur Dioxide Samples Collected by the Federal Reference Method, Report EPA-600/4-76-024, U. S. Environmental Protection Agency, Research Triangle Park, NC 27711 (1976).

INDOOR AIR POLLUTION IN RESIDENTIAL BUILDINGS

C. D. Hollowell and G. W. Traynor

INTRODUCTION

Air pollution research has focused almost exclusively on pollution in the outdoor environment and has virtually neglected the indoor environment, even though the major portion of the population spends far more time indoors than outdoors. The importance of indoor air pollution has only recently been recognized. Table 1 lists the sources and types of indoor air pollutants which have been identified in residential buildings. The significance of indoor air pollution is expected to have a large impact (1) on the overall assessment of the effect of air pollution on human health, (2) on the design of epidemiological studies that must consider indoor as well as outdoor air pollution, (3) on energy conservation strategies for buildings that might restrict indoor-outdoor air exchange, and (4) on the need for more stringent control of air pollution from indoor combustion sources.

Table 1. Indoor air pollution in residential buildings.

SOURCES	POLLUTANT TYPES
OUTDOOR	
Ambient Air	SO_2, NO, NO_2, O_3, Hydrocarbons, CO, Particulates
Motor Vehicles	CO, Pb
INDOOR	
Building Construction Materials	
Concrete, stone	Radon
Wallboard	Formaldehyde
Paint	Mercury
Insulation	Formaldehyde, Sulfates
Building Contents	
Heating and cooking combustion appliances	CO, SO_2, NO, NO_2, Particulates
Furnishings	Organics, Odors
Natural gas; water service	Radon
Human Occupants	
Metabolic activity	CO_2, NH_3, Odors
Human Activities	
Cigarette Smoke	CO, NO_2, HCN, Organics, Odors
Aerosol spray devices	Fluorocarbons, Vinyl Chloride
Cleaning and cooking products	Hydrocrbons, Odors, NH_3
Hobbies and crafts	Organics

The Lawrence Berkeley Laboratory (LBL) indoor air pollution research project, initiated in 1975, is designed to study the chemical and physical behavior of indoor combustion-generated air pollution in residential and commercial buildings. The broad goals of this project are (1) to characterize indoor air pollution; (2) to identify the important sources, abundance, and fate of indoor air pollutants; (3) to study the abatement of indoor air pollutants; (4) to characterize exposures of the occupants to the important air pollutants; (5) to study the health and welfare effects; and (6) to assess the impact of various energy-conservation strategies on indoor air quality.

The Energy Conservation Standards for New Buildings Act of 1976[1] calls for promulgation of performance standards for all new residential and commercial buildings by 1980. It is expected that the results of this LBL project will provide valuable insight into the impact on indoor air quality of various energy conservation measures for buildings. It is essential that this impact be considered in the development of energy conservation performance standards for new and existing buildings required by this Act.

The work reported here represents the current status of ongoing field and laboratory studies of this project. The initial goal of these studies has been to examine in detail the sources, rates of emissions, dispersion, transformations, and fates of gaseous and aerosol air pollutants in residential buildings. Laboratory and field measurements are conducted with the LBL Mobile Atmospheric Research Laboratory (MARL),[2] which is capable of remote, multipoint sampling for such pollutants as SO, NO, NO_2, CO, O_3, and for aerosol size and chemistry. Measurements on laboratory- and field-collected aerosol samples are performed by x-ray fluorescence (XRF), photoelectron spectroscopy (also known as electron spectroscopy for chemical analysis--ESCA), infrared spectroscopy (IR), and combustion and wet chemistry techniques to characterize particulate species such as total sulfur, total nitrogen, $SO_4^{=}$, NO_3^{-}, NH_4^{+}, Pb, Fe, Zn, and total carbon. Aerosol size measurements for the range 0.01-1.0 μm are performed by condensation nuclei formation and electrical mobility techniques.

The principal objective of the field study has been to obtain qualitative data on the relationship of indoor to outdoor air pollutant concentrations as a function of gas cooking and heating appliance use. Six occupied single-family residential buildings were studied in 1975 for gaseous and particulate air pollutant levels under typical occupancy conditions of cooking and heating.[3] This field study clearly demonstrated that gas stove use under poor ventilation conditions can result in elevated levels of CO, NO, NO_2, and even SO_2 and particulate sulfur. High levels of NO and NO_2 were observed in the one house where the effect of a forced-air gas-fired central heating system was studied.

The duration of the elevated levels of CO, NO, and NO_2 from gas combustion appliances may be under 1 hour for gas stove use but may be continuous for gas-fired heating system use during cool seasons. Levels of CO and NO_2 in the field study were found to approach or exceed existing U.S.A. ambient air quality standards. Nitrogen dioxide levels in kitchens of houses with gas stoves were observed to be as high as 1000 μg/m^3 with one top burner operating for less than 30 minutes and as high as 1700 μg/m^3 with the oven operating for 20 minutes. Concentrations of NO_2 were observed to be as high as 1200 μg/m^3 for 8 hours in the bedroom of a house with a forced-air gas-fired heating system operating under normal conditions. These NO_2 concentrations can be compared with the short-term recommended U.S. and promulgated foreign NO_2 air quality standards (~400 μg/m^3 for 1 hour).[4]

ACCOMPLISHMENTS DURING 1977

Laboratory studies now in progress in experimental rooms and buildings are designed to identify various parameters which affect rates of emissions from gas-fired cooking and heating appliances and short- and long-term air pollution levels from such appliances in the indoor environment. The parameters include appliance type and its operating characteristics (for example, fuel/air mixture, flame temperature and geometry), and reduced ventilation and air infiltration rates expected to be imposed as energy conservation measures. Work in progress concerns the dispersion, transformations, and ultimate fate of combustion-generated indoor pollutants. The physical and chemical transformations depend on the many constituents (gaseous and particulate) present in the air, on the effects of temperature and humidity, and on the effects of walls and other materials. This phase of the study involves detailed analysis and experiments with various ventilation and air circulation systems.

Studies using an experimental room with an air volume of 27 m^3 have characterized the emissions from a new gas stove operating in the room with air exchange rates from 1/4 to 10 air changes per hour. Well-constructed new single-family houses have air exchange (ventilation and infiltration) rates on the order of 0.5-1.0 air changes per hour (ACPH). Older houses and most other new houses have air exchange rates of 0.8-1.5 ACPH or higher. Energy conservation measures which would limit the air exchange rate in new houses to 0.2 to 0.5 ACPH are now being considered by state governments and the federal government.

The laboratory studies have shown that gas stoves generate extremely high concentrations of such species as CO, NO, NO_2, respirable aerosols (size <1.0 μm), and particulate sulfur when the air exchange rate is controlled to less than 1 ACPH. The results of several experiments are shown in Figs. 1 and 2. These figures illustrate the levels of CO and NO_2 observed in an experimental chamber under various ventilation rates from 0.24 to 7.0 ACPH. The results are compared with air quality standards. Various NO_2 standards are given in Table 2.

While these laboratory studies do not necessarily duplicate "real world" situations, they clearly demonstrate the types and levels of air pollutants one could expect under low air exchange rates for buildings; such rates may be required in order to meet recent energy conservation performance standards for buildings. Such "real world" findings have already been

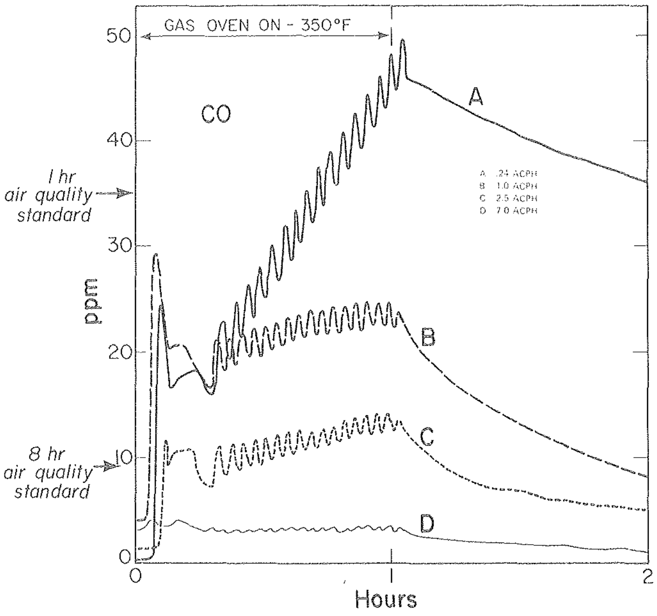

Fig. 1 Carbon Monoxide concentrations in a 27m^3 experimental room at various air exchange rates. Gas oven operated for 1-hour at 350°F. (XBL 772-304A)

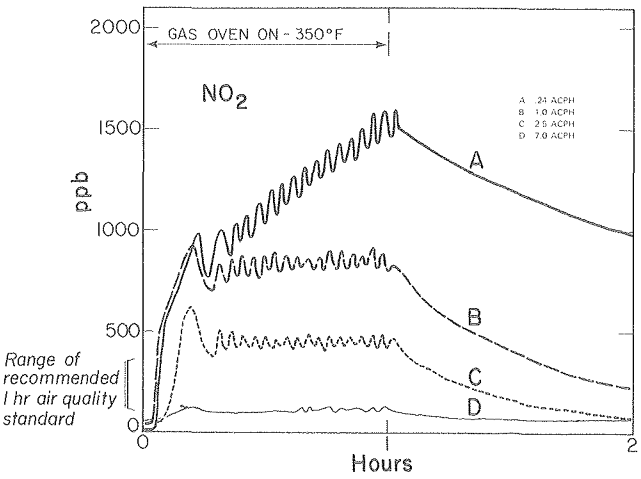

Fig. 2 Nitrogen dioxide concentrations in a $27 m^3$ experimental room at various air exchange rates. Gas oven operated for 1-hour at 350^oF. (XBL 772-306A)

Table 2. Recommended and promulgated short-term NO_2 air quality standards.

Country	Short-term NO_2 Air Quality Standard (0.1 ppm 190 g/m^3)	Status
Canada (Ontario)	0.2 ppm/1 hr 0.1 ppm/24h hr	promulgated promulgated
Japan	0.02 ppm/24 hr	promulgated
U.S.A.	0.1-0.35 ppm/1 hr	recommended
West Germany	0.15 ppm/short-term exposure	promulgated
WHO/UNEP	0.10-0.17 ppm/1 hr	recommended

demonstrated in field experiments with six "leaky" houses where air exchange rates were on the order of a few air changes per hour.

PLANNED ACTIVITIES FOR 1978

Laboratory investigations now in progress include detailed studies of particulate sulfur, nitrogen, and carbon compounds in the indoor environment. Also of particular interest are the high NO_2/NO ratios (~1:1) observed in the laboratory and field studies. In addition to NO and NO_2, considerable attention is being given to such gaseous species as HCN and NH_3 and particulate species as NO_3^-, NH_4^+, and organic nitrogen compounds.

In most systems, NO_2 accounts for less than 5% of the NO_x emissions, but higher values can be encountered when flames are rapidly quenched. One probable explanation is that NO_2 is formed in high concentrations by reactions of NO with HO_2 and/or OH, and that the NO_2 may be reduced subsequently by reactions with oxygen atoms. Evidence for this is provided by Merryman and Levy[5] and by numerical simulations by Kendall et al.[6] Possible intermediate species in such a process include HCN, NH_3, amines, and various nitrates. The concentrations of some of these compounds in the post-combustion gas may be significant, and we plan in 1978 to quantitatively characterize HCN, NH_3, and other gaseous nitrogen compounds in the indoor environment.

We have also observed elevated indoor particulate nitrogen levels from gas stoves and heating systems in recent experiments. The analyses have been performed by proton activation analysis (for total N) and ESCA (for NH_4^+, NO_3^-, and organic amines). A recent paper by Benarie[7] reports higher levels of NH_4^+ and NO_3^- inside buildings than outside; these results are similar to our findings. Although the results of our study are not definitive, they clearly indicate the need for systematic studies to assess the significance of particulate nitrogen compounds in the indoor environment. These studies will be continued in 1978.

We plan to quantitatively characterize HCN and NH_3 with laser optoacoustic spectroscopy techniques developed at LBL, as well as with conventional colorimetric and ion specific electrode techniques. Quantitative characterization of particulate species will be performed by dichotomous air sampling while analysis will be achieved by proton activation, ESCA, x-ray fluorescence, and possibly gas chromatography mass spectrometry. Systematic laboratory and field studies will focus on specific particulate nitrogen compounds (NH_4^+, NO_3^-, amines, etc.).

Laboratory studies will permit detailed quantitative characterization of various indoor combustion-generated nitrogen compounds in order to ascertain the important species to monitor routinely in our field studies. The work on the nitrogen compounds will focus on aspects of indoor air pollution research which have not been previously investigated.

Combustion-generated indoor air pollution will be studied in several occupied residential buildings in 1978. The buildings will be selected on the basis of residential building type, indoor combustion sources, occupancy patterns, and air circulation, ventilation, and infiltration factors.

Other indoor environments in which people spend considerable time are commercial buildings, such as office buildings and schools, and other public or semipublic buildings. Modern commercial buildings are usually engineered so that the circulation and infiltration of air are controlled. Public health considerations often require certain minimum air ventilation rates, usually to control odors and to decrease the possibility of transmission of infectious agents. However, significant attention is seldom given to the public health role of air pollution generated by indoor sources. Indoor air pollution in such public buildings will be studied in subsequent phases of this project.

REFERENCES

1. Energy Conservation Standards for New Buildings Act of 1976, U. S. Public Law 94-385, 90 Stat. 1125, 42 USC (August 14, 1976).
2. C. D. Hollowell and T. Novakov, "Mobile Atmospheric Research Laboratory," in Novakov, T., et al., Atmospheric Aerosol Research Annual Report, 1976-77, Lawrence Berkeley Laboratory Report LBL-5214
3. C. D. Hollowell, R. J. Budnitz, G. D. Case, G. W. Traynor, Generation of Gaseous and Particulate Air Pollutants from Indoor Combustion Sources: I. Field Measurements 8/75-10/75, Lawrence Berkeley Laboratory Report LBL-4416.
4. C. D. Hollowell, R. J. Budnitz, and G. W. Traynor, Combustion-Generated Indoor Air Pollution, Lawrence Berkeley Laboratory Report LBL-5918.
5. E. L. Merryman and A. Levy, Nitrogen Oxide Formation in Flames: The Roles of NO_2 and Fuel Nitrogen. Paper presented at the Fifteenth Symposium (International) on Combustion, Tokyo (August, 1974).
6. R. M. Kendall, J. T. Kelly, and W. S. Lanier, Prediction of Premixed Laminar Flat Flame Kinetics Including the Effects of Diffusion. Paper presented at the Stationary Source Combustion Symposium, Atlanta, Georgia (September, 1975).
7. M. Benarie, B. T. Chuong, and A. Nonat, Pollution Particulaire a l'Intrieur et a l'Exterieur d'un Local, Sci. Total Environ. 7, 283 (1977).

ATMOSPHERIC AEROSOL RESEARCH GROUP

T. Novakov,* S.-G. Chang,† C. D. Hollowell,† H. Rosen,† W. H. Benner, H. A. Brendel, R. Brodzinsky, M. Clemenson, R. L. Dod, R. D. Giauque, L. Gundel, A. D. Hansen, S. S. Markowitz, G. E. Mason, P. J. Pagni, R. C. Schmidt, G. W. Traynor, R. Toosi and L. Wroth

INTRODUCTION

During the early days of environmental awareness, primary particulate emissions were easily visible; smoke or soot was the first air pollutant to be recognized and controlled. In fact, the word "smog" was coined from the words "smoke" and "fog." In more recent times, improvements in combustion technology and the use of better-grade fuels have led to the virtual elimination of visible smoke emissions. The emphasis of air pollution control slowly shifted away from primary particulate emissions toward controlling gaseous emissions. This trend culminated in southern California with the concept of Los Angeles-type photochemical smog, which is believed to contain neither smoke nor fog. According to a widely held view, the haze over the Los Angeles air basin on polluted days is due almost entirely to the photochemical conversion of certain invisible gases to light-scattering particles. In recent years there has also been a trend to consider aerosol pollution elsewhere in the United States, and in the world, as an essentially photochemical phenomenon. Control strategies based on the above view naturally stress the control of gaseous emissions, especially those responsible for the formation of ozone. Ozone, the principal product of photochemical processes, is considered essential for the formation of photochemical haze. Thus the control of pollution aerosol particles remains linked largely with present control strategy for oxidant and precursor gases.

Over the past 5 years, the principal research objective of LBL's Atmospheric Aerosol Research Group has been to assess the contribution of primary particulates to the ambient particulate burden, and to evaluate the role of these primary particles in the formation of secondary aerosol species. We chose this research objective because there is considerable evidence that primary carbonaceous or soot particles remain major contributors to atmospheric pollution.

The difference between our concepts of soot and visible smoke is largely confined to the size of the particles. Smoke consists of large particles that are responsible for the opacity of plumes. Soot is any carbonaceous particulate material emitted from sources, even if these do not produce visible plumes or smoke. In most cases, soot particles are very small when emitted, having diameters of the order of 100 Å, and are therefore invisible to the naked eye.

Soot can also be described as a chemically complex carbonaceous material that consists of a "graphitic" component and an organic component. There are significant differences in the overall properties of the two components. For example, the graphitic component is nonvolatile, insoluble in organic solvents, and is a strongly light-absorbing material. In contrast, the organic component of soot is volatile, soluble in solvents, and does not appreciably absorb light. We have previously found that as much as 80% of the ambient particulate carbon collected in different parts of California is in the form of soot.[1,2]

Another view, which we have advocated over the years, is that soot particles are not only a major constituent of ambient particles, but also are a catalytically and surface-chemically active material, largely responsible for the formation of sulfates resulting from fossil fuel combustion.[1] For example, we have expressed the view that the catalytic formation of sulfate on soot particles is expected to occur in the open atmosphere, and especially in or near combustion sources, where both SO_2 and soot concentrations are highest.[1] We have also stated that the soot-catalyzed SO_2 oxidation plays a major role in atmospheres characterized by high concentrations of particulate carbon.

This annual report describes the results obtained during 1976-1977. The individual papers contained in the report attempt to provide answers to the following questions:

1. What fraction of the ambient particulate carbon is of primary origin?
2. What is the role of primary particulate carbon in the atmospheric oxidation of sulfur dioxide to sulfate?
3. What is the role of primary particulate carbon in the formation of suspended nitrogenous species?

The first section deals with the chemical and physical characterization of ambient and source particulates. The research reported in this section should provide at least a partial answer to the question of what fraction of the ambient particulate carbon is of primary origin. Two novel approaches have been used for this purpose: the first involves application of the optical absorption technique; the second uses laser Raman spectroscopy. The results show that the absorbing species in ambient and source particulate samples are "graphitic" soot and that a major fraction of the carbonaceous component of ambient aerosol particles in the San Francisco Bay Area and in the Los Angeles Air Basin are of primary origin.

The second section reviews our recent work on the role of primary particulate carbon in atmospheric reactions. We have extended our work on the role of soot particles as catalysts for SO_2 oxidation by studying the effect of liquid water on the soot-catalyzed reaction. The effects of liquid water are important because in plumes liquid water may condense on the soot particles. Furthermore, soot particles may encounter liquid water in their passage through fogs and clouds. This "wet" mechanism is much more efficient for SO_2 oxidation than the corresponding "dry" mechanism that we have suggested previously.[1] A model calculation of the new formation of H_2SO_4 in a plume and in ambient air is presented for the "wet" and "dry" mechanisms. The results show that the "wet" mechanism yields a conversion rate that is in agreement with experimental observations.

The third section describes some of our field results. The principal aim of our field program is the study of winter air pollution in the San Francisco Bay Area. These winter episodes are characterized by both low oxidant concentrations and high particulate concentrations. The particulates are produced either by sources or by atmospheric reactions, but presumably not by ozone-related reactions. These results demonstrate that even in the virtual absence of ozone, there is still a severe air pollution problem whose abatement will require measures different from those designed for oxidant control.

CHARACTERIZATION OF AMBIENT AND SOURCE PARTICULATE SAMPLES

1. Characterization of the Carbonaceous Component of Ambient and Source Particulate Samples by an Optical Absorption Technique and Raman Spectroscopy

One major uncertainty in air pollution research is the extent to which the carbonaceous aerosol particle burden is caused by secondary reactions, or by primary emissions. Such a determination is clearly necessary for designing an effective control strategy. However, due to the complex nature of the samples, it has been a difficult analytical problem to develop methods for discriminating between these two sources of carbon. One distinct feature of primary emissions is that they appear to have a large "graphitic" soot component. This component offers an attractive tracer for primary emissions, since it has some unique physical properties. These include a high oxidation threshold, and a large and uniform absorptivity throughout the visible spectral region, which we suggest leads to the blackish or grayish appearance of ambient and source particulate samples. It should be emphasized that "graphitic" soot represents only one component of the primary carbonaceous aerosol particles, which in general also contain a large nonabsorbing and volatile organic fraction.

Here we report on measurements of the absorbing properties of ambient samples collected in winter at Berkeley, California, and in summer at Anaheim, California. These results are compared with measurements made on various source particulate samples. A strong correlation between the carbon content and the absorptivity of the collected particulates is observed. This correlation, in combination with measurements of the wavelength dependence and temperature dependence of the absorptivity, suggests that the absorbing species is "graphitic" soot. Figure 1a shows striking similarity in the dependence of the absorptivity on the carbon content for the Berkeley and Anaheim particulate samples. This is true in spite of the fact that several of the Anaheim samples were taken under high oxidant conditions, which are expected to promote secondary production of aerosol particles. Also, the absorptivity per unit mass of carbon for these ambient samples is found to be quite similar to that of various mobile source exhaust samples as shown in Fig. 1b. These results seem to indicate that a large fraction of the carbonaceous aerosol particles in the summer and winter episodes investigated is primary in origin. Further studies are under way to test the generality of these results under a wide range of atmospheric conditions and for a variety of combustion sources.

Particulate samples were collected simultaneously on 1.2-μm Millipore filters, and on quartz fiber filters that had been prefired to remove all combustible carbon. The total carbon on the quartz fiber filters was determined by combustion in an oxygen atmosphere, followed by separation and measurement of the evolved CO_2 with a gas chromatograph/thermal conductivity detector system.[3] After correction for differing flow rates, these values were then used to calculate the total carbon loadings on the corresponding Millipore filters by an apparatus incorporating a 1-mW He-Ne laser as a light source (λ = 0.6328 μm) and a photomultiplier as a detector. Essentially all of the light transmitted through the filter was collected and focused onto the photomultiplier by an f/1 lens. The average transmission through blank filters was assigned a value of 100%. This technique for measuring absorptivity is based on a principle similar to that of the opal glass technique developed by Lin et al.[4] The attenuation measured in the above fashion should be primarily due to absorption rather than scattering because most of the radiation scattered from ambient aerosol particles is in the forward direction and therefore should not contribute to the attenuation since it is collected by a lens of small f-number.

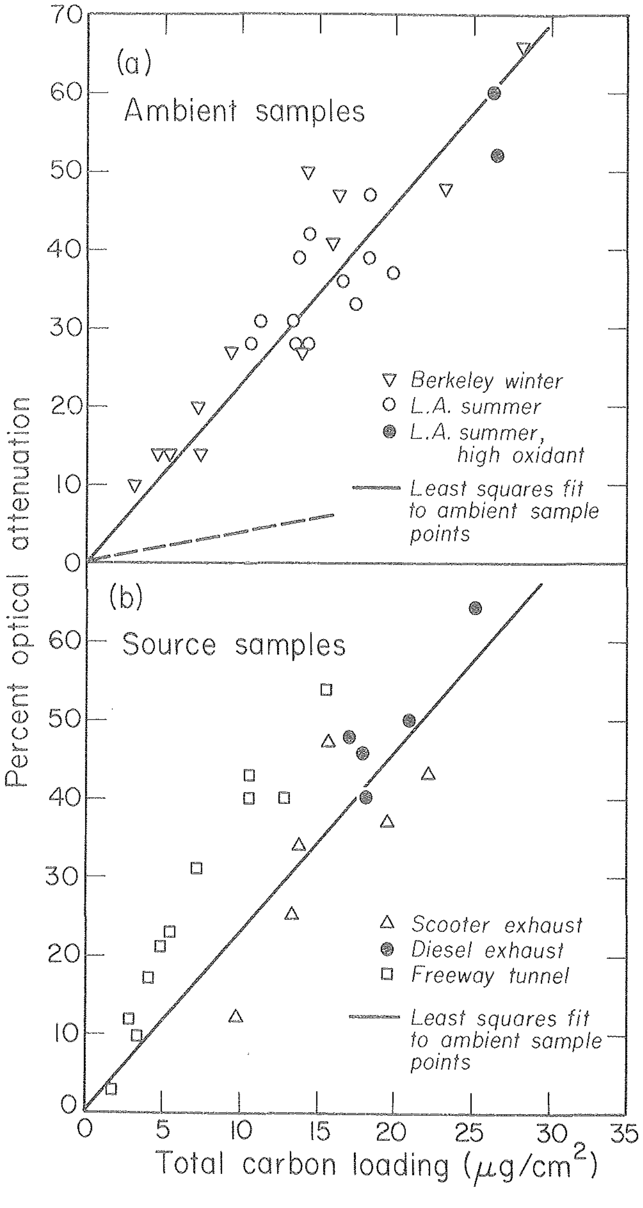

Fig. 1. (a) Optical attenuation vs total carbon loading for ambient samples collected in Berkeley, CA, in the winter and in Anaheim, CA, in the summer. The peak ozone levels for the daily summer samples ranged from 30 ppb to 270 ppb. The points designated by a solid circle have ozone levels ⩾250 ppb. The dashed line corresponds to the theoretical prediction from a mass balance calculation using Pb as a tracer and assuming the dominant sources of primary particulate carbon are automobiles. (b) Optical attenuation vs total carbon loading for various mobile source samples.
(XBL 779-2015)

The following particulate samples were used in these experiments: (1) ambient samples collected in the winter in Berkeley, California (sampling times from 15 min-4 hr; flow rate, ≈ 70 liters/min); (2) ambient samples collected in the summer in Anaheim, California (sampling time 24 hr; flow rate, ≈ 7 liters/min); (3) tunnel samples collected in a storage room between two bores of the Caldecott Tunnel, on a major San Francisco Bay Area commuter route with a traffic flow of approximately 10^5 vehicles/day; (4) garage samples collected from the rear of an underground parking garage, in which the automobile traffic flow was approximately 35 vehicles/hr, with an average stay of 1-2 hr; (5) diesel exhaust samples from a small air-cooled engine; (6) motor scooter exhaust samples from a two-stroke engine operating at a slow idle; and (7) soot samples generated by a very rich acetylene flame.

We have measured the attenuation and total carbon content of a number of ambient and mobile-source exhaust samples. These results are shown in Figs. 1a and 1b. In all cases there is a strong correlation between the carbon content and the attenuation. Since sulfur and nitrogen species in the form of common salts such as ammonium sulfate and ammonium nitrate are nonabsorbing in the visible region, and since there are no significant amounts of transition metals like Fe in these samples, we suggest that the absorption is due to the carbonaceous component of the aerosol particles.

It should be emphasized that the coverage of these samples is very light (≈ 1 monolayer of particles or less); and yet the absorptivity is quite high, implying that the refractive index of the absorbing species has a large imaginary part. The material most likely to be responsible for this absorption is "graphitic" soot, which has the requisite high imaginary index of refraction (n_I = 0.46),[5] and has been shown to be a major species in both ambient and source samples.[6]

In order to gain a better understanding of the nature of these highly absorbing species, we have measured the wavelength and temperature dependence of the absorptivity for ambient, tunnel, and laboratory-generated soot samples, shown in Figs. 2 and 3. The absorptivity shows a 1/λ wavelength dependence to within 20% over the visible spectral region (4500 Å - 7000 Å) as expected for a wavelength independent imaginary index of refraction (and evidenced by the gray or black color of these samples). This result is consistent with the hypothesis that the absorption is due primarily to "graphitic" soot, since it has been shown that the imaginary index of refraction of both acetylene and propane soot is essentially constant throughout the visible region.[5] In fact it is difficult to find many organic species that meet this criterion. Of the the 13,000 organics listed in the 54th edition of the CRC Handbook, only 5 are gray or black in appearance.

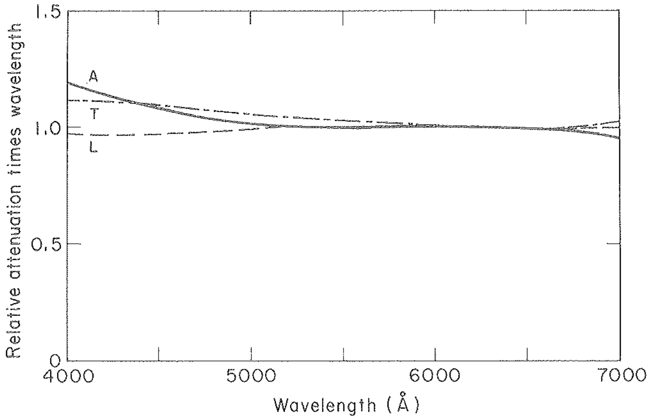

Fig. 2. Plot of the product of absorptivity and wavelength vs wavelength for A - ambient samples, T - tunnel samples, and L - laboratory-generated soot samples. Such a plot would be flat for a wavelength-independent imaginary index of refraction. (XBL 777-1307)

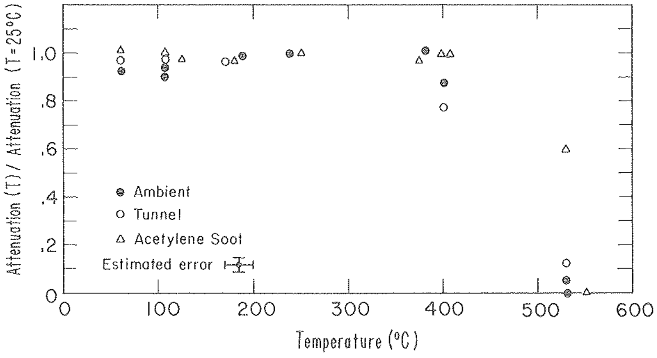

Fig. 3. Plot of the ratio of the absorptivity of various samples after heat treatment at temperature T to the absorptivity at T = 25°C as a function of heat treatment temperature. The heat treatment procedure consisted in heating the sample in air for 1/2 hr at the prescribed temperature. (XBL 777-1308)

The temperature dependence of the absorptivity was determined by measuring the absorptivity of particulates collected on quartz fiber filters before and after heat treatment at various temperatures. The heat treatment procedure consisted of heating the sample at the prescribed temperature for 30 min in air. The results of these measurements are plotted in Fig. 3, which shows clearly that in all cases the absorbing species are stable in air until approximately 400°C, and then undergo what is presumably a rapid oxidation process to essentially disappear around 500°C. Note that this threshold is similar to that of polycrystalline graphite.[7] The stability of the absorbing species at elevated temperatures again suggests that they are graphitic in structure, as most other organic species expected to be present in ambient and tunnel samples should oxidize or vaporize at significantly lower temperatures.

All these results strongly suggest that the absorptivity of urban aerosol samples is due to their "graphitic" soot content. Since "graphitic" soot seems to offer a very attractive tracer for primary emissions, we would like to obtain more direct evidence that this is indeed the case. The Raman spectrum[6] of ambient and source particulate samples clearly shows the presence of "graphitic" species as shown in Fig. 4. We have measured the Raman spectrum and absorptivity of the same sample, and then compared the integrated intensity of the "graphitic" Raman mode near 1600 cm^{-1} with the optical absorptivity. These measurements were done on acetylene soot samples, highway tunnel samples, and ambient samples collected in Berkeley, Fremont, and Anaheim, California. The results are shown in Fig. 5. Within experimental error these data show that there is a direct correspondence between the optical absorptivity and the Raman intensity for all samples studied.

If we take the Raman intensity as a measure of the "graphitic" soot content of the aerosol particles, then these results show that the optical absorptivity is also a quantitative measure of this species. The most obvious explanation for this correlation in these very different samples is that the absorptivity is due to the "graphitic" soot component of the aerosol particles. In the future we will study other source and ambient samples to see if the correspondence is generally valid.

The characterization of the carbonaceous component of ambient aerosol particles in terms of primary and secondary species is crucial to the determination of any effective control strategy. In this respect the results shown in Figs. 1a and 1b could have important implications. The similarity between the absorbing properties of the winter and summer ambient samples, and the mobile source samples, is quite striking and can be interpreted to mean that a large fraction of ambient particulate carbon is primary in origin. It would seem quite fortuitous for secondary ambient atmospheric processes to generate carbonaceous species that just happen to have similar absorbing properties to mobile source samples. It is

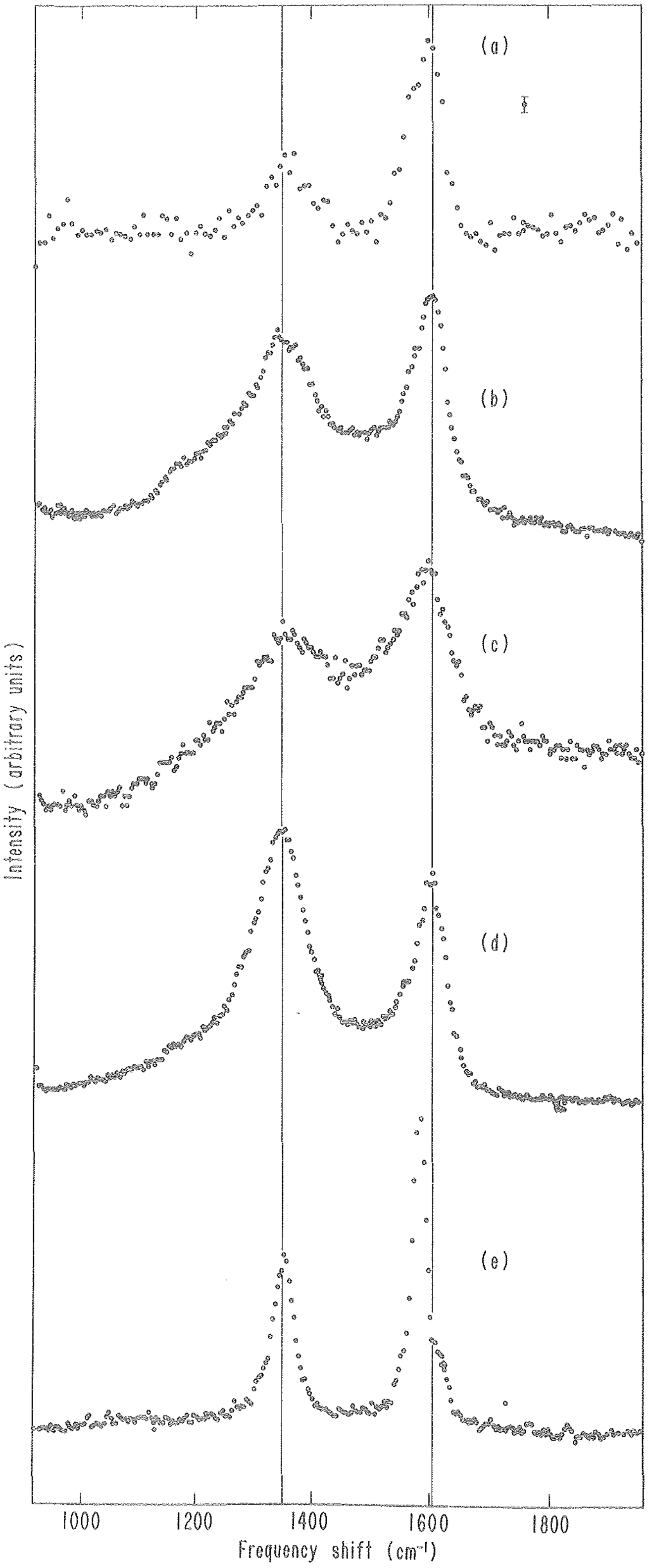

Fig. 4. Raman spectra between 920 and 1950 cm^{-1} of: (a) Ambient samples collected in 1975 as part of EPA's RAPS program. The sample was collected on a dichotomous sampler and was in the small size range fraction. (b) Automobile exhaust collected from a number of cold starts of a poorly tuned automobile using lead-free gas and having no catalytic converter. (c) Diesel exhaust. (d) Activated carbon. (e) Polycrystalline graphite. (XBL 767-3091)

also evident from the strong correlation between the absorptivity and carbon content that "graphitic" soot seems to constitute an approximately constant fraction of the total carbon content of the ambient samples, even for oxidant levels exceeding 250 ppb (see Fig. 1a). This is expected from primary emissions, but not from secondary processes, which would be expected to show more variability depending on atmospheric conditions (relative humidity, gas concentrations, oxidant level, etc.).

It has been suggested that most of the carbonaceous species in the Los Angeles Air Basin in the summer are of secondary origin, based on the concept of mass balance using Pb as a tracer.[8,9] Most of the primary carbon is assumed to originate from mobile sources, while the contribution of other sources relative to the autmobile is estimated from an emission inventory. The contribution of mobile sources is determined by assuming that such emissions are characterized by a C/Pb ratio of ≈ 1.7.[9] In the ambient samples, C/Pb ratios of the order of 10 are found, and the deviation from the automotive C/Pb ratio, after taking into account a small contribution from other sources, is attributed to the secondary production of organic carbon. Both the summer and winter episodes that we have investigated show a similar discrepancy (C/Pb ≈ 10 in the ambient samples and C/Pb ≈ 1 in the tunnel samples). If we were to use the same analysis as above, and further assume that black species ("graphitic" soot) are not produced in secondary processes, an approximate prediction of the absorptivity vs carbon content for our ambient samples would be given by dividing the slope of least squares fit of the tunnel points by 10. This line is shown in Fig. 1a and clearly does not agree with the ambient measurements.

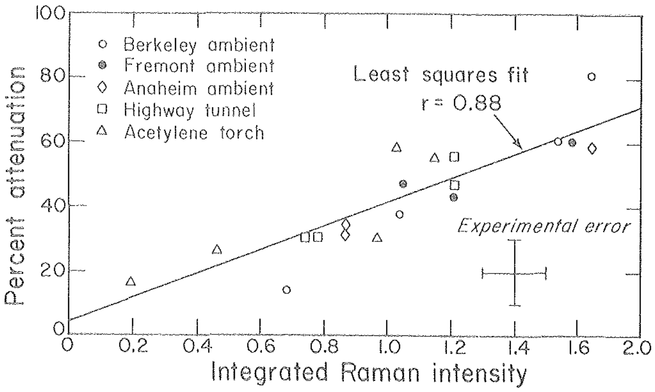

Fig. 5. A plot of integrated Raman intensity of the 1600 cm^{-1} mode vs percent optical attenuation at 6328Å for ambient acetylene soot and tunnel samples. (XBL 782-177)

This disagreement may be due to the fact that sources other than automobiles (e.g., diesels, home heating, aircraft, industry) make a major contribution to the carbon balance. It is also possible that there are some difficulties in using Pb as a tracer for mobile source emissions. For example, differences in the transport properties of lead and carbon could affect the C/Pb ratio. Also, we have found that the C/Pb ratio may depend markedly on driving conditions. Tunnel samples typically had a C/Pb ratio of $\simeq 1$, while parking garage samples taken under "start-stop" conditions had a C/Pb ratio of $\simeq 8$. This is quite reasonable since under these conditions we would expect the combustion process to be more incomplete and therefore produce more carbonaceous emissions.

ATMOSPHERIC CHEMISTRY

1. Catalytic Oxidation Of SO_2 on Carbon in Aqueous Suspension

The relative importance of different mechanisms responsible for the oxidation of sulfur dioxide to sulfate has not been established with certainty. One set of important mechanisms involves the oxidation of SO_2 in water droplets by dissolved O_2.[10] This reaction is slow, except in the presence of a catalyst, such as the metal ions Mn^{2+}, Fe^{3+}, and Cu^{2+},[11-16] or ammonia.[11,17,18] However, concentrations of these catalysts in the atmosphere are small.

We have previously suggested[19] that soot particles produced from the incomplete combustion of fossil fuel are an efficient catalyst for the oxidation in humid air of SO_2 to sulfate. This behavior is similar to that of activated carbon, whose catalytic properties are well known.

In our previous experiments, it was shown that the soot-catalyzed oxidation of SO_2 is more efficient when prehumidified, rather than dry, air is used to dilute the SO_2. However, the specific role of water was not made clear in these experiments. The effect of liquid water on the soot-catalyzed reaction is important because liquid water may condense on the soot particles in plumes, and the soot may also encounter clouds and fog during transport through the atmosphere.

The purpose of the research described here is to investigte the oxidation of SO_2 in an aqueous suspension of soot particles. The reaction was studied in systems containing various concentrations of sulfurous acid and suspended carbonaceous particles. Soots that were produced by the combustion of acetylene and natural gas, as well as that produced by a diesel engine, were used in this study and were found to be good catalysts. The results obtained with these combustion-generated soots are essentially reproduced by suspensions of similar concentrations of activated carbon (Nuchar).[20] Since it is difficult to reproducibly prepare soot suspensions, suspensions of Nuchar were used as a model system. The majority of results reported are therefore obtained using the model system. The range of carbon concentrations used in the suspensions were from 0.004% to 0.63% by weight, which corresponds to the concentrations of carbon expected in water droplets in the open atmosphere and in plumes.

A 6% H_2SO_3 solution (Baker & Adamson reagent grade) was mixed with distilled H_2O to a desired initial concentration in a 200-ml volume. This solution was contained in a 250-ml Erlenmeyer flask and stirred with a Teflon-coated magnetic stirrer. Varying weights of Nuchar C-190 were added to this solution, and the concentration of H_2SO_3 (or $SO_2 . H_2O$) was monitored by iodometric titrations during the course of the reaction. At convenient time intervals, 4- or 10-ml aliquots were removed and filtered in a sintered glass funnel. A known excess of I_2 was added and backtitrated with 1.00×10^{-3} M $Na_2S_2O_3$ with a starch indicator. All runs were done at room temperature ($\sim 20^oC$) and were open to the air. The pH of the reaction mixture was measured using a Beckman 4500 digital pH meter with a probe combination electrode (Beckman #39013). Each experiment lasted approximately 30 min to 1 hr.

Figures 6 and 7 illustrate some of the specific features of the oxidation of H_2SO_3 by dissolved oxygen in aqueous suspensions of Nuchar and of various soots. The concentration of H_2SO_3 is plotted vs the reaction time. It is apparent from these data that the disappearance of H_2SO_3 occurs in a two-step process. The rate of the initial disappearance is so fast that it could not be followed by the analytical technique employed in this investigation. The second process is manifested by a much slower linear reduction in H_2SO_3 concentration.

In order to investigate the reaction mechanism, a series of experiments were done with Nuchar as a model catalyst. The essential results obtained from these experiments are:

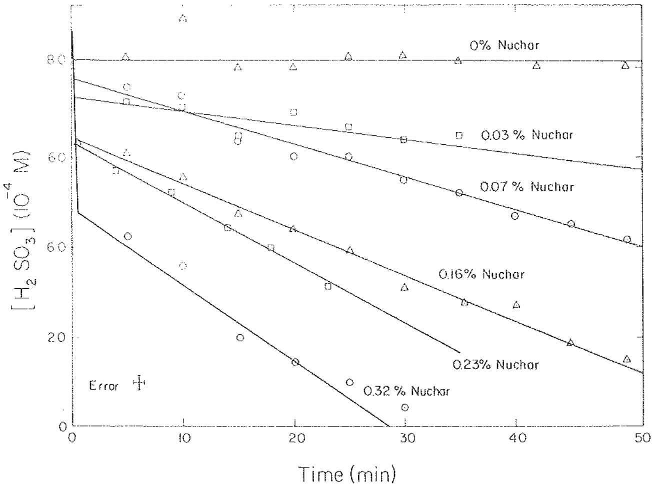

Fig. 6. H_2SO_3 concentration vs time for various Nuchar concentrations. The initial H_2SO_3 concentration was 8.85×10^{-4} M.
(XBL 7710-2070)

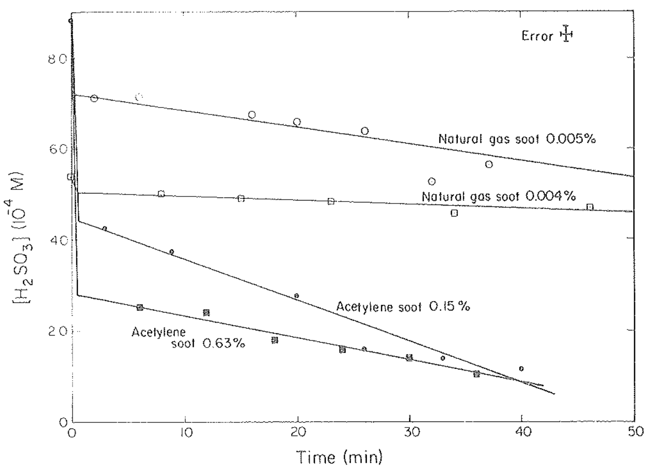

Fig. 7. H_2SO_3 concentration vs time for acetylene and natural gas soot suspensions.
(XBL 7710-2065)

1. The reaction rate is zero order with respect to the $SO_2.H_2O$ concentration (Fig. 8) and first order with respect to the carbon concentration (Fig. 9).
2. The reaction rate is pH independent (Fig. 10).
3. There is a mass balance between the destruction of H_2SO_3 and the production of H_2SO_4.[21]

Based on these experimental observations, the following reaction mechanism may be proposed:

$$C_x + O_2^1 \underset{k_{-1}}{\overset{k_1}{\rightleftarrows}} C_x \cdot O_2^1 \quad ; \quad C_x \cdot O_2^1 + S \underset{k_{-2}}{\overset{k_2}{\rightleftarrows}} C_x \cdot O_2^1 \cdot S$$

$$C_x \cdot O_2^1 \cdot S + S \underset{k_{-3}}{\overset{k_3}{\rightleftarrows}} C_x \cdot O_2^1 \cdot S^2 \quad ; \quad C_x \cdot O_2^1 \cdot S^2 \xrightarrow{k_4} C_x + 2SO$$

Assuming that the reaction follows the condition of equilibrium adsorption, and that $k_2[S] \gg k_{-2}$ and $k_3[S] \gg k_{-3}$, one can obtain the rate of acid formation:

$$\frac{d[SO]}{dt} = k[C_x][O_2]^n$$

where C_x = soot, S = sulfite species, SO = sulfate species, n = 0.7. The value of k was taken to be 1.8×10^{-4} 1/sec-g at 20°C. This numerical value represents the average of the rate constant determined from natural gas and acetylene soot.

Using this rate law, we can make an estimate of the formation of H_2SO_4 under ambient conditions. We assume the following concentrations for the various ambient species: 0.01 ppm of SO_2, 10μg/m^3 of soot, and 0.1 g/m^3 of liquid water. We also assume an ambient temperature of 20°C. Under these conditions, we calculate a production of H_2SO_4 of 1.8 μg/m^3-hr, corresponding to a conversion rate of 4.4%/hr. This rate is comparable to the rates observed in the atmosphere.[22] We therefore suggest that the soot-catalyzed reaction may play an important role in the formation of sulfates in the atmosphere.

2. A Plume Model for the Soot-Catalyzed Oxidation of SO_2

It is important to predict the spatial distribution of pollutants caused by sources such as power plants. Much work has been done on the dispersion of pollutants. However, chemical reactions are usually neglected so that many models do not give information on the secondary pollutants formed in the plume.

Gaseous reactions have recently been taken into consideration in a few photochemical smog models.[23] Freiberg[24] has recently studied the iron-catalyzed oxidation of SO_2 in water droplets in a dispersing plume. We have developed a model describing the catalytic oxidation of SO_2 to sulfuric acid on soot particles in

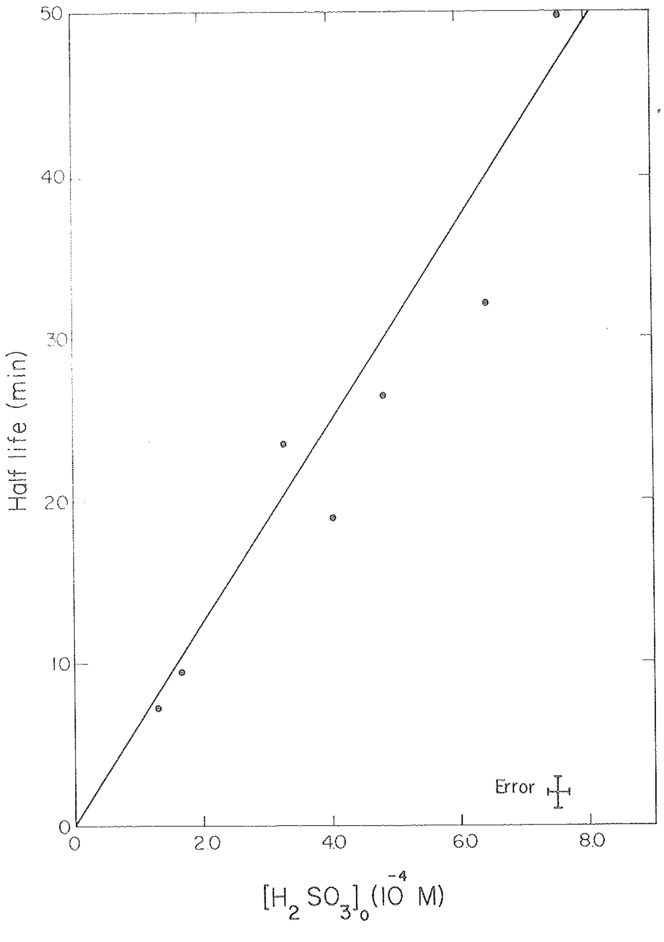

Fig. 8. Reaction half-life vs initial H_2SO_3 concentration. Plot shows zeroth order dependence with respect to H_2SO_3.
(XBL 7710-2064)

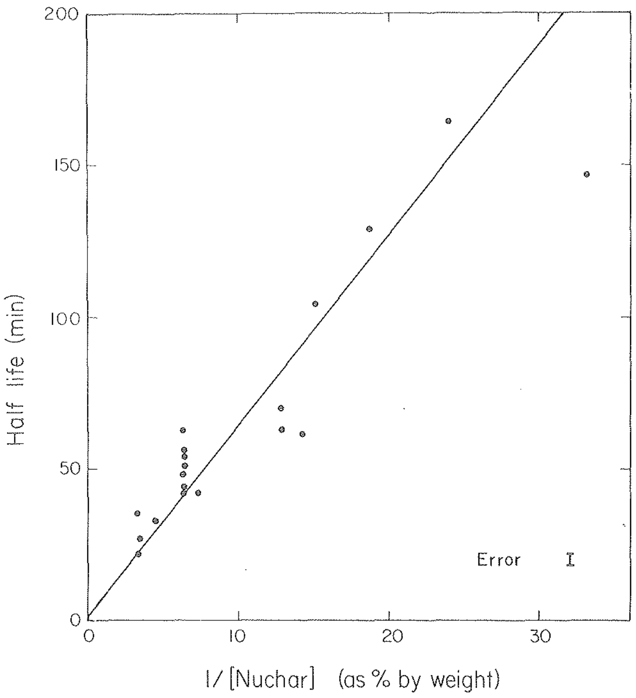

Fig. 9. Reaction half-life vs reciprocal of Nuchar concentration. Plot shows first order dependence with respect to Nuchar. (XBL 7710-2067)

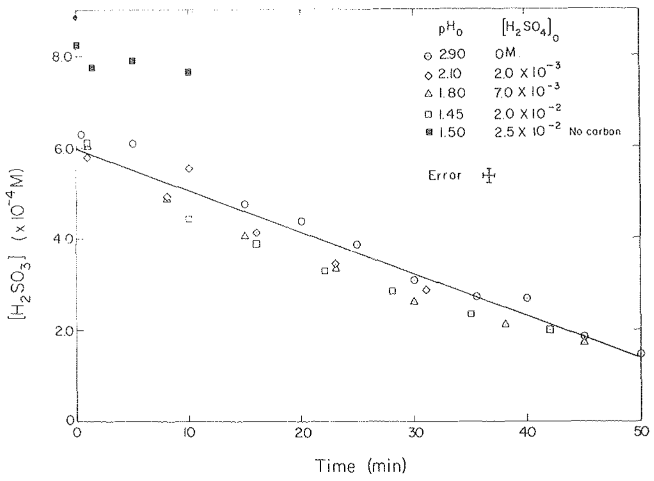

Fig. 10. H_2SO_3 concentration vs time at a Nuchar concentration of 0.16% by weight at various pH's and H_2SO_4 concentrations. The initial H_2SO_3 concentration was 8.85×10^{-4} M. (XBL 7710-2066)

a dispersing stack plume of a coal-fired power plant, under dry conditions and when liquid water is condensed on the particles.

This model is an extension of Ref. 25 to include chemical reactions in the plume. We assume velocity, density, and pollutant concentration profiles are similar at all sections normal to the plume. Atmospheric turbulence is assumed to be much smaller than turbulence generated by the plume. Geometry and coordinate systems chosen are shown in Fig. 11. A cross section of the plume at a direction normal to plume trajectory is a circle of diameter 2b. The relationship between such a coordinate system and the Cartesian system is given by

$$z = \int_0^s \sin\theta \, ds \quad ,$$

$$x = \int_0^s \cos\theta \, ds \quad .$$

Conservations of mass, momentum (in $\bar{r}$ and in θ directions), energy, and N species present constitute (N + 4) differential equations, which can be solved to obtain density, velocity, radius, angle of plume, and concentrations of the N species present. Initial conditions are determined at the stack exit.

As a special case, it is assumed that all the profiles are top hats. This reduces the equations to a set of ordinary differential equations, which are then nondimensionalized and integrated. Nondimensionalization was made with respect to two characteristic length scales: ℓ_b, the buoyancy length scale, and ℓ_m, the momentum length scale; and to a characteristic time scale ω^{-1}, which is the characteristic time for oscillation of a plume about its equilibrium position in the atmosphere. A detailed mathematical formulation and derivation, and the method of computation, will be given in another LBL report.

Conservation of chemical species j can be written as

$$\frac{d}{ds} \int C_j u dA = \varepsilon C_{j,\infty} + \int w_j'' \, dA \quad ,$$

where C_j is the concentration at any point inside the plume, $C_{j,\infty}$ is the background ambient

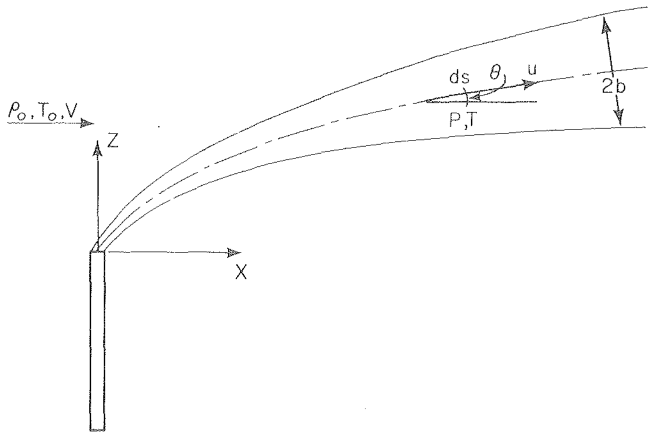

Fig. 11. Coordinate system, P, T, and u are the potential density, absolute temperature, and velocity; b is half the plume diameter, and V is wind velocity. (XBL 7710-2048)

concentration, ε is the entrainment rate, and w''_j is the rate of production of the species j in the model

$$w''_{H_2O} = w''_{carbon} = 0 \quad ,$$

$$w''_{SO_2} = -\frac{64}{98} \; w''_{H_2SO_4} \quad .$$

In modeling the production of H_2SO_4 in a plume, we have considered separately both the SO_2-air-soot-H_2O vapor and SO_2-air-soot-H_2O liquid mechanisms. The kinetic data for SO_2 oxidation on soot particles in air and H_2O are not available in the literature. Therefore we use the rate expression obtained in Refs. 26-28 with activated carbon as a catalyst. Data obtained with activated carbon obviously represent an approximation; no data exist on actual soots, however. When water is in liquid form, the reaction rate law was derived from our experimental study described in this report. For this "wet" oxidation mechanism, we also assume that the temperature is constant (20°C) during the entire course of transport, and that there is no evaporation of liquid water. The particle growth due to the vapor pressure lowering effect of the sulfuric acid formed in the droplets was neglected.

The calculations which are summarized below have been worked out using data given in Ref. 29 for a TVA coal-fired power plant:

Velocity at the stack exit = 10 m/sec
Wind velocity = 3 m/sec
Stack diameter = 8.2 m
Temperature excess at the stack = 95°C
Flux of SO_2 emissions = 1500 g/sec
Soot = 0.36 g/m^3
H_2O vapor: 10 g/m^3
H_2O liquid: 34 g/m^3

The centerline plume trajectory, temperature, and horizontal velocity are plotted in Figs. 12 and 13 as the plume travels downwind. Maximum plume rise occurs at distance $x = \pi \ell_b S$, where S is the stratification parameter defined as the ratio:

$$\frac{\text{flow time for an element of plume to reach its final height}}{\text{flow time required for the plume to be bent over appreciably in a cross wind}}$$

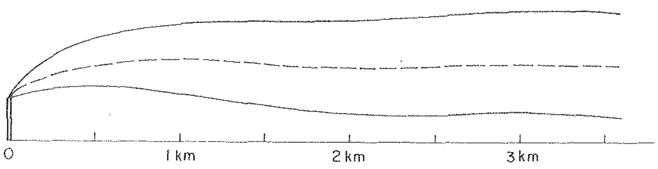

Fig. 12. Plume trajectory. The dotted line is the centerline. Note the periodic nature of the plume due to the stratification. The plume eventually stabilizes at its maximum rise. (XBL 7710-2155)

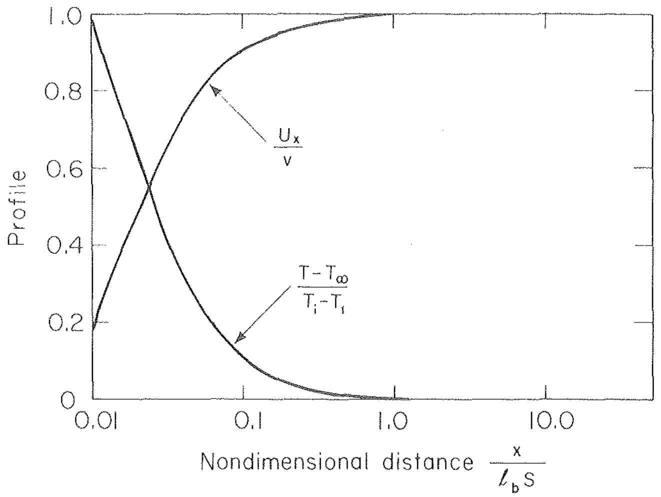

Fig. 13. Dimensionless temperature and velocity distribution inside the plume as a function of distance downstream from the stack. U_x is the component of velocity in the horizontal x direction. (XBL 7710-2060)

The concentration of sulfuric acid and the percent of total conversion of SO_2 as a function of time of transport and the distance from the stack is plotted in Figs. 14 and 15 for SO_2-air-soot-H_2O(vapor) and SO_2-air-soot-H_2O(liquid) mechanisms, respectively. The results show that the rate of oxidation of SO_2 on carbon particles is slow when the relative humidity is low and there is no water condensation on the surface of the particles. However, the rate is very fast in the presence of liquid

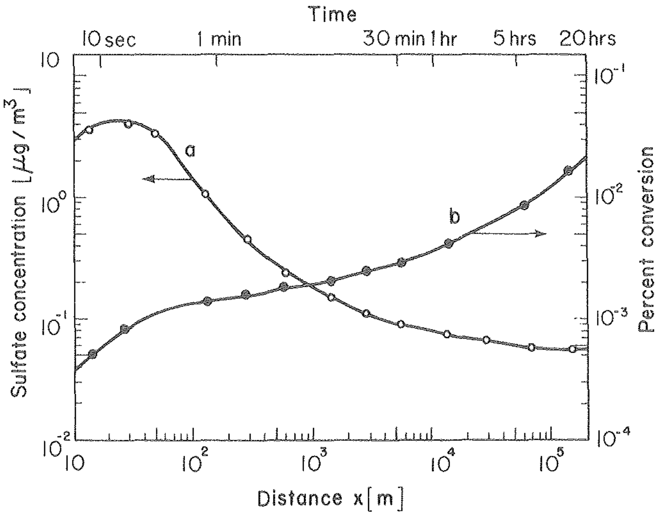

Fig. 14. The concentration of sulphuric acid (a) and the percent of total conversion of SO_2 (b) as the function of time of transport and the distance from the stack for SO_2-air-soot-H_2O (vapor). (XBL 782-188)

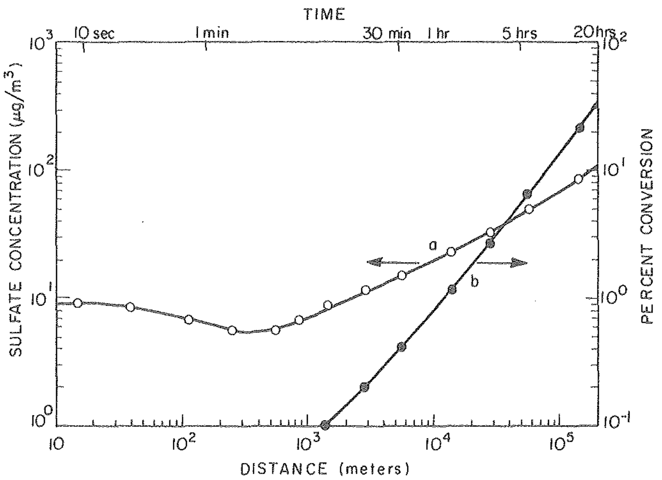

Fig. 15. The concentration of sulphuric acid (a) and the percent of total conversion of SO_2 (b) as the function of time of transport and the distance from the stack for SO_2-air-soot-H_2O (liquid). (XBL 782-4615)

H_2O. In this case the model calculation yields a conversion rate of about 1% per hour, which is in substantial agreement with experimental observations.

3. Photodecomposition of Lead Bromochloride

Most lead in the atmosphere, especially in urban areas, originates from combustion of gasoline containing antiknock additives. The dominant chemical form of lead in automobile exhaust is lead bromochloride.[30] Field experiments indicate that the halogen-to-lead ratio decreases with aerosol age,[31-34] presumably as the result of photodecomposition. Pierrard[35] has studied the photodecomposition of PbBrCl in carbon tetrachloride. However, the absorption spectrum, molar extinction coefficients, and quantum coefficients for this process have not been reported previously. We have obtained this information by means of uv-visible, x-ray photoelectron, and x-ray fluorescence spectroscopy.

Vacuum-evaporated PbBrCl films were used throughout this study. The films were deposited in a Varian vacuum vapor deposition chamber ($\sim10^{-5}$ torr) onto quartz substrates for absorption spectrum measurements, and aluminum substrates for quantum efficiency studies. The thickness of the PbBrCl deposits was measured with a Varian interference microscope.

The absorption spectra were obtained with a Cary 118 recording spectrophotometer. Figure 16 shows the absorption spectra between 700 and 300 nm of PbBrCl (dashed line), PbBrCl irradiated with natural sunlight (dotted line), and PbBrCl irradiated with a 200-W mercury arc after being exposed to natural sunlight for 2 hr (solid line). The PbBrCl film was darker after arc irradiation. This is presumably due to the formation of PbO species that are highly absorbing in the visible spectral region. The thickness of the vacuum-evaporated PbBrCl film was 196.5 ± 6.7 nm. Assuming a value of 6 g/cm³ for the density of the PbBrCl film (based on the unit cell volume given in Ref. 36), the molar extinction coefficients of PbBrCl at 525, 475, 350, and 300 nm were calculated to be 9.66×10^2, 7.06×10^2, 1.20×10^3, and 1.82×10^4 ℓ/mole-cm.

The rate of photodecomposition was studied at 252, 475, 350, and 300 nm. Figure 17 illustrates the use of XPS in monitoring the changes in concentrations of the various species during the course of the PbBrCl photodissociation.

After a 5-min *in-vacuo* irradiation of PbBrCl by the 200-W mercury arc, $4f_{5/2,7/2}$ peaks corresponding to metallic lead appear at binding energies of 141.5 and 136.6 eV.[37] The rate of production of metallic lead is initially fast but approaches saturation with continued irradiation.

Angularly resolved XPS measurements[38] were performed to find the extent to which the PbBrCl photolysis was confined to the sample surface. For a sample irradiated by the mercury arc for about 4 hr, there is a marked increase in the relative intensity of metallic lead to lead halide when the photoelectron escape angle is low. This increase, shown in Fig. 18, implies a higher concentration of metallic lead on the surface of the film than in the bulk. The mean free path of electrons in metallic lead[39] is about 2.0 nm at a kinetic energy of 1350 eV. We have calculated the mean free path of electrons in PbBrCl to be about 2.5 nm, using the formula in Ref. 39. Therefore, the ratios of metallic lead to total lead concentrations represent only a thin surface layer, not

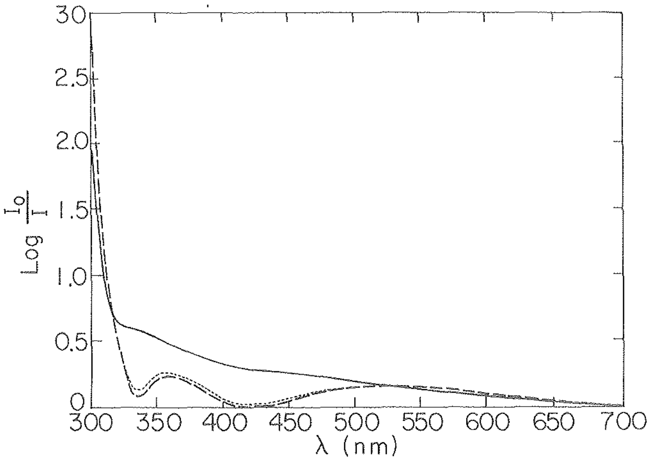

Fig. 16. - - - - Absorption spectrum of PbBrCl thin film at 20°C.
------- Absorption spectrum of PbBrCl after a 1-hr exposure in air to natural sunlight at 20°C at a level of 95 mW/cm².
——— Absorption spectra of PbBrCl after a 2-hr additional irradiation by a 200-W mercury arc at a level of 20 mW/cm².
(XBL 776-1129)

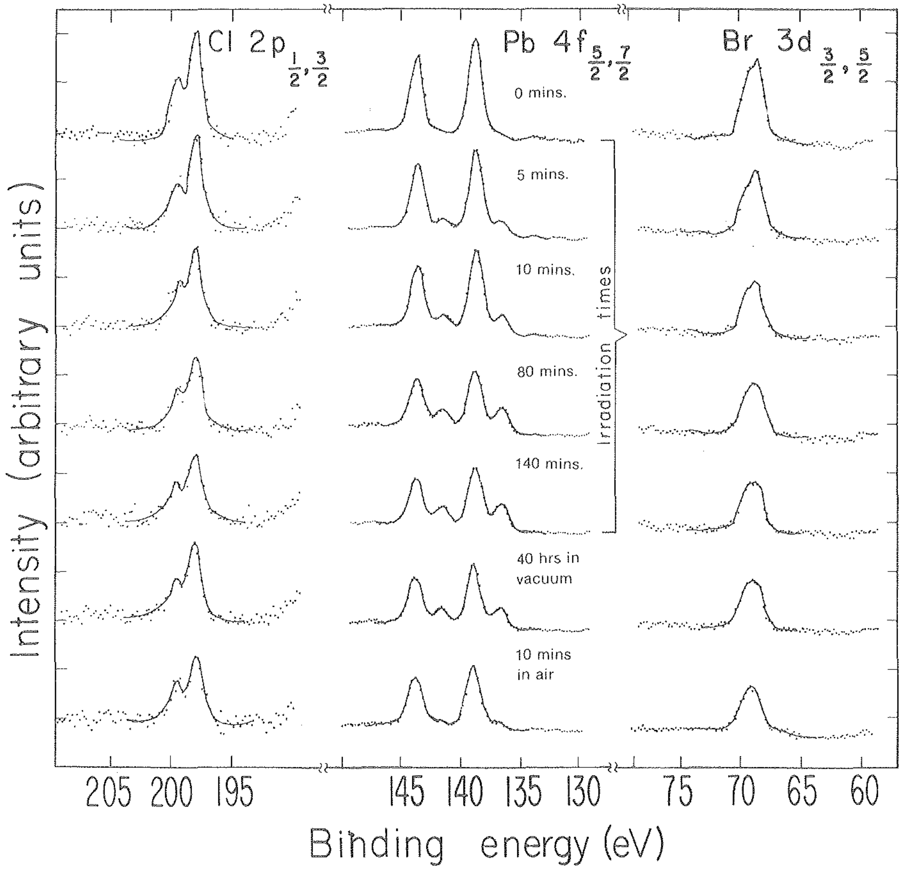

Fig. 17. XPS spectra of PbBrCl showing changes in intensity of reactant and product peaks with increasing irradiation. (XBL 776-1130)

the entire PbBrCl film (~200 nm thick). However, we can calculate the bulk lead/lead halide ratio for the entire sample by using the Beer-Lambert equation and the molar extinction coefficients reported earlier. This is done by multiplying the lead/lead halide ratio (for the sample surface), determined from XPS, by the factor $(I_0-I_3)\ \ell_1 \cos(90-\theta)/[(I_0-I_1)+(I_2-I_3)]\ \ell_2$. I_0 is the intensity of the radiation incident on the surface of the PbBrCl film; I_1 is the intensity of the radiation after penetrating a distance $\ell_1 \cos(90-\theta)$, where ℓ_1 is the electron mean free path and θ is the photoelectron escape angle; I_2 is the intensity of the radiation that reaches the surface layer after it penetrates the entire thickness (ℓ_2) of the film and after it reflects from the aluminum backing; and I_3 is the intensity of the radiation as it emerges from the surface of the sample. From this ratio and from the x-ray fluorescence results, we can calculate the amount of halogen lost as a function of the irradiation time. The quantum efficiency can then be calculated according to the following equation:

$$\phi_\lambda = \frac{\Delta}{Jt(I_0-I_3)/I_0} \quad ,$$

where ϕ_λ is the quantum efficiency at wavelength λ, Δ is the amount of bromine or chlorine lost in number of atoms/cm^2 during the irradiation time t (in seconds), and J is the photon flux in number of photons/cm^{2}sec. We have calculated the quantum efficiencies at 350 and 300 nm for chlorine and bromine when the irradiation

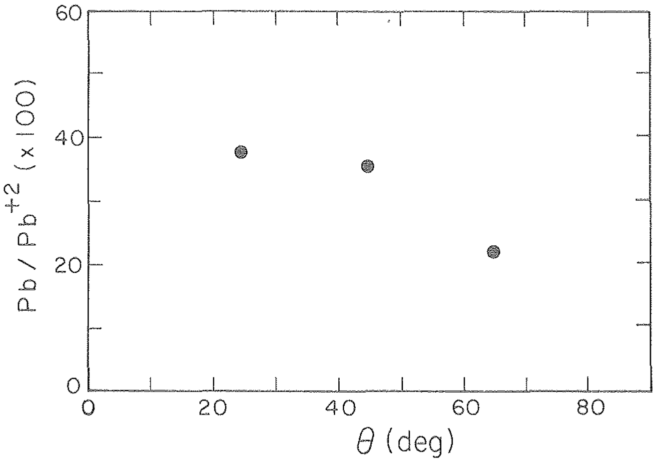

Fig. 18. Relative intensity of metallic lead to lead halide as a function of the photoelectron escape angle. (XBL 776-1131)

time (t) approaches zero. The results are listed in Table 1. The quantum efficiencies at 525 and 475 nm are negligible because no obvious photolysis of PbBrCl was observed at these wevelengths.

4. Heterogeneous Reactions of Polynuclear Aromatic Hydrocarbons and Soot Extracts with NO_2

Polycyclic aromatic hydrocarbons (PAH) can be produced directly from the combustion of fossil fuel and are always associated with soot particles.[40] Many PAH are known to be carcinogenic. Also, PAH may undergo chemical modification as a result of irradiation by sunlight[41] or by reaction with pollutant gases[42] to produce modified forms that may have enhanced health-hazard potential. We have begun a study of the reactions of selected PAH with NO_2 in order to assess their influence on the fate of PAH in ambient carbonaceous particulate material.

Heterogeneous reactions of PAH with NO_2 have not been investigated extensively before this study. However, their reactions with HNO_3 in solution produce nitro-substituted compounds and quinones.[43] Anthracene and perylene were chosen as prototypes for this work because of their availability, occurrence in particulate extracts,[44] and reactivity toward nitration in solution.[43] Finely ground hydrocarbon samples (~0.3 g) were exposed to 25-100 torr NO_2 in a light-tight, evacuated, stainless-steel reaction vessel at room temperature. For both anthracene and perylene, the pressure dropped continuously and stabilized after 1/2 hr exposure to NO_2. Not much change in pressure was observed after longer monitoring (12-24 hr). NO was produced during the reaction and was observed as a blue condensation product after the reaction. Column chromatography, with neutral alumina as the stationary phase and toluene as eluent, was used to separate the hydrocarbon products from the starting material and from each other. These fractions were crystallized by evaporation from a toluene solution. Infrared spectra of the separated hydrocarbons in KBr pellets were recorded on a Perkin-Elmer 621 grating spectrometer and representative spectra are shown in Fig. 19.

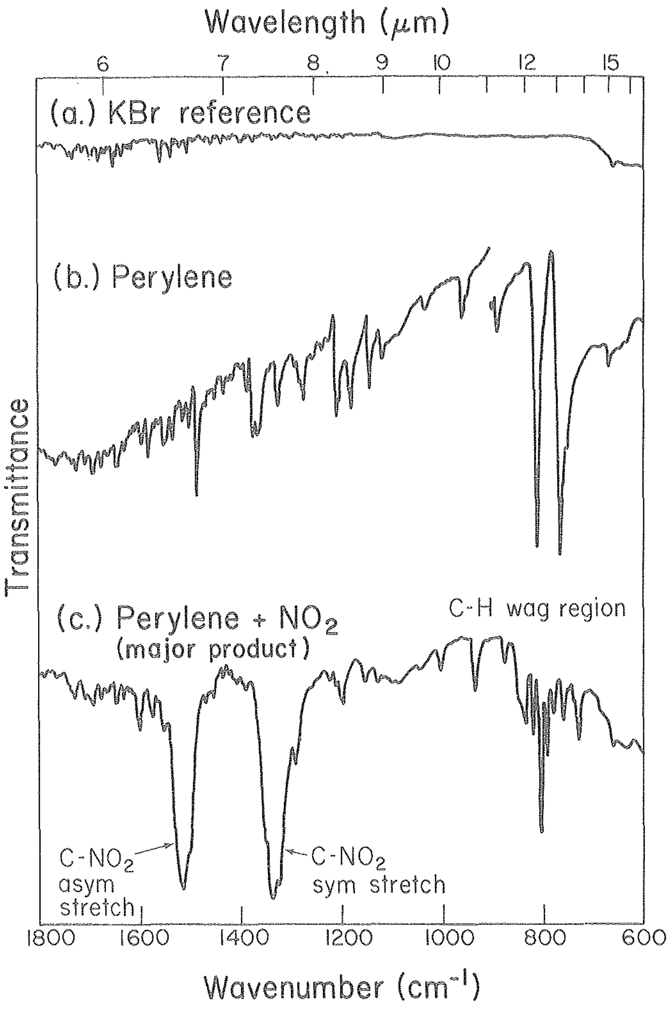

Fig. 19. Infrared absorption spectra in KBr: (a) KBr reference; (b) perylene; (c) perylene + NO_2 major reaction product (3-nitroperylene). (XBL 7710-2094)

Experiments were also performed to test the effects of water vapor on the NO_2-anthracene reaction and of humid air on the NO_2-perylene reaction. Table 2 summarizes the experimental

Table 1. Quantum efficiencies for the production of bromine and chlorine during the photodissociation of PbBrCl.

Wavelength (nm)	Photon Flux (Photons/cm^2 sec)	Film Thickness (nm)	Total Irradiation Time (hr)	Δ_{Br} [a] (μg/cm^2)	Δ_{Cl} [b] (μg/cm^2)	ϕ_{Br}	ϕ_{Cl}
350	5.85×10^{13}	179	9.5	1.72	0.55	0.038	0.027
300	2.5×10^{13}	179	2	2.30	0.90	0.35	0.31

[a] Δ_{Br} = loss of bromine after irradiation.

[b] Δ_{Cl} = loss of chlorine after irradiation.

Table 2. Summary of experimental conditions and results.

Reactants[a]	Products (30-min Exposure)	Estimated Yield[b]	$C-NO_2$ asym str (cm^{-1})	$C-NO_2$ sym str (cm^{-1})	Aromatic C-H wag[c]
Anthracene(white) + NO_2	9-nitroanthracene(orange)	10%	1508(m)	1363(m)	p879(s),832(w), 768(m),p719(s)
Anthracene + NO_2 + H_2O	9-nitroanthracene	Not Available	1510(m)	1363(w)	p878(s),833(w), 770(m),p720(s)
Perylene(orange) + NO_2	3-nitroperylene(bright red)	7-10%	1517(s)[d]	1339(s)[d]	836(w),820(w), p808(m),791(w), 778(w),p760(w), 730(w)[d]
	1-nitroperylene(?)(dark red)	$\lesssim$ 5%	–[e]	–[e]	p810(s),p764(s)
Perylene + NO_2 + H_2O + air	3-nitroperylene	10%	1520(s)	1340(s)	See above
	1-nitroperylene(?)	$\lesssim$ 5%	–[f]	–[f]	–[f]
Kerosene soot(benzene) (extract) + NO_2(dk brown)	Aromatic nitro compounds (dark red)(24-hr exposure)	Not available	1523(s)[g]	1338(s)[g]	898(w),798(m)

[a] Typical initial conditions: 2.0 x 10^{-3} mole PAH, 3 x 10^{-3} mole NO_2 (4 x 10^{-4} mole H_2O, air to ambient pressure).

[b] Mole percent, based on mass of separated products, identified as listed.

[c] C-H wag frequencies of parent PAH are preceded by p. Intensities are indicated as s-strong, m-medium, and w-weak.

[d] The strength of nitro absorptions and disruption of C-H wag pattern suggests more than one nitro group per molecule.

[e] Apart from a strong absorption at 1452 cm^{-1}, the spectrum is identical to that of unreacted perylene.

[f] No spectra available.

[g] Broad.

conditions and the assignments for the various spectral features observed in all experiments.

Characteristic nitro aromatic absorptions appear in all reaction products of 30-min and longer exposures to NO_2. These occur in the regions 1515 ± 8 cm^{-1} (asymmetric $C-NO_2$ stretch) and 1350 ± 13 cm^{-1} (symmetric $C-NO_2$ stretch). Strong aromatic nitro absorptions are also observed in kerosene soot benzene extract solids exposed to NO_2 for 24 hr. Out-of-phase C-H wagging vibrations of PAH (900-700 cm^{-1}) show absorption frequencies that are characteristic of both the number of adjacent hydrogen atoms per ring and ring substitution.[45] Polar substituents usually introduce new C-H wagging vibrations, and this effect is particularly noticeable in the nitroperylene product (Fig. 19c).

Comparison with published spectra[46] shows that the anthracene reaction product is 9-nitroanthracene, whether or not water vapor is present with NO_2. For perylene the reaction products are the same when perylene reacts with NO_2 alone or in the presence of humid air. The major nitroperylene product has a melting point range (207-210°C in argon) close to that of 3-nitroperylene (210-212°C),[47] compared with 277-279°C for perylene. However, elemental analysis and the severe disruption of the CH wag absorption modes indicate that the compound may have more than one nitro group per molecule.

These results suggest that reactions of PAH with NO_2 may occur in stagnant polluted atmospheres, under nonphotochemical conditions. Nitro PAH may have enhanced toxicity compared with PAH.[42] Nitro PAH are readily reduced to amines,[48] since the nitro group activates PAH toward reaction with electron-rich nucleophiles such as NH_3. The nitro group also influences the photochemical behavior of these compounds,[49] and could affect the fate of particulate PAH. To assess the relative importance of these reactions in source and ambient particulate chemistry, we plan to measure reaction rates and to investigate reactions when the PAH are adsorbed on activated carbon, under photochemical and nonphotochemical conditions.

FIELD STUDIES

1. Characterization of Winter Air Pollution Episodes

One of the aims of our field studies is to establish what differences, if any, can be found in the chemical composition of urban aerosol particles in winter and in summer, i.e., when the photochemical activity is low and when it is intense. It is important to understand the relative contributions of both nonphotochemical reactions and photochemical (ozone-olefin) reactions in the formation of aerosol particulate air pollution. This is especially important because existing pollution controls are specifically aimed at the control of photochemical oxidant, which is believed to be an essential precursor for the formation of particulates from gaseous pollutants such as SO_2, NO, and certain hydrocarbons.

We have recently initiated an extensive field study to characterize winter and summer air pollution episodes. The work reported here represents the first phase of this field program. During winter months the San Francisco Bay Area has frequent, intense particulate air pollution episodes in spite of low or negligible ozone concentrations. The initial work has focused on a characterization of aerosol particles during typical winter air pollution episodes. The program will be extended into the summer months when the photochemical oxidant is at maximum concentrations. A comparison of the chemical composition of the aerosol particles sampled under these two distinctly different conditions should identify the species associated specifically with oxidant-related aerosol-particulate-forming reactions and should lead to a better understanding of the significance of nonphotochemical, especially heterogeneous, reactions in the formation of secondary particulates. During the course of these field studies, the LBL Mobile Atmospheric Research Laboratory (MARL)[50] will be used at several San Francisco Bay Area locations during both photochemical and nonphotochemical seasons. The field laboratory, MARL, is a self-contained unit designed to provide a complete chemical and physical characterization of the gaseous and particulate portions of the ambient aerosol. It is capable of supporting field studies at almost any location and is readily movable to new sampling sites without requiring extensive time and effort. It contains the latest state-of-the-art air pollution monitoring and sampling equipment, meteorology instrumentation, automatic calibration equipment, and data acquisition and control systems necessary for routine measurements and special studies in the field.

We have characterized two episodes during the winter of 1976-1977. These results are shown in Figs. 20 and 21. In early November 1976, an episode occurred characterized by warm temperatures, low relative humidity, and generally stagnant air, as seen in Fig. 20a. The light-scattering coefficient, b_{scat}, reached extremely high values during midday, as did the particle volume and concentration of condensation nuclei (Fig. 20e). The most striking feature in the gas data is the high NO_2 and very low NO concentration. NO_2 exhibits maximum concentrations at midday, concurrent with the maximum concentrations of primary gaseous pollutants such as CO and SO_2. Ozone concentrations remained at the background level throughout the day. The diurnal concentration variations of total suspended particulates, particulate carbon, nitrogen, sulfur, lead, bromine, and chlorine are also shown in Fig. 20. The particulate nitrogen concentrations were obtained by both combustion and proton activation analysis.

Sulfur, lead, bromine, and chlorine concentrations were obtained by x-ray fluorescene. It is of interest to note that the nitrogen concentrations are about a factor of 5 higher than the sulfur concentrations. The detailed particulate composition for the November episode is tabulated in Table 3. Comparisons of the concentrations of C, S, and N compounds determined by various techniques at LBL and Battelle, Columbus Laboratories,[51] are given.

The nitrogen content of the aerosols was determined at LBL by a novel, sensitive, and nondestructive activation analysis technique. The close agreement between our results and those determined by combustion analysis is shown in Table 3. The results of the time-dependence of the nitrogen content of the atmospheric aerosol particle samples are shown in Figs. 20 and 21, where results for sulfur, lead, and bromine are also displayed. It is evident that the nitrogen, sulfur, lead, and bromine concentrations "track" one another. Thus our proton activation analysis for relatively low concentrations of total nitrogen in comparatively low-mass samples of atmospheric aerosol particles has been successfully demonstrated as a practical analysis.

The lateness of the season, with relative shortness of daylight hours and the low angle of the solar radiation, prevented conditions that could be classified as a photochemical episode. Photochemistry was also inhibited by sporadic high cloudiness during the period. In spite of these conditions, a heavy air pollution episode was experienced in the San Francisco Bay Area. The Bay Area Air Pollution Control District (BAAPCD) described the episode as a "winter mix" of high levels of suspended particulates, NO_2, and CO.[52]

A less severe episode in February 1977 was monitored, as shown in Fig. 21. Temperatures were moderate to warm, relative humidity rather high, and stagnation conditions prevailed. This episode did not last as long as the November one, but it was monitored from inception, following a light rain, until its breakup by marine intrusion (see chlorine data, Fig. 21). Direct comparisons between the data taken in this episode and those taken in November are subject to some uncertainty, due to a change of sampling location to a lower elevation within Berkeley. Similarities in the ozone, carbon monoxide, and sulfur dioxide concentrations and diurnal variations are evident in Figs. 20 and 21. Nitrogen oxides, however, show a reversal to a regime more dominated by NO in February. This may be due to a different set of local sources or to a shorter history of episode development. Similarly, there is a reversal in the concentrations of particulate sulfur and nitrogen, with the February episode showing substantially more particulate sulfur. No change in the chemical character of the particulate sulfur and nitrogen was observed by ESCA between the two episodes, with the sulfur being entirely in the form of sulfate, and the nitrogen being composed of approximately 25% nitrate, 25% ammonium, and 50% organic-type nitrogen.

During these two winter episodes of low photochemical activity, significant concentrations of carbon, sulfur, and nitrogen were present in the aerosol particles. The results show high concentrations of particulate sulfur and gaseous and particulate nitrogeneous species, and low concentrations of SO_2.

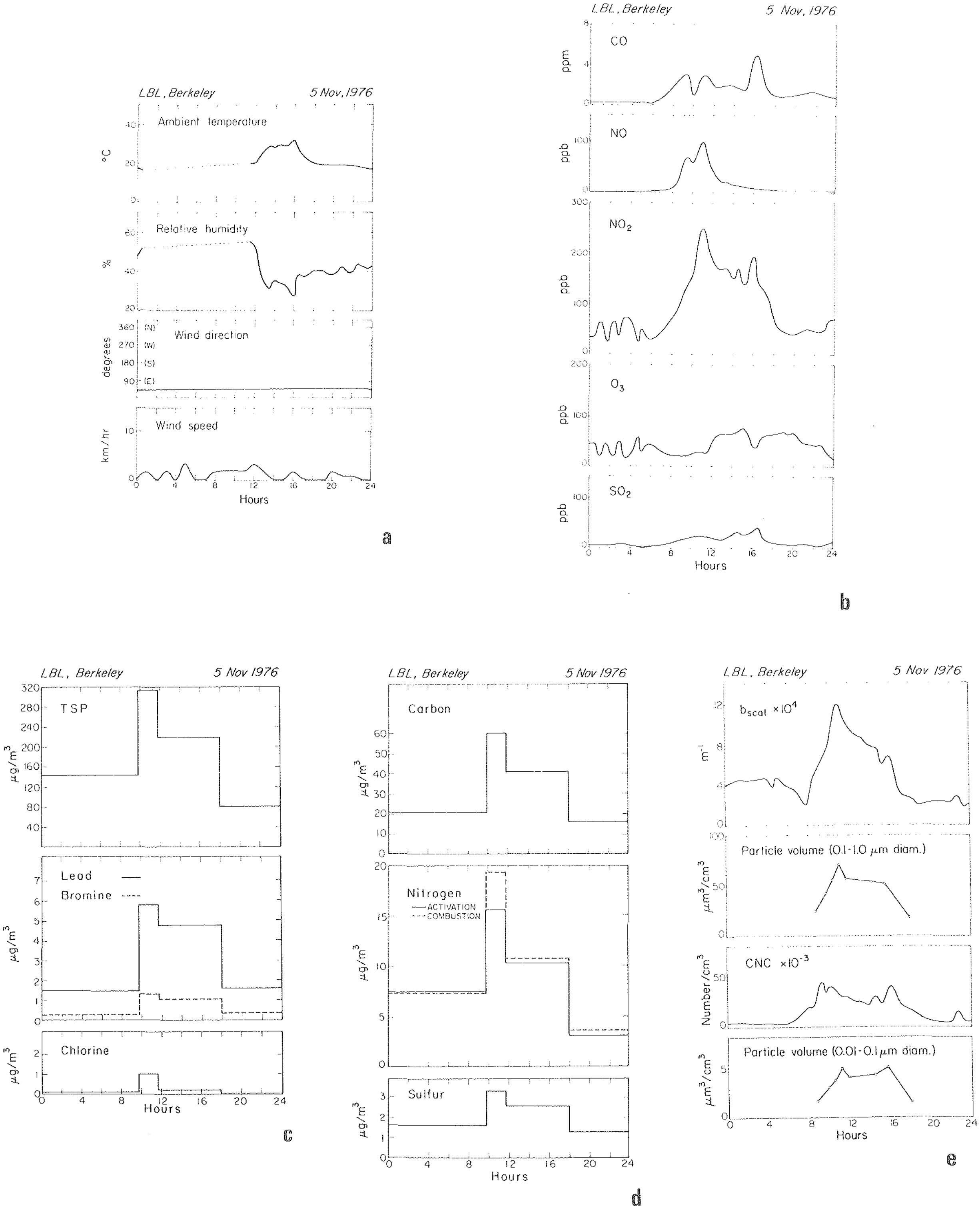

Fig. 20. November episode. (XBL 7711-10634)

The sulfate-to-SO_2 ratio is similar to that observed in the South Coast Air Basin during photochemical smog episodes. This indicates either significant primary sulfate, significant nonphotochemical SO_2-to-sulfate conversion, or both. The presence of a low level of oxidant and the area-wide use of predominantly low-sulfur fuels did not alleviate the problem of high nitrogen (gaseous and particulate) and particulate sulfur species, nor was the development of visibility restriction (comparable to a moderate-to-severe South Coast Air Basin photochemical smog episode) prevented.

The initial results of these studies indicate that the aerosol particulate composition of a nonphotochemical air pollution episode is similar in composition to "photochemical" episodes

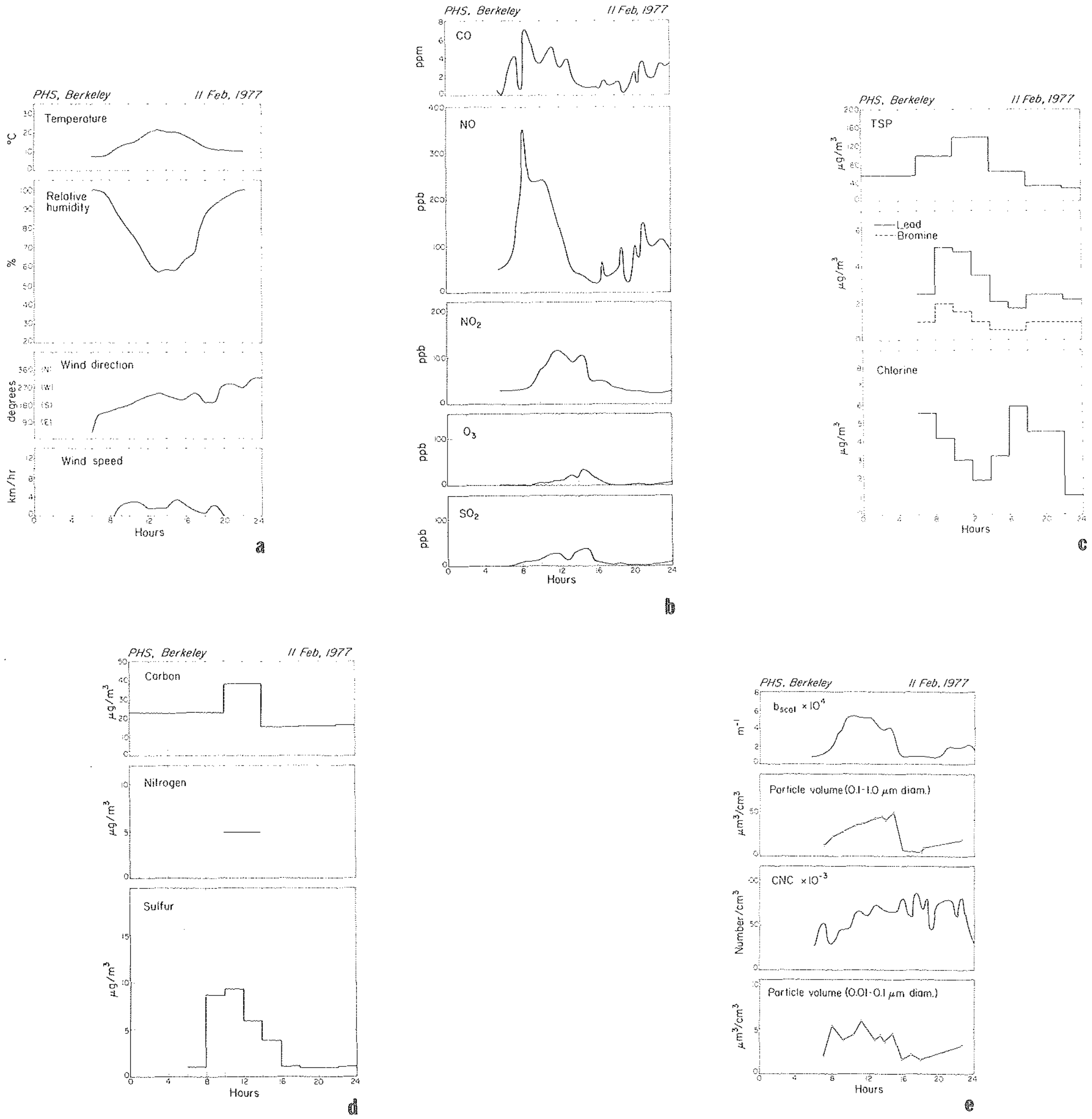

Fig. 21. February episode.

and give strong support to the thesis that nonphotochemical reactions play a significant role in particulate aerosol formation in both summer and winter urban air pollution episodes in California. More extensive studies of winter and summer air pollution episodes are currently in progress. These studies should help to assess both the significance of heterogeneous and homogeneous reactions in the formation of carbon, sulfur, and nitrogen-containing aerosol particles and also the relative importance of humidity and various potentially important catalysts (e.g., carbon) for SO_2 conversion.

2. Primary Sources of Particulate Carbon

Primary emissions of particulate carbon (soot) appear to make a major contribution to the ambient particulate burden.[53,54] The relative importance of the various industrial, domestic, and mobile sources responsible for these emissions, however, has not been well documented. Preliminary measurements of the particulate carbon emission factors for three natural-gas-fired stationary sources are presented in this report.

Particulate emissions were collected on prefired absolute quartz fiber filters from a 70,000-lb steam generator on the UCB campus, a 300,000-Btu/hr boiler at LBL used for heating a laboratory building, and a 36,000-Btu/hr domestic-type hot water heater (30 gal). During sampling of the steam generator, enough heat was transferred from the stack gases to the filter holder to prevent water condensation on the filter. For the boiler and water heater, the filter holder was heated to ~225°F with a length of electrical heating tape. The volumetric flowrate of stack gas from the steam generator was calculated from operating parameters supplied by the plant superintendent. The stack gas flowrate from the boiler

Table 3. Particulate composition ($\mu g/m^3$), November 5-6, 1976.

Collection Date			11-4/5-76	11-5-76	11-5-76	11-5/7-76	11-5/6-76	11-6-76
Collection Time			18:39(11-4)- 9:45(11-5)	9:54- 11:40	11:48- 18:00	18:05(11-5)- 11:20(11-6)	18:05(11-5)- 22:00(11-6)	11:25- 22:00
Mass	TSP = 0.31 $g/m^3 \cdot b_{scat}$		143	313	229			81
Carbon	Total C, combustion (LBL)		21.56	60.54	40.94			15.96
	Total C, Combustion (Battelle)		23.75	62.64	38.01			15.82
Sulfur	Total S, XRF (LB)		1.63±0.16	3.37±0.34	2.60±0.26	1.30±0.13		1.63±0.16
	$SO_4^=$ (as S), wet chemistry (Battelle)		3.31	4.32	5.20		1.28	
Nitrogen	Total N, proton activ. anal. (LBL)		7.53	15.60	10.29		3.06	
	Total N, combustion (Battelle)		7.40	19.15	11.14		3.69	
	NH_4^+ (as N)	Proton Activ. Anal. and ESCA (LBL)	1.9-2.3	~4	~3		~1.0	
	Organic N(as N)		3.8	~8	~4		~1.2	
	NO_3^- (as N)		1.5-1.9	~4	~3		~1.0	
	NO_3^- (as N), wet chemistry Battelle)		5.07	14.16	5.87		2.58	
Hydrogen	Total H (Battelle)		13.19	64.88	23.12		5.25	
Calcium	Total Ca	XRF (LBL)	1.67±0.07	4.07±0.16	3.98±0.16	1.16±0.05		1.50±0.06
Iron	Total Fe		2.40±0.10	5.36±0.21	6.12±0.24	2.00±0.08		2.36±0.09
Zinc	Total Zn		0.13±0.01	0.98±0.04	0.63±0.03	0.10±0.01		0.10±0.01
Bromine	Total Br		0.32±0.01	1.36±0.05	1.10±0.04	0.35±0.01		0.37±0.01
Lead	Total Pb		1.53±0.06	5.77±0.23	4.78±0.19	1.66±0.07		1.76±0.07

and water heater were determined from pitot tube measurements. The filter samples were analyzed for carbon by a combustion technique in which the filters were combusted in an oxygen atmosphere and the evolved carbon was catalytically converted to CO_2. The CO_2 was measured by gas chromatography. Results are shown in Table 4.

The data reported here indicate that the production of primary particulate carbon depends critically on combustion conditions and operating parameters. The production of carbon was greater during the time in which the boiler was ignited. This was undoubtedly due to an improper mixture of gas and air in the burner. The data also indicate that properly controlled combustionprocesses (industrial) have a much smalle remission factor for carbon than less properly maintained burners (domestic). The average emission factor per Btu of energy appears to be approximately two orders of magnitude higher for the domestic sources than for the steam generating plant. Industrial combustion of natural gas usually occurs at a constant rate (e.g., steam generation at nearly constant production without restarts). Industrial boilers are also maintained to produce the best economic return. Such maintenance includes frequent tuneups. Many domestic water heaters and furnaces are not maintained as carefully.

If the preliminary emission factors reported here are a reasonable approximation of the true emission factors, then the domestic use of natural gas in the Bay Area could produce as much as 100 times more particulate carbon than industrial use. A summary of these conclusions is presented in Table 5.

FOOTNOTES AND REFERENCES

*Principal Investigator
†Co-principal Investigator

1. T. Novakov, S.-G. Chang, and A. B. Harker, Sulfates as Pollution Particulates: Catalytic Formation on Carbon (Soot) Particles, Science 186, 259 (1974).

2. S.-G. Chang and T. Novakov, Formation of Pollution Particulate Nitrogen Compounds by NO-Soot and NH_3-Soot Gas Particle Surface Reactions, Atmos. Environ. 9, 495 (1975).

3. A similar system is described by P. K. Mueller,R. W. Mosley, and L. B. Pierce, Carbonate and Non-Carbonate Carbon in Atmospheric Particulates, in Proceedings of the 2d International Clean Air Congress, New York, Academic Press, (1971).

Table 4. Particulate carbon released during combustion of natural gas.

Source	μg C/Btu	Ratio to Steam Gen.	Comments
50,000-b steam/hr generator, campus	0.005	1	Exhaust gas flowrate calculated from CH_4 feed rate, stoichiometry, and 2% excess O_2, at 310°F (pitot tube was not available at this time for Q meas.). Sampling rate measurements could be off a little.
Domestic water heater, Bldg. 44	2.81	562	Sample collection began ~5 sec after ignition.
(same day)	1.85	370	Sample collection began 3.5 min after ignition.
	$\bar{x}$=2.33	$\bar{x}$=466	
Boiler in 73A	1.29	258	Sample collection began 1-2 min after ignition.
(same day)	1.00	200	Sample collection included initial puff of particles at ignition but stack was warmer than usual.
Boiler in 73A	0.27	54	Boiler had been running ~0.5 min before sampling started.
(same day)	0.15	30	Sample included initial puff of particles, but entire sample period = 4 min.
Boiler in 73A	0.46	92	Ave. of 4 determinations in which the first 0.5 min of the firing cycle was sampled.
(same day)	0.20	40	Sample collection began 0.5 min after ignition and extended for a total of 3.0 min.
	$\bar{x}$=0.56	$\bar{x}$=112	

Table 5. Emissions of particulate carbon from combustion of natural gas in the Bay Area.

Source	Carbon Emission Factor		Natural Gas Consumption[a]	Carbon Production (μg/day)	
Commercial use of natural gas	0.005 μg/Btu	$\frac{1}{200}$	8×10^{11} Btu/day	4×10^{9}	$\frac{1}{125}$
Domestic use of natural gas	1.0 μg/Btu		5×10^{11} Btu/day	5×10^{11}	

[a] BAAPCD figures for the San Francisco Bay Area in 1975.

4. C.-I. Lin, M. Baker, and R. J. Charlson, Absorption Coefficient of Atmospheric Aerosol: A Method for Measurement," App. Op. 12, 1356, (1973).

5. W. H. Dalzell and A. F. Sarofim, Optical Constants of Soot and Their Application to Heat-Flux Calculations, J. Heat Trans. 91, 101 (1969).

6. H. Rosen and T. Novakov, Raman Scattering and the Characterization of Atmospheric Aerosol Particles, Nature 266, 708 (1977); H. Rosen and T. Novakov, Identification of Primary Particulate Carbon and Sulfate Species by Raman Spectroscopy, Lawrence Berkeley Laboratory, Report LBL-5912 (to be published in Atmos. Env.)

7. See, for example, Union Poco Comparison Chart, Publication PGI-S-2021, Poco Graphite, Inc., 1601 South State Street, Decatur, TX 76234.

8. S. K. Friedlander, Chemical Element Balances and Identification of Air Pollution Sources, Env. Sci. Techn. 7, 235 (1973).

9. G. M. Hidy, et al. Characterization of Aerosols in California (ACHEX): Final Report, Science Center, Rockwell International, Report SC524.25FR (1974).

10. H. F. Johnstone and P. W. Leppla, The Solubility of Sulfur Dioxide at Low Partial Pressures, J. Am. Chem. Soc. 56, 2233 (1934).

11. C. Junge and T. G. Ryan, Study of the SO_2 Oxidation in Solution and its Role in Atmospheric Chemistry, J. Meteorol. Soc. 84, 46 (1958).

12. H. F. Johnstone and D. R. Coughanowr, Absorption of Sulfur Dioxide from Air, Ind. Eng. Chem. 50, 972 (1958).

13. M. J. Matteson, W. Stöber, and H. Luther, Kinetics of the Oxidation of Sulfur Dioxide by Aerosols of Manganese Sulfate, Ind. Eng. Chem. 8, 677 (1969).

14. J. Freiberg, The Mechanism of Iron Catalyzed Oxidation of SO_2 in Oxygenated Solutions, Atmos. Environ. 9, 661 (1975).

15. J. Freiberg, Effects of Relative Humidity and Temperature on Iron-Catalyzed Oxidation of SO_2 in Atmospheric Aerosols, Environ. Sci. Tech. 8, 731 (1974).

16. J. Freiberg, The Iron Catalyzed Oxidation of SO_2 to Acid Sulfate Mist in Dispersing Plumes, Atmos. Environ. 10, 121 (1976).

17. W. D. Scott and P. V. Hobbs, The Formation of Sulfate in Water Droplets, J. Atmos. Sci. 24, 54 (1967).

18. J. M. Miller and R. G. de Pena, Contribution of Scavenged Sulfur Dioxide to the Sulfate Content of Rain Water, J. Geophys. Res. 77, 5905 (1972).

19. T. Novakov and S. G. Chang, Catalytic Oxidation of SO_2 on Carbon Particles, AIChE Symposium Series 72, 255 (1975).

20. For previous works related to this subject, see M. Hartman and R. W. Coughlin, Oxidation of SO_2 in a Trickle-Bed Reactor Packed with Carbon, Chem. Eng. Sci. 27, 867 (1972) and references therein.

21. For further details see H. Rosen, Atmospheric Aerosol Research Annual Report 1976-77 Lawrence Berkeley Laboratory Report LBL 6819 (1977).

22. F. B. Smith and G. H. Jeffrey, Airborne Transport of Sulfur Dioxide from the U.K., Atmos. Environ. 9, 643 (1975).

23. S. D. Reynolds, P. M. Roth, and J. H. Seinfeld, Mathematical Modeling of Photochemical Air Pollution--I. Formulation of the Model, Atmos. Environ. 7, 1033 (1973); P. M. Roth, P. J. W. Roberts, and M.-K. Liu, Mathematical Modeling of Photochemical Air Pollution--II. A Model and Inventory of Pollutant Emissions, Atmos. Environ. 8, 97 (1974); S. D. Reynolds, M.-K. Liu, T. A. Hecht, P. M. Roth, and J. H. Seinfeld, Mathematical Modeling of Photochemical Air Pollution--III. Evaluation of the Model, Atmos. Environ. 8, 563 (1974).

24. J. Freiberg, The Iron Catalyzed Oxidation of SO_2 to Acid Sulfate Mist in Dispersing Plumes, Atmos. Environ. 10, 121 (1976).

25. D. P. Hoult, J. A. Fay, and L. J. Forney, A Theory of Plume Rise Compared with Field Observations, J. Air Pollut. Control Assoc. 19(8), 585 (1969).

26. K. Yamamoto, M. Seki, and K. Kawazoe, Rate of Oxidation of Sulfur Dioxide on Activated Carbon Surfaces, Nippon Kagaku Kaishi 6, 1046 (1972).

27. I. Sugiyama, K. Kawazoe, and K. Yamamoto, Effect of Particle Size of the Activated Carbon Pellets on the Rate of Sulfur Dioxide Oxidation, Nippon Kagaku Kaishi 6, 1052 (1972).

28. K. Yamamoto, M. Seki, and K. Kawazoe, Effect of Sulfuric Acid Accumulation on the Rate of Sulfur Dioxide Oxidation on Activated Carbon Surface, Nippon Kagaku Kaishi 7 1268 (1973).

29. S. B. Carpenter, et al., Full-Scale Study of Plume Rise at Large Coal-fired Electric Generating Stations, J. Air Pollut. Control Assoc. 18(7), 458 (1968).

30. D. A. Hirschler, L. F. Gilbert, F. W. Lamb, and L. M. Niebylskr, Lead Compounds in Automobile Exhaust Gas, Ind. Eng. Chem. 49, 1131 (1957).

31. R. L. Lininger, R. A. Duce, J. W. Winchester, and W. R. Matson, Chlorine, Bromide, Iodine, and Lead in Aerosols from Cambridge, Massachusetts, J. Geophys. Res. 71, 2457 (1966).

32. E. L. Jernigan, B. J. Ray, and R. A. Duce, Lead and Bromine in Atmospheric Particulate Matter on Oahu, Hawaii, Atmos. Environ. 5, 881 (1971).

33. J. A. Robbins and F. L. Snitz, Bromine and Chlorine Loss from Lead Halide Automobile Exhaust Particulates, Environ. Sci. Tech. 6, 164 (1972).

34. California Air Environment (University of California) 6, 5 (1977).

35. J. M. Pierrard, Photochemical Decomposition of Lead Halides from Automobile Exhaust, Environ. Sci. Tech. 3, 48 (1969).

36. G. Calingaert, F. W. Lamb, and F. Meyer, The Lead Chloride-Lead Bromide System, J. Am. Chem. Soc. 71, 3709 (1949).

37. K. S. Kim, T. J. O'Leary, and N. Winograd, X-Ray Photoelectron Spectra of Lead Oxides, Anal. Chem. 45, 2214 (1973).

38. C. S. Fadley, R. J. Baird, W. Siekhaus, T. Novakov, and S. Å. L. Bergstrom, Surface Analysis and Angular Distributions in X-Ray Photoelectron Spectroscopy, J. Electron Spectros. 4, 93 (1974).

39. D. R. Penn, Quantitative Chemical Analysis by ESCA, J. Electron Spectros. 9, 29 (1976).

40. K. W. Boyer and H. A. Laitenen, Automobile Exhaust Particulates: Properties of Environmental Significance, Environ. Sci. Technol. 9, 457 (1975); J. B. Edwards, Combustion: Formation and Emission of Trace Species, Ann Arbor, Ann Arbor Science, 1974, p. 64.

41. B. D. Tebbens, M. Mukai, and J. F. Thomas, Fate of Arenes Incorporated with Airborne Soot: Effect of Irradiation, Am. Ind. Hyg. Assoc. J. 32, 365 (1971); B. D. Tebbens, J. F. Thomas, and M. Mukai, Fate of Arenes Incorporated with Airborne Soot, Am. Ind. Hyg. Assoc. J. 27, 415 (1966).

42. National Academy of Science, Biological Effects of Atmospheric Pollutants: Particulate Polycyclic Organic Matter, Washington, U. S. Govt. Printing Office, 1970.

43. J. G. Hoggett, R. B. Moodie, J. R. Penton, and K. Schofield, Nitration and Aromatic Reactivity, Cambridge, Cambridge University Press (1971); A. Streitweiser, J. I. Branman, and J. B. Bush, Application of the Molecular Orbital ω-technique to Aromatic Substitution, Tetrahedron 19, Suppl. 2, 379 (1963); M. J. S. Dewar, T. Mole, and E. W. T. Warford, Electrophilic Substitution. VI. The Nitration of Aromatic Hydrocarbons; Partial Rate Factors and Their Interpretation, J. Chem. Soc. 3581 (1956).

44. R. C. Pierce and M. Katz, Dependency of Polynuclear Aromatic Hydrocarbon Content on Size Distribution of Atmospheric Aerosols, Environ. Sci. Technol. 9, 347 (1975); C. Golden and E. Sawicki, Ultrasonic Extraction of Total Particulate Aromatic Hydrocarbons from Airborne Particles at Room Temperature, J. Intern. Anal. Chem. 4, 9 (1975); R. C. Lao, R. S. Thomas, H. Oja, and L. Dubois, Application of a GC-MS Data Processor Combination to the Analysis of the Polycyclic Aromatic Hydrocarbon Content of Airborne Pollutants, Anal. Chem. 45, 906 (1973); R. J. Gordon, Distribution of Airborne Polycyclic Aromatic Hydrocarbons Throughout Los Angeles, Environ. Sci. Tech. 10, 370 (1976).

45. M. P. Groenewege, Some Regularities in the Infrared Spectra of Aromatic Compounds in the C-H Wagging Region, Spectrochim. Acta 11, 579 (1964); C. G. Cannon and G. B. B. M. Sutherland, The Infrared Absorption Spectra of some Aromatic Compounds, Spectrochim. Acta 4, 373 (1951).

46. C. J. Pouchert, ed., Aldrich Library of Infrared Spectra, Milwaukee, Aldrich Chemical Company, 1975.

47. J. T. Looker, Mononitration of Perylene, Preparation of Structure Proof of the 1 and 3 Isomers, J. Org. Chem. 37, 3379 (1972).

48. J. March, Advanced Organic Chemistry, New York, McGraw-Hill, 1968.

49. E. Havinga and J. Cornelisse, Aromatic Photosubstitution Reactions, Pure and Appl. Chem. 47, 1 (1976).

50. C. D. Hollowell and T. Novakov, "Mobile Atmospheric Research Laboratory," in Atmospheric Aerosol Research, Annual Report 1975-76, Lawrence Berkeley Laboratory Report LBL-5214 (1976).

51. Analyses performed by Chester W. Spicer, Battelle, Columbus Laboratories, Columbus, OH 43201.

52. Air Currents, Bay Area Air Pollution Control, 20, 1977).

53. T. Novakov, S. G. Chang, and A. B. Harker, Sulfates as Pollution Particulates: Catalytic Formation on Carbon (Soot) Particles, Science 186, 259 (1974).

54. H. Rosen, A. D. A. Hansen, R. L. Dod, and T. Novakov, Application of the Optical Absorption Technique to the Characterization of the Carbonaceous Component of Ambient and Source Particulate Samples, presented at the Fourth Joint Conference on Sensing of Environmental Pollutants, New Orleans, Louisiana, November 6-11, 1977; Lawrence Berkeley Laboratory Report LBL-6844 (1977).

VISIBLE LIGHT AND OZONE DAMAGE TO MAMMALIAN MEMBRANES

L. Packer, R. Mehlhorn, A. Quintanilha,
B. Aggarwal and J. Maguire

INTRODUCTION

The main objective of this project is to characterize and understand damage to biological membranes of various mammalian cell types, so as to put its physiological significance into proper perspective. The environmental research program at LBL has been keenly interested in assessing levels of air pollution[1,2] and in understanding the formation and transport of particulate and gaseous pollutants from fossil fuel combustion.[3] However, a detailed understanding of how biological membranes interact with the environment[4] is incomplete. Our efforts have concentrated on the study of damage processes affecting membranes, in particular those that involve free radical reactions. During 1977 we continued our studies[5-9] on the effects of visible light and oxygen on the function and structure of several cellular membrane types. It was our working hypothesis that in the presence of endogeneous membrane photosensitizers (flavins or hemes) and oxygen, visible light would generate damaging species of oxygen, viz., superoxide radicals (O_2^-), singlet oxygen ($'O_2$) and perhaps hydroxyl radicals ($OH\cdot$). These could then react with enzymes and lipids, altering both the metabolism and the structure of subcellular organelles. We have recently extended our work to include the effects of ozone (O_3), a potent atmospheric pollutant, on biological membranes.

ACCOMPLISHMENTS DURING 1977

Mitochondrial Electron Transport Studies

We have reported that human diploid cells, on exposure to visible light[6] >400 nm and oxygen[7] >10%, lose their capacity to proliferate, while ultrastructural studies of four types of cells in culture indicated the presence of numerous damaged mitochondria in the illuminated cells.[10] Our previous studies[6] indicated that maximum photokilling of WI-38 cells occurs by illumination in the wavelength region of maximum absorption by flavins, which are known to be primarily associated with the flavoenzymes in mitochondria. Indeed, the exposure to visible light of mitochondrial inner membranes in the presence of exogenous flavins accelerated the rate of, but did not change appreciably the pattern of, inactivation of flavin-linked dehydrogenases and oxidases.[5]

Further studies have shown[9,11] that visible light in the presence of oxygen inactivates the electron transport and energy coupling mechanisms in mitochondria. The respiratory chain (Fig. 1) shows a pattern of inactivation by visible light in the following order of sensitivity: succinate dehydrogenase (complex II) ≥ ubiquinone > choline dehydrogenase > NADH dehydrogenase (complex I) > iron-sulfur centers. The cytochromes do not seem to be affected. The inactivation of the energy transducing functions of the mitochondria appears concomitantly with the inactivation of flavoprotein dehydrogenases (at about the same rate as the inactivation of succinate dehydrogenase). Loss of energy coupling is shown by a decline in ATP synthesis and transmembrane potentials, and by an increase in ATP hydrolysis. Lipid peroxidation also occurs, and may well be related to the increase in ionic and H^+ permeability of the mitochondrial membrane, which is associated with the uncoupling and the decline in transmembrane potentials.

Flavins seem to be the endogeneous photosensitizers responsible for the primary processes of inactivation of the respiratory chain. The evidence can be summarized as follows:

1. All the inactivated dehydrogenases are flavin enzymes. This is consistent with the sensitivity to light of purified flavin enzymes.
2. All types of endogenous flavins of the mitochondria were gradually lost during illumination.
3. Reduction of flavins during illumination, by incubation of mitochondria in the presence of substrates and electron transport inhibitors, protects against inactivation. This is expected since flavins in their reduced state absorb much less visible light.

In addition to visible light and a photosensitizer, the inactivation of respiratory functions seem also to require the presence of oxygen. Inactivation did not occur under nitrogen, and was significantly enhanced by increasing the oxygen concentration in the gas phase. The way in which oxygen may be involved is summarized in Fig. 1. Under aerobic conditions, flavins consume oxygen to generate either singlet

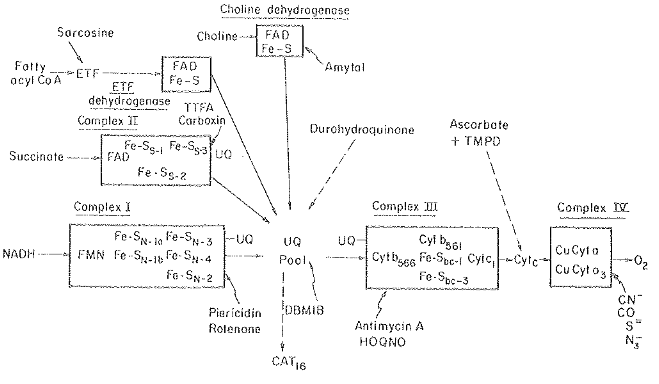

THE MITOCHONDRIAL RESPIRATORY CHAIN

Fig. 1. The respiratory chain of mitochondria. Fe-S, iron-sulfur center; Cyt, cytochrome; UQ, ubiquinone; FAD and FMN, Flavin containing coenzymes; and ⇝, inhibitory sites and substances. (XBL 776-3539)

oxygen 'O_2 or superoxide radical O_2^-. The formation of O_2^- radicals by the reduction of ubiquinone in the respiratory chain has also previously been demonstrated. Purified iron-sulfur proteins have been shown to generate O_2^-.

As indicated in Fig. 2, a spontaneous dismutation of O_2^- could lead to the formation of singlet oxygen 'O_2 and it has been suggested that O_2^- can react with its own dismutated product to form the hydroxyl radical OH·.

All these radicals have been implicated in the formation of lipid peroxides and in the cross-linking of proteins.

Evidence of the destructive potential of singlet oxygen for the electron transport chain comes from the effects of externally added photosensitizers, Eosine Y and methylene blue, which are singlet oxygen generators. They dramatically accelerate the light-dependent inactivation of succinate dehydrogenase.

Several superoxide, singlet oxygen and hydroxyl radical quenchers have been tested for their protective role, but none were effective. It is still not clear to what extent H_2O_2 or the oxygen radicals are the damaging species. The main problem lies in the difficulty of localizing radical generation and radical quenching activity at the membrane level. In fact it may be that some of these radicals are generated in membrane regions that are inaccessible to the quenchers, so that no protection is achieved.

Free Radical Detection with Spin Traps

Nitroxide spin traps were used to assay free radical production during illumination of inner mitochondrial membranes. It was shown that nitroxides were reduced to diamagnetic hydroxylamines, and that the reduced nitroxides were oxidized to the paramagnetic species in light dependent reactions. In addition, a third reaction was observed that destroyed the nitroxides. The latter reaction is presumed to involve direct coupling of light induced radicals, R·, with the N-oxyl residue of the nitroxide molecule. Evidence for the coupling mechanism proposed above comes from the failure to recover the paramagnetic nitroxide by a variety of oxidation schemes, and from the chromatographic behavior of the destruction products.

The spin reduction and destruction assay (henceforth referred to as spin loss) was used to identify the photosensitizer responsible for the free radical production. Centrifugation experiments showed that the pigment was released from the membranes slowly at 37°C, while the spin loss effect increased over a period of about 2 hr. Fluorescence assays showed that the flavin content of the supernatant increased linearly over the same time period. An action spectrum of spin loss coincided with the absorption spectrum of flavin mononucleotide (FMN), as shown in Fig. 3. These and other experiments demonstrate unequivocally that flavins released from the inner mitochondrial membrane, interact with membrane-derived substrates, and release free radicals into the aqueous phase.

Preliminary experiments have shown a similar pattern of spin loss when inner mitochondrial membranes were treated with ozone. In the ozone experiments another spin trap, 5,5-dimethy-1-pyrroline-1-oxide (DMPO), was used to demonstrate hydroxyl radical involvement in membrane damage. The different spin trapping assays vary in their specificity for reactive free radicals, and thus offer the opportunity to characterize

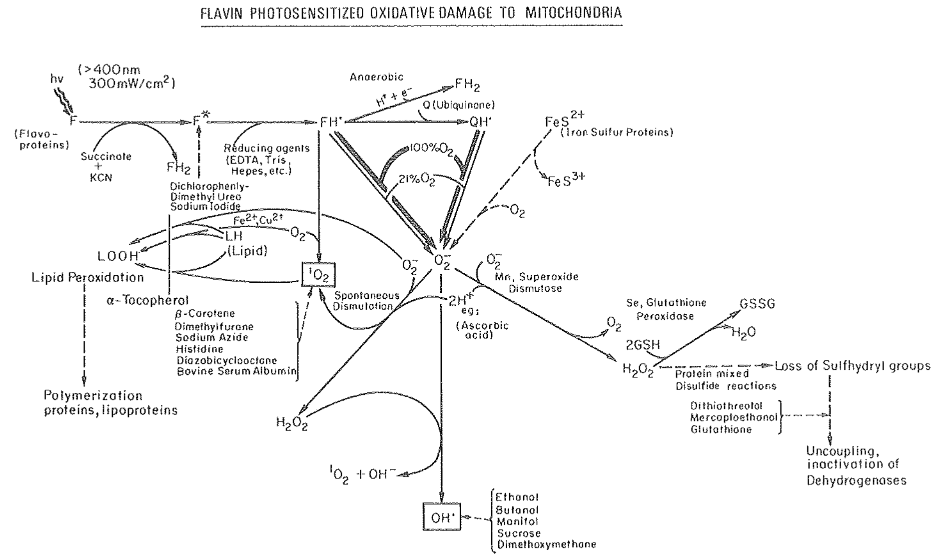

Fig. 2. Proposed mechanisms for generation of activated species of O_2 by the mitochondrial respiratory components. (XBL 7710-3922)

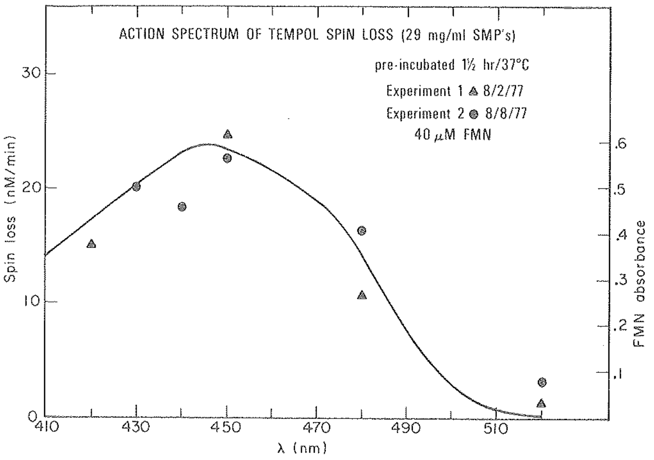

Fig. 3. The spin probe TEMPOL was incubated with mitochondrial inner membranes and illuminated with light of the indicated wavelengths using 10 nm bandwidth interference filters. The solid points represent rates of spin loss measured with a Varian E109-E electron paramagnetic resonance spectrometer. The solid line represents an absorption spectrum of flavin mononucleotide (FMN). (XBL 7710-3877)

the temporal sequence of free radical reactions in pollutant stressed membranes.

Hypatocyte Studies

The effect of visible light on isolated mitochondria may be different from that on mitochondria in intact cells. Furthermore, mitochondria are just one of many organelles within cells. In order to study the intracellular effect of oxygen and visible light damage we used isolated suspensions of rat liver cells (hepatocytes) to try to identify cellular targets of damage. The primary response observed was destabilization of various subcellular membranes in the following order: lysosomes > mitochondria ⩾ peroxisomes > plasma membranes. Enzymatic latency was used as a measure of membrane instability.

The secondary response of hepatocytes to visible light exposure was the destruction of various enzimatic activities located in different cell compartments.

Probably the most interesting finding that has come out of these studies has been that the first cellular enzyme to be destroyed by visible light is catalase, a peroxisomal enzyme. Since catalase is responsible for the breakdown of hydrogen peroxide, the destruction of catalase may cause accumulation of H_2O_2 within the cell. The damaging effects of H_2O_2 on cells are well known from ionizing radiation studies. The sequence of enzyme inactivation following catalase destruction is as follows: cathepsin c > succinate dehydrogenase ⩾ acid phosphatase > glucose 6-phosphatase > urate oxidase. Whether the inactivation of these enzymes was initiated by heme or by flavingenerated free radicals is still not known. Inactivation of catalase in vitro by visible light has previously been observed.[12] Other studies have also shown that lysosomes are susceptible to free radical attack.[13]

Lipid peroxidation occurred in all the cellular components studied. It seems, therefore, that oxygen and visible light damage to intact cells is a multicomponent phenomenon, involving the destruction of a complex metabolic system that is made up of energy generating components (e.g., mitochondria), protective enzymes (e.g., catalase), and lipid structure.

Last year[4] we reported that vitamin E protected against lipid peroxidation in mitochondria, but not against enzyme inactivation. The same is true in hepatocytes when exposed to visible light in the presence of exogenous added vitamin E. In the case of animals grown under deficient and supplemented diets of vitamin E, some protection of enzyme inactivation could be observed. It is not clear whether this is due to different light absorption of the two kinds of membranes (with or without vitamin E diet), or to a protective free radical scavenging action of the vitamin E in the membrane.

Ozone Studies

Ozone is a strong oxidizing agent, mainly produced in urban environments by the photochemical decomposition of nitrogen oxides produced by pollution. It is known to oxidize sulfhydryl groups and initiate peroxidation of lipids. It may therefore cross-link proteins and increase the permeability of lipid membranes, leading to inactivation of enzymes and to the incapacity of membranes to sustain ionic or proton gradients. We have begun studies of ozone effects on mitochondria, and have been able to show that on short exposures (~5 min) to high concentrations of O_3 (~10 ppm), the outer membrane of mitochondria affords very little protection to the enzymes localized in the inner membrane. Furthermore, using inverted inner membranes of mitochondria, we have also shown that the inner surface of this membrane is more sensitive to damage than the outer surface. This is in agreement with previous findings from our laboratory[14] that indicate a higher concentration of SH groups on the inner surface. Using a spin-label technique that monitors surface charge in membranes,[15,16] we have evidence that upon treatment with ozone the outer surface of mitochondrial membranes seems to become more positively charged. This would alter the ionic distribution close to the membrane surface, thereby affecting proton uptake rates and probably the coupled ATP synthesis.

Lipid Integrity Studies with Model Membranes

Millipore filter membranes, impregnated with different lipids, were exposed to ozone and their conductivities were measured. Breakdown of the membranes was observed over a period of minutes for highly unsaturated lipids. Very little conductance increase was noted in highly saturated lipid mixtures such as the mammalian "lung surfactant" fraction of lipids. The protective effects of lipid soluble antioxidants were also studied. The preliminary experiments have demonstrated the value of this test system for the study of pollutant damage to membrane lipids.

PLANNED ACTIVITIES FOR 1978

Having identified some steps in the temporal sequence of events involved in enzymatic and membrane structure damage in mitochondria and hepatocytes, we will endeavor to clarify the following:

1. Which of the species: O_2^-, $'O_2$, OH·, or peroxides is primarily responsible for damage? Spin trapping assays will be developed to study the generation of hydroxyl radicals. How do the effects of each of the above species change after successive inactivation of the various cellular protective enzymes, in particular catalase, which we have shown to be particularly sensitive to damage in intact cells. This will allow us to determine whether both visible light damage and O_3 damage involve similar active oxygen and peroxide species.

2. The lipid impregnated millipore assay system will be used to characterize the role of specific lipids in the propagation of damage. Lung surfactant is composed principally of lipids and there has been no sensitive assay for the function of surfactant, other than to observe changes in surface tension measured on a Langmuir trough. As surfactant is believed to line the entire alveolar air interface within the lung, all gas exchange must occur through the surfactant system. It is thus very important to monitor how O_3 can alter surfactant. Dr. Maguire, who recently joined our laboratory, has recently described[17] the best characterized preparation of rabbit lung surfactant currently available.

To characterize surfactant damage we will isolate rabbit lung surfactant lipids and incorporate them into a millipore filter. Dr. P. Shieh, in our laboratory, has found that increases in electrical conductance of these membranes, after ozone treatment, provides one of the most sensitive methods to evaluate damage to natural lipids. The method will be adapted for a detailed study on both surfactant lipids and lipids from other lung cell membranes. One strategy that seems promising is to employ two lipid-impregnated filter membranes in parallel--the outer one impregnated with surfactant lipid and the inner with lipid from other lung cell preparations. After exposure to ozone, the outer membrane (containing surfactant lipid) is removed. The degree of protection it had afforded the inner membrane can then be deduced.

We have already demonstrated that this system works well and are now evaluating levels of ozone damage and antioxidant protection by vitamin E in this system. Membranes will also be isolated from animals grown on diets supplemented with natural and artificial antioxidants such as dl-α-tocopherol, which will alter the threshold level of pollutant-initiated damage.

With this new assay system we can make rapid progress in identifying lipids that are susceptible or resistant to ozone damage, and in finding optimum conditions for reducing the damaging level of ozone.

REFERENCES

1. C. D. Hallowell, R. J. Budnitz, G. W. Traynar and W. Winkelstein, Jr., Lawrence Berkeley Laboratory Report 5982, 164-166 (1976).

2. C. D. Hallowell, S. T. Sacks, W. Winkelstein, Jr., D. M. Austin and D. W. Merrill, Jr., Lawrence Berkeley Laboratory Report 5982, 166-168 (1976).

3. T. Novakov, M. Clemenson, S. Chang, R. Dod, R. Giangne, C. Hallowell, S. Markowitz, P. Pagni, H. Rosen and R. Toossi, Lawrence Berkeley Laboratory Report 5982, 170-185 (1976).

4. L. Packer, B. Aggarwal, A. Quintanilha and R. Mehlhorn, Lawrence Berkeley Laboratory Report 5982, 183-186 (1976).

5. B. B. Aggarwal, Y. Avi-Dor, H. M. Tinberg and L. Packer, Biochem. Biophys. Res. Commun. 69, 362-368 (1976).

6. O. M. Pereira, J. R. Smith and L. Packer, Photochem. Photobiol. 24, 237-242 (1976).

7. L. Packer and K. Fuehr, Nature (London) 267, 423 (1977).

8. L. Packer and J. Walton, Chem. Tech. 7, 276-281 (1977).

9. B. B. Aggarwal, A. T. Quintanilha, R. Cammack and L. Packer, Biochim. Biophys. Acta (in press).

10. L. Packer, K. Fuehr, J. Walton, B. Aggarwal and Y. Avi-Dor, Lawrence Berkeley Laboratory Report 5299, 92-95 (1975).

11. A. T. Quintanilha and L. Packer, Proc. Natl. Acad. Sci. USA 74, 570-579 (1977).

12. R. L. Mitchel and I. C. Anderson, Science 150, 74 (1965).

13. A. C. Allison, I. A. Magnus and M. R. Young, Nature (London) 209, 874-878 (1966).

14. H. M. Tinberg and L. Packer, in Membrane Bound Enzymes, Vol. 1 (A. Martonosi, ed.), Plenum Pub. Co., New York, 1976, pp. 171-198.

15. R. J. Mehlhorn and L. Packer, Methods in Enzymology, Academic Press, NY (in press).

16. A. T. Quintanilha and L. Packer, FEBS Lett. 78, 161-165 (1977).

17. J. J. Maguire, S. A. Sheley, J. E. Paciga and J. U. Balis, Prep. Biochem. 7, 415-425 (1977).

APPLICATIONS OF NEUTRON ACTIVATION ANALYSIS (NAA) TO ENERGY AND ENVIRONMENTALLY RELATED PROBLEMS

F. Asaro, H. V. Michel, J. P. Fox and D. F. Mosier

INTRODUCTION

Elemental abundances have been measured by many different methods involving neutron activation. These methods generally use brief, low-flux neutron irradiations for predominant elements, longer, high-flux irradiations for elements present in trace amounts, or combinations of both. Analyses may be automated and computerized. They may range from low precision determinations of one element to simultaneous measurements, or groups of simultaneous measurements, that are made with high precision and encompass a significant fraction of the natural elements. Measurements can be completely instrumented, with little or no sample preparation or may entail extensive chemical and physical separations before or after the neutron irradiation. The topics covered in this report will be generally restricted to instrumented, multi-element analyses of radioactive species by neutron activation methods for oil shale research, in which precision and accuracy have been stressed.

ACCOMPLISHMENTS DURING 1977

In prior years, high precision techniques have been developed for measurements of many elements in various earth-like materials. These methods were successfully applied to raw oil shales and to the solid residues (spent shales) from thermal processing (retorting) of the shales. An example of analysis of a spent shale sample is shown in Table 1.

In addition, techniques of measurement for individual elements were improved. Molybdenum measurements have interferences from the fission of U in the samples, and Se has a large interference due to Hf. Techniques for removing these interferences were developed, which resulted in values comparable to those obtained elsewhere by other techniques. Further work with calibrated standards is needed for accurate measurements with good reproducibility. Methods for more precise measurements of Cr at the 1-10 ppm level were determined by removing the interferences due to Ta, as well as the known ones due to Fe and Nd. A systematic comparison of high precision NAA measurements by LBL and the Hebrew University of Jerusalem was extended from 6[1] to 23[2] elements. General techniques and applications of high precision NAA measurements were published.[3]

Sample preparation techniques previously applied to geothermal waters were successfully applied to oily waters. The sample water is weighed and evaporated to dryness at temperatures of 60-80°C in Nalgene bottles of 500 ml capacity. After evaporation, the tops of the bottles are cut off and the residue is removed and weighed.

Measurements were made on 100 mg samples of the residue. It is necessary to weigh the residue each time it is sampled, in order to monitor changes in the residue mass due to water evaporation or absorption. With these methods of sample preparation, and the normal NAA methods used for solid samples applied to the evaporated residues, the measurements were precise and accurate enough to determine inhomogeneity in the primary sampling of the oil shales.

Specifically, there was more Na in the spent shale and oily water fraction, after normalization for the yields of these two products, than appeared in the raw shale. Thus better methods of primary sampling of the raw and spent shales need to be used to evaluate carefully the distribution of the various elements in the retort fractions.

PLANNED ACTIVITIES FOR 1978

With the techniques developed in this research, it is planned to start fingerprinting oil shale deposits as a function of depth. This

Table 1. Abundances and precision of measurement of major, minor and trace elements in a spent shale.

Element		Element	
Ag	1.4±0.4[a]	Lu	0.204±0.018
Al%	4.24±0.14	Mg%	4.02±0.58
Au	<0.04	Mn	365±7
Ba	568±17	Mo	34.8±7.0
Ca%	11.9±0.7	Na%	2.502±0.016
Cd	<12	Nd	22.1±0.9
Ce	49.29±0.23	Ni	38.0±5.4
Cl	<1360	Rb	89.5±4.1
Co	11.7±0.2	Sb	3.12±0.19
Cr	42.2±0.8	Sc	6.697±0.030
Cs	5.81±0.14	Sm	3.414±0.011
Dy	2.65±0.09	Ta	0.5363±0.0039
Eu	0.74±0.010	Tb	0.402±0.016
Fe%	2.35±0.03	Th	7.612±0.051
Hf	2.15±0.07	Ti%	0.15±0.03
In	<0.24	U	6.614±0.047
Ir	<0.01	V	92±17
K%	1.99±0.19	W	1.8±0.4
La	15.8±0.8	Yb	1.43±0.02

[a] Entries after the ± signs are 1σ values of the estimated precision. The estimate is based on errors in counting the gamma radiation, errors in subtraction of interference effects, and calibration errors (Mo). Limits are 2σ values of the precision.

will determine to what extent different layers of shale can be distinguished chemically, and whether or not the same layer can be identified in different areas. This will be useful in selecting locations for *in situ* retorting facilities. Extensive measurements of raw and spent shales and oily waters will be made to determine the distribution of trace elements from the raw shale in the retort products. Similar measurements will be made on oils, tars, and waters relevant to *in situ* coal gasification. Techniques of measurement of oils will be investigated to couple sensitivity of measurement with precision.

REFERENCES

1. J. Yellin, I. Perlman, F. Asaro, H. V. Michel and D. F. Mosier, *Comparison of Neutron Activation Analysis for the Lawrence Berkeley Laboratory and the Hebrew University*, Archaeometry (in press) and Lawrence Berkeley Laboratory Report LBL-5298 (1976).
2. J. Yellin, I. Perlman, F. Asaro, H. V. Michel and D. F. Mosier, *Neutron Activation Analysis of Complex Mixtures--An Interlaboratory Study*, HUAL 3, preprint of the Hebrew University of Jerusalem Laboratory for Archaeometry, Institute of Archaeology and Faculty of Science (1977).
3. F. Asaro, *Applied Gamma-Ray Spectrometry and Neutron Activation Analysis*, Proc. of the combined XX Colloquium Spectroscopicum Internationale and the 7th Intern. Conf. on Atomic Spectroscopy, Prague, Czechoslovakia 1977 (to be published).

ASSESSMENT OF THE OFFSHORE COMMERICAL SAND AND GRAVEL POTENTIAL ON THE CENTRAL CALIFORNIA CONTINENTAL SHELF*

P. Wilde, J. Sandusky, W. B. N. Berry and W. Niebuhr

INTRODUCTION

Sand and gravel are the second most valuable nonpetroleum mineral commodities produced in California. In 1973, sand and gravel accounted for a dollar value of $162,290,000, or 21% of the value of minerals produced in the state.[1] However, the growth of metropolitan areas, which on one hand increases the demand for sand and gravel as aggregate, on the other hand produces situations that inhibit or will eventually prevent utilization of many land based aggregate resources. The recognition of potentially available sand and gravel bars and banks will provide planners with accessible and recoverable sources of aggregate, with which to meet the needs of the urban areas around San Francisco and San Jose. If the potentially useful sand and gravel deposits are identified at this stage of long-range planning, then appropriate consideration of the ecological consequences of mining these deposits may be considered before the real need exists. This project concerns the identification of sand and gravel deposits in the central California near-shore areas that may be considered for their commercial potential.

The University of California Museum of Paleontology has among its collections a group of about 3,000 samples taken from the California continental shelf and beach areas north of Point Conception. Many of these samples (hereafter referred to as the HEL collection) have been examined for grain size distribution. We will use the HEL collection and the data concerning marine sediment grain size to compile maps showing the distribution of grain sizes on the central California offshore, and permitting the analyses of this distribution. The maps will also help in defining bodies bearing sand and larger particles of commercial value.

ACCOMPLISHMENTS DURING 1977

The project objectives for 1976-77 were to (a) ensure that the HEL Collection is stored in an orderly manner and that the information in the computer base correlates with the actual sample locations and descriptions; and (b) display four grain size parameters: (1) median grain size, (2) sorting coefficient, (3) skewness, and (4) kurtosis, for stations in the collection where sufficient grain size analytical work has been done. The purpose of these maps is a preliminary delineation of the potential economic offshore sand and gravel deposits.

At the end of the project year we have produced:

(1) A correlated computer printout catalog of the HEL collection, including HEL stations in consecutive order; position in latitude and longitude; sampling device; sampling time in hours, day, month, year; depth; location-intertidal, shelf, beach, etc.; sediment description; key to publication of data; and field number. Raw grain size data will be in an additional section of the catalog by consecutive HEL number weight of seive catch in grams; by standard mesh number; millimeters, and phi units.[2]

(2) A strip-map atlas (see Fig. 1) showing locations of stations and individual maps of the grainsize statistics; median grain size, sorting coefficient, skewness, and kurtosis for the central California offshore area.[3]

FOOTNOTE AND REFERENCES

*Project funded by Department of Commerce/Sea Grant (R/CZ-37).

1. F. F. Davis and J. R. Evans, Mineral Production in California, Calif. Geol. 27, 128 (1974).

2. P. Wilde, W. Niebuhr, J. Sandusky, and W. B. N. Berry, Catalog of Sediment Samples in the Hydraulic Engineering Laboratory Collection Housed in the Paleontological Museum, Lawrence Berkeley Laboratory Report, UCID-4003 (1978).

3. P. Wilde, J. Sandusky, W. Niebuhr, and W. B. N. Berry, 1978, Atlas of Grain Size Parameters of Surface Sediments on the Central California Continental Shelf, UCID (to be published).

OCEANOGRAPHIC DATA OFF THE WEST COAST OF THE UNITED STATES: NITINAT FAN SHEET 46-49°N

P. Wilde, T. Chase* and W. R. Normark*

A series of oceanographic compiliation sheets for the area off the west coast are being undertaken in cooperation with the U. S. Geological Survey. The aim of this study is to provide a map of convenient size that:

1. Summarizes the oceanographic data to date for a particular area.
2. Can be used as a base map for geologic investigations.
3. Can be a working chart during shipboard operations.
4. Can be easily revised as new information becomes available.

The format for the Nitinat fan sheet consists of a base map at oceanographic plotting scale 1:748,602, at 47°N latitude, with depth contours at 100 meter intervals. The base map is supplemented with a series of mini base maps, where items of special interest are plotted. The mini-maps include geolographic features, earthquake epicenters, bottom sediment and heat flow stations, free air gravity anomaly, magnetic lineations, seismic reflection and refraction, coastal reflection surveys, monthly surface currents and sea surface temperatures, and percentage of frequency of seas greater than 8 ft by season. Selected seismic reflection profiles are shown at various scales. A temperature-salinity diagram for an east-west transect of the area is given to identify water masses in the region.

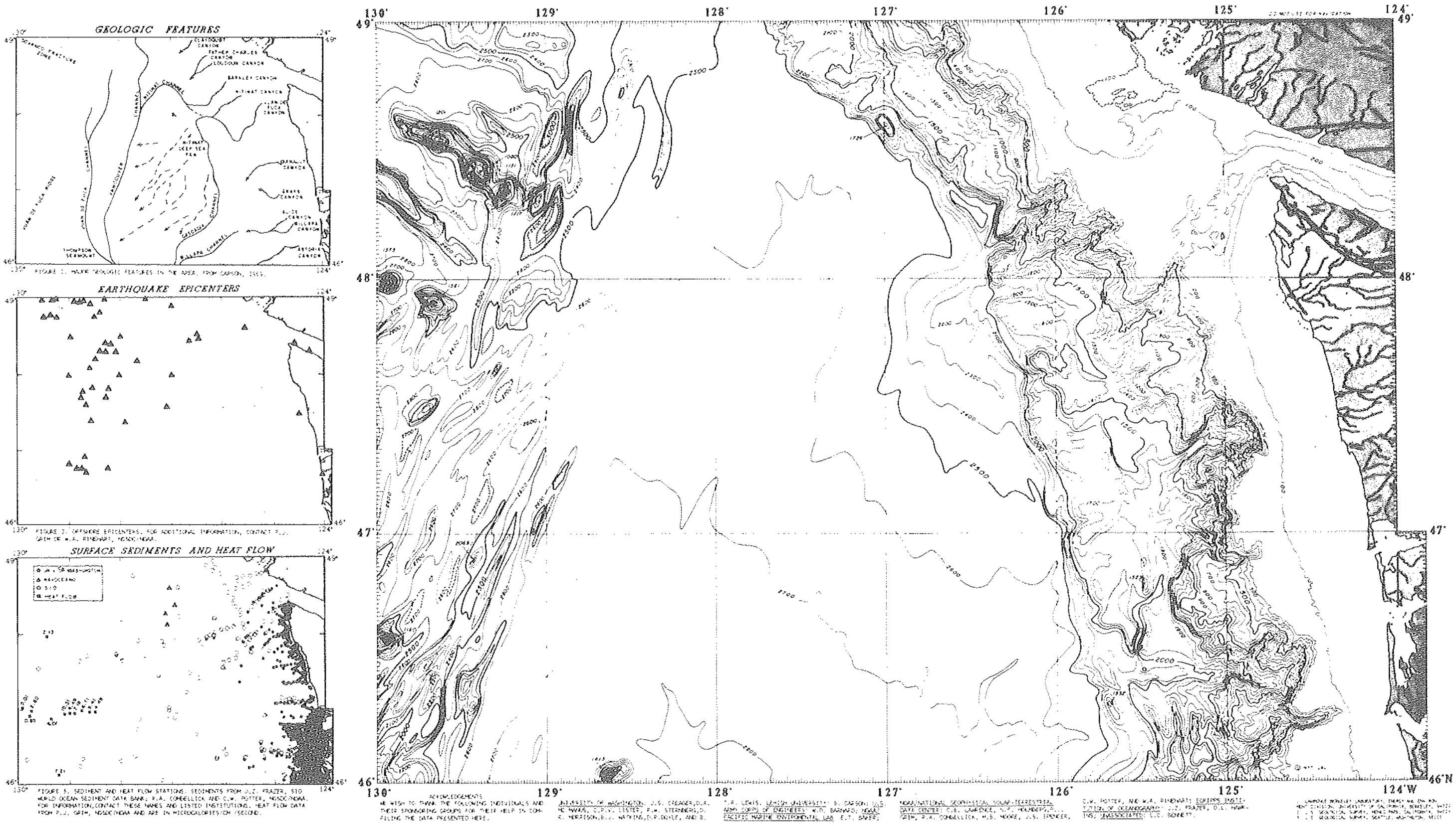

Fig. 1. Format for the Nitinat fan sheet.

For actual navigation, a table of available NOAA-NOS sailing and general charts is shown. Finally, pertinent oceanographic and particularly marine geologic references are listed. The mini-maps, tables, and diagrams are useful as indices to available data in a more detailed form. Each data source is listed so the reader/user can contact the groups responsible for the data for additional information.

FOOTNOTE AND REFERENCES

[*] U. S. Geological Survey, Pacific Arctic Marine Geology Branch, Menlo Park, California.

1. T. E. Chase, W. R. Normark, and P. Wilde, Oceanographic Data of the Monterey Deep-Sea Fan, IMR Tech. Rept. Series TR-58, University of California, San Diego (1975).
2. P. Wilde, W. R. Normark, and T. E. Chase, Oceanographic Data Off Central California 37°-40°N including the Delgada Deep-Sea Fan, Lawrence Berkeley Laboratory Report, PUB-92 (1976).
3. P. Wilde, T. E. Chase, W. R. Normark, and J. A. Thomas, Oceanographic Data Off Washington 46°-49° North including the Nitinat Deep-Sea Fan, Lawrence Berkeley Laboratory Report, PUB-223 (1977).

Instrumentation Development

SENSITIVE OPTOACOUSTIC DETECTION OF CARBON MONOXIDE BY RESONANCE ABSORPTION

R. Gerlach and N. M. Amer

The carbon monoxide molecule (CO) is of interest for a variety of reasons. CO plays a crucial role in the CO-OH-CH_4 cycle responsible for cleansing the troposphere.[1] Furthermore, it is a dangerous air pollutant and has been implicated in the formation of smog.[2]

The most widely used techniques for the detection of CO are: 1) conventional infrared absorption--this approach suffers from interference, particularly from N_2O, and although adequate for many applications, is incapable of ultra-low concentration detection; 2) gas chromatography, which is highly sensitive, but is elaborate and time-consuming.

We have combined the concept of optical resonance absorption with laser optoacoustic spectroscopy to achieve sensitive (0.15 ppm) and interference-free detection of CO.

We used a cw gas discharge CO laser capable of oscillating on transitions in the fundamental $1 \to 0$ band of CO,[3] around 4.75 μm, as well as on higher vibrational bands. Operation on transitions in the $1 \to 0$ band was essential because only these transitions are resonantly, and hence strongly, absorbed by CO molecules in their ground vibrational state. Laser transitions in higher vibrational bands are generally not resonant with those in the fundamental $1 \leftarrow 0$ band; and while resonant with hot band transitions, the latter produce very little absorption at typical ambient temperatures.

Two types of optoacoustic cells were investigated for comparison: an acoustically nonresonant cell which was operated in its 1/f frequency response region, and a resonant cell which was driven at the frequency of its first radial resonance. Both cells were calibrated by measuring the optoacoustic signals for gas mixtures of known CO concentration. We used gas mixtures from National Bureau of Standards having concentrations 49.3 ± 0.5, 95 ± 0.9, and 476 ± 5 ppm and centified mixtures from Matheson having concentrations 6, 11, and 29 ppm (all ±5%) of CO in N_2. Mixtures of other concentrations were prepared by diluting the NBS mixtures with N_2.

The dependence of optoacoustic signal on CO concentration is summarized in Table 1, and illustrated in Fig. 1 for the $P_{1-0}(11)$ transition. Above a certain background-equivalent concentration, and up to the maximum concentration investigated, 476 ppm, the signal is proportional to CO concentration. Below the background-equivalent concentration, the signal approaches a nonzero value of $\sim$0.04 μV/mW for all four transitions as concentration approaches zero. This is an optoacoustic signal which disappears when the laser beam is blocked. It is also observed with pure N_2 in the cell. We attribute this background signal to heating of the walls and/or windows of the cell by the beam, which has a 1 cm diameter at $1/e^2$ intensity traversing the cell.

In practice our limit of lowest detectable concentration for the nonresonant cell was set by the background signal, which allowed the detection of $\sim$1.5 ppm for the three resonant transitions. For the $P_{2-1}(12)$ transition, the CO absorption is much weaker but the power available was much larger, so that at a given concentration the observed signal to noise ratio was comparable to that for the resonant transitions. However, the higher power resulted in an increase in the background signal which was equivalent to a CO concentration of 15 ppm. Additional disadvantages of this nonresonant transition will be pointed out later.

The other optoacoustic cell used in this experiment was an acoustically resonant cavity with a Q (defined as the resonant frequency divided by the full width at $1/\sqrt{2}$ response) of 760.

With the resonant cell, for the $P_{1-0}(10)$ transition we observed a signal of 7.5 nV/(mW ppm) which, with a noise level of 5.5 nV and a typical laser power of 5 mW, gives a signal-to-noise ratio of unity at a concentration of 0.15 ppm. The minimum detectable concentration was limited only by electrical noise, with no background signal observable. By comparison, for the same laser transition, the nonresonant cell would give a signal-to-noise ratio of unity at 0.4 ppm, but had a background-equivalent concentration of 1.5 ppm.

We investigated the dependence of the optoacoustic signal on pressure for both cells, since in the presence of interference, use of low pressure might be desirable. For the acoustically nonresonant cell, as the pressure of the CO-N_2 mixture was reduced from 760 Torr to 75 Torr, the signal observed for the resonant $1 \to 0$ laser transitions was found to be nearly independent of pressure, increasing slightly as pressure was decreased. This is reasonable since in the pressure-broadened regime, for constant percentage of absorbing gas, the absorption coefficient at line center remains constant. Below 75 Torr the signal fell off rapidly as Doppler broadening began to dominate, causing the absorption coefficient at line center to decrease in proportion to the pressure. For the optically nonresonant transition, $P_{2-1}(12)$,

Table 1. Performance of the system using the acoustically nonresonant cell.

Laser transition	Typical output power (mW)	Optoacoustic signal per unit power per unit CO concentration (nV/(mW ppm))	Noise-equivalent CO concentration (ppm)	Background-equivalent CO concentration (ppm)
$P_{1-0}(9)$	2	31.2	0.8	1.5
$P_{1-0}(10)$	5	27.7	0.4	1.5
$P_{1-0}(11)$	5	28.9	0.4	1.5
$P_{2-0}(12)$	51[a]	3.9	0.3[a]	15

[a] Maximum rather than the typical power, obtained by optimizing the lasing gas mixture for 2 → 1 transitions. Noise-equivalent concentration computed using the maximum power value.

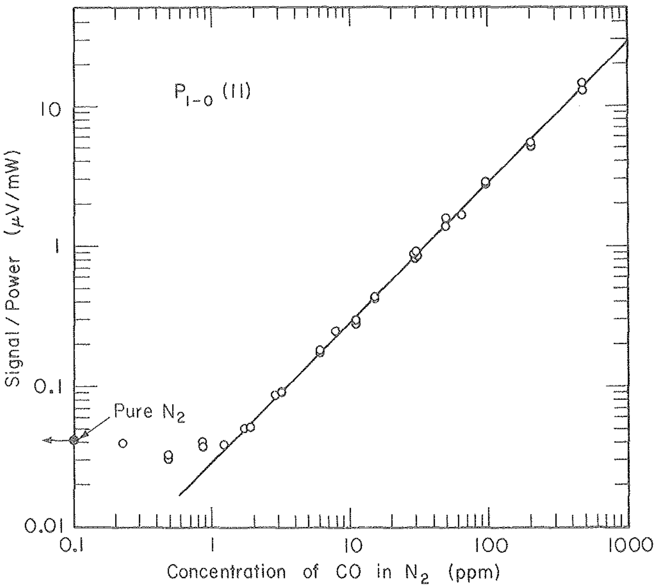

Fig. 1. Concentration dependence of nonresonant optoacoustic signal for $P_{1-0}(11)$ transition. (XBL-779-1920)

in the range from ~200 Torr to 760 Torr the signal was observed to fall off linearly with decreasing pressure due to the narrowing of the absorption line. At lower pressures the signal appeared to vary as a higher power of pressure. For an interfering species whose absorption line did not coincide closely with the laser line, the optoacoustic signal would have a pressure dependence similar to that described for the $P_{2-1}(12)$ transition. By lowering the pressure, the interfering absorption line is narrowed, and unless it is in very close coincidence with the laser wavelength, its absorption will be decreased. In contrast, the absorptivity of the resonantly absorbing gas to be detected remains constant, independent of pressure, until Doppler broadening begins to dominate. Hence, selectivity is improved as pressure is decreased.

In the case of the acoustically resonant cell, even for an optically resonant transition, the signal was found to depend linearly on pressure, even though the absorbed power is independent of pressure in the pressure-broadened regime. The reason is that as pressure decreased, the Q of the acoustical resonance decreases. Although the sensitivity of this system to an interfering species will then be decreased relative to the resonantly absorbing gas by decreasing the pressure, the signal-to-noise ratio will be degraded.

Thus, it appears that the acoustically nonresonant cell has an advantage for low pressure operation, since the signal, and hence signal-to-noise ratio, remains constant as pressure is decreased, whereas for the resonant cell, it falls off linearly with decreasing pressure. Also, the background signal, which limits the sensitivity of the nonresonant cell at atmospheric pressure, has been found to depend approximately linearly on pressure, and would be less troublesome for low pressure operation.

To assess the effect of interference from atmospheric absorption, we estimated atmospheric absorption coefficients for each of the laser transitions from computer-generated atmospheric transmission spectra.[4] For atmospheric pressure, temperature of 296°K, and relative humidity of 65%, these coefficients were compared to our estimated absorption coefficients to obtain equivalent CO concentrations which would result in the same absorption. The equivalent concentrations were 0.25 ppm for $P_{1-0}(9)$, 0.09 ppm for $P_{1-0}(10)$, 0.08 ppm for $P_{1-0}(11)$, and 0.43 ppm for $P_{2-1}(12)$. Due to the 0.25 cm^{-1} resolution folded into the computed spectra,[4] the equivalent CO concentrations may be somewhat higher for the $P_{1-0}(9)$ and $P_{1-0}(10)$ transitions, since these appear to lie close to the centers of atmospheric absorption lines, where finite resolution would result in an underestimate of the absorption coefficient. On the other hand, the $P_{1-0}(11)$ and $P_{2-1}(12)$ absorption coefficients are more likely to be overestimated since these lines lie far from the centers of atmospheric absorption lines.

While the atmospheric absorption coefficient for the $P_{2-1}(12)$ transition is not large, it appears as a high equivalent CO concentration due to the weak absorption of CO at that wavelength. Use of low pressures to eliminate this interference is not practicable because, as discussed above, it is not a resonantly absorbed transition.

Of the four transitions we have investigated, $P_{1-0}(11)$ offers the best combination of sensitivity and freedom from interference.

Recent combustion studies have shown that N_2O can be a serious interferer in determining the concentration of CO with monitoring instruments using broad-band, incoherent light sources (e.g., nondispersive infrared analyzers).[5] The interference stems from the overlap of the 4.5 μm and 4.67 μm absorption bands of N_2O and CO, respectively. This finding motivated us to test the selectivity of our detector since, in principle, detection by resonance absorption should result in the unambiguous determination of CO concentration. We tested a mixture of 4200 ppm of N_2O in N_2 at atmospheric pressure using our acoustically nonresonant detector and observed no signals above the usual background level. We also tested a mixture of 4200 ppm of N_2O and 49 ppm of CO and found that the observed optoacoustic signals did correspond to those obtained for 49 ppm of CO in the complete absence of N_2O.

No attempt was made to increase our detectivity beyond 0.15 ppm. This sensitivity was limited in part by the low output power of our laser. In this connection, it is of interest to note that a chemical laser capable of emitting almost one watt on transitions in the 1 → 0 band of CO has been reported.[6] The use of such laser would easily extend our detectivity to the sub-ppb level.

ACKNOWLEDGMENT

This work was supported by E.P.A under IAG-D5-E681, and by the Department of Energy.

FOOTNOTE AND REFERENCES

*Complete version of this work has been accepted for publication in Applied Physics Letters.

1. N. D. Sze, Science 195, 673-675 (1977).
2. K. Westberg, N. Cohen, and K. W. Wilson, Science 171, 1013-1015 (1971).
3. N. M. Amer and R. Gerlach, Lawrence Berkeley Laboratory Report, LBL-6854 (November 1977); N. Djeu, Appl. Phys. Lett. 23, 309-310 (1973).
4. R. J. Nordstrom, J. H. Shaw, W. R. Skinner, J. G. Calvert, W. H. Chan, and W. M. Uselman, "Computer-Generated Long-Path Air Spectra," EPA-600/3-77-026, available from Environmental Sciences Research Laboratory, E.P.A., Research Triangle Park, North Carolina 27711.
5. C. D. Hollowell and G. W. Traynor, to be published.
6. W. Q. Jeffers, H. Y. Ageno, C. E. Wiswall, and J. D. Kelley, Appl. Phys. Lett. 29, 242-244 (1976).

THE ROLE OF BUFFER GASES IN OPTOACOUSTIC SPECTROSCOPY*

L. Thomas, III, M. J. Kelley, and N. M. Amer

INTRODUCTION

Little attention has been given to the role of the buffer gas (defined as the optically non-absorbing gaseous component in optoacoustic detectors) in optoacoustic spectroscopy. In principle, the molecular weight, and the thermodynamic and transport properties of the buffer gas should have a significant impact upon the optoacoustic signal. One would also expect the energy transfer between the absorbing species and the buffer gas to play an important role in optoacoustic detection.

We have investigated the dependence of the optoacoustic signal on the following physical properties of the buffer gas: molecular weight and isotopic efects, heat capacity, thermal conductivity, and viscosity. The following series of noble, diatomic, and polyatomic gases were studied: Ne, Ar, Kr, Xe, N_2, CO, N_2O, $^{12}CO_2$, $^{13}Co_2$, and SF_6. The optically absorbing molecule in our case was CH_4 whose ν_3 absorption band lies conveniently in near coincidence with the 3.39 μm output of He-He lasers.

In the case of a binary gas mixture, for a cylindrical cell the acoustic resonant frequencies are given by[1]

$$f_{mnp} = \frac{\bar{v}_s}{2}\left[\left(\frac{\alpha_{mn}}{r}\right)^2 + \left(\frac{p}{\ell}\right)^2\right]^{1/2} \qquad (1)$$

where f_{mnp} is the frequency at which the acoustical modes occur. The eigenvalues m, n, and p refer to radial, azimuthal, and longitudinal modes, respectively; r is the radius and ℓ the length of the cavity, α_{mn} is the m^{th} zero of the derivative of the Bessel function

$dJ_n(\pi\alpha)/d\alpha$, and $\bar{v}_s$ is the sound velocity in a mixture of ideal gases (and is given by $\bar{v}_s = (\bar{\gamma}\ RT/M)^{1/2}$, where R is the ideal gas constant). We determine the effective specific heat ratio $\bar{\gamma}$ and the average molecular weight $\bar{M}$ for the mixture from

$$\bar{\gamma} = \frac{x\ C_p^b + (1 - x)\ C_p^a}{x\ C_v^b + (1 - x)\ C_v^a} \quad ;$$

$$\bar{M} = xM^b + (1 - x)\ M^a$$

where C_p, C_v^b, C_p^a, and C_v^a are the heat capacities of the buffer and absorbing gases, respectively; M^b and M^a are their molecular weights; and x is the fractional concentration of the buffer gas.

From Eq. (1) it can be seen that the acoustic resonant frequencies are partially determined by the combined properties of the buffer and absorbing gases. In our case since $x >> (1 - x)$, the acoustical behavior of the cell will largely be determined by γ and M of the buffer gas.

EXPERIMENTAL RESULTS

In Fig. 1 we show typical acoustical excitation spectra for pure CH_4 and for 0.9% Ch_4 inN_2 and Xe; and in Table 1 we summarize our results. The agreement between the observed resonance frequencies and those calculated from Eq. (1) is excellent. Furthermore, our experimentally deduced velocity of sound for the different gases tested agrees to within $\leqslant$0.8% of the calculated values. The discrepancy is attributable to uncertainties in the temperature and dimensions of the cell. As predicted, when the molecular weight of the buffer gas is increased, the resonance frequencies of the cavity shift to lower values.

In Table 1 we list the signal-to-noise ratio (S/N) as well as the experimentally and theoretically derived quality factor Q for different buffer gases. It can be seen that Xe enhances significantly the amplitude of the optoacoustic signal and yields the highest S/N observed. The largest experimental Q obtained was that of SF_6, with CO_2 proving to be the most dissipative.

It should be noted that the amplitude of the optoacoustic signal is a function of: (1) the heat capacity of the mixture, (2) the laser power absorbed, (3) the modulation frequency, (4) the vibrational relaxation times of CH_4, and (5) damping effects of the buffer gas. The first four contribute to the power going into the sound wave, and the last mechanism determines the Q of the resonances.

Assuming that boundary layer losses are the dominant dissipation mechanism, a theoretical Q can be obtained from[2,3]

$$\frac{1}{Q_{cal}} = \frac{1}{\ell}\left[d_v + (\bar{\gamma} - 1)\ d_h\left(1 + \frac{\ell}{r}\right)\right] \qquad (2)$$

where the viscous boundary layer thickness $d_v = (2\eta/\rho\omega)^{1/2}$, the thermal boundary layer thickness $d_h = (2\kappa/\rho C_p\omega)^{1/2}$, η is the viscosity, κ the thermal conductivity, ρ the density of the gas mixture, and ω is the frequency.

The ratio Q_{exp}/Q_{cal} is an indication of the relative significance of different energy dissipating mechanisms in the optoacoustic cavity. A value of unity for this ratio indicates that

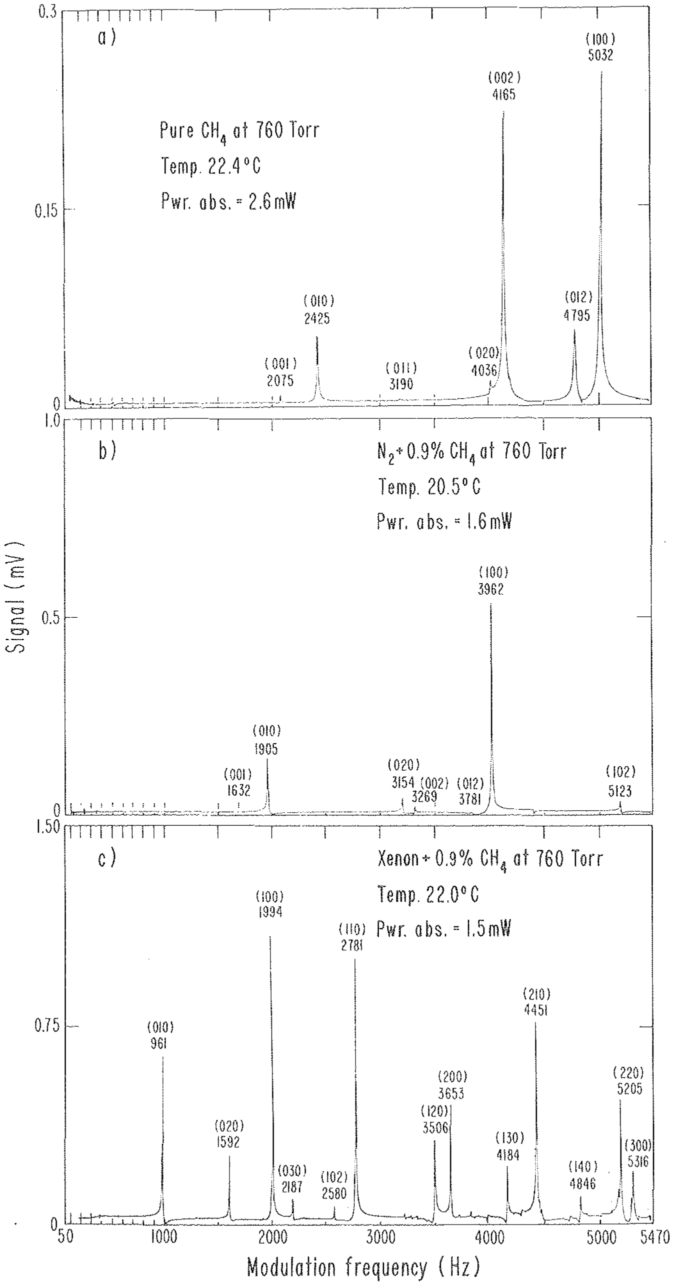

Fig. 1. Typical acoustically resonant optoacoustic spectra. (XBL 7710-2099)

Table 1. Summary of experimental results.[a]

Buffer Gas[b]	f_{100}(Hz)[c]	Q_{exp}[d]	Q_{exp}/Q_{cal}	S/N
Ne	5074	554	0.56	3800
Ar	3619	694	0.62	6300
Kr	2495	832	0.86	11000
Xe	1995	903	0.95	14000
CO	3967	929	0.63	4900
N_2	3966	1030	0.71	5700
$^{12}CO_2$	3030	250	0.16	1400
$^{13}CO_2$	2994	270	--	1700
N_2O	3009	673	0.43	3300
SF_6	1522	1220	0.99	5500

[a] C_p, κ and η were obtained from Ref. 6. F_{100}, Q_{exp}, Q_{exp}/Q_{cal}, and S/N for CH_4, without buffer gas, are 5033 Hz, 500, 0.24, and 2800, respectively.
[b] Spectroscopic grade.
[c] Typical uncertainty 1 Hz; f_{100} values agree to better than 0.8% with those calculated from Eq. (1).
[d] Q measured at half-power; typical uncertainty 5%.

the viscous and thermal dissipations at the cell wall are the sole sources for sound energy loss. When $Q_{exp}/Q_{cal} < 1$, additional dissipating mechanisms have to be invoked in order to explain this discrepancy. For the case of diatomic and polyatomic molecules, one must take into account the irreversible energy transfer from the sound wave to the molecule. As a consequence, one would expect the characteristic relaxation times governing these transfer rates to affect the value of Q.

Typical resonant optoacoustic spectra contain three useful quantities; the frequency, the Q, and the amplitude of the signal. An illustration of their utility is given in the following two examples:

1) It is of interest to investigate the ability of optoacoustic spectroscopy to mass-resolve[4] two isotopes of the same molecular species. Figure 2 shows the acoustic signatures for the first radial mode of $^{12}C^{16}O_2$ and $^{13}C^{16}O_2$. As expected, due to the mass difference, the frequency of the (100) mode shifts from 3032 Hz to a lower value of 2994 Hz, which is in complete agreement with the theoretical prediction of Eq. (1).

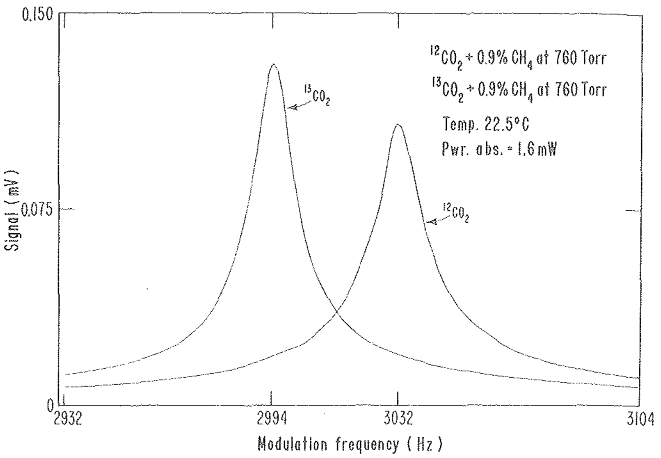

Fig. 2. First radial mode of the isotopically substituted pair $^{12}CO_2$ and $^{13}CO_2$. (XBL 7710-2098)

2) To verify the sensitivity of our approach to differences[4] in γ, when the molecular weight is very nearly identical, we determined the (100) resonance frequency for N_2O and $^{12}CO_2$ whose molecular weights are 44.013 and 44.010; and whose γ's are 1.301 and 1.287, respectively. From Eq. (1) the first radial mode for N_2O and $^{12}CO_2$ should occur at 3009 and 3030 Hz, respectively. In Fig. 3 we present the experimental spectra which agree very well with the predicted values and which correspond to a difference of only 1.8 m/sec in the sound velocity in the two gases.

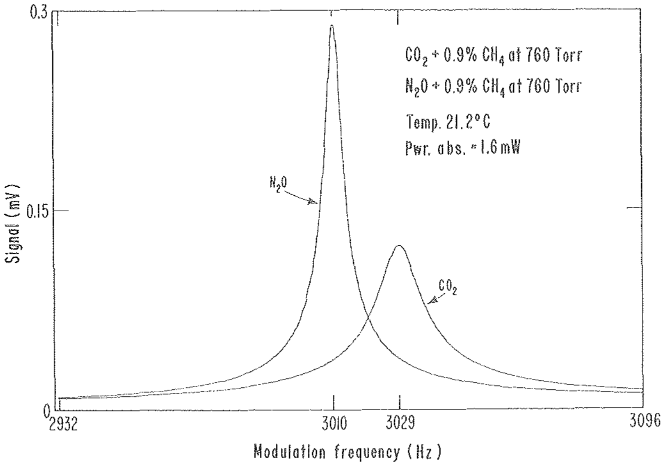

Fig. 3. First radial mode of $^{12}CO_2$ and N_2O. (XBL 7710-2100)

CONCLUSIONS

The practical implications of our results are manifold. First, with respect to extending the flexibility and sensitivity of optoacoustic spectroscopy, we have shown that it is no longer necessary to limit the applicability of laser optoacoustic spectroscopy to species whose absorption must match available laser radiation. Instead, "doping" with a relatively small amount of an optically absorbing gas yields optoacoustic signatures of non-absorbing materials. We have also demonstrated that for a fixed cavity dimension, the molecular weight of the buffer gas can serve as a means of shifting the frequency of the acoustical resonances to any region of interest for the purpose of optimizing S/N. Furthermore, irrespective of the frequency dependence on molecular weight, the use of such buffer gases as Xe enhances the sensitivity of optoacoustic detection. A consequence of both results is that, in the case where resonant optoacoustic detection is desirable, it now becomes possible to construct miniature resonance optoacoustic detectors by employing the appropriate high molecular weight buffer gas. Such a compact, room temperature detector can be of use in, for example, conventional and Fourier infrared spectroscopy and in gas chromatography-infrared analyzers.

Secondly, our findings point to the potential of this technique as a versatile analytical tool for "coarse" mass spectrometry and isotope analysis, for gas analysis, and for monitoring chemical reactions via changes in heat capacity and sound velocity.[5]

Finally, we have shown that quantities such as γ and v_s can now be measured readily by optoacoustic spectroscopy.

Extensions of various aspects of this work are currently being pursued in our laboratory.

FOOTNOTES AND REFERENCES

*Complete version of this work has been accepted for publication in Applied Physics Letters.

1. P. M. Morse, Vibration and Sound (McGraw-Hill, New York, 1948).
2. R. D. Kamm, J. Appl. Phys. 47, 3550 (1976).
3. P. M. Morse and K. U. Ingard, Theoretical Acoustics (McGraw-Hill, New York, 1968); P. M. Morse and K. U. Ingard, in Handbuch der Physik, S. Flügge, ed. (Springer-Verlag, New York, 1961), Vol. XI, part 1.
4. Frequency resolution will depend on the linewidth of the resonance mode; i.e., the Q, which is gas dependent.
5. A. Einstein, Preuss. Akad. Wiss., Berlin, Ber. 24, 380 (1920).
6. K. Raznjevic, Handbook of Thermodynamic Tables and Charts (McGraw-Hill, New York, 1976); JANAF Thermodynamical Tables (U. S. Nat. Bur. Stand., NBS 37, 1971); J. C. McCoubrey and N. M. Singh, Trans. Farad. Soc. 53, 877 (1957).

MINIATURE WAVEGUIDE CO_2 LASER

R. Gerlach and N. M. Amer

INTRODUCTION

Gas lasers made from very narrow bore discharge tubes (on the order of a few hundred times the optical wavelength) have many attractive features.[1] Very high gain coefficients (inversely proportional to diameter) and high output power per unit volume can be achieved; and since narrow bore lasers work best at high pressures, they are capable of wideband tunability by virtue of pressure broadening. In such lasers the free-space modes used in conventional lasers have high diffraction losses, negating the benefit of high gain coefficient. However, there exist other low-loss modes in which the optical field behaves as a guided wave confined by the dielectric walls of the discharge tube. For this reason such lasers are known as waveguide lasers.

Our goal is the development of a CO_2 waveguide laser for use as part of an optoacoustic system for detecting ammonia. Ruggedness and compactness are the chief advantages of a waveguide laser over a conventional CO_2 laser for this application. The waveguide laser might also be useful for other experiments, such as injection locking of a TEA CO_2 laser, where the wide tunability of the waveguide laser would make it possible to utilize a greater part of the large TAE laser linewidth than would be possible with a conventional CO_2 laser.

Most of the waveguide CO_2 lasers which have been reported were constructed from either glass (usually fused silica) or beryllia ceramic (BeO) tubes. The latter material is vastly superior in performance because of its excellent thermal conductivity, but it is expensive and, due to its high toxicity, is difficult to work with. A compromise can be achieved with alumina ceramic (Al_2O_3). This material has a thermal conductivity between that of BeO and glass, is relatively inexpensive, and is non-toxic. The results of our first experiments with an alumina laser tube are reported here.

ACCOMPLISHMENTS DURING 1977

We began by using a tube of 1/4 in. outer diameter and 1/8 in. (3.2 mm) inner diameter. The reason for using such a large diameter was that for smaller diameters, diffraction of the beam emerging from the ends of the waveguide results in high beam divergence, requiring short focal length concave mirrors to refocus the beam into the ends of the waveguide.

Since we had only flat mirrors, we chose to lessen the diffraction effects by using a tube diameter somewhat large for CO_2 waveguide lasers, but still much smaller than is common in conventional CO_2 lasers.

Due to its diameter, the waveguide nature of our laser is questionable. With a cavity length of 38 cm, a 3.2 mm aperture gives a Fresnel number of only 0.66 at wavelength 10 microns. Fox and Li[2] have calculated that for this Fresnel number, the fundamental free-space mode of a planeparallel cavity would have a power loss of more than 25% per pass. Due to the high gain of the laser, oscillation of this mode cannot be ruled out in spite of the losses. However, the diffraction losses for the TEM_{10} free-space mode are 60% per pass, which would seem to make oscillation on this mode unlikely. Since we have in fact observed lasing on higher transverse modes by varying the cavity alignment, we interpret this as evidence that we obtained waveguide, rather than free-space, modes.

We used a tube 11-3/4 in. long (see Fig. 1). The ends of the laser were 1/4 in. x 1/8 in. x 1/4 in. stainless steel swage-type male run tees on which the 1/8 in. male pipe thread portion has been milled off at Brewster's angle. (A large bore glass laser tube employing a similar scheme has been described previously.[3]) These tees were attached to the ends of the ceramic tube with teflon ferrules. Sodium chloride windows were epoxied to the Brewster angle faces. The fittings at the ends of the tube served as electrodes for the discharge. A slow flow of gas through the laser was maintained, and gas entered and left the tube through polyethylene tubing attached to the side outlets of the tees. A mixture of 70% He, 20% N_2, and 10% CO_2 was used. Inlet and outlet pressures were measured with a 200 Torr Wallace & Tiernan gauge.

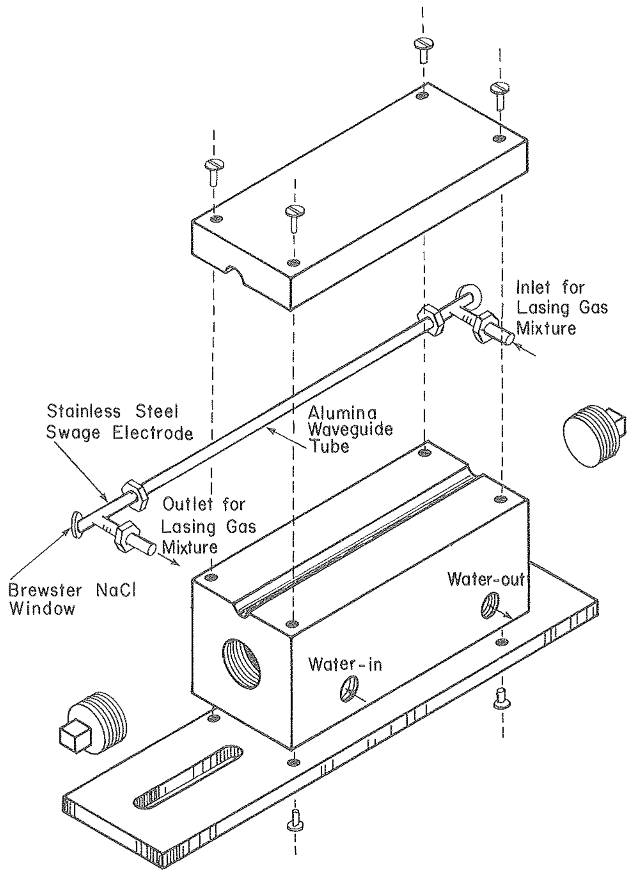

Fig. 1. Schematic diagram of the miniature waveguide laser. (XBL 78 614)

The ceramic tube rested in a 1/4-in. diameter round groove in a water-cooled aluminum block 9 in. long. An uncooled aluminum slab, also with a round groove, was screwed down on top of the tube. The tube fit snugly in the grooves, and thermal contact was improved by use of silicone grease.

The optical cavity consisted of two flat mirrors, one a dielectric coated copper high reflector and the other a dielectric coated ZnSe mirror with 95% reflectivity at 10.6 μ.

We examined the performance of the laser as a function of pressure, current, and flow rate for pressures up to 78 Torr and currents up to 10 mA. The highest output power, 4.6 W, was obtained with an average pressure (average of inlet and outlet pressures) of 56 Torr and a current of 10 mA. At average pressure 61 Torr, the power increases by about 40% as the pressure drop across the tube (due to flow) is increased from 0 to about 5 Torr; above 5 Torr the power remains constant. At 56 Torr and 10 mA, the voltage drop across the tube is about 10.4 kV, and when the voltage drops across the ballast and current regulator are added, the total supply voltage needed is 15 kV. Higher voltages are needed at higher pressures.

At the highest pressure investigated, 78 Torr, an output of 3.3 W could be obtained. The ability of the laser to operate at such a high pressure suggests that wide tuneability should be possible; however, for the present laser length, the tunability would be limited by the free spectral range of the cavity (about 390 MHz). A shorter tube would have to be used for wider tuneability.

PLANNED ACTIVITIES FOR 1978

Our next step is to employ smaller bore versions of this same design. We will also be using shorter tube lengths for wider tuneability, where a grating will be incorporated in the cavity for single line operation.

REFERENCES

1. J. J. Degnan, Appl. Phys. 11, 1-33 (1976).

2. A. G. Fox and T. Li, Bell Syst. Tech. J. 40, 453 (1961).

3. N. Amer and R. Gerlach, E&E Div. Annual Report, 1975.

THE DEVELOPMENT AND APPLICATION OF X-RAY FLUORESCENCE ANALYTICAL TECHNIQUES

R. D. Giauque, R. B. Garrett, and L. Y. Goda

INTRODUCTION

X-ray fluorescence (XRF) techniques are being developed and applied to support programs which require trace multielement chemical analysis. Over the past year we have contributed to programs which: (1) studied the distribution of elements in spent oil shale, shale oil, and retort waters obtained from oil shale retorting experiments, so that potential environmental control problems associated with shale oil production may be anticipated; (2) assessed the contribution of primary particulates to the ambient particulate burden and evaluated the role of primary particulates in the formation of secondary aerosol species; (3) determined the impact of emissions from catalyst-equipped cars on air quality for automobile-related pollutants; and (4) studied problems associated with industrial solid waste management.

ACCOMPLISHMENTS DURING 1977

An XRF method for the determination of 40 elements of atomic number 22 (Ti) and higher, in both geochemical and industrial waste management samples (e.g., coal fly ash and sludge pond residues), has been established.[1] Pulverized samples are mixed 1:4 with sulfur powder and prepared in the form of pressed disks. In addition to acting as a binder, the sulfur matrix dominates the absorption properties of the specimen disks. Thus, matrix absorption corrections can be determined for a single specimen and applied to the analyses of a wide range of samples. Standardization is achieved with nebulized multielement solution deposits, as well as two single-element vacuum vapor deposited thin-film standards. Using two 25-min. analysis periods, results are typically accurate to within ±5% when x-ray counting statistics are not the limiting factor. Table 1 lists the results for NBS Standard Reference Material 1633, Trace Elements in Coal Fly Ash, and serves as an illustration of the capability of this method.

The above method has been applied to programs in which it was necessary to determine the concentration of a broad range of metals in solid wastes, including those from energy generation, prior to waste disposal. In one brief study, the XRF results from analysis of ashes, collected from the fireboxes of ships using Bunker sea oil, has led to reclamation of metals. These wastes, which previously had been dumped, were found to contain relatively high concentrations (percent range) of vanadium, chromium, and nickel. These metals are now being recovered commercially.

Table 1. Comparison of XRFA results for NBS SRM 1633, trace elements in coal fly ash (μg/g ± 2σ unless otherwise indicated).

Element	XRF	NBS	Ref. 2
Ti	0.86%±0.11	...	0.74%±0.03
V	195±156	214±8	135±15
Cr	159±115	132±2	127±6
Mn	528±104	493±7	496±19
Fe	6.22%±0.48	...	6.2%±0.3
Co	130	(38)	41.5±1.2
Ni	101±7	98±3	98±9
Cu	133±4	128±5	...
Zn	126±14	210±20	216±25
Ga	41±7	...	...
Ge	26±5	...	...
As	63±7	61±6	58±4
Se	11±1	9.4±0.5	10.2±1.4
Br	6±2	...	12±4
Rb	108±4	(112)	125±10
Sr	1342±20	(1380)	1700±300
Y	60±5	...	62±10
Zr	290±7	...	301±20
Nb	28±2	...	...
Mo	25±5	...	...
Ru	3±2	...	...
Rh	4	...	...
Pd	4	...	...
Ag	4	...	...
Cd	4	1.45±0.06	...
In	3±2	..	0.32±0.10
Sn	5±2	...	...
Sb	4±3	...	6.9±0.6
Te	5	...	...
I	6	...	2.9±1.2
Cs	10	...	8.6±1.1
Ba	2670±85	...	2700±200
La	82±20	...	82±15
Ce	160±23	...	146±15
Ta	22	...	1.8±0.3
W	19	...	4.6±1.6
Hg	12	0.14±0.01	...
Pb	72±5	70±4	75±5
Th	21±3	(24)	24.8±2.2
U	9±6	11.6±0.2	12.0±0.5

We are assisting in a study of the partitioning of trace elements in simulated *in-situ* oil shale retorting experiments. Using previously developed XRF methods we have analyzed a series of samples of oil shale, and of suspended particulates collected from retort waters. It is hoped that potential problems associated with the disposal of residues from the production of shale oil may be established on a quantitative basis. A variety of analytical methods are being used for these studies.

PLANNED ACTIVITIES FOR 1978

X-ray fluorescence thin specimen techniques are being developed for the determination of elements of atomic number 22 (Ti) and higher in liquid samples. Less than 0.5 ml of liquid will be required for analysis. We plan to determine the concentrations of a broad range of metals in shale oils and liquid wastes.

Another method will be established for the determination of 22 trace elements in coal specimens. Coal samples are to be mixed 1:1 with sulfur powder and specimens, which are infinitely thick for the radiations of interest, are to be prepared. Compton scattered MoK excitation radiation will serve as an internal standard to compensate for matrix absorption effects, and also as a measure of spectral background intensity.[3] Multielement standard solutions deposited on microcrystalline cellulose powder, mixed 1:1 with sulfur powder, will be used for standardization.

To date, we have not been successful in establishing an accurate XRF method for the determination of sulfur in coal. Sulfur can be present in many forms such as sulfates, sulfides, and various organic compounds. Using pressed disks, unreasonably low results have been obtained for sulfur when present as pyrite, due to particle size effects. This occurs because the particles of pyrite have not been ground sufficiently fine, i.e., $<2\mu$, so that the samples are homogeneous for the x-ray energies selected for analysis. We have attempted to stabilize matrix effects and minimize the particle size required. To do this, samples were ground and blended 1:4 with sodium carbonate, which serves as a high absorbing substance for S K x-rays. However, the results still have been low. Further attempts will be made to prepare specimens for which particle size effects are not a critical problem.

REFERENCES

1. R. D. Giauque, R. B. Garrett and L. Y. Goda, Anal. Chem. 49, 1012 (1977).
2. J. M. Ondov, W. H. Zoller, I. Olmez, N. K. Aras, G. E. Gordon, L. A. Rancitelli, K. H. Abel, R. H. Filby, K. R. Shah, and R. C. Ragaini, Anal. Chem. 47, 1102 (1975).
3. C. E. Feather and J. P. Willis, X-Ray Spect. 4, 41 (1976).

APPLICATIONS OF NEUTRON ACTIVATION ANALYSIS (NAA) TO ARCHAEOLOGY AND THE HUMANITIES

F. Asaro, H. V. Michel and D. F. Mosier

INTRODUCTION

Neutron activation analysis (NAA) reveals elemental abundances of an object, and, therefore may yield information on where an ancient object (artifact) was made. If the techniques of making the artifact have varied with time in the past, then these types of measurement occasionally may give information on when an artifact was made.

The program in NAA, for which University of California students and faculty in archaeology and the humanities have done a significant proportion of the work, consists of three areas: studies of ancient pottery, obsidian research, and studies of brass. The neutron activation analysis done at LBL is part of a measurement system in which about 50 elements are sought by NAA. Approximately 40 are usually detected in materials whose composition is similar to the earth's crust, and about 30 are measured with good precision and accuracy.

STUDIES OF ANCIENT POTTERY

A type of pottery from the Eastern Mediterranean called Tel El Yahudiyah Ware was thought to have a Palestinian origin. By NAA, eight out of twenty-one sherds of this ware, found in Cyprus, were shown to have originated in the Nile Delta. Eight others probably originated in Egypt, and the remaining five were consistent with an Egyptian origin.[1] None of the sherds matched known Palestinian or Cypriot chemical composition groups for pottery. This work suggests that subgroups of this pottery type, which were thought to have originated in Palestine or Cyprus, originated in Egypt. However, the style of the distinctive decoration in the ware (prolific puncture designs in the pottery), did not originate in Egypt. It was known from other work that a subgroup of this ware, from an earlier period than those just discussed, was made in Palestine. This earlier subgroup was studied in the present work, and found to be very different in its pottery chemistry than the later wares. It was found that x-ray fluorescence measurements could distinguish adequately between the major pottery compositional groups from Egypt, Eastern Cyprus and coastal Palestine.

The NAA measurements were applied to another type of problem, the search for the lost city of Wassukanni. Wassukanni was the capital of the Mitanni, a powerful people in northern Syria and Mesopotamia during the latter part of the eighteenth dynasty in Egypt. A king of the Mitanni, Tusratta, wrote letters on clay tablets to the Pharoah and to his daughter, the Pharoah's wife. These tablets were found in the Egyptian archives and dispersed. Through the courtesy of the Staatlich Museum in Berlin and the British Museum in London, a number of these tablets have been sampled and the powders analyzed by NAA. The chemical profile of these tablets has been compared[2] with those from the areas in northern Syria.[3] The profiles were completely different, and it appears as if Wassukanni were elsewhere. Currently about 900 samples from Northern Syria are being analyzed by X-ray fluorescence as a sorting tool. An estimated 10-15% of these will be analyzed by NAA. If a chemical match can be found between surface sherds from one of the Syrian tells, and only one match is found, the tell will probably be excavated.

In another study, neutron activation measurements of blue-glazed pottery from ancient Siraf on the Persian Gulf indicated that the pottery was imported from Mesopotamia. From this it was deduced that possibly a cornerstone of the Mesopotamian economy in Islamic times was due to the export of blue-glazed pottery.[4]

STUDIES OF OBSIDIAN

An outline of the functions of a national center for obsidian research was prepared. The report stressed that obsidian from archaeological sources can be very homogeneous. If sophisticated techniques of measurement such as NAA can be used to characterize obsidian from different sources, then inexpensive methods of measurement may be adequate for reliable source determination of artifacts. This is particularly true if the more sophisticated measurements are made on those samples whose origin is left uncertain by the more inexpensive techniques.

About fifty samples of Peruvian obsidian artifacts were used to define five major chemical compositional groups. A sixth was known from other measurements. About three additional groups were found, each of which contained only a few artifacts. It was determined that abundances of Ba and Sr would suffice to distinguish all groups, and that these could be easily measured with sufficient accuracy (15%) by two x-ray fluorescence (XRF) runs. In one run the 60 keV ray of ^{241}Am was used to excite Ba atoms in the obsidian producing measureable Ba x-rays. In the other run, Ag x-rays excited Sr atoms and produced measureable x-rays of Sr. Approximately 800 samples were measured by the x-ray fluorescence techniques and reliable identifications were made on approximately 90% of the samples. The NAA runs were made on the remaining 10% which comprised around eighty artifacts. Seven new groups were identified, four having at least two members. Nearly all ambiguities were resolved with this combined XRF-NAA system.[5] One chemical abundance group was pinpointed to a specific source in Quispisisa (over 270 km from the coast) by analysis of geological samples.[6]

From this work, which lasted four years, trading and exchange patterns of obsidian were suggested which could apply to a period of over several thousand years. As an example, prior to the beginning of the Huari empire at 600 AD, Cuzco type obsidian was rarely found more than a short distance outside the Cuzco area. During the flourishing of the Huari empire it was found as far away as 1000 km to the north.

We also studied[6] Mesoamerican obsidian from ancient workshops in the El Chayal area of Guatemala. Artifacts previously found in Belize (British Honduras) were found to agree nearly exactly in chemical abundance patterns with the workshop obsidian from Guatemala. Another study showed that previously postulated trading patterns in Belize were slightly in error. A nodal center for different trade routes, suggested to be Lubantuum in Belize, was found to be more likely Wild Cane Cay, nearer the coast of Belize.[7]

STUDIES OF BRASS

Recently a chemical study was made of the Plate of Brass, the inscribed plate presumably left by Sir Francis Drake when he visited California in 1579. A detailed investigation of the Plate's authenticity was initiated by the Bancroft Library[8] of the University of California at Berkeley. As part of that study, neutron activation, emission spectroscopy, x-ray fluorescence and atomic absorption measurements were made at our laboratory. X-ray fluorescence and neutron activation measurements were also made at the Research Laboratory for Archaeology and the History of Art at Oxford University in England. The agreement between the two sets of studies was generally excellent. As an example, the Oxford laboratory obtained 34.8% for the abundance of zinc by x-ray fluorescence and our laboratory obtained 35.0% by neutron activation. From the various measurements it was concluded at LBL that the plate was not authentic. The abundances of the major and trace elements indicated that the plate was manufactured between the eighteenth and the twentieth centuries, most probably the late nineteenth or early twentieth century. The study indicated that Elizabethan brasses should have higher levels of Pb, Zn, Fe, As, Sb, Ni, Ag and Au than modern brasses.

FUTURE PROJECTS

The search for Wassukanni will be continued with studies of Turkish pottery, if Syrian pottery does not match our chemical profile from King Tusratta's clay tablets. If profiles of tablets from other important "lost" ancient cities in Syria can be developed they will be compared with the "library" of Syrian chemical abundance patterns acquired in the Wassukanni project.

Peruvian obsidian artifacts will be measured to study the trading patterns of ancient Chavin. By analyses of additional source obsidian, attempts will be made to determine exact locations where obsidian corresponding to the major compositional types was mined. Attempts will be made to study Ecuadorian obsidian sources and artifacts.

In Mesoamerica more detailed studies of source obsidian from Ixtepeque Volcano in Guatemala will be reported. Studies will be made, in collaboration with the University of Texas, of Texas obsidian.

Further measurements of Elizabethan brasses will be made in collaboration with the U. C. Berkeley Bancroft Library. One or more astrolabes from the sixteenth century will be measured to see if the levels of impurities in Elizabethan rolled brass conforms to criteria found for cast brasses of that period.

REFERENCES

1. M. Artzy and F. Asaro, "Origin of the Tell El-Yahudiyah Ware," Lawrence Berkeley Laboratory, LBL-4399. (Submitted to the Journal for Archaeological Science.)
2. A. Dobel, F. Asaro and H. V. Michel, Neutron Activation Analysis and the Location of Wassukanni, to be published by Orientalia.
3. T. E. Davidson and H. McKerrell, Iraq 38, 45-56 (1976).
4. D. Whitehouse, Proceedings of the Intern. Conf. of Application of Techniques of Physical Science to Medieval Ceramics, Berkeley (in press).
5. R. Burger and F. Asaro, "Trace Element Analysis of Obsidian Artifacts from the Andes: New Perspectives on Pre-Hispanic Economic Interaction in Peru and Bolivia," Lawrence Berkeley Laboratory Report, LBL-6343, June 1977. Also to be published in Spanish by Revista del Museo Nacional, Lima, Peru.
6. F. Asaro, H. V. Michel, R. Sidrys and F. Stross, "High-Precision Chemical Characterization of Major Obsidian Sources in Guatemala," Lawrence Berkeley Laboratory Report, LBL-5984, April 1977. Also to be published by American Antiquity.
7. F. H. Stress, H. R. Bowman, H. V. Michel, F. Asaro and N. Hammond, "Mayan Obsidian Trade in Southern Belize," Lawrence Berkeley Laboratory Report, LBL-5220, February 1976. Also to be published by Archaeometry.
8. J. D. Hart, "The Plate of Brass Reexamined," Publication of the University of California at Berkeley Bancroft Library, 1977.

ACQUISITION OF A GAS CHROMATOGRAPH/MASS SPECTROMETER

A. S. Newton and W. Walker

INTRODUCTION

In response to the requirements of several research programs, the laboratory has acquired a gas chromatography mass spectrometer (GC/MS). The system contains its own data system. Because of the variety of samples expected from research groups with diverse interests, it was necessary to obtain the greatest possible flexibility in the GC/MS data handling system. A state-of-the-art system was necessary to avoid early obsolescence.

DISCUSSION

Complete specifications were written for the expected and desired performance of each part of the system and for the system as a whole. The specifications were written to assure best operation within the widest latitude of instrumental parameters. The gas chromatograph requirements included: isothermal or temperature programmed operation, with a temperature range of subambient to 300^{o}; the capability to accommodate either packed columns or capillary columns; and a "Grob" type injection block for capillary column operation which enables efficient utilization of very small samples and maximizes chromatographic separations.

The interface between the gas chromatograph and the mass spectrometer required a separate temperature control, a separator to remove the bulk of the helium carrier gas from packed columns before the eluate is introduced into the ion source of the mass spectrometer, and a direct inlet line of very low volume and minimum length to introduce the total eluate from a capillary column to the mass spectrometer ion source. The interface must also provide a connection for introducing reagent gases for chemical ionization studies. All interface connections are glass or glass-lined stainless tubing.

The mass spectrometer requirements included: a resolution capability $M/\Delta M = 4000$ at $M/z = 1000$; a mass scan from $M/z = 2$ to $M/z = 1000$, with the range within these limits being adjustable; a minimum scan time of less than 0.5 sec, with a reset time of less than 0.01 sec. This fast scan capability is necessary for operation with high efficiency capillary columns which can yield chromatographic peaks with a width of less than 1 sec; longer scan times or longer reset times result in apparently broadened GC peaks and decrease the ability of the system to separate components of complex mixtures. Mass spectrometer operation in either the EI (electron impact) or CI (chemical ionization) mode of the excitation was also required.

A desirable data system must be capable of storing the large amount of information generated by a mass spectrometer in a short time period. Furthermore, in order to effectively identify compounds, the system must rapidly retrieve and manipulate this data. Modern computers with high speed random access disk drives provide this capability. Such a computer, with appropriate software, becomes a powerful tool in data treatment and presentation of results. Notably, "libraries" of mass-spectral patterns of known compounds may be used to help determine the identity of unknown components in samples.

No single piece of commercial equipment met all our specifications and requirements. The Finnigan model 4023 met more of the requirements than other commercially available equipment, and therefore was purchased. Delivery was made in early July, 1977; the next three months were spent installing, debugging, and operating the equipment in order to check for compliance to specifications.

The equipment purchased consists of a Finnigan model 9610 gas chromatograh with its own microprocessor control, a model 4000 mass spectrometer with its controls, an Incos 2300 data system which includes a Nova 3/12 computer, a Wangco T2222 dual density dual disc driver with removable platters, a Tektronix-4010-1 terminal, a Versatec 800A hard copy unit, and a 300/1200 baud modem.

Each of us has taken three week-long courses on the interpretation of mass spectra, the operation and maintenance of the GC/MS system, and the theory and use of the data system.

Some twenty samples have been run through the GC/MS, and the mass spectral data for each chromatographic peak have been compared to spectral libraries for identification. Most of these samples were from model compound studies in various coal liquefaction processes. The samples varied in complexity from three chromatographic peaks to as many as thirty peaks. In these samples most of the resolved chromatographic peaks have been identified.

We expect a period of increased understanding of the capabilities and limitations of the GC/MS system, as more complex samples are run and operational experience is gained. The GC/MS provides a powerful additional analytical capability to the laboratory.

EXTENSION OF THE ZEEMAN ATOMIC ABSORPTION TECHNIQUE TO FIFTEEN ELEMENTS

T. Hadeishi and R. D. McLaughlin

INTRODUCTION

The funded development of the Zeeman atomic absorption (ZAA) technique began in 1972. The object at that time was to develop an instrument that would determine the amount of mercury in foodstuffs as rapidly as possible and with as little sample pretreatment as possible. The method was so successful that additional funding was obtained for extension to other elements and other sample types.

The instrument works by shining a light beam through a furnace which contains the sample to be analyzed. As the furnace is heated, the atoms of the elements of interest are vaporized, which causes the light beam to be absorbed in proportion to the number of atoms in the sample. The Zeeman effect modifies the light in such a manner that the instrument automatically corrects for absorption and scattering of the light by smoke and vapors not due to the element of interest.[1-4]

Recently, the technique has been applied to the analysis of materials resulting from the retorting of oil shales, i.e., raw shale, spent shale, shale oil and retort water. Hg, As, Se, Cd, Pb and Zn were determined in these materials. In addition a number of different sample types (i.e., coal, coal fly ash, bovine liver, orchard leaves, pottery and oil) were analyzed to determine the applicability of this method to different sample matrices. These samples were National Bureau of Standards reference materials except for the oil, which is a standard material commonly used in the analysis of fossil fuels. In every case the ZAA results agreed with other methods of analysis.

ACCOMPLISHMENTS DURING THE CURRENT CALENDAR YEAR

One of the difficulties in extending this technique to a larger number of elements is the construction of the light source. In order to make a compact instrument the light source must fit between the poles of a permanent magnet with a gap of one centimeter. During the past year this problem was solved by using the configuration pictured in Fig. 1. This discharge tube is made of readily available parts (swagelok fittings and automobile spark plugs) and is capable of exciting the spectra of both refractory materials and volatile materials in the small space between the poles of the magnet. Both RF and DC power are superimposed on the electrodes, which allows a high degree of control of the discharge. The discharge is confined by the magnetic field to a plane perpendicular to the field direction. For this reason the lamp is referred to as an MCL (magnetically confined lamp).

The cathode is usually made by drilling a 1/4-in. deep hole in a 10-24 stainless steel screw. This hole is then packed with the material whose spectrum is required. The MCL is first evacuated, the RF and DC power supplies are next

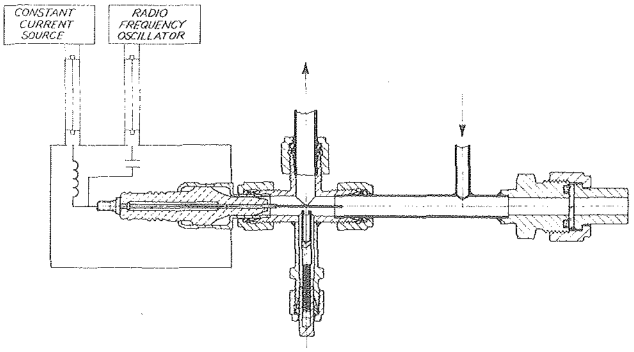

Fig. 1. Schematic of the magnetically confined lamp. (XBL 782-7032)

turned on, and the pressure is then adjusted to about 100 microns by allowing argon to flow into the system through the port shown in the figure. Experience with the MCL so far indicates that the spectrum of all the elements that are presently analyzed by atomic absorption techniques may be produced.

The goal of the work for the 1977 calendar year was to excite the spectrum of as many elements as possible using this new light source. In addition the lower limit of detection was determined for these elements. Table 1 lists the results and compares the sensitivities of the ZAA technique with the conventional atomic absorption method. The atomic absorption sensitivities were obtained with hollow cathode lamps that resulted from years of development effort directed toward obtaining a high intensity, stable, long-lived light source. To date the sensitivity of the MCL lamp is comparable, and in most cases better, than that of the hollow cathode lamp. As the MCL becomes more widely used, improvements in its operation characteristics will presumably occur.

Because of interest in continuous monitoring of the off gases from retorting of shale oil, one ZAA instrument was adapted to be an on-line mercury monitor. This was attached to the controlled state oil shale retort at Laramie Energy Research Center in Laramie, WY. We sought to determine whether the mercury comes out at a continuous rate as the flame front moves through the shale, or whether it condenses in the cool region ahead of the flame front, to come out at the end of the run. By using the ZAA monitoring instrument it was determined that the second description was the correct one.

Table 1. Comparison of MCL and hollow cathode Lamp.

Element	MCL LLD (pg)[a]	HCL Sensitivity[b]
Ag	5	8
As	100	160
Au	20	60
B	1,000	-
Ca	20	3
Cd	10	2
Fe	30	50
Ga	50	1,200
In	300	200
Pb	30	80
Pt	1,500	750
Sb	400	500
Se	400	3,000
Zn	7	0.7

[a] Amount of element that results in signal to noise ratio of 2.

[b] Amount of element causing 1% absorption (data from "Handbook of Spectroscopy," J. W. Robinson, Ed., CRC Press, 1974).

The results with this instrument have been very exciting. This work should be extended to determine more elements in samples of importance to the production of energy in its many forms. It is possible that funding for this research will result from discussions now in progress at Laramie Energy Research Center.

REFERENCES

1. T. Hadeishi, "Isotope-shift Zeeman effect for trace elements detection: An application of atomic physics to environmental problems," Appl. Phys. Lett. 21, 438 (1972).

2. D. A. Church, T. Hadeishi, L. Leong, R. D. McLaughlin, and B. D. Zak, "Two-chamber furnace for flameless atomic absorption spectrometry," Anal. Chem. 46, 1352 (1974).

3. T. Hadeishi, D. A. Church, R. D. McLaughlin, B. D. Zak, N. Nakamura, and B. Chang, "Mercury monitor for ambient air," Science 187, 348 (1974).

4. Tetsuo Hadeishi and R. D. McLaughlin, "Zeeman atomic absorption determination of lead with a dual chamber furnace," Anal. Chem. 48, 1009 (1976).

DEVELOPMENT OF A MILLIMETER-WAVE SPECTROMETER FOR ENVIRONMENTAL RESEARCH

B. Leskovar, W. F. Kolbe

INTRODUCTION

The purpose of this project is to develop the physical method of microwave rotational spectroscopy as a technique for the rapid and sensitive detection of gaseous pollutants and other atmospheric constituents.

Our calculations [1,2] have shown that favorable transitions for a number of species exist in the frequency region near 70 GHz. A sensitive microwave spectrometer operating in this frequency band has been designed and constructed. The spectrometer consists of a semiconfocal Fabry-Perot cavity,[3] a phase-locked microwave source and a low-noise superheterodyne receiver. The cavity can be electrically tuned by means of a piezoelectric transducer to enable it to track the microwave source. Work is under way to evaluate and optimize the performance of this instrument.

ACCOMPLISHMENTS DURING 1977

Microwave Spectrometer Development

During the past year the development and evaluation of the superheterodyne microwave spectrometer has continued. Measurements were made of small concentrations of the pollutant sulfur dioxide diluted in nitrogen using the 6(1,5)-6(0,6) rotational transition at 68982.1 MHz. In order to increase the system sensitivity, two forms of modulation followed by phase sensitive detection were investigated.

In the source modulation scheme the phase-locked signal oscillator is frequency modulated at 33 Hz and the piezoelectric tuned Fabry-Perot cavity is made to track these frequency excursions by means of a feedback signal from the receiver. The detected signal from the gas is approximately proportional to the derivative of the absorption lineshape. Figure 1 shows the results of a typical measurement, in this case SO_2 diluted to a concentration of 970 ppm and measured with a short detector time constant of 20 msec. With longer time constants (up to several seconds) the sensitivity is correspondingly increased. The results of these measurements are reported in greater detail in Ref. 4.

A second modulation scheme was also investigated in which a high voltage square wave electric field at 19 KHz was used to Stark modulate the molecular transition. The high voltage modulation signal was applied between the two mirrors of the Fabry-Perot cavity, which was modified by insulating and moving the spherical mirror to within 1 cm of the flat mirror. Measurements of dilute samples of SO_2 using this apparatus indicate a sensitivity about half of that obtainable with source modulation. This difference was attributed to the significant reduction in cavity Q resulting from the close proximity of the two mirrors.

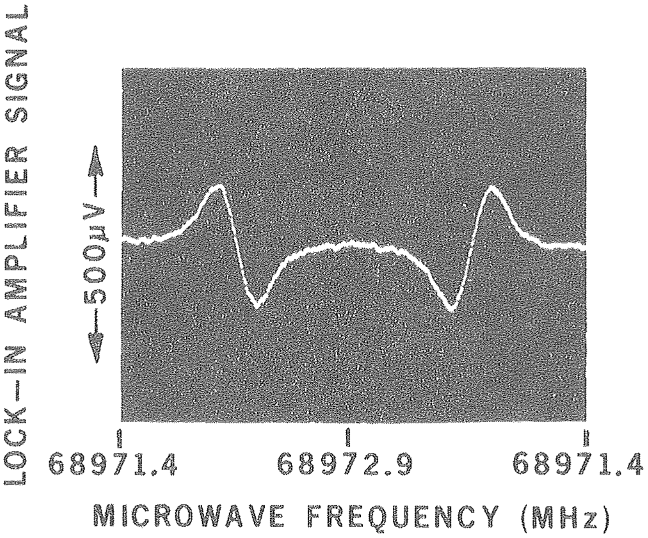

Fig. 1. Detected absorption signal for 970 ppm SO_2 in N_2 using source modulation and a time constant of 20 msec. The signal is presented twice due to the triangular sweep used. (XBB 781-288)

Noise Measurements

As has been shown,[5] the sensitivity of the spectrometer system is determined by the noise contributions of the signal source, the microwave cavity, and the receiver. Our measurements with the present system indicate that the major contribution to the overall system noise comes from the FM or phase noise generated by the source oscillator. This noise is converted by the slope of the cavity response curve into AM noise before reaching the receiver.

In the spectrometer system the microwave source is phase-locked to the 152nd harmonic of a frequency synthesizer. Within the bandwidth of the phase-lock loop, the phase noise is determined by the spectral purity of the synthesizer degraded by 44 dB due to the multiplication process. Measurements of the phase noise of the synthesizer and of the phase-locked microwave source were made using a narrow band spectrum analyzer. Modifications to the spectrometer system are under way which will reduce the contribution of FM noise reaching the receiver. These changes should significantly improve the overall sensitivity.

Fabry-Perot Cavity

Based on our experience with the present cavity,[6] a new Fabry-Perot cavity has been constructed and is presently being tested. Two features have been incorporated into its design which should result in better performance. The first is a more rigid mounting for the piezoelectric driver together with a spherical mirror of reduced mass. This should increase the stability of the cavity tracking system. The second is an improved input and output cavity coupling structure which will reduce cavity losses. In addition, the cavity and enclosure has been designed with a minimum of exposed metallic surfaces, which will permit the study of unstable molecular species such as SO and O_3.

Data Processing System

A data processing system incorporating a PDP 11/34 computer has been put into operation. This system is based on a CAMAC interface to the spectrometer. All of the necessary CAMAC modules to control the spectrometer and to provide signal averaging capabilities have been designed and constructed. These include a real time clock to provide accurate timing, a multiplexed analog-to-digital converter for data acquisition, and a digital interface to control the synthesizer frequency. A stepping motor and controller have also been incorporated to provide automatic tuning of the Fabry-Perot cavity. The necessary software to drive these modules is in the final stages of development.

PLANNED ACTIVITIES FOR 1978

We plan during the next year to complete the interfacing of our spectrometer with the data processing system. This will enable us to make more rapid and accurate measurements of various gases. Our sensitivity should be significantly improved through the use of more efficient signal averaging and digital filtering techniques. In addition, we will incorporate a number of design changes in the spectrometer electronics as suggested by our measurements of the past year. Finally, the performance of the new Fabry-Perot cavity will be evaluated and measurements of unstable species such as SO will be made.

REFERENCE

1. W. F. Kolbe, B. Leskovar, H. Buscher, J. Mol. Spectros. 59, 86 (1976).
2. W. F. Kolbe, H. Buscher and B. Leskovar, J. Quant. Spectr. Rad. Transf. 18, 47 (1977).
3. H. T. Buscher, B. Leskovar and W. F. Kolbe, "Application of Microwave Fabry-Perot Resonantors in Instrumentation for Air Pollution Research," Lawrence Berkeley Laboratory Report, LBL-4469, Feb. 1976.
4. W. F. Kolbe and B. Leskovar, "Millimeter-Wave Spectrometer for Pollution Research," Lawrence Berkeley Laboratory Report, LBL-6128, Feb. 17, 1977.
5. B. Leskovar, D. B. Hopkins and W. F. Kolbe, "Optimal Design Criteria for Millimeter-wave Spectrometers," in Proc. Fifth European Microwave Conference, 1975 (Hamburg, September 1-4, 1975), pp. 228-232.
6. B. Leskovar, H. T. Buscher and W. F. Kolbe, "Piezoelectri-Tuned Microwave Cavity for Absorption Spectrometry," U.S. DOE Patent pending, Serial No. 825,503, August 17, 1977.

IN SITU THERMAL CONDUCTIVITY MEASUREMENTS IN CALIFORNIA LAKES: INSTRUMENTAL DEVELOPMENTS

J. Oldson and P. Wilde

Terrestrial heat flow may be approximated by: $q = -K(dT/dZ)$, where K = thermal conductivity; and (dT/dZ) = thermal gradient. In general, for oceanographic and shallow measurements in lakes by probes, (dT/dZ) is measured and K is estimated or measured on a separate sample. To improve the quality of heat flow values calculated from probes, a heat flow system has been developed which measures both the thermal gradient and the thermal conductivity in place. Thermal conductivity measurements are made taking advantage of the self-heating characteristics of the same thermistors used for gradient measurements. After the temperature of the ambient environment is taken by reading each thermistor at low current or neglible self-heating, the currents passing through each thermistor are simultanously increased to induce self-heating. To prevent conduction of the self-heat along the probe, each thermistor is insultated from the probe. Accordingly, the apparent temperature rise with time for each thermistor is a function of how rapidly the self-heat dissipates into the environment; in short, it is a function of the thermal conductivity of the sediment in the vicinity of each thermistor. For the present model, heat dissipation is about a thousand times larger than that obtaining in gradient measurements which have a power dissipation per thermistor of only 5 to 10 mW. Thus the system can be powered easily by batteries. Calibration of the thermistors for thermal conductivity measurements is made in the laboratory, by comparison with materials of known thermal conductivity and water content. The system has been tested at over 200 stations in the Salton Sea, Clear Lake, and Mono Lake areas of California.

REFERENCES

1. J. Oldson, E. Binnal, F. Parks, W. Low, and P. Wilde, "A Geothermal Prospecting

Heat Flow System for Thermal Gradient and Thermal Conductivity Measurements," in Gothermal Investigations of California Submerged Lands: California State Land Commission Report, Part B, 1976, 44p.

2. J. Oldson, P. Wilde, E. Welday, and R. Martin, "In Situ Thermal Conductivity Measurements for Heat Flow Determinations in Marine and Lacustrine Environment," EOS, Trans. Am. Geophys. Union 58 (6) 515.

THE SURVEY OF INSTRUMENTATION FOR ENVIRONMENTAL MONITORING

D. A. Mack, Y. C. Agrawal, N. M. Amer, P. Bhardwaja,
C. D. Hollowell, G. A. Morton, D. L. Murphy,
A. V. Nero, and M. S. Quinby-Hunt

INTRODUCTION

Environmental quality control is essential to our health and economic well-being. In the past decade, it has become clear that even trace quantities of certain pollutants can be detrimental to our health. Numerous highly sophisticated analytical procedures have been developed to detect these pollutants. To aid laboratories in choosing among the techniques and instruments available for monitoring and analysis, Lawrence Berkeley Labortory (funded initially by the National Science Foundation, ERDA and now the Department of Energy) has conducted a survey titled Instrumentation for Environmental Monitoring (LBL-1). The survey covers instrumental methods suitable for measuring radiation, examining biomedical specimens, and studying the environmental quality of air and water.

Material concerning a wide variety of environmental pollutants is also presented. The characteristics, forms, and effects of pollutants are discussed along with physical and regulatory control strategies.

The survey, contained in six loose-leaf volumes, is divided into four volumes: AIR, WATER, RADIATION, and BIOMEDICAL. The contents are listed in Table 1. Further description may be found a brochure[1] issued by the Technical Information Division of Lawrence Berkeley Laboratory. More than five thousand copies have been distributed to date.

Table 1. Contents of the survey of instrumentation for environmental monitoring, LBL-1.

Vol. 1 AIR	Vol. 2 WATER	Vol. 3 RADIATION	Vol. 4 BIOMEDICAL
Parts 1 and 1A: Gases Calibration Sampling[a] SO$_2$ NO$_x$ Oxidants Carbon Monoxide Hydrocarbons Part 2: Particulates Sampling[a] Mass Size Chemical Composition Haxardous Pollutants: Mercury Beryllium, Asbestos, Lead Noise	Calibration Sampling[a] Data Analysis Metal Nitrogen, Phosphorous, Sulfur Biological Pollutants: BOD, COD, DO, TOC Pesticides Phenolics Petrochemicals Oil and Grease Physical Parameters: pH, turbidity temperature, radiation	By Radiation type Alpha Radiation Beta Radiation X- and Gamma Radiation Gamma Spectrometry Neutrons Personal Dosimetry By Radonuclide Tritium Krypton-85 Strontium-89 and 90 Iodine-129 and 131 Radon-222 and its daughters Radium Uranium Plutonium	Carbon Monoxide SO$_2$ Asbestos Mercury Cadmium Lead Pesticides Radiation

[a] in progress

CURRENT AND FUTURE ACTIVITIES

The instrumentation and techniques used for analysis of environmental samples develop so rapidly that information regarding the state-of-the-art techniques can become outdated in a year or two. Our understanding of the sources, effects and methods of controlling pollutants also increases and changes yearly. This past year has been spent primarily bringing extant sections up-to-date. The entire RADIATION volume is being redone. The introduction material (which includes for the first time a discussion of the biological effects of radiation), and the sections on radiation (by radiation type) are essentially complete. The section on instrumentation by radionuclide is in progress.

In the AIR, WATER, and BIOMEDICAL volumes, the sections on trace element determination are being rewritten and updated. The background material and sections on instrumentation for Metals-in-Water are nearly complete and will be adapted for use in the section on Composition of Particulates in AIR (pt. 2), and for the discussion of the same techniques for determining trace-element concentrations in biological specimens. Sections on Sampling of Particulates (AIR, pt. 2) and Data Analysis (WATER) are also in progress.

FOOTNOTES

1. Available from the Technical Information Division, Lawrence Berkeley Laboratory, University of California, Berkeley, California, 94720.

Combustion Research

INTRODUCTION

Combustion of fossil fuels is our primary source of energy and is likely to remain so for quite some time. Two important factors in using this valuable, non-renewable resource are the efficiency of utilization of the fuel and the generation of pollutants which contaminate our environment. The combustion system used to burn the fuel and transfer the heat to either a working medium or the ultimate source is one of the most important steps in the long chain of processes which convert the fuel to energy from its original state. The aim of combustion research and development is to improve the overall efficiency of combustion systems while minimizing the pollution generated and the cost.

A combustion system typically involves a complex interaction of chemical and fluid mechanical phenomena. It is a fertile field for sophisticated research and development which draw on the academic disciplines of high temperature chemical kinetics and turbulent fluid mechanics. A number of the most recent experimental and theoretical research techniques, such as laser based instrumentation, molecular beam techniques, and powerful computational and numerical analysis techniques in fluid mechanics can be fully exploited in well planned programs of combustion research.

The initiation of research on problems associated with coal combustion is discussed in the first two articles. Coal is by far our largest fossil fuel research and we believe that its utilization can be significantly improved by a vigorous and farsighted research program. The first article describes a study of the combustion of solid coal and coal related fuels under conditions of slow heating rates. The research summarized in the second article is aimed at understanding and controlling the formation of submicron particulates in pulverized coal combustion.

The subsequent twelve articles summarize research projects covering a wide variety of combustion problems. Several are directly related to pollution problems; in particular there is a coordinated program aimed at developing clean burning internal combustion engines. Another important general area being studied (in three experimental and two theoretical projects) is the complex interaction of fluid mechanical turbulence with combustion heat release.

THE COMBUSTION OF COAL AND COAL RELATED FUELS IN AN OPPOSED FLOW DIFFUSION FLAME

W. K. Chin and R. F. Sawyer

INTRODUCTION

The utility of the opposed flow diffusion flame (OFDF) apparatus for the laboratory study of the combustion of gaseous, liquid, and polymer fuels has been demonstrated by a number of researchers. We have employed this configuration to study the steady state of combustion of graphite, pulverized coal, and solvent refined coal in an opposed flow of oxygen/nitrogen or oxygen/argon. The advantages of this geometry lie primarily in the ability to observe the combustion of coal and coal related or derived fuels in a particularly well controlled, steady state environment. While the heating rates, which are known to be important to the pyrolysis and combustion of coal, are considerably less than is typical of the burning of pulverized coal, they are in the range of applicability to the *in situ*, fluidized bed, and possibly stoker fed combustion of coal. Unlike most other experimental methods, the technique appears to be suitable for the study of a number of coal derived or coal related fuels such as coal, pressed pulverized coal, char, coke, solvent refined coal, and coal liquid--thereby providing a means of observing the combustion of these fuels under comparable combustion conditions.

ACCOMPLISHMENTS DURING 1977

The fuel holder and oxidizer nozzle are contained in a 10 cm diameter pyrex cross to eliminate external disturbances, to aid in the collection of product gases, and to allow operation at below atmospheric pressure if desired. One horizontal side of the cross serves as a viewing port, and the other provides access for temperature and gas sampling probes. The oxidizer enters through the top port and the fuel feed mechanism through the lower port. The sample feed system provides accurate placement and control of the location of the fuel surface to within ten micrometers. A laser beam and photodiode detector are used to sense the burning fuel surface, providing a signal to a stepping motor which automatically positions to the 12.7 mm diameter fuel rods. Linear regression rate measurements are obtained directly from a counter driven by the stepping motor feeding sample. Due to the substantial radiation loss from most surface burning fuels, including coal, it is not possible to burn some samples in air and an oxygen enriched flow is required.

Graphite, pressed pulverized coal, and solvent refined coal were selected for study to demonstrate the suitability of the method to this family of fuels and to provide a comparison among related solid fuels. Pressed pulverized coal was selected because of the chemical and physical homogeneity which such a material exhibits, especially in contrast to coal itself which is highly anisotropic and presents difficulty in insuring constancy from sample to sample. The pressed pulverized coal samples were prepared from Pittsburgh seam pulverized coal under 35 mesh (417 micrometer) sieve. The pulverized coal has significant ash content, about 6%. Rods were prepared in a plunger and die apparatus with and without the addition of a binder. Varying sample water content was obtained through dessication. Density, void volume, and pore size distribution of the pressed coal samples were found by porosimetry using a 400 MPa mercury intrusion porosimeter capable of measuring pore size from 70 down to 0.003 micrometers.

Burning rates were measured as linear regression rates for several sample compositions and under a range of oxidizer flow rates and oxygen concentrations. A typical record of the regression rate history of a pressed-pulverized coal sample is shown in Fig. 1. The irregularities are caused by the buildup and removal of an ash layer. Burning rate reproducibility was within eight percent, demonstrating the consistency of the sample preparation method. The effect of oxygen concentration was investigated by burning samples under a constant oxidizer flow velocity of 380 cm/sec and a varying oxygen fraction. The regression rate shows oxygen mole fraction or concentration dependency of the 0.74 power. Some selected burning rates for graphite, coal, and comparison materials are presented in Table I.

Temperature distribution within the solid phase during steady state combustion was obtained by an imbedded fine thermocouple. In this steady state burning, the measured temperature variation with time is equivalent to the instantaneous spatial temperature variation. It was found as expected, that the surface temperature increases with oxygen concentration in the oxidizer flow. Thermal diffusivities of the burning coal were extracted from the temperature measurements.

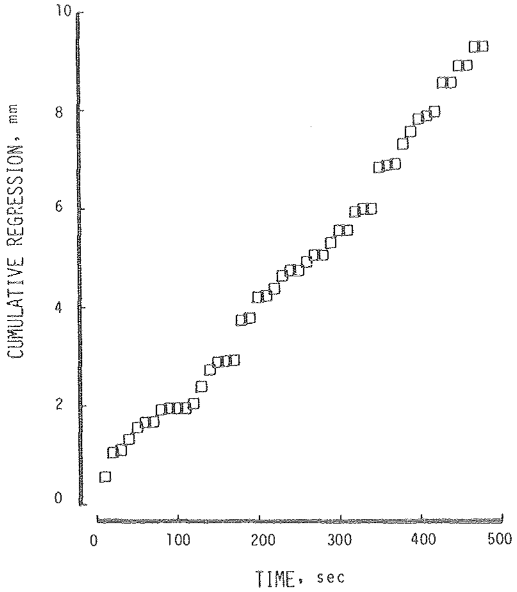

Fig. 1. Experimental regression curve for pressed pulverized coal burning in a mixture of .30 O_2 + .70 N_2; oxidizer blowing velocity, 380 cm/sec; sample density, 0.92 gm/cm^3. (XBL 782-7390)

Table 1. Burning rate data for selected solid fuels.

Material	Density (gm/cm^3)	O_2 Velocity (cm/sec)	Burning Rate (gm/sec)	Burning Rate (mm/sec)
Polymethyl Methacrylate	1.176	253	0.0137	0.0922
Maple Wood	0.731	253	0.0059	0.0640
Graphite I	1.528	589	0.0083	0.0427
Graphite II	1.334	479	0.0047	0.0279
Coal C-2[a]	1.097	253	0.0047	0.0340
Coal B-4-1[b]	0.950	253	0.0040	0.0330
Coal B-3-2[c]	0.902	253	0.0043	0.0279

[a] Pressed pulverized coal, no binder.

[b] Pressed pulverized coal, with binder, unsieved.

[c] Pressed pulverized coal, with binder, sieved.

CONDENSATION OF ASH AND TRACE METALS FROM PULVERIZED COAL COMBUSTION

P. Sherman and F. Robben

INTRODUCTION

Particulate emissions from sources burning coal have long been a health and environmental problem. Although much progress has been made in the development of devices for cleaning the effluent (such as electrostatic precipitators), there is considerable evidence that the collection of submicron particles formed from the combustion of coal is very inefficient. There is also evidence that the trace metals present in the coal are concentrated in the fly ash; in particular there appears to be an increase in the concentration of some metals with the decrease of particle size. These small particles which enter the atmosphere are the ones which are most easily ingested into the lungs and thus are more of a health hazard. The intelligent control of such particulate emissions by either modifications in the design of coal burning equipment or in the design of exhaust clean-up equipment requires as a first step an understanding of the mechanisms of formation of the particulates. Such understanding is also necessary in the consideration of environmental restrictions which should be placed on the burning of coal in the future.

At present, there is no good way of predicting the formation of the submicron particulates or any of their characteristics. Much more new information is necessary in order to obtain any predictive model for the generation of submicron particles. In particular, information is necessary relating the formation and growth of particles to the many combustion parameters. The condensation of vaporized ash, along with trace metals, is one suggested model for the formation of these submicron particles. The increase in concentration of the trace metals in these small particles is consistent with the formation and growth of these particles by condensation; further, rudimentary calculations using estimated combustion conditions support a condensation model.

ACCOMPLISHMENTS DURING 1977

In order to investigate the formation of particulates generated by the combustion of pulverized coal and to study the controlling parameters, a laboratory arrangement where appropriate measurements can be made was chosen as the first step. A simple system consisting of

1) an air-pulverized coal injection-conveyor system;

2) a burner for turbulent pre-mixed flow of pulverized coal, air and gaseous fuel;

3) a sample for the collection of submicron particulates on a substrate appropriate for electron microscope analysis has been designed and constructed.

Controlled variations in flow rates and fuel/air ratios can be made in the laboratory arrangement to change residence times, temperatures and temperature gradients, velocities and velocity gradients. A schematic of the present experimental arrangement is shown in Fig. 1. A jet ejector using air as a carrier gas entrains the pulverized coal from a hopper and blows the air-powder mixture through 3 mm diameter tubing into the 12 mm diameter vertical tube-burner. Gaseous fuel and air are metered, mixed in the vertical tube-burner, and burned with the flame stabilized at the tube exit. Oxygen enriched air may be used to facilitate burning the coal without gaseous fuels.

The sampler is evacuated with a vacuum pump so that a supersonic jet impinges on the collector surface. A cleaved mica surface with a thin evaporated carbon layer will be used as the collecting surface in the initial experiments. Transmission electron microscopy will be used to measure the particle sizes. A very sensitive spectroscopic technique known as Zeeman shifted atomic absorption, developed at Lawrence Berkeley Laboratory, will be used to measure the trace metal concentrations.

PLANNED ACTIVITIES FOR 1978

The apparatus described above will be used to evaluate the measurement techniques and then to try to obtain some information on the formation of submicron particles in this particular burner. Collection of samples from industrialized pulverized coal combustors may also be carried out in order to obtain more data on the emission of small particulates from commercial combustors.

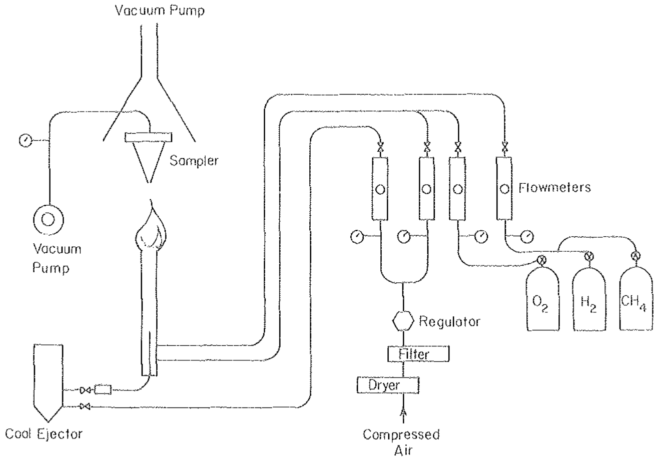

Fig. 1. Schematic of a pulverized-coal-burning experimental arrangement. (XBL 781-2380)

SECONDARY POLLUTANTS FROM AMMONIA INJECTION NO_x CONTROL PROCESSES

N. J. Brown, R. F. Sawyer, and A. K. Gordon

INTRODUCTION

Consideration of odd-nitrogen compounds (essentially all nitrogen containing compounds other than N_2) as air pollutants has been primarily focused upon the nitrogen oxides, NO and NO_2, with occasional interest in ammonia. The oxides of nitrogen result either directly or indirectly in atmospheric nitrogen dioxide, photochemical smog, nitrate compounds, and probably other compounds whose role in air pollution is less well defined.

Combustion sources both of the mobile and stationary types are recognized as the primary sources of the oxides of nitrogen. The two principal sources of nitrogen oxides in the combustion of conventional fuels are oxidation of atmospheric molecular nitrogen (thermal NO_x) and oxidation of nitrogen containing compounds in the fuel (fuel nitrogen NO_x). Until recently, the former has been the dominant source of NO_x; however, in combustion processes using crude oil, coal and shale derived fuels, and some refinery gases, fuel nitrogen can be a significant and even dominant source of NO_x. The amount of fuel nitrogen contained in fossil fuel can vary considerably with negligible amounts in natural gas, significant amounts found in distillate fuels, and amounts from 0.5 to 3 percent in heavier fuels (residual oil, coal, coal derived, and shale derived fuels). The amount of fuel nitrogen NO_x produced in combustion processes increases with the fuel nitrogen content of the fuel. Fuel nitrogen nitric oxides may account for more than half of the nitric oxides emitted from the combustion of high nitrogen content oil or coal in power plants.

The mechanism of fuel NO_x production, although not understood, appears favored under conditions different from those which enhance thermal NO_x production. Consequently, the various control strategies used in the United States to meet NO_x emission standards, namely the modification of the combustion processes to reduce thermal production, are ineffective in reducing fuel NO_x.

A new NO_x control technology has been patented by Exxon Research and Engineering Company which selectively removes NO from combustion effluents through homogeneous reaction with ammonia and oxygen. This process is distinctly different from other technologies in that it removes NO_x after its formation rather than attempting to prevent its formation. Thus, the process offers the possibility of removing both thermal and fuel NO_x. This process has been demonstrated commercially in Japan and is likely to be proposed for use in California for the control of oxides of nitrogen from stationary sources. The major question regarding this process is its potential for formation of secondary pollutants, especially at operating conditions different from those which are optimal for the reduction of oxides of nitrogen.

In recognition that NO_x removal through NH_3 addition now appears to be a viable control process for stationary combustion sources, a new research program sponsored by the California Air Resources Board has been initiated at Lawrence Berkeley Laboratory which is directed toward identification and quantification of the nitrogen containing products formed from the addition of ammonia. This research will be performed in a laboratory scale combustion tunnel with a well-controlled experimental environment. A test sequence is planned to examine product formation associated with 1) optimum ammonia addition conditions, 2) off-design ammonia addition conditions, 3) optimum and off-design ammonia addition conditions with an oil fuel rather than the propane of the first two test series, and 4) the effect of fuel additives and impurities on the nitrogen-containing products formed. The overall objective of this research is to provide a framework to assist the California Air Resources Board in assessing potential pollution hazards associated with application of the ammonia addition control process to reduce stationary source emissions.

ACCOMPLISHMENTS DURING 1977

A premixed, laminar flat flame is being used to provide a prototype combustion environment for developing and testing gas analysis procedures. A new burner which was designed and fabricated at Lawrence Berkeley Laboratory has been characterized, and its ability to support a stable, reproducible one-dimensional flame has been ascertained. Radial and axial temperatures and velocity profiles have been determined for a series of propane/air flames. An analytical scheme for N_2 and NO has been developed. A laboratory combustion tunnel has been designed utilizing a propane/air burner followed by a reaction duct, including a temperature controller, ammonia injector and sampling ports.

PLANNED ACTIVITIES FOR 1978

A continuing review of developments in the field of ammonia addition control technology will be conducted through examination of the open technical literature and direct contact with individuals and groups working in this field. This information is essential to the study of the secondary pollutant potential of the process. The combustion tunnel will be constructed and its performance will be characterized. A series of experiments varying fuel nitrogen additive type and concentration and equivalence ratio will be conducted to assess the ammonia addition process. N_2, NO and NH_3 concentrations will be measured as a function of time following the ammonia addition. Other nitrogen compounds which are products of the control process will be determined. The effect of operating at off-design conditions of temperature and mixture ratio will be determined.

CATALYZED COMBUSTION IN A BOUNDARY LAYER

R. Schefer, F. Robben, R. K. Cheng, and I. Namer

INTRODUCTION

Studies have indicated that considerable promise exists in the use of surface catalysis in the combustion process to reduce the associated pollution.[1] Results have shown that catalytically supported combustion makes possible the efficient burning of a variety of fuels under fuel lean pre-mixed conditions with a substantial reduction in thermal NO$_x$ levels. Surface catalysis is very effective in this application by initiating and speeding up the combustion reactions so that complete combustion can be attained under conditions where stable combustion is difficult or impossible to achieve using conventional combustors.

The principal objective of the present research is to improve the understanding of high temperature heterogeneous catalysis of combustion reactions and the coupling with the homogeneous reactions and the fluid mechanics. Combustion in the laminar boundary layer of a heated flat plate with a free stream flow of premixed fuel and air involves most of the important physical and chemical processes of catalytic combustion systems while providing a geometry which facilitates experimental study and numerical modeling. The experimental configuration used in the present study consists of a thin quartz plate with vacuum deposited platinum heating strips mounted over an open, atmospheric pressure jet of premixed hydrogen and air. Electrical heating of the platinum strips is used to heat the plate surface to temperatures approaching 1400°K. The plate may be used to study catalysis of combustion by a platinum surface, or may be coated with various other catalytic and noncatalytic materials. Current diagnostic techniques include laser-Doppler velocimetry for measurement of velocity, Rayleigh scattering for the measurement of density, and optical pyrometry for measurement of temperature. In addition, a variant of the Schlieren technique known as deflection mapping has given considerable insight into the boundary layer behavior under combustion conditions. Future measurements may include species concentration profiles utilizing Raman scattering of laser light and gas sample probing in conjunction with a gas chromatograph-mass spectrometer system.

ACCOMPLISHMENTS DURING 1977

Detailed density measurements were obtained over SiO and SiO$_2$ "noncatalytic" surfaces and with a platinum catalytic surface for equivalence ratios from 0.0 to 0.3 and plate temperatures up to 1250°K.[2] Measurements with the silicon dioxide surface indicated no gas phase combustion of lean hydrogen-air mixtures at surface temperatures up to 1250°K. This was determined by comparison of experimental and calculated thermal boundary layer profiles and boundary layer thicknesses. The numerical results show a very marked thickening of the thermal boundary layer in the zone of maximum energy release rate, as well as a peak in the temperature profile. Neither of these was present in the experimental results. In Fig. 1 thermal boundary layer thickness is plotted as a function of distance from the plate leading edge for equivalence ratios from 0 to 0.1. As shown, the measurements agree well with numerical calculations for no combustion, and thus it is concluded that no gas phase reactions were occurring under these conditions.

Similar results were found with a catalytic platinum plate where no gas phase reaction was apparent up to a surface temperature of 1200°K. However, significant surface combustion was measured at plate temperatures less than 900°K. Preliminary measurements indicate that surface heat release rates can be determined from the change in power input to the plate heating strips as fuel is added. Such measurements will be useful in evaluating the effectiveness of various catalytic surfaces.

The numerical calculations were carried out based on a numerical finite difference solution of the governing differential equations for laminar boundary layer flow and combustion over a heated flat plate.[3] A detailed hydrogen-air reaction mechanism with 13 reactions and 8 chemical species was used. Results for a lean ($\phi = 0.1$) H$_2$/air mixture over a heated constant temperature ($T = 1100^{\circ}$K) noncatalytic plate indicate the existence of several stages of combustion. These include an initial induction period during which

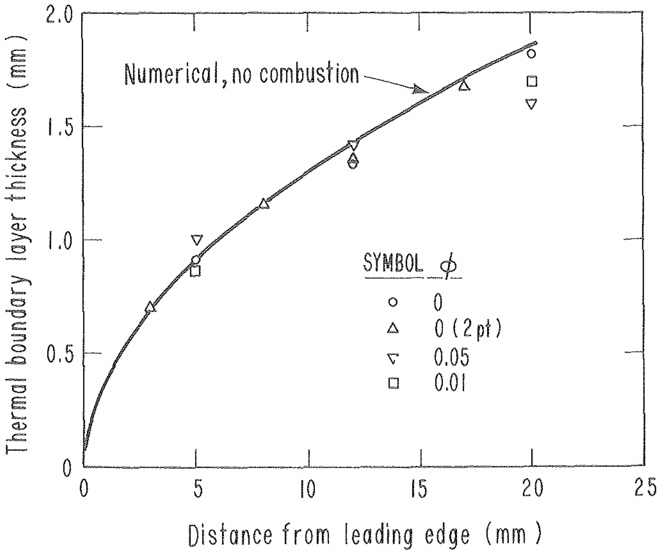

Fig. 1. Comparison of measured thermal boundary layer thickness ($T/T_\infty = 2.0$) at hydrogen-air equivalence ratios of 0.0, 0.05, and 0.10. Silicon dioxide coated plate with surface temperature of 1250°K and free stream velocity 3.17 m/s. Also shown is the numerical result for combustion. (XBL 779-2011)

radical concentrations increase with little associated heat release and a downstream region of rapid heat release during which the boundary layer rapidly thickens. Typical species concentration profiles for this case are shown in Fig. 2 as a function of nondimensional distance above the plate. The results shown are for a distance of 1.98 mm from the plate leading edge.

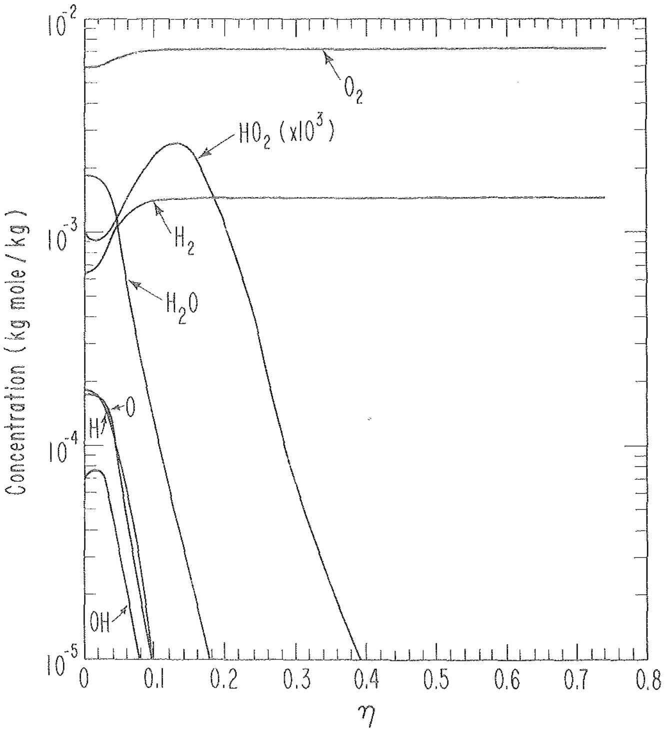

Fig. 2. Concentration profiles as a function of nondimensional distance above plate noncatalytic plate. X = 1.89 mm from leading edge. H_2/air combustion. $\phi = 0.1$, $T_{wall} = 1100K$, $U_\infty = 3.17$ m/s. (XBL 779-2006)

A simplified model was formulated for a catalytic surface based on equilibrium conditions for species diffusing from the surface, and calculations were carried out for the same conditions as with the noncatalytic surface. The equilibrium wall was found to act as a source of radicals very near the plate leading edge. Further downstream it behaves as a sink for radicals and results in a delay of the onset of homogeneous combustion.

PLANNED ACTIVITIES FOR 1978

More extensive data will be taken over platinum and SiO_2 plates. This data will include measurements over a greater range of equivalence ratios and plate temperatures under conditions in which gas phase and surface reactions occur simultaneously. Alternate catalytic and noncatalytic surfaces and additional fuels such as methane and propane will be studied. Further development of data reduction techniques should allow accurate determination of the relative importance of surface as opposed to gas phase reactions and heat release. A more realistic model for surface reaction will also be developed.

REFERENCES

1. W. S. Blazowski, and D. E. Walsh, Combust. Sci. Technol. 10, 233 (1975).

2. F. Robben, R. Schefer, Y. Agrawal, and I. Namer, Catalyzed Combustion in a Flat Plate Boundary Layer I. Experimental Measurements and Comparison with Numerical Calculations, Paper 77-37, Fall Meeting, Western States Section of the Combustion Institute, Stanford, CA, October 17-18, 1977. Also Lawrence Berkeley Laboratory Report LBL-6841 (1977).

3. R. Schefer, and F. Robben, Catalyzed Combustion in a Flat Plate Boundary Layer II. Numerical Calculations, Paper 77-38, Fall Meeting, Western States Section of the Combustion Institute, Stanford, CA, October 17-18, 1977. Also Lawrence Berkeley Laboratory Report LBL-6842 (1977).

TECHNIQUES FOR THE STABILIZATION OF LEAN COMBUSTION SYSTEMS

J. W. Daily, A. K. Oppenheim, and R. F. Sawyer

INTRODUCTION

A program has been underway for the past three years to study problems associated with stabilizing lean pre-mixed, pre-vaporized gas turbine combustors. The work has focused on the development and utilization of a two-dimensional model gas turbine combustor fitted with quartz side windows which allow optical studies of the combustion phenomena. The combustor itself has a variable fuel inlet system to allow study of separate fuel-air addition and combustion characterizing pre-mixed, pre-vaporized fuel-air addition. Air preheat of up to 600° Kelvin is also possible to simulate compressor heating. The combustion of lean pre-mixed fuel-air mixtures is of special interest for simultaneous emissions reduction and maintenance of combustion efficiency.

ACCOMPLISHMENTS DURING 1977

A number of experiments have been run using the two-dimensional burner. Initial work involved the mapping of temperature, velocity and composition fields within the burner using conventional probe techniques, flow visualization through high-speed schlieren motion pictures, establishment of blow-out characteristics, and observation of transient behavior at blow-out. More recent work involves the application of advanced laser-based spectroscopic diagnostics, especially that of Rayleigh scattering density measurements.

The gas turbine combustor test section is constructed so that fuel and air are mixed and passed through a flow straightener. The mixture is then accelerated over a rearward facing step, and a flame is stabilized in the recirculation zone which exists behind the step. Recent work on large scale eddy structures and turbulent shear flows has given a new direction to our understanding of such flow fields. One of the basic findings of this research program has been the firm establishment of experimental evidence for such large scale motion. Analysis of still photographs and high-speed schlieren motion pictures reveals several results, some of which were not expected:

1. Long exposure time schlieren pictures, 20 milliseconds or longer, show a well-defined region immediately behind the step which is commonly referred to as the recirculation zone.
2. Shorter exposure schlieren pictures, 1 millisecond, show a pattern of large eddies which grow downstream to a size of the order of the chamber height and intrude into the recirculation zone.
3. The color high-speed schlieren motion pictures confirm the pattern of the large scale structure observed in the still pictures, and reveal additional details, both qualitative and quantitative, including the formation of the eddies, their shedding frequency spectrum, growth rate, coalescence and intermittent intrusion into the recirculation zone. Flow patterns for both non-reacting and reacting flows have been observed and compared.

PLANNED ACTIVITIES FOR 1978

The study of transient phenomena within the burner is underway. It is anticipated that the information gathered in studying more steady flows will be of help in understanding such transient behavior.

PERTURBATION OF A FLAME FRONT BY A VORTEX SHEET

R. K. Cheng, I. Namer, F. Robben, R. Schefer, and L. Talbot

INTRODUCTION

The propagation of flames in premixed fuel-oxidizer gas in the presence of fluid mechanical turbulence is an important feature of many practical combustion systems. This problem has been studied at some length; however, there is no satisfactory theoretical model for such a flame front, nor is there much experimental data which are able to differentiate between the various theoretical models, or suggest alternative models. The research program summarized here is intended to give greater insight into the interaction of a flame front with a turbulent flow.

Turbulent flow consists of fluctuations in the velocity. The small scale fluctuations may be random and uncorrelated, but, at least in many situations, the larger scale fluctuations consist of vortices which are often well correlated. It is presently popular to refer to this aspect of turbulent flows as "coherent structures." It is also presently believed that combustion and flame propagation in turbulent fluids may be dominated by these larger scale coherent structures. In the present research these vortices are simulated by the Karman vortex sheet shed by a cylinder, which is located upstream of a stabilized flame front in an otherwise laminar flow. Time and space resolved density and velocity measurements are made by laser light Rayleigh scattering and laser Doppler velocimetry, respectively. A phase locked signal averaging technique will be used to obtain the density and flow fields associated with the disturbance of the flow and flame front by the vortices shed from the cylinder.

Although the experimental data are measured point by point, plotting of these data at a given phase time related to the original and repetitive vortex structure will give a series of "pictures" of the vortex as the flame propagates through it. Such pictures will most likely consist of contour plots of density and velocity at various phase times. Such a complete picture should help evaluate the validity of the wrinkled laminar flame theory as well as lead to a better quantitative understanding of flame generated turbulence and the dilation of eddies as they pass through an oblique plane flame.

ACCOMPLISHMENTS DURING 1977

Most of the experimental facility has been completed and preliminary measurements have been made on two flow configurations.[1] Measurements on a flame stabilized on a heated 0.25 mm platinum wire in a 5 cm open jet showed rather large fluctuations in flame position due to the turbulent mixing eddies at the interface between the jet and the surrounding air. We concluded that this flow configuration would not be suitable for the proposed study. By enclosing the flow in a 5 cm square channel with pyrex walls, the flame stability was greatly increased. In this case, a 3.2 mm rod was used to create a Karman vortex sheet, generated at a frequency of 22 Hz, and measurements of the turbulent density fluctuations through the flame front were made. Perturbations of the flame front outside and upstream of the region of the vortices in the wake of the rod were found. To our knowledge, such perturbations have not been discussed in the literature. We have attributed them to the overall disturbance of the flow field by the fluctuating flame front.

PLANNED ACTIVITIES FOR 1978

In order to implement the phase locked signal averaging technique, a PDP-11 computer will be used to correlate and signal average the measurements. A hot wire will sense the vortex shedding frequency and phase, and thus give a time reference for the computer controlled measurements. This hot wire will be located in the wake of the cylinder, upstream of the flame front, and will give minimal disturbance to the flow.

REFERENCE

1. I. Namer, Y. Agrawal, R. K. Cheng, F. Robben, R. Schefer, and L. Talbot, Interaction of a Plane Flame Front with the Wake of a Cylinder, Paper 70-50, Fall Meeting, Western States Section of the Combustion Institute, Stanford, CA, October 17-18, 1977. Also University of California Report FM-77-3.

TURBULENT COMBUSTION IN A BOUNDARY LAYER

R. K. Cheng, F. Robben, R. Schefer, H. Dwyer and L. Talbot

INTRODUCTION

This report presents the status of and the future plans for the study of turbulent combustion in a boundary layer over a flat heated surface. The main objective of this program is to further the understanding of the complex mechanisms involved in combustion in turbulent environments. Our present goal is to look for correlations between the parameters of the coherent turbulent structures and the thermodynamic as well as chemical properties associated with combustion reactions through experimental measurements of density and flow velocity. For this purpose, turbulence will be initiated by controlled sources placed in the stream ahead of or within the boundary layer. These sources will be a vibrating rod or obstacle of some sort. The results should help establish an experimental foundation for the development of numerical models of turbulent combustion processes.

ACCOMPLISHMENTS DURING 1977

The present experimental facility is similar to the one used for the surface catalyzed combustion study. The range of Reynolds numbers possible with a platinum coated quartz plate is too low to approach the transition to turbulence in a viscous boundary layer. We have designed and are constructing a vertical wind tunnel with a 2.5 cm square modular test section where one of the walls will be lined with heating elements to heat the boundary layer. This modular design allows a much greater length for growth of the boundary layer than the flat plate configuration, resulting in larger Reynolds numbers approaching that necessary for transition to turbulence.

Diagnostics involve measurement of flow velocity by hot wire anemometry, laser Doppler velocimetry and laser particle tracking of gas density by Rayleigh scattering of laser light, and of the temperature of the heated surface by optical pyrometry. The measurements will be phase-locked to the disturbance frequency so that the details of the coherent disturbances can be measured.

Some measurements of the velocity fluctuations in a non-reacting turbulent boundary layer have been carried out. Results were obtained using a quartz plate placed in an open air jet of 16 m/sec velocity. A stainless steel wire mesh was attached to the exit of the nozzle to disturb the flow. Velocity profiles of the boundary layer and the fluctuation intensities at different locations along the quartz plate were measured by a hot wire probe. Attention was paid to the growth of the fluctuation intensity as a function of location in the flow field.

A novel diagnostic technique involving photographic particle tracking combined with laser fringe anemometry has been tested in a nonreacting open jet flow as well as in a v-shaped flame stabilized on a heated wire. It was conceived by F. J. Weinberg of Imperial College, University of London, and may be applied to this study. This method is based on using a light sheet from a laser to illuminate light scattering particles seeded in the flow. The light sheet is both separated into fringes and interrupted at a known frequency so that the system can utilize both Doppler fringe anemometry and photographic particle tracking. Particle tracking gives the spatial distribution of velocities at one instant of time, and this type of information complements that obtained simultaneously from laser Doppler anemometry. Results of particle tracking in a v-shaped natural gas-air flame stabilized on a heated platinum wire is shown in Fig. 1.

PLANNED ACTIVITY FOR 1978

The vertical 2.5 cm square wind tunnel will be completed in the early part of 1978. Detailed velocity and density data will be obtained in the disturbed boundary layer over a non-heated, heated, and heated-with-combustion surface. These data will be checked for similarities in well-known dimensionless variables and analyzed to seek correlation with parameters such as disturbance frequency and combustion heat release.

A larger horizontal combustion wind tunnel will be designed with a channel about 12 cm square and one heated wall. This configuration will result in boundary layer Reynolds numbers greater than 10^5, so that measurements on coherent disturbances can be made in the range of transition to turbulence.

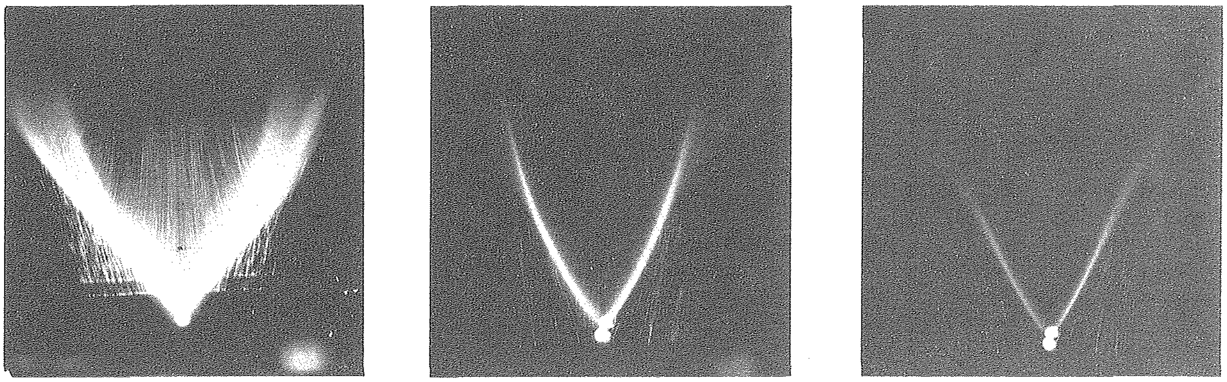

Fig. 1. Records of particle tracking in a V-shaped flame taken at three different exposure times (from left to right 1/2, 1/10, 1/25 sec) to vary particle track density. (XBB 782-2364)

NUMERICAL STUDIES OF LAMINAR AND TURBULENT COMBUSTION

A. J. Chorin, P. Concus, and P. Bernard

INTRODUCTION

In these studies we are developing computational techniques for analyzing turbulent combustion phenomena, such as those that occur in an internal combustion engine. Our goal is the construction of realistic models that are suitable for comparison with experiment and are capable of being used for design purposes. The specific features of the methods we are developing are (1) the use of sampling and random choice procedures and (2) the use of "dictionaries" of known phenomena as building blocks in the numerical schemes. These features allow us to overcome the major difficulties that have hindered the application of other numerical techniques to the study of physical combustion phenomena. Our methods, unlike others, have little or no numerical diffusion (and thus no cell Reynolds number restrictions), i.e., they can deal realistically with high Reynolds number flow. Because they are based on sampling rather than averaging, they can take into account the effect of organized structures (coherent eddies) in a flow. This feature is very important because real chemical phenomena are greatly affected, perhaps even determined, by the existence of coherent eddies and will not be accurately modelled if these coherent eddies are not taken into account.

ACCOMPLISHMENTS DURING 1977

We have continued to work on the development of random choice and random vortex methods for the analysis of turbulent and/or combusting flow. A course graining method, which represents a substantial advance over previously available methods, has been developed.[1] A new version of the vortex method, more accurate and computationally more efficient than previous versions, has been developed and analyzed.[2,3] These two methods have been combined in a computer program that analyzes turbulent boundary layers and bursting sequences for flow in a model cylinder-piston assembly. This is the first such program ever written capable of performing these calculations. It was observed that the bursting sequences dominate the turbulence and are the probable origin of intermittency in the flow.

PLANNED ACTIVITIES FOR 1978

Computer programs are being written for studying turbulent and laminar fluid transport based on the methods we have developed which do away with the introduction of artificial numerical diffusion. We plan to incorporate into these programs the means for solving numerically the ordinary differential equations of chemical kinetics so that chemically reacting flows can be treated. We expect to initiate a substantial and coordinated effort to model flows of practical interest, e.g., flow in the interior of a motored internal combustion engine and flow induced during a jet ignition process. We expect to work closely in this effort with experimentalists and engineers.

REFERENCES

1. P. Bernard, The Computation of the Mean Properties of Turbulent Flows in the Method of Coarse Graining, Lawrence Berkeley Laboratory Report, LBL-6455 (1977).

2. A Chorin, Vortex Sheet Approximation of Boundary Layers, Lawrence Berkeley Laboratory Report, LBL-6443, 1977 (to appear in J. Comp. Phys.).

3. O. Hald and M. del Prete, Convergence of Vortex Methods for Euler's Equations, Lawrence Berkeley Laboratory Report, LBL-6752, September 1977 (to appear in Math. Comp.).

NUMERICAL ANALYSIS OF FLOW FIELDS GENERATED BY ACCELERATING FLAMES

J. Kurylo, H. A. Dwyer, and A. K. Oppenheim

INTRODUCTION

The specific problem with which we are concerned is: steady flame propagates in an essentially unconfined combustible gas mixture. At a given moment its speed changes abruptly. The question is what happens then? The disturbances associated with this process may trigger the transition to detonation or they may die down leading eventually to the establishment of another steady state solution. Since the outcome depends on the law governing the flame propagation speed, while the experiments are relatively easy to perform, and a good deal of data on the transition to detonation in gaseous media is available in the literature, the numerical technique we are presenting should be instrumental in revealing such laws under a variety of conditions of practical interest. The phenomenon of a relatively rapid change in the flame propagation speed is well established in combustion literature. It is due to the effects of turbulence, and it has been exploited for many years in the form of the so-called Shchelkin turbulizers used in detonation research. More recently it has been employed by Wagner and his associates[1] for the study of unconfined explosions.

ACCOMPLISHMENTS DURING 1977

A new computational technique has been developed taking into account sharp discontinuities and their interactions, since their existence has been so prominently established by optically recorded experiments pertaining to this field of study.[2-4] For this reason the algorithm is set in Eulerian coordinates and is based on the use of a floating shock fitting technique[5] that has been generalized to treat all the discontinuous wave processes that can occur in the flow field. The basic algorithm used in this connection is that of MacCormack,[6] a non-centered difference scheme applied to conservation equations expressed in divergence form. The technique consists of predictor and corrector steps made, respectively, on a simple forward and backward difference scheme of first order accuracy, while the combined two-step process has a second order accuracy.

The computational scheme is capable of treating four types of discontinuities: shock waves, contact surfaces, deflagrations, and detonations. If these discontinuities propagate without interacting with each other nor with a plane, line, or point of symmetry, they are considered to be well separated and their position in the flow field established by the floating discontinuity technique. According to our algorithm, a discontinuity requires six to eight spatial grid points for its handling. This set of points defines its zone of influence. For each type of discontinuity, the computations handle such a zone with subroutine.

Of particular importance in the computational scheme is proper handling of deflagrations since the differentiating algorithm of the conservation equations cannot be applied across them. Through preliminary studies we have found that most of the difficulties are obviated by making sure that deflagration fronts are treated as discontinuities that always pass through computational grid points. This principle has been adopted as one of the keys of our technique: at each time interval the Eulerian computational grid is shifted throughout the whole flow field so that it moves with the velocity of the deflagration.

When the discontinuities are not well separated and their zones of influence tend to overlap, more elaborate differentiating algorithms are required in order to make sure that differentiation, applicable only to continuous portions of the flow field, are not carried out across a discontinuity.

The strategy adopted for the application of our technique is as follows. First the time-step is computed by the Courant-Friedrichs-Lewy stability condition, assuring that the numerical domain of dependence at every point in the flow field includes that of the set of hyperbolic partial differential equations governing the solution. Gas-dynamic parameters for all grid points of the flow field at the next time interval are then computed by applying the MacCormack predictor-corrector scheme as if there were no discontinuities involved in the problem. The types of discontinuities present in the flow field are then identified and located. By the use of appropriate subroutines the motion of the discontinuities and the flow fields around them are thereupon determined.

When the discontinuities tend to interact, subroutines for treating multi-discontinuity systems are invoked. After the interaction has terminated and the discontinuities become well separated, their positions are properly reordered and the computations continued in a routine manner.

REFERENCES

1. K. J. Dorge, D. Pangritz, and H. G. Wagner, Acta Astronautica 3, 1067 (1976).

2. G. D. Salamandra and I. K. Sevastyanova, Combustion and Flame 7, 169 (1963).

3. P. A. Urtiew and A. K. Oppenheim, Proceedings of the Royal Society A295, 13 (1966).

4. P. A. Urtiew and A. K. Oppenheim, 11th Intern. Symp. on Combustion, 665-670 (1967).

5. M. D. Salas, AIAA Journal 14, 583 (1976).

6. R. W. MacCormack, AIAA Paper 69-354, p. 6 (1969).

STRONG IGNITION LIMITS FOR METHANE-HYDROGEN MIXTURES

R. K. Cheng and A. K. Oppenheim

INTRODUCTION

This program pertains to dynamic properties of combustion in a homogeneous gas mixture. When such mixtures are brought uniformly and rapidly to a state of high temperature by a shock wave, they can either generate a blast wave or burn without exhibiting any gas-dynamics effects. The strong ignition limit is a line of demarcation between the two cases. It is usually expressed in terms of a curve on the plane of pressure and temperature of states at which the induction process takes place. The limit is determined experimentally by the use of the reflected shock technique. As a useful and essential by-product, induction time data are obtained. The strong ignition limit is, in effect, a specific measure of the capability of a given combustible gas mixture for transition to detonation and hence of the tendency to knock. This is relevant to a wide variety of combustion phenomena ranging from unconfined explosions on one hand, and reciprocating internal combustion engines on the other.

The gas-dynamic properties of exothermic processes induced behind reflected shocks have been explored in a program of studies conducted in the 1970's at the University of California, Berkeley. The structure of the flow field generated by the exothermic process associated with strong ignition was determined for hydrogen and for methane. Experimental observations were made by means of cinematographic laser schlieren and interferometric techniques. Their prominent features were confirmed by computations based on the currently available chemical kinetic data. On the basis of experience thus acquired, a simple experimental technique was developed for the determination of the strong ignition limit and the concomitant measurement of induction times. The latter involves the use of piezoelectric pressure transducers as time of arrival meters for fronts of pressure waves generated by the exothermic process.

ACCOMPLISHMENTS DURING 1977

A systematic investigation has been carried out of the strong ignition limit in a two-fuel system, methane and hydrogen. The scope of our experimental program covers a full range of compositions including two methane-oxygen mixtures, two hydrogen-oxygen mixtures, and seven different methane-hydrogen-oxygen mixtures, all diluted by 90% argon. A composition diagram for all the eleven test mixtures used is given in Fig. 1. Initial conditions behind the reflected shock were in the range of 800°K to 2500°K in temperature and 1.4 atm to 3 atm in pressure. In all, some 800 viable experimental runs were performed. The gasdynamic effects of combustion were observed for a number of experimental cases by cinematographic laser schlieren and interferometric techniques, while the bulk of data was deduced from pressure transducer records.

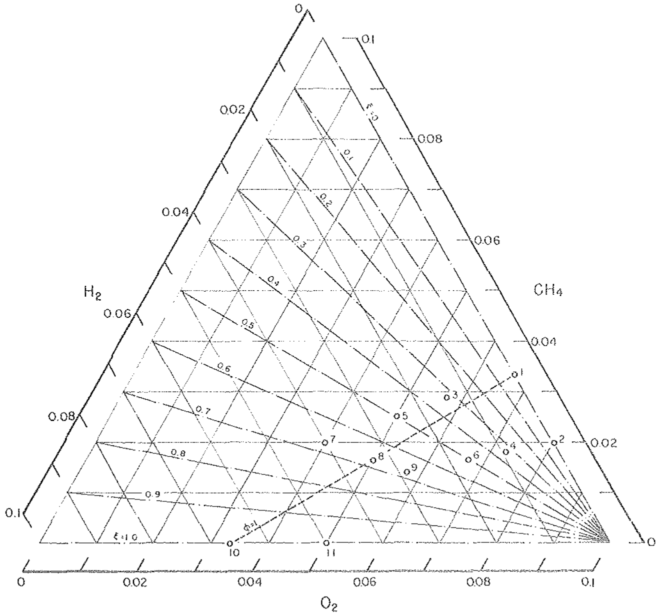

Fig. 1. Mixture compositions. (XBL 782-7388)

Strong ignition limits for all the test mixtures are shown in Fig. 2. The numbers refer to compositions specified in Fig. 1. Continuous lines represent experimental data reduced by non-linear regression. The chain-broken lines are the classical "explosion" limits, the lower bounds of self-sustained exothermic reactions. The broken lines were obtained from correlation formulae.

As manifested by our results, the addition of hydrogen has a significant effect on the strong ignition limit of methane, lowering considerably the temperature level at which it occurs.

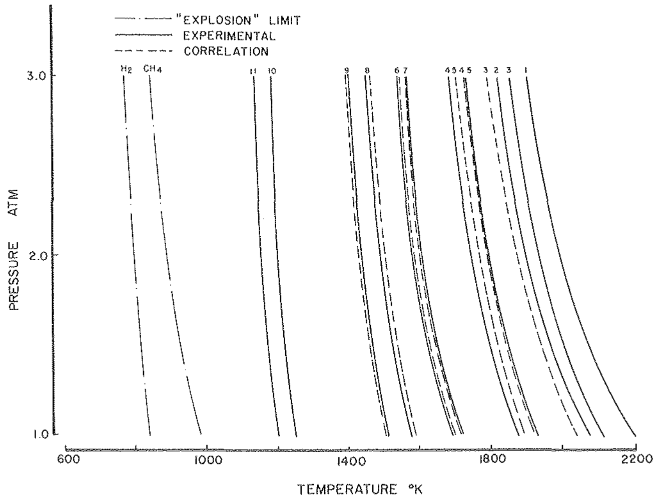

Fig. 2. Strong ignition limits. (XBL 782-7387)

LASER-INDUCED FLUORESCENCE SPECTROSCOPY APPLIED TO TURBULENT COMBUSTION FLOWS

J. W. Daily and C. Chan

One technique that shows great promise as a diagnostic tool for measuring species concentrations is that of laser-induced fluorescence spectroscopy (LIFS). The method consists of illuminating the gas with a laser source tuned to an absorption line of the species of interest. The molecules are excited, reradiating spontaneously, and fluorescence is observed at 90° to the laser beam. The beam diameter and the collection optics define the spatial resolution which may be as fine as 0.1 to 0.5 mm.

Our work has proceeded in three areas. The first deals with the use of saturated fluorescence to measure species concentrations in flames. The second has been the study of chemical decay processes by observing fluorescence decay. The third has been the study of the collisional redistribution process and near resonant Rayleigh enhancement.

The primary difficulty with using laser induced fluorescent spectroscopy to make density measurements has been that collisional de-excitation in high pressure flames completely dominates radiative de-excitation causing fluorescence quenching. In our work we have overcome this difficulty by using a laser source of sufficient intensity to saturate the exciting transition. Preliminary work with sodium has demonstrated the feasibility of the technique, and linear curves of growth for sodium atom concentration have been obtained. The dynamic range of the measurement is approximately two orders of magnitude, limited at low number densities by detectability limit considerations and at high number densities by radiative trapping.

Chemical reaction rates of the excited species may be examined by the fluorescent technique. If the characteristic decay time for the species of interest is of comparable length to the exciting pulse, chemical decay may be observed directly. We have observed such decay and are in the process of making measurements for a range of flame conditions.

One problem that exists for atomic fluorescence spectroscopy is that fluorescence trapping severely limits the dynamic range. One potential method for overcoming this limitation is to observe the enhanced Rayleigh scattering near resonance, rather than the fluorescence signal itself. If the laser is detuned from resonance slightly, then the spectrum of the scattered light consists of a Rayleigh scattering line at the laser frequency, a fluorescent signal which is caused by collisional redistribution of energy to the resonant state, and perhaps a three photon signal if the laser intensity is sufficiently large. We have observed the Rayleigh and the resonance peaks in sodium in flames. We have demonstrated that the Rayleigh component is not significantly trapped at number densities much higher than that for which fluorescence trapping becomes important.

We are now presently examining the use of laser induced fluorescence spectroscopy to measure radical species concentrations in flames and to study chemical reaction rates of such species.

REACTIVE AND INELASTIC SCATTERING OF $H_2 + D_2$

N. J. Brown and D. M. Silver*

INTRODUCTION

Combustion science is concerned with chemistry and fluid mechanics and the coupling between them. A detailed knowledge of combustion chemistry remains elusive since multistep mechanisms prevail and individual reaction steps are difficult to isolate for experimental study. The application of theoretical kinetics to combustion chemistry has been rather limited relative to the experimental effort; however, some theoretical considerations are often used to eliminate potential reaction steps in a proposed chemical mechanism. One such idea is that bimolecular reactions between stable molecules generally have high reaction barriers, and thus relatively small rate coefficients. This idea has been challenged for simple exchange reactions.[1] To further investigate the feasibility of such bimolecular reactions, a theoretical study of a prototype reaction, $H_2 + D_2$ exchange, was undertaken.

This four part study involved the construction of four H_4 potential energy surfaces and the investigation of the inelastic and reactive scattering of $H_2 + D_2$ on them. The dynamics are treated quasi-classically and this formalism incorporates the following three approximations: (1) treating the dynamics with classical mechanics, (2) restricting initial molecular energies to experimentally determined eigenenergies, and (3) using Monte Carlo techniques to compute average final state properties of several collisions with identical initial energy configurations. The results of the scattering study are presented in terms of reaction probabilities, average final state properties of the molecules, and average final state energy distributions. The effects of alignment and surface properties are examined.

The initial study[2] of this set made use of a simple model potential energy surface of the London type which had an anomalously low reaction barrier (when compared to ab initio results) in the square planar saddle point configuration. This type of surface has become increasingly popular for molecular scattering calculations because of its relative ease of construction. Hence the purpose of this particular study was to provide a prototype calculation of a bimolecular reaction process occurring on a London surface. The total system energy considered in the study was less than the H_2 dissociation energy. The only reaction observed was the four center exchange reaction forming two HD molecules, and the probability of this reaction decreased with increasing initial vibrational energy since vibrational energy decreased the probability for the favored reaction geometry.

A second study employing a semi-empirical valence bond type surface was conducted at total energies of 150 kcal/mole. Four reaction paths were found.

$H_2 + D_2 \rightarrow 2H + D_2$ (hydrogen dissociation) (1)

$H_2 + D_2 \rightarrow H_2 + 2D$ (deuterium dissociation) (2)

$H_2 + D_2 \rightarrow HD + H + D$ (single exchange) (3)

$H_2 + D_2 \rightarrow 2HD$ (double exchange) (4)

The particular path followed by the reactants was found to be extremely sensitive to the system's initial energy configuration. In general, total reactivity was directly related to the amount of initial vibrational energy in the system, and specific reactivity along the four paths was related to the distribution of initial vibrational energy between the reactant molecules.

ACCOMPLISHMENTS DURING 1977

Three potential energy surfaces have been computed using valence bond theory to generate a simple model wave function. The surfaces are constructed using the semi-empirical treatment of the London-Eyring-Polanyi-Sato type, but modified to include all overlap and multiple exchange integrals. Different parameterizations have been used to generate the three surfaces. The surfaces are compared with ab initio results and, in the limit of removing one of the atoms to infinity, to H_3 results. Figure 1 shows a projection and equi-potential contour map for the London and one of the valence bond surfaces for the rectangular arrangement of four atoms. The contour intervals are one-tenth of the H_2 dissociation energy. The two surfaces are drawn to identical scale.

The results of a comparative scattering study investigating reactivity and energy transfer on the three valence bond surfaces and on a London surface have been analyzed. The calculations were performed at energies greater than the dissociation energy of molecular hydrogen. Reactivity and energy transfer characteristics have been related to surface properties. It is anticipated that two papers describing this work will be completed and submitted for publication.

FOOTNOTE AND REFERENCES

*Applied Physics Laboratory, The Johns Hopkins University, Laurel, MD 20810.

1. N. J. Brown and D. M. Silver, J. Chem. Phys. 65, 311 (1976).

2. N. J. Brown and D. M. Silver, J. Chem. Phys. 68 (1978).

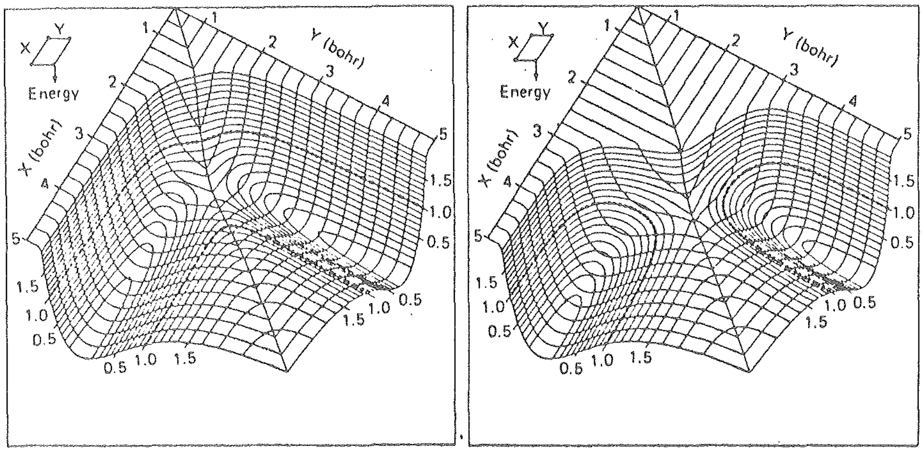

Fig. 1. Projections of Equi-potential contour maps for a London and valence bond semi-empirical H_4 potential energy surface.

JET IGNITION STUDIES

A. K.. Oppenheim, F. C. Hurlbut, F. A. Robben,
K. Teichman, K. Hom, and H. E. Stewart

INTRODUCTION

Practically all combustion systems used today are, in effect, mixing controlled. In most, fuel is either introduced into the combustion chamber separately from air or it is deliberately not mixed well so that the process by which the two are brought in contact with each other is significantly slower than the chemical reaction of combustion and can serve, therefore, as means for control. Such systems have the unfortunate attribute of automatically adjusting themselves so that the production of pollutants is maximized. The flame front, where the exothermic reaction is initiated, establishes itself at the stoichiometric contour, promoting the attainment of a maximum possible temperature that enhances the generation of the largest quantity of nitric oxide. This is true, irrespective of the overall fuel-air ratio at which the system operates. Moreover, in approaching the flame in the absence of oxygen, the fuel pyrolyzes to unburned hydrocarbons and soot.

This state of affairs exists whenever there is insufficient time for fuel to vaporize and diffuse uniformly throughout the oxidant prior to the exothermic process of combustion. One could improve the situation, therefore, by the development of systems where the fuel is pre-vaporized, the reactants are premixed and preheated while combustion occurs in the presence of as much diluent, provided by excess air and exhaust gases, as is necessary in order to maintain the maximum temperature at an optimum level for efficient operation of the energy conversion system for which the combustor serves as the heat source.

Work on the development of such systems is currently in progress. The major problems encountered are due to the progressively more difficult ignition and slower combustion process as the amount of diluent in the pre-mixed combustible medium is increased. We intend to supply the background knowledge required to solve these problems.

In spark ignition engines using near stoichiometric mixtures, combustion is initiated at a point by a relatively weak spark forming a single laminar flame kernel. With the use of significantly leaner mixtures, weak spark discharge is insufficient for ignition and, as a consequence of a lower temperature level due to dilution, the laminar flame, even if successfully initiated, would be too slow for satisfactory operation. One has to resort to other means that provide zonal or multi-point ignition sources so that, by creating a multitude of flames, sufficiently high overall rate of combustion can be achieved in spite of the relatively low individual flame speed. In principle this can be accomplished by the use of jets of active radicals that offer the prospect of sufficiently good penetration and distribution of ignition sources for such purpose.

The fact that jets of active radicals offer attractive means for ignition of lean mixtures has been known for quite some time and the technical literature is full of publications bearing evidence of this fact. Most of these publications are primarily concerned with the operation of some particular device; relatively few of them report studies on fundamental properties of such ignitions systems. Jet ignition can be considered as an advanced version of the stratified charge concept. The main difference is that, instead of a flame torch--a typical feature of conventional stratified charge systems--jet ignition is based on the use of distributed active radicals. There are two ways by which the radicals can be generated: by combustion or by electrical discharge.

Combustion generated radical jet ignition has been developed at the Institute of Chemical Physics in Moscow on the basis of theoretical studies by Semenov[1] and the experimental research program conducted by Gussak.[2,3] Semenov presents his theory in three parts. First he sets out the fundamental concepts by which he demonstrates that chain kinetic processes, in their simplest cases, constitute autocatalysis by ultimate products. Secondly he considers the limitations imposed by the interaction between active particles, and thirdly he analyses wall effects. The work of Gussak and his associates at the Institute led to the establishment of the concept of Avalanche Activated Combustion (or LAG, its acronym in Russian), and to the development of a variety of practical devices for its technological realization. As its name implies, the LAG process is based on the exploitation of active radicals to provide an abundance of chain carriers, especially hydrogen atoms, that significantly enhance the chain-branching steps and, hence, the rate of the reaction at relatively low temperatures corresponding to combustion of mixtures whose composition is far from stoichiometric proportions. In order to generate the radicals, the process is based on the use of an extra-rich mixture (equivalence ratio of an order of 2) in a pre-combustion chamber, while the charge in the main chamber can be ultra-lean (equivalence ratio of 0.5, or less at part loads). An investigation to test the viability of the LAG process in an internal combustion engine, conducted at General Motors, demonstrated its positive effect on the reduction of emissions of carbon monoxide and oxides of nitrogen, but was otherwise inconclusive.

A considerable amount of work has been done on the development of plasma jet ignition systems for automotive applications. A fundamental program of studies of plasma jets has been carried out by Weinberg and his associates at the Imperial College, University of London. After laying the groundwork in a book on electrical aspects of combustion,[4] Weinberg conducted a study of the effectiveness of different plasmas for enhancing combustion rates in a steady flow system. Under investigation at the same time was the effect of mixing, achieved by the use of a magnetic field, both to sustain combustion under stirred flow conditions and to enhance ignition. Nitrogen was found to be most effective for flame stabilization under steady flow conditions. Its plasma was subsequently demonstrated to provide practical means for the removal of soot and the reduction of NO concentration in exhaust products. In a parallel study to that reported here, in which Weinberg collaborated with us, distinct effects of various chemical species used for the plasma jet on the ignition of an ultra-lean methane-air mixture were observed, with methane showing clear superiority in this respect over hydrogen and nitrogen.

ACCOMPLISHMENTS DURING 1977

Preliminary experiments were carried out using a cylindrical, stainless steel vessel, fitted with optical glass windows 9 cm in diameter at a distance of 9 cm between their inner faces. Figure 1 is a photograph of the vessel showing at the right the instrument plug, fitted with inlet tubing for the test gas, and the plasma plug on top.

The combustion radical jet generator is shown in Fig. 2. Its body is made out of hexagonal steel stock, and the combustion chamber it provides is in the form of a cylinder 45 mm long and 3.6 mm in diameter; the effective volume of the gas used for the generation of the jet is thus 460 mm.^{3} For a stoichiometric methane-oxygen mixture we used, at a pressure of 1 atm and a temperature of 20°C, this corresponds to 5J of energy expended for the projection of the jet.

The plasma radical jet generator is shown in Fig. 3. The unit consists of the electrode and porcelain insulator of a Champion J-61Y spark plug which is fitted into a teflon insert, forming the side-walls of the discharge chamber; the main body and the bushing holder on top were made out of brass. The discharge chamber is cylindrical in shape, 6.1 mm long and 2.4 mm in diameter, providing a volume of 28 mm^3 for the gas used in the production of the production of the plasma jet. At the exit, the plasma generator is furnished with an orifice plate which is attached to the body by three small screws. For the current study we employed primarily an orifice 1.2 mm in diameter, while an alternative one 2 mm in diameter was used only to investigate the influence of its size on the properties of the jet.

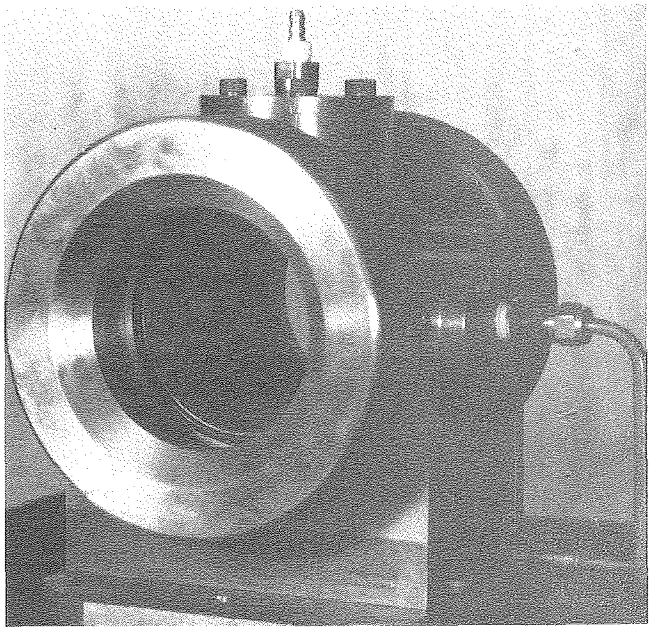

Fig. 1. Explosion vessel. (XBB 782-3371)

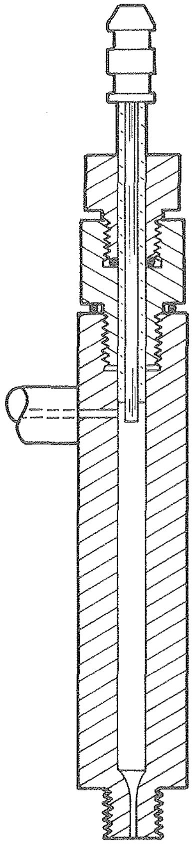

Fig. 2. Combustion jet generator. (XBL 782-7381)

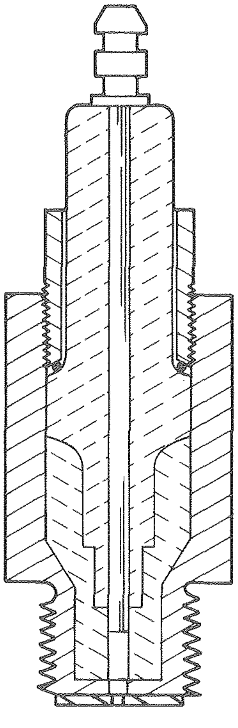

Fig. 3. Plasma jet generator. (XBL 7711-11333)

Major results of the peliminary studies are in the form of schlieren flash photographs obtained with an open shatter camera using a sub-microsecond spark discharge in air as a point light source. An example of such records is shown in Fig. 4. The figure consists of a set of four photographs depicting a sequence of events taking place under the same operating conditions. Each of them was taken from a different experiment, and the sequence obtained by shifting the time delay used for triggering the light source, while the vessel was filled initially with a methane-air mixture at atmospheric pressure and room temperature. The equivalence ratio of the mixture was 0.5, corresponding to 5% volumetric fraction of methane. Under such conditions this was below the normal flammability limit which, according to data of the U. S. Bureau of Mines, is at 5.3%. The orifice diameter was 2.4 mm while the energy discharged in the plasma generator was 2.5 J. The first photograph was taken 1 msec after the discharge was initiated. Here one observes the turbulent plume propagating towards the center of the enclosure. Superimposed on it is the direct image of the light emitted by the jet due to the illumination of the plasma. In the next photograph taken at 10 msec, the combustion has started, appearing in the form of a turbulent flame kernel. In the next frame, at 50 msec, the combustion front acquired a laminar flame structure, and, in the last frame at 100 msec, it reached the walls of the vessel.

Our preliminary studies of jet ignition have led to the following conclusions:

(1) If the initial velocity of the jet is sufficiently high, its gasdynamic properties are, in general, the same, irrespective of whether it has been formed by combustion or by electric discharge.

(2) The jets enter the combusion chamber in the form of turbulent plumes which are embedded in blast waves headed by hemispherical shock fronts.

(3) The blast wave effects are dissipated by the time combustion starts. The latter always occurs in the turbulent zone of the plume.

(4) Combustion is initiated as a set of turbulent flames which later tend to acquire a more laminar structure. This is in direct contrast to the sequence of events associated with spark ignition.

(5) The depth of penetration of the jet depends on its initial velocity, which can be controlled by the specific energy used for its production as well as by the size of the orifice through which it is injected.

To sum up, insofar as its fluid mechanic properties are concerned, jet ignition offers the following advantages:

(a) A controllable depth of penetration, providing the capability for starting the combustion process at any desired location within the charge

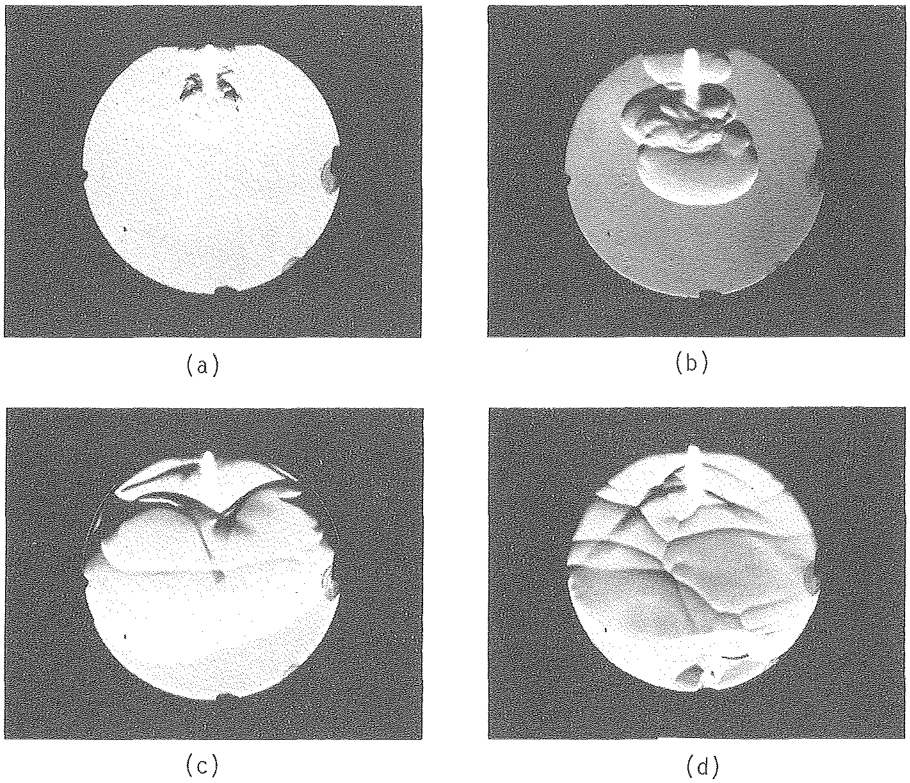

(a) (b) (c) (d)

Fig. 4. Schlieren flash photographs of events associated with ignition produced by plasma jet. Discharge energy: 2.5J, Orifice diameter: 2.4 mm. (a) 1 msec, (b) 10 msec, (c) 50 msec, (d) 100 msec. (XBB 782-2372)

and, in particular, protecting the process from the destructive effects of walls.

(b) Zonal pre-turbulization, furnishing optimum conditions for ignition and thus enhancing the combustion of lean mixtures.

(c) Wide dispersion of ignition sources, yielding multi-point initiation of combustion--a feature of particular importance to lead mixtures for it yields high overall rates in spite of relatively low individual flame speeds.

PLANNED ACTIVITIES FOR 1978

The major effort in the next phase of this research program is to be spent on a systematic study of the fluid mechanic properties of the jets and their effectiveness as ignitors.

The combustion generator investigation will include the following effects:

(1) chemical composition of fuel,
(2) chemical composition of oxidizer--ranging from pure oxygen to air--and its relative amount, the equivalence ratio,
(3) method of ignition--single or multi-source,
(4) pressure and temperature of combustion products ahead of the ejection nozzle,
(5) shape and size of the ejection nozzle and its orientation at the exit, as it governs the formation of the shear layer--the actual source of turbulence.

The plasma generator investigation will focus on the following features:

(1) size and shape of the discharge cavity,
(2) size of orifice controlling the momentum of the jet
(3) net amount of electrical energy expended in the discharge,
(4) shape of the discharge power pulse and its duration,
(5) electro-magnetic stirring or explusion
(6) chemical composition of medium used for the production of plasma.

The most important properties of the process of jet ignition are chemical in nature. These will be studied by two associated programs of research. One will concentrate on optical measurements using conventional spectroscopy at first and later, as they become available, laser-based fluorescence and scattering techniques. The other will be concerned with the measurement of time-resolved local concentrations using a molecular beam sampling technique associated with a quadrupole mass spectrometer. This strategy is based upon the premise that non-interactive laser-based instruments are not yet developed to a point where they can be relied upon for a program of studies involving the acquisition of knowledge about a novel process, such as ours. Hopefully, they may become available in time for our experiments to serve as a convenient proving ground for testing their performance.

REFERENCES

1. N. N. Semenov, "On Types of Kinetic Curves in Chain Reactions," Comptes Rendus (Doklady) de l'Academie des Sciences de l'URSS (I) 43, 8: 342-348; (II) 44, 2: 62-66; (III) 44, 6: 241-245 (1944).
2. L. A. Gussak, "High Chemical Activity of Incomplete Combustion Products and a Method of Prechamber Torch Ignition for Avalanche Activation of Combustion in Internal Combustion Engines," Paper 750890, presented at SAE Automobil engineering Meeting, Michigan (Oct. 1975).
3. L. A. Gussak and M. C. Turkish, "LAG-Process of Combustion and Its Application in Automobile Gasoline Engines," Stratified Charge Engines, I. Mech. E., London, 137-145 (1976).
4. J. Lawton and F. Weinberg, "Electrical Aspects of Combustion," Clarendon Press (Oxford, England), xv + 355 pp (1969).

ENGINE COMBUSTION WITH EXCESS AIR

K. H. Chu, J. W. Daily, R. Greif, H. Heperkan, N. Ishikawa, M. Nikanjam,
A. K. Oppenheim, R. F. Sawyer, O. I. Smith, K. Y. Teichman, and S. Young

INTRODUCTION

A square piston, single-pulse, compression-expansion machine has been employed to study reciprocating engine combustion under well controlled laboratory conditions simulating the operation of a spark ignition engine. The single-pulse machine, built by researchers in the Department of Mechanical Engineering, has the unique feature of providing optical access to the entire combustion process. This work was originally sponsored by the National Science Foundation/ Research Applied to National Needs but during 1977 came under Department of Energy support. Current studies are on the combustion of lean mixtures because of the advantages such mixtures offer in terms of increased fuel economy and reduced pollutant emissions in comparison with conventional engine combustion which occurs at mixture ratios near to the stoichiometric amount.

The research is being conducted under four major tasks: (1) ignition process, directed by Professor A. K. Oppenheim, (2) flame propagation phenomena, directed by Professor R. F. Sawyer (who also serves as principal investigator for the project), (3) wall quenching processes, directed by Professor John W. Daily, and (4) heat transfer phenomena, directed by Professor R. Greif. In all cases the recording of the combustion events through high speed schlieren cinematography provides detailed information on the complex engine combustion processes. In all cases methane has been used as a model hydrocarbon fuel because of the information available on its oxidation kinetics.

ACCOMPLISHMENTS DURING 1977

Studies of ignition processes have demonstrated the ability to ignite mixtures beyond their ordinary lean flammability limits through use of both chemical and plasma torch igniters. Detailed information on jet ignition is presented in the preceding article.

A postulated process of "bulk quenching," which is brought about during the piston expansion period in the combustion of mixtures near the lean flammability limit, has been observed and measured. Such processes, which prevent the completion of combustion and result in reduced efficiency and increased hydrocarbon emissions, present a constraint upon the operation of "lean burn" engines. This work has included a cooperative effort with the Lawrence Livermore Laboratory which has provided a computer based model of the quench model.

A second and generally dominant mechanism controlling the emission of hydrocarbons from engines is the quenching of combustion in a thermal boundary layer which is a necessary consequence of cold combustion chamber walls. This boundary layer is scraped off the wall into a vortex through the motion of the piston. The nature of this "roll-up" vortex has been observed to be strongly influenced by the piston and cylinder head geometry.

Unsteady, time-resolved heat transfer to the end wall of the combustion chamber has been measured using a thin-film platinum resistance thermometer during the combustion stroke without combustion. A theoretical laminar boundary layer model is in good agreement with the experimental observations. Time varying heat transfer coefficients are extracted from the heat flux data and show a non-monotonic variation.

PLANNED ACTIVITIES FOR 1978

Ignition studies are focused on gaining an understanding of the importance of radical species produced in the plasma to the initiation of the combustion processes. Flame propagation studies are to be extended to a range of hydrocarbon fuels with the objective of providing energy release rate data of use to combustion chamber design. Wall quenching studies will focus upon the fate of the roll-up vortex produced during the exhaust stroke. Heat transfer measurements are being extended to cases with combustion.

GPO 794-890/277